UNIVERSITEIT GENT

FACULTEIT FARMACEUTISCHE WETENSCHAPPEN

SYNTHESIS AND BIOLOGICAL EVALUATION OF PYRIMIDINE NUCLEOSIDES AND NUCLEOSIDE PHOSPHONATES

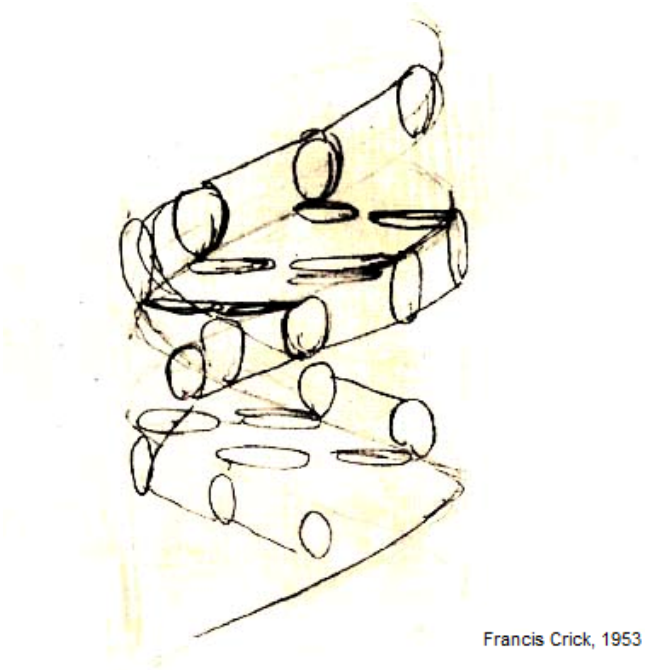

Francis Crick, 1953

Apr. Sara Van Poecke

Promoter

Prof. Dr. Apr. Serge Van Calenbergh

Academic year 2011-2012

UNIVERSITEIT GENT

SYNTHESIS AND BIOLOGICAL EVALUATION OF PYRIMIDINE NUCLEOSIDES AND NUCLEOSIDE PHOSPHONATES

Apr. Sara Van Poecke

Thesis submitted to the Faculty of Pharmaceutical Sciences to obtain the degree of Doctor in Pharmaceutical Sciences

Promoter
Prof. Dr. Apr. Serge Van Calenbergh

Academic year 2011-2012

TABLE OF CONTENTS

DANKWOORD

De afgelopen jaren waren uitdagend, leerrijk en fascinerend, zo nu en dan gekruid met een snuifje ontgoocheling, frustratie en moedeloosheid. Deze pagina is gericht aan al diegene die me steunden in goede en kwade dagen en die me hielpen daar waar mogelijk. Dit werk was er nooit gekomen zonder jullie. Een welgemeende dikke merci.

Een bijzonder woord van dank aan mijn promotor Prof. Serge Van Calenbergh. Je wist door welke moeilijke periode ik ging en toch heb je me de kans gegeven om deze uitdaging aan te gaan. Je verhaal over hoe ik openbloeide in het labo tijdens mijn thesis klinkt me nog steeds als muziek in de oren. Bedankt voor de vele tips, aanmoedigingen en goede begeleiding gedurende de voorbije 4 jaar.

Bedankt ook aan de vele collega's die de revue passeerden: Izet, Annelies, Ineke, Liesbeth, Steven, Ulrik, Radim, Thomas, Nora, René, Kiran, Martijn, Joren, Shari & Jolien. Nora, jou wil ik in het bijzonder bedanken voor de vele toffe jaren die we samen in het labo doorbrachten. Ik was zó blij toen je erbij kwam. Eindelijk een vrouwelijke collega, gedaan met gesprekken over voetbal en duiken. Na 3 jaar lief en leed gedeeld te hebben is het voor mij afgelopen. Ook voor jou is het einde in zicht, ik wens je bijzonder veel succes bij het finaliseren van je werk!

Een welgemeend woord van dank gaat eveneens uit naar de mensen die me geholpen hebben met allerlei zaken tijdens mijn onderzoek: Prof. Dr. Jan Balzarini voor het testen van de TK-2 inhibitoren en de antivirale componenten, Dr. Hélène Munier-Lehmann for testing the TMPKmt inhibitors, Prof. Kendall Harden and Prof. Kenneth Jacobson for the biological evaluation of the $P2Y_2$ ligands, Bart Lucas voor het opnemen van de fluorescentie spectra, Davy Sinnaeve voor het uitvoeren van allerlei NMR experimenten en het agentschap voor Innovatie door Wetenschap en Technologie voor het financiële luik van dit werk.

Mijn ouders, broers, goede vrienden en familie: bedankt voor de interesse, de steun en om er altijd te zijn voor mij.

Bruno, toen ik je leerde kennen was ik al volop bezig in het labo. Ik zie nog voor me hoe je je wenkbrauwen fronste toen ik je vertelde over mijn reactieschema's, reacties, kolommen, NMR's enz. De laatste tijd was het wellicht iets minder uitbundig en met een beetje schrik voor wat komen zal ... Oprecht dank voor al je geduld, steun en begrip.

SUMMARY

Modification of naturally occurring nucleosides is an important area in the search for new agents with therapeutic potential. The work presented herein focuses on modified pyrimidine nucleosides as well as nucleoside phosphonates. The first part presents the synthesis and biological evaluation of several thymidine kinase 2 inhibitors. In the second part, the synthesis and biological evaluation of a series of new TMPKmt inhibitors will be discussed. The third part is dedicated to the search for new $P2Y_2$ receptor ligands and in the last part, the synthesis and antiviral activity of a series of nucleoside phosphonates will be presented.

Thymidine kinase 2 (TK-2) is a mitochondrial deoxynucleoside kinase that plays an important role in the first phosphorylation of pyrimidine nucleosides needed for mtDNA synthesis. Furthermore, it is assumed that TK-2 could be involved in the mitochondrial toxicity associated with antiviral nucleoside analogues. However, there are still many open questions related to the real contribution of TK-2 to these issues. Potent and selective TK-2 inhibitors could be valuable tools to unravel the role of TK-2 in mitochondrial deoxytriphosphate pools and homeostasis, and may help to clarify the contribution of TK-2 catalyzed phosphorylation of antiviral drugs to the mitochondrial toxicity of these agents. Two series of thymidine analogues that were originally designed as TMPKmt inhibitors, were evaluated for their inhibitory activity against a panel of other nucleoside kinases (TK-1, TK-2, herpes simples virus 1 and varicella zoster virus TK). Several substituted 3'-thiourea derivatives of β-dThd proved highly inhibitory to and selective for human mitochondrial TK-2 compared to related kinases. As it was demonstrated that the 3'-substituent of these analogues was responsible for extra interactions with TK-2, we decided to investigate if the thiourea moiety, earlier described as the perpetrator of toxicity, could be replaced by alternative linkages to connect the C-3' atom of the deoxyribose moiety to several substituents. In Chapter 2 we explored thymidine analogues containing a triazole ring instead of the thiourea moiety. Therefore, a series of 1,4- and 1,5-disubstituted 3'-(1,2,3-triazol-1-yl)-3'-deoxy-β-D-thymidine analogues was synthesized via Huisgen [3+2] cycloaddition. Combination of a favorable 3'-(4-substituted-1,2,3-triazole) moiety with a (*E*)-5-(2-bromovinyl)-substituent, known as a privileged scaffold for TK-2 binding, resulted in several potent and selective TK-2 inhibitors, e.g., compound **1.66** (IC_{50} = 0.036 μM). Chapter 3 described the synthesis and biological evaluation of several thymidine and BVDU analogues containing a substituted amine, guanidine or 1,5-disubstituted tetrazole instead of a thiourea. The latter modification resulted in analogue **1.100** (IC_{50} = 0.014 μM) which is the most potent and selective TK-2 inhibitor reported so far.

Mycobacterial thymidine monophosphate kinase (TMPKmt) catalyses the reversible phosphorylation of thymidine monophosphate to thymidine diphosphate in *Mycobacterium tuberculosis*. Because its crucial role in thymidine metabolism and in view of its low sequence identity with the human isoenzym, TMPKmt represents an attractive target for blocking the mycobacterial DNA synthesis. To gain further insight into the S.A.R. of several thiourea analogues known for their inhibitory activity against TMPKmt, different analogues of these lead compounds were synthesized including 3'- and 5'-modified

α- and β-derivatives. In addition, several analogues were synthesized in which the 4-oxygen was replaced by a more lipophilic sulfur atom. In both the 3'- and 5'- modified thymidine analogues, the anomer that places the thymine base trans to the aromatic substituent showed the best TMPKmt inhibition. Several compounds showed an inhibitory potency in the low micromolar range, with the 5'-arylthiourea 4-thio-α-D-thymidine analogue **2.24** being the most active one (K_i = 0.17 μM).

The $P2Y_2$ receptor is a G-protein coupled receptor belonging to the purinergic receptor family which is activated by ATP and UTP. $P2Y_2$ agonists are promising potential therapeutics for cystic fibrosis, while $P2Y_2$ antagonists exhibit anti-inflammatory and neuroprotective properties. UTP as well as most reported analogues are sensitive to enzymatic degradation. Replacement of the α-phosphate group of UTP by an isosteric phosphonate group didn't result in an increased metabolic stability. The resulting uridine 5'-phosphonodiphosphate (**3.6**) suffered from complete chemical hydrolysis to the corresponding 5'-phosphonate (**3.7**) in the buffer storage solution. Surprisingly, when tested in its pure form, compound **3.7** showed partial $P2Y_2$ receptor agonist activity while being inactive at the $P2Y_4$ receptor. In PART III, we introduced several (hetero)aromatic substituents at C-5 of the 5'-methylene phosphonate analogue **3.7**. All 5-modified analogues caused $P2Y_2$-dependent IP_3 accumulation but none of the phosphonate analogues had the same maximal activity as UTP. Within this series, a 5-(2-furanyl) modification (**3.49**) gave the highest efficacy, while 5-(4-fluorophenyl) substitution (**3.46**) afforded the highest potency. Remarkably, these analogues failed to inhibit activity of UTP down to the level of activity seen with the 5-modified analogues alone as would be expected for classical partial agonists. A possible explanation for this phenomenon is that these phosphonates are producing their effects by interacting with a receptor site distinct from the orthosteric site. In addition, we also envisaged replacement of the 2'-OH group of compound **3.7** with a 2'-chloro and a 2'-amino group. Both 2'-modified analogues gave marginal activation of the receptor. Another phosphonate bio-isostere of uridine 5'-monophosphate, obtained by the inversion of the 4'-CH_2-O group of uridine monophosphate, was significantly less active than the lead phosphonate.

A number of C-5 modified 2'-deoxypyrimidine analogues are known to possess potent and selective antiviral activity. However, relatively few examples of 5-(hetero)aryl-modified nucleosides with promising antiviral activity have been reported. This may be due to the fact that these nucleosides are not efficiently converted into their triphosphate form. This led us to investigate a small series of 2'-deoxyuridine analogues that combine different aromatic substituents at position 5 of the base with a 5'-methylene phosphonate group to bypass a possibly difficult first intracellular phosphorylation step. An unexpected anomerisation during the last step of the synthesis allowed us to investigate the β- as well as the α-anomers of the corresponding phosphonates. None of these analogues exhibited significant antiviral activity.

SAMENVATTING

Het modificeren van nucleosiden is een veelgebruikte methode in de zoektocht naar nieuwe verbindingen met therapeutisch potentieel. In dit werk wordt gefocust op gemodificeerde pyrimidine nucleosiden en nucleoside fosfonaat analogen. In het eerste deel wordt de synthese en biologische evaluatie van een aantal thymidine kinase 2 inhibitoren voorgesteld. Het tweede deel behandelt de synthese en evaluatie van nieuwe TMPKmt inhibitoren. Het derde deel is gewijd aan de zoektocht naar $P2Y_2$ liganden gevolgd door een laatste deel waarin de synthese en antivirale activiteit van nucleoside fosfonaten beschreven wordt.

Thymidine kinase 2 (TK-2) is een mitochondriaal deoxynucleoside kinase dat een belangrijke rol speelt in de eerste fosforylering van pyrimidine nucleosiden nodig voor mtDNA synthese. Daarnaast zou TK-2 ook betrokken zijn bij de mitochondriale toxiciteit geassocieerd met nucleoside-analoog therapie. Er zijn echter nog vele vragen omtrent de bijdrage van TK-2 in beide processen. De synthese van potente en selectieve TK-2 inhibitoren zou een belangrijk hulpmiddel kunnen zijn in het onderzoek naar de rol van TK-2 in mitochondriale deoxynucleoside trifosfaat pools en homeostase, alsook naar de bijdrage van TK-2 gekatalyseerde fosforylering in de mitochondriale toxiciteit van antivirale middelen. Twee reeksen thymidine analogen die oorspronkelijk gesynthetiseerd werden als TMPKmt inhibitoren, werden getest voor hun inhiberende werking op verschillende TK's (TK-1, TK-2, Herpes Simplex TK 1 en varicella zoster virus TK). Een aantal gesubstitueerde 3'-thioureum derivaten van β-dThd vertoonden een hoge en selectieve inhiberende activiteit voor humaan TK-2 in vergelijking met de andere kinasen. Aangezien de substituent op het C-3' atoom van het deoxyribose gedeelte verantwoordelijk bleek voor extra interacties maar de thioureum functie in het verleden reeds toxische nevenwerkingen veroorzaakte, werd op zoek gegaan naar alternatieve linkers tussen C-3' en de verschillende substituenten. In hoofdstuk 2 werd de thioureum functie vervangen door een triazool ring. Hiervoor werd via Huisgen [3+2] cycloadditie een reeks 1,4- en 1,5-digesubstitueerde 3'-(1,2,3-triazol-1-yl)-3'-deoxy-β-D-thymidine analogen gesynthetiseerd. Combinatie van de meest actieve 3'-(1,2,3-triazol-1-yl) modificatie met een (*E*)-5-(2-bromovinyl) substituent, die een positieve invloed op TK-2 affiniteit heeft, leverde een aantal zeer potente en selectieve TK-2 inhibitoren op (bv. verbinding **1.66**, IC_{50} = 0.036 µM). In hoofdstuk 3 werd de synthese en biologische evaluatie van een aantal thymidine en BVDU analogen beschreven waarin de thioureum functie vervangen werd door een gesubstitueerde amine, guanidine of 1,5-digesubstitueerde tetrazool linker. Deze laatste modificatie resulteerde in analoog **1.100** (IC_{50} = 0.014 µM), de meest potente en selectieve TK-2 inhibitor beschreven tot dusver.

Mycobacterieel thymidine monofosfaat kinase (TMPKmt) katalyseert de reversibele fosforylering van thymidine monofosfaat naar thymidine difosfaat in *Mycobacterium tuberculosis*. Zijn essentiële rol in het thymidine metabolisme gecombineerd met een lage aminozuur sequentie overeenkomst met het humane iso-enzym (TMPKh), maken van TMPKmt een aantrekkelijk target voor het blokkeren van de mycobacteriële DNA synthese. Om een beter inzicht te krijgen in de S.A.R van een aantal gekende

thioureum analogen die TMPKmt inhiberen, werden in deel II verschillende structurele varianten van deze lead verbindingen gesynthetiseerd waaronder 3'- en 5'- gemodificeerde α- en β-derivaten. In sommige analogen werd tevens het zuurstofatoom op positie 4 van de base vervangen door het meer lipofiele zwavel. Zowel voor de 3'- als 5'-gemodificeerde analogen, gaf het anomeer waarbij de thymine base trans stond ten opzichte van de aromatische substituent de beste TMPKmt inhiberende activiteit. Verschillende analogen vertoonden een K_i in de lage micromolaire concentratie, met het 5'-arylthioureum 4-thio-α-thymidine analoog **2.24** als meest actieve verbinding (Ki = 0.17 μM).

De $P2Y_2$ receptor is een G-proteïne gekoppelde receptor die behoort tot de familie van de purinerge receptoren en die geactiveerd wordt door ATP en UTP. $P2Y_2$ agonisten zijn potentiële geneesmiddelen voor de behandeling van mucoviscidose, terwijl $P2Y_2$ antagonisten anti-inflammatoire en neuroprotectieve eigenschappen bezitten. UTP, alsook de diverse reeds gerapporteerde UTP analogen zijn onderhevig aan enzymatische degradatie. Vervanging van de α-fosfaat groep van UTP door een isostere fosfonomethylgroep leidde in het verleden niet tot de verhoopte toename in metabole stabiliteit. Uridine 5'-fosfonodifosfaat (**3.6**) onderging chemische hydrolyse tot het overeenkomstige 5'-methylfosfonaat (**3.7**) in de bufferoplossing voor bewaring. Opmerkelijk hierbij was dat **3.7** zich als aan partiële $P2Y_2$ receptor agonist gedroeg terwijl het inactief was ten opzichte van de $P2Y_4$ receptor. In deel III werden analogen gesynthetiseerd waarbij de 5'-methylfosfonaat groep van **3.7** gecombineerd werd met verschillende (hetero)aromatische substituenten op C-5. Alle analogen veroorzaakten een $P2Y_2$ receptor afhankelijke IP_3 accumulatie maar geen enkel fosfonaat had hetzelfde maximaal effect als UTP. Een 5-(2-furanyl) modificatie (**3.49**) bezat de hoogste efficacy terwijl een 5-(4-fluorofenyl) (**3.46**) substitutie de hoogste potency vertoonde. Opmerkelijk hierbij was dat de analogen er niet in slaagden de activiteit van UTP te inhiberen tot het activiteitsniveau van de 5-gemodificeerde analogen alleen zoals te verwachten voor klassieke partiële agonisten. Mogelijks veroorzaken de fosfonaten hun effect via een allosterisch werkingsmechanisme. In een tweede reeks analogen werd de 2'-OH groep van verbinding **3.7** vervangen door een 2'-chloor en een 2'-amino. Beide analogen vertoonden een matige activatie van de $P2Y_2$ receptor. Analoog **3.68**, een fosfonaat bioisosteer van uridine 5'-monofosfaat verkregen door omkering van de 4'-CH_2-O groep van uridine monofosfaat, veroorzaakte slechts een beperkte receptor activatie.

Een aantal C-5 gemodificeerde 2'-deoxypyrimidine analogen zijn gekend omwille van hun potente en selectieve antivirale activiteit. Binnen deze groep is slechts een beperkt aantal 5-(hetero)aryl derivaten gerapporteerd. Mogelijks is dit te wijten aan een inefficiënte omzetting tot hun actieve trifosfaat vorm. Om dit na te gaan werden in deel IV de synthese en antivirale activiteit van een kleine reeks 2'-deoxyuridine analogen beschreven die verschillende aromatische substituenten op C-5 combineerden met een 5'-methylfosfonaat functie. Introductie van dit fosfonaat zou de eerste en vaak moeilijkste fosforylering stap moeten overbruggen. Een onverwachte anomerisatie in de laatste synthese stap liet toe om de antivirale activiteit van zowel de β- als de α- fosfonaten te onderzoeken. Geen enkel analoog vertoonde een significante antivirale activiteit.

LIST OF ABBREVIATIONS

ACV	Acyclovir
ADP	Adenosine 5’-diphosphate
AIDS	Acquired immune deficiency syndrome
Ala	Alanine
AMP	Adenosine 5’-monophosphate
Ara-C	Arabinofuranosyl cytosine
Ara-T	Arabinofuranosyl thymine
Ara-U	Arabinofuranosyl uracil
Arg	Arginine
ASL	Airway surface liquid
Asn	Asparagine
Asp	Aspartic acid
ATP	Adenosine 5’-triphosphate
AZT	3’-Azido-3’-deoxythymidine, zidovudine
AZTTP	3’-Azido-3’-deoxythymidine 5’-triphosphate
AZTMP	3’-Azido-3’-deoxythymidine 5’-monophosphate
BAIB	Bis(acetoxy)iodobenzene
BCG	Bacille Calmette-Guérin
BCN	Bicyclic nucleoside analogue
BVaraU	1-β-D-arabinofuranosyl-(*E*)-5-(2-bromovinyl)uracil
BVDU	(*E*)-5-(2-Bromovinyl)-2’-deoxyuridine
C	Cysteine
CaCC	Ca^{2+} regulated Cl^- channel
cAMP	Cyclisch adenosine 5’-monophosphate
$CCID_{50}$	Cell culture infection dose 50%
CDC	Centers for Disease Control and Prevention
cdN	Cytosolic 5’-deoxyribonucleotidase
CF	Cystic fibrosis
CFTR	Cystic fibrosis transmembrane regulator
CMV	Cytomegalovirus
COSY	Correlation spectroscopy
CTP	Cytidine 5’-triphosphate
CuAAC	Copper catalyzed azide-alkyne cycloaddition
Cys	Cysteine
D	Aspartic acid
d4T	3’-Deoxy-2’,3’-didehydrothymidine
DAG	Diacylglycerol
dAMP	2’-Deoxyadenosine 5’-monophosphate

dATP	2’-Deoxyadenosine 5’-triphosphate
DBU	1,8-Diazabicyclo[5.4.0]undec-7-ene
dCK	Deoxycytidine kinase
dCMP	2’-Deoxycytidine 5’-monophosphate
dCyd	2’-Deoxycytidine
ddT	3’-Deoxythymidine
DEPT	Distortionless enhancement by polarization transfer
dFdC	2’,2’-Difluoro-2’-deoxycytidine, Gemcitabine
dFdU	2’,2’-Difluoro-2’-deoxyuridine
dGK	Deoxyguanosine kinase
dGMP	2’-Deoxyguanosine 5’-monophosphate
DMAP	4-Dimethylaminopyridine
Dm-dNK	*Drosophila melanogaster* deoxyribonucleoside kinase
DMF	Dimethylformamide
DMSO	Dimethylsulfoxide
dN	Deoxyribonucleoside
DNA	Deoxyribonucleic acid
dNDP	Deoxynucleoside 5’-diphosphate
DNC	Deoxynucleotide carrier
dNK	Deoxynucleoside kinase
dNMP	Deoxynucleoside 5’-monophosphate
dNTP	Deoxynucleoside 5’-triphosphate
DOTS	Directly observed treatment short course
dTDP	Thymidine 5’-diphosphate
dThd	Thymidine
dTMP	Thymidine 5’-monophosphate
dTTP	Thymidine 5’-triphosphate
dUMP	2’-Deoxyuridine 5’-monophosphate
dUrd	2’-Deoxyuridine
E	Glutamine acid
EBV	Epstein-Barr virus
EC_{50}	Half maximal inhibitory concentration
E. coli	*Escherichia coli*
EdU	5-Ethyl-2’-deoxyuridine
EL	Extracellular loop
ENaC	Epithelial Na^+ channel
ENT	Equilibrative nucleoside transporter
ESI-MS	Electrospray ionization-mass spectrometry
F	Phenylalanine
FIAU	1-(2-deoxy-2-fluoro-β-D-arabinofuranosyl)-5-iodouracil

GDP	Guanosine 5’-diphosphate
Gln	Glutamine
Glu	Glutamine acid
GPCR	G protein-coupled receptor
GTP	Guanosine 5’-triphosphate
H	Histidine
HAART	Highly active anti-retroviral therapy
HBV	Hepatitis B virus
HCMV	Human cytomegalovirus
HCV	Hepatitis C virus
HEL	Human embryonic lung
HIV	Human immunodeficiency virus
HPLC	High performance liquid chromatography
HSV	Herpes simplex virus
IBX	2-Iodobenzoic acid
IC_{50}	Half maximal inhibitory concentration
IdU	5-Iodo-2’-deoxyuridine
Ile	Isoleucine
IP_3	Inositol 1,4,5-triphosphate
IR	Infrared
IUATLD	International Union Against Tuberculosis and Lung Disease
K_i	Affinity constant
*K*m	Michaelis constant
Lys	Lysine
M. bovis	*Mycobacterium bovis*
MCC	Minimum cytotoxic concentration
MD	Molecular dynamics
mdN	Mitochondrial 5’-deoxyribonucleotidase
MDR	Multidrug resistant
MDS	Mitochondrial depletion syndrome
Met	Methionine
MIC	Minimum inhibitory concentration
Ms	Methanesulfonyl
MCT	Methanocarbathymidine
mtDNA	Mitochondrial DNA
M. tuberculosis	*Mycobacterium tuberculosis*
N	Northern
N	Nucleoside
NAATs	Nucleic acid amplification tests
NADH	Nicotinamide adenine dinucleotide

NBS	*N*-bromosuccinimide
NDP	Nucleoside 5'-diphosphate
NDPK	Nucleoside 5'-diphosphate kinase
NK	Nucleoside kinase
NMP	Nucleoside 5'-monophosphate
NMPK	Nucleoside 5'-monophosphate kinase
NMR	Nuclear magnetic resonance
NOE	Nuclear Overhauser effect
NOESY	Nuclear Overhauser effect spectroscopy
NT	NH_2-terminus
OXPHOS	Oxidative phosphorylation
PCR	Polymerase chain reaction
PDB	Protein data base
PFU	Plaque forming unit
Phe	Phenylalanine
PIP_2	Phosphatidylinositol 4,5-bisphosphate
PLC	Phospholipase C
Pol-γ	Polymerase gamma
PPD	Purified protein derivative
ppm	Parts per million
PRPP	5-Phospho-α-D-ribosyl-1-pyrophosphate
R	Arginine
RB-2	Reactive Blue 2
RNA	Ribonucleic acid
RNR	Ribonucleotide reductase
ROE	Rotating-frame Overhauser enhancement
ROESY	Rotating-frame Overhauser effect spectroscopy
RP-HPLC	Reversed phase high performance liquid chromatography
RT	Reverse transcriptase
S	Southern
S.A.R	Structure-activity relationship
SD	Standard deviation
SEM	Standard error of the mean
SI	Selectivity index
TB	Tuberculosis
TBAF	Tetra-*n*-butylammonium fluoride
TBDMS	*tert*-Butyldimethylsilyl
TEMPO	(2,2,6,6-Tetramethylpiperidin-1-yl)oxyl
TFA	Trifluoroacetic acid
THF	Tetrahydrofuran

Thr	Threonine
TK-1	Thymidine kinase 1
TK-2	Thymidine kinase 2
TLC	Thin layer chromatography
TM	Transmembrane region
TMPK	Thymidine monophosphate kinase
TMPKec	Thymidine monophosphate kinase of *Escherichia coli*
TMPKh	Human thymidine monophosphate kinase
TMPKmt	Thymidine monophosphate kinase of *M. tuberculosis*
TMPKy	Yeast thymidine monophosphate kinase
TMSBr	Bromotrimethylsilane
TOF	Time of flight
Tr	Triphenylmethyl
Tyr	Tyrosine
UDP	Uridine 5'-diphosphate
UK	United Kingdom
USA	United States of America
UTP	Uridine 5'-triphosphate
Val	Valine
V_m	Maximum velocity
VSV	Vesicular stomatitis virus
VV	Vaccinia virus
VZV	Varicella zoster virus
WHO	World health organisation
XDR	Extensively drug resistant
Y	Tyrosine

NUCLEOSIDE NOMENCLATURE

Since IUPAC nomenclature does not allow rapid visualization of modified nucleosides, the typical nucleoside notation starts from the name of the natural nucleoside, to which the chemical modifications at the different positions are added. This nomenclature is generally accepted in the nucleoside chemistry and is therefore used throughout this work. As these conventions can lead to misinterpretations if changes on the nucleoside structure alter the parent nucleoside too much, sometimes the IUPAC nomenclature will be used (e.g., compounds **1.67** and **1.68** (PART I) and the (2'-deoxy)uridine phosphonate derivatives described in PARTS III and IV). In addition, the generally used numbering system for nucleosides is depicted in Figure I.

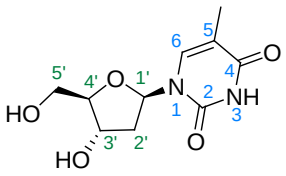

Figure I. Generally used numbering system for nucleosides.

PREFACE

Modification of naturally occurring nucleosides has been proven a successful strategy in the search for new drugs. Structural modifications of nucleosides have given rise to widely used drugs such as zidovudine (Retrovir®) and acyclovir (Zovirax®), which demonstrates that this strategy offers interesting opportunities to synthesize new therapeutically useful compounds.

This work comprises four different parts that, from a target point of view, don't have much in common except that these targets all use a nucleoside or a nucleotide as endogenous ligand. Hence, from a chemical point of view, interesting similarities may be uncovered in the substrate-based design of compounds capable of modulating these targets.

In PART I, efforts will be made to synthesize highly active and selective inhibitors for human mitochondrial thymidine kinase 2. Thymidine kinase 2 inhibitor **1.43**, a 3'-modified analogue of the natural ligand thymidine, will be used as a template to synthesize new compounds in which the toxic thiourea group is replaced with an alternative linker (Figure II). Based on the structural relationship of TK-2 and thymidine monophosphate kinase and some of their inhibitors, PART II aims at evaluating selected TK-2 inhibitors for their inhibitory activity against mycobacterial thymidylate kinase to gain further insight into the S.A.R. of known TMPKmt inhibitors.

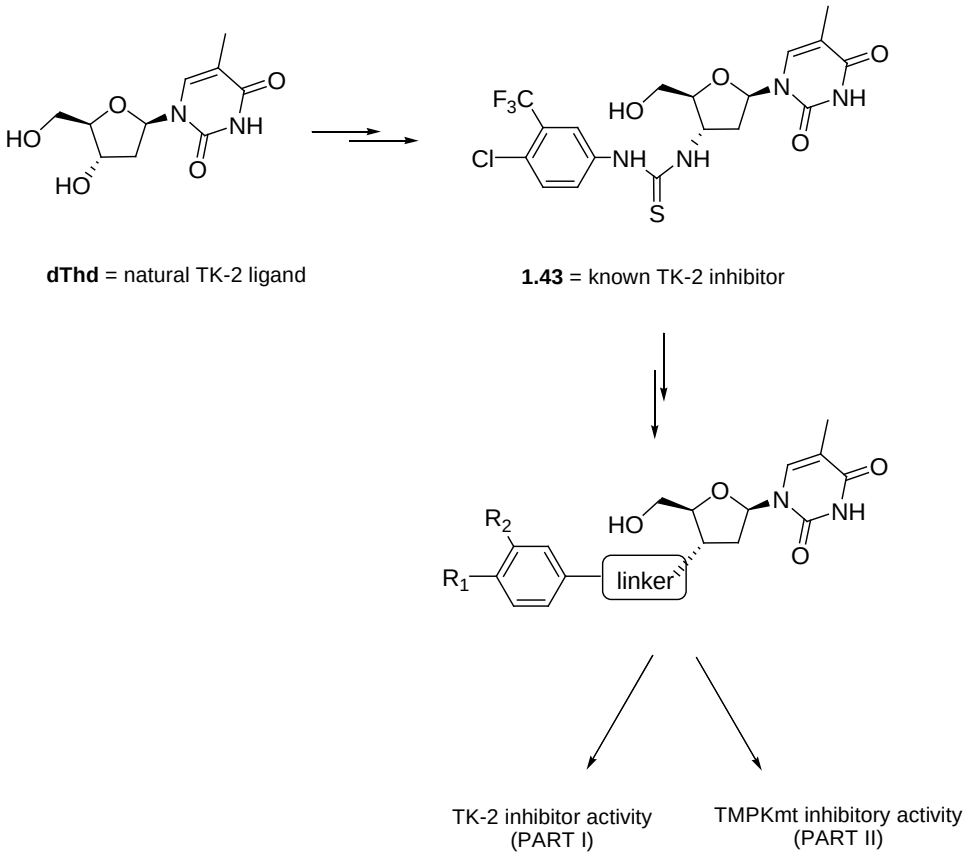

dThd = natural TK-2 ligand

1.43 = known TK-2 inhibitor

Figure II

In the third part, attempts will be made to increase the potency of a known $P2Y_2$ ligand, compound **3.7**, by introducing aromatic substituents at position 5 of the uracil base (Figure III). The same chemical modifications will be carried out in search for new nucleoside analogues possessing antiviral activity (PART IV). The only difference is that for putative $P2Y_2$ receptor ligands we will start from uridine (in analogy with the natural ligand UTP), while as possible agents acting against DNA viruses, 2'-deoxyuridine will be used as a nucleoside scaffold.

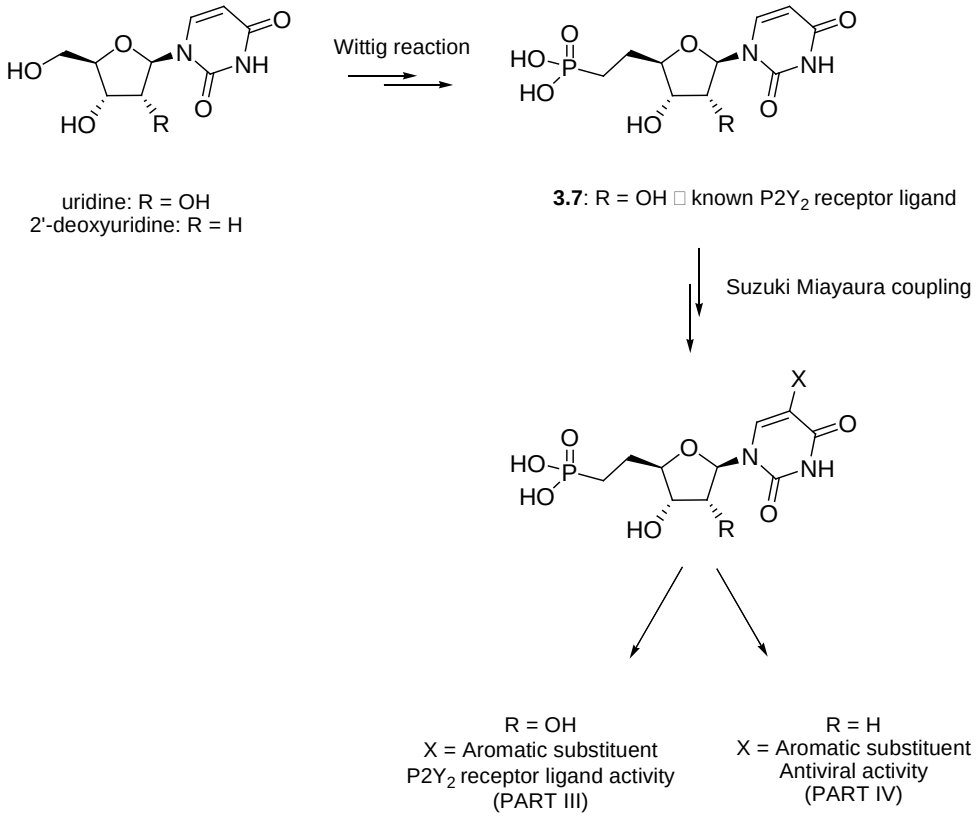

Figure III

PART I

3’-MODIFIED THYMIDINE ANALOGUES AS POTENT TK-2 INHIBITORS

1 INTRODUCTION

1.1 DEOXYRIBONUCLEOTIDES

DNA replication and repair strongly depends on a balanced pool of the four deoxyribonucleoside triphosphates (dNTPs). In most living organisms the synthesis of these essential building blocks is performed by two pathways: the *de novo* and the salvage pathway. Most organisms can synthesize purine and pyrimidine nucleotides from low-molecular-weight precursors in amounts sufficient for their needs. These so-called *de novo* pathways are essentially identical throughout the biological world. Most organisms can also synthesize nucleotides from nucleosides or bases that become available either via the diet or through enzymatic breakdown of nucleic acids. These processes are called salvage pathways, because they involve the utilization of preformed purine and pyrimidine compounds that would otherwise be lost in biodegradation (Figure I.1).[1]

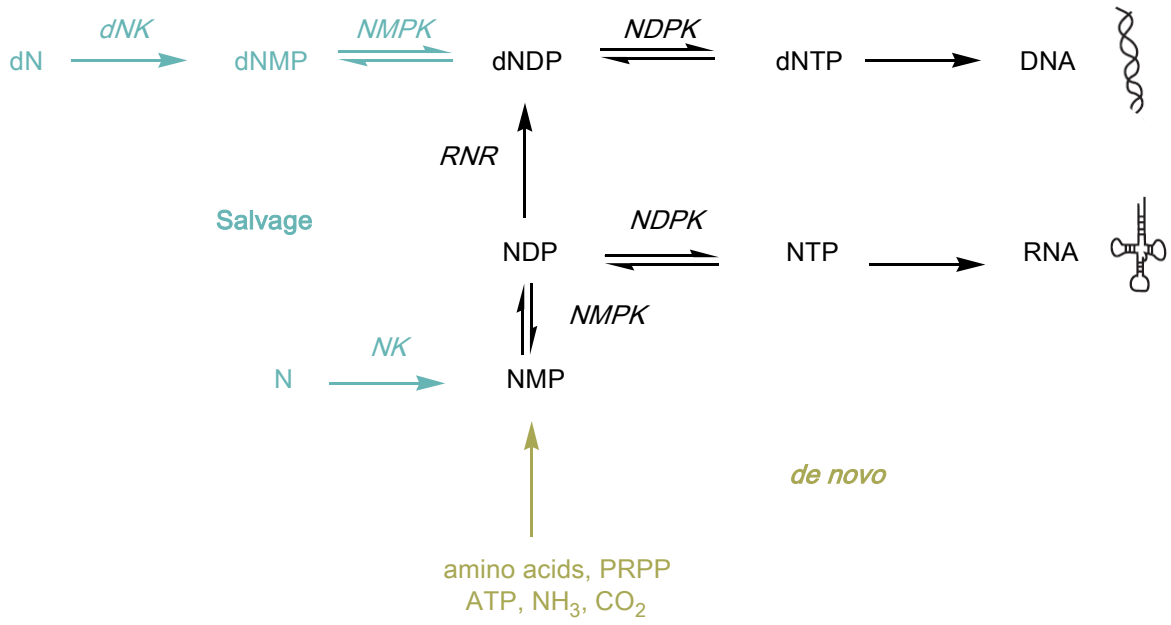

dN = deoxynucleoside, dNK = deoxynucleoside kinase, dNMP = deoxynucleoside monophosphate, NMPK = nucleoside monophosphate kinase, dNDP = deoxynucleoside diphosphate, NDPK = nucleoside diphosphate kinase, dNTP = deoxynucleoside triphosphate, DNA = deoxynucleic acid, RNR = ribonucleoside diphosphate reductase, NDP = nucleoside diphosphate, NTP = nucleoside triphosphate, RNA = ribonucleic acid, NMP = nucleoside monophosphate, NK = nucleoside kinase, N = nucleoside, PRPP = phosphoribosyl pyrophosphate, ATP = adenosine triphosphate.

Figure I.1. The *de novo* and salvage pathways of (deoxy)ribonucleotides.

1.1.1 The *de novo* Pathway

In mammalian cells the majority of the deoxyribonucleotides are synthesized by the *de novo* pathway (Figure I.1). In proliferating cells this pathway is the main provider of dNTPs needed for DNA replication.[2,3] Initially, ribonucleoside monophosphates are synthesized from low molecular weight precursors like ribose, amino acids, CO_2 and NH_3.[2] The monophosphates are then further phosphorylated to their diphosphate counterparts by nucleoside monophosphate kinases (NMPK). The regulatory step in the *de novo* synthesis of deoxyribonucleotides is the reduction of the 2'-hydroxyl group of the ribonucleoside diphosphate to the corresponding deoxyribonucleoside diphosphate. This reaction is catalyzed by ribonucleotide reductase (RNR).[2] The final step in the *de novo* pathway is the addition of the third phosphate group in a reaction catalyzed by a family of nucleoside diphosphate kinases (NDPK).

1.1.2 Salvage Pathway

A complementing and less energy demanding salvage pathway is found in quiescent or terminally differentiated cells. During the salvage pathway, extracellular (deoxy)nucleosides ((d)Ns) originating from degraded cells or nutrients are transported into the cell via non-specific nucleoside carrier proteins and undergo three successive phosphorylation steps. In the first step, deoxyribonucleoside kinases (dNKs) and ribonucleoside kinases (NKs) phosphorylate deoxyribonucleosides or ribonucleosides, respectively. Addition of negative charges in form of phosphates will trap the phosphorylated nucleosides inside the cell. The continued phosphorylation of the monophosphates to their corresponding diphosphates and triphosphates occurs in two subsequent reversible steps that are catalyzed by nucleoside monophosphate kinases and nucleoside diphosphate kinases (Figure I.1).[4]

An alternative salvage pathway synthesizes nucleoside 5'-phosphates directly from free bases. This route involves the reversible transfer of a free base to the ribose of 5-phospho-α-D-*ribo*-1-pyrophosphate (PRPP) catalyzed by a phosphoribosyl transferase.[1]

1.2 DEOXYNUCLEOSIDE KINASES

Before being built in DNA, deoxynucleosides require activation into their triphosphate form by different enzymes. As described above, deoxynucleoside kinases catalyze the first of three phosphorylation steps. Besides their role in the salvage pathway, dNKs are instruments in the activation of nucleosides that are used against cancer cells and/or viruses.[5] They catalyze the initial, and often limiting, first phosphorylation step in the conversion of the nucleoside analogues into their active form.

In mammalian cells, four cellular deoxynucleoside kinases can be found including two cytosolic enzymes, thymidine kinase 1 (TK-1) and deoxycytidine kinase (dCK), as well as two mitochondrial enzymes, thymidine kinase 2 (TK-2) and deoxyguanosine kinase (dGK). Three of the kinases (dCK, TK-2 and dGK) are evolutionary closely related and their amino acid sequences share 40% identity. Several nucleoside triphosphates can act as phosphate donors, with ATP being accepted by all dNKs. Besides their different localization, these enzymes have variable and overlapping substrate specificities as well as different patterns of expression according to the cell cycle and the nature of origin of the cell (Figure I.2).[6,7]

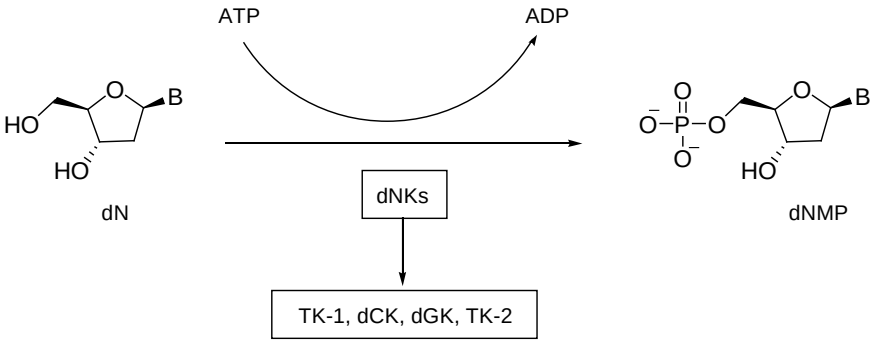

Figure I.2. Phosphorylation reaction catalyzed by deoxynucleoside kinases.[8]

In addition, the fruit fly *Drosophila melanogaster* contains only one single deoxyribonucleoside kinase (*Dm*-dNK) that was cloned by two independent groups in the late 1990s.[7,9] Johansson *et al.* showed that *Dm*-dNK is closely related to the human deoxyribonucleoside kinase family, in particular with TK-2. However, in contrast to human enzymes, *Dm*-dNK is a multisubstrate nucleoside kinase. It phosphorylates all the natural nucleosides as well as several anticancer and antiviral nucleoside analogs, although pyrimidine nucleosides are the preferred substrate.[9] The catalytic rate of deoxyribonucleoside phosphorylation of *Dm*-dNK depends on the substrate, but is generally 10 to 100-fold higher than that of mammalian enzymes.[10]

1.3 THYMIDINE KINASES (TK-2 vs. TK-1)

1.3.1 Localization and Expression

In mammals there are two enzymes able to phosphorylate thymidine: a cytosolic (TK-1) and a mitochondrial (TK-2) enzyme. TK-1, which was cloned in 1983, is expressed only in S-phase cells,[11] while TK-2 is expressed in most tissues throughout the whole cell cycle with the highest expression in liver, pancreas, muscles and brain.[12][13,14] In many resting cells, such as nerve and muscle cells, TK-2 is the only pyrimidine deoxynucleoside phosphorylating enzyme expressed. In these tissues, where *de novo* synthesis of DNA precursors is undetectable,[12] TK-2 is likely to be responsible for the supply of deoxyribonucleotides required for mitochondrial DNA synthesis. The physiological role of TK-2 is not well defined but in cells with no TK-1 activity, TK-2-mediated phosphorylation of thymidine leads to a product that finally gets into mitochondrial DNA.[15]

1.3.2 Substrate Specificities

1.3.2.1 Thymidine Kinase 2

Human TK-2 utilizes thymidine (dThd, **1.1**), 2'-deoxycytidine (dCyd, **1.2**) and 2'-deoxyuridine (dUrd, **1.3**) as substrates but with different efficiency and kinetic mechanisms. dThd is the preferred substrate while ATP (**1.4**) and CTP (**1.5**) can be used as phosphate donors (Figure I.3).[16]

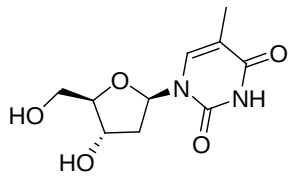

1.1

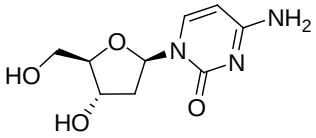

1.2

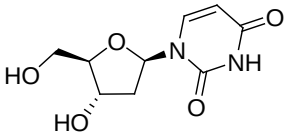

1.3

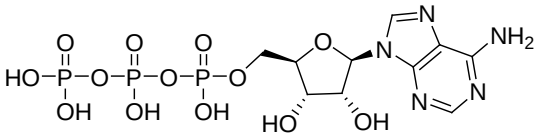

1.4

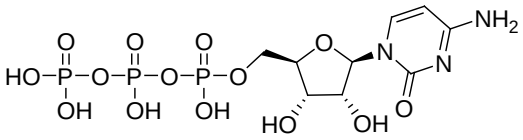

1.5

Figure I.3

Concerning nucleoside analogues used as antivirals, the anti-HIV drug 3'-azido-3'-deoxythymidine (AZT, zidovudine, **1.6**) is a poor substrate for TK-2, although its level of phosphorylation is significant in non-dividing tissues.[8] Other drugs that are well phosphorylated by TK-2 include the antiherpetic drugs 1-(β-D-arabinofuranosyl)thymine (Ara-T, **1.8**), (*E*)-5-(2-bromovinyl)-2'-deoxyuridine (BVDU, **1.10**) and its arabinosyl counterpart 1-β-D-arabinofuranosyl-(*E*)-5-(2-bromovinyl)uracil (BVaraU, **1.11**). Another compound that is effectively recognized by TK-2 is 1-(2-deoxy-2-fluoro-β-D-arabinofuranosyl)-5-iodouracil (FIAU, **1.12**), a potent anti-hepatitis B nucleoside analogue (Figure I.4).[6,16,17,18]

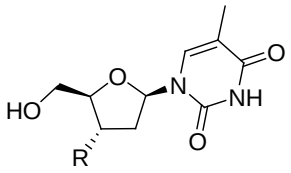

1.6: R = N_3
1.7: R = F

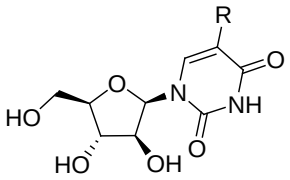

1.8: R = CH_3
1.9: R = H

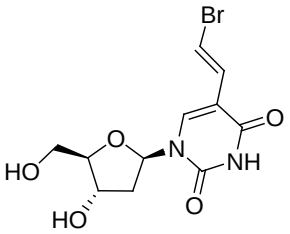

1.10

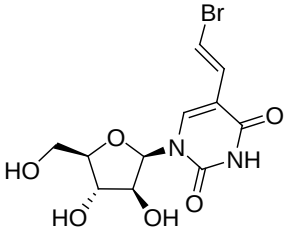

1.11

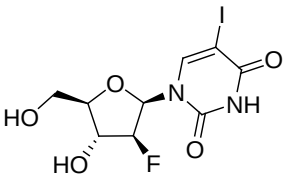

1.12

Figure I.4

In addition, 3'-deoxy-3'-fluoro-β-D-thymidine (**1.7**) and ribothymidine (**1.13**) are phosphorylated as well, but with relatively low efficiency. Other substrates are 1-β-D-arabinofuranosyluracil (Ara-U, **1.9**), 2'-deoxy-2',2'-difluorouridine (dFdU, **1.14**) and a few 5-substituted dUrd analogues (e.g., halogen, amino or ethyl).[6,16,17] 2'-Deoxycytidine analogs with a 5-modification, such as 5-(2-chloroethyl) (**1.15**) and 5-(2-bromovinyl) (**1.16**), showed activity with TK-2, and modifications of the sugar moiety, such as gemcitabine (dFdC, **1.17**) and 1-β-D-arabinofuranosylcytosine (Ara-C, **1.18**), are also accepted but with low efficiency (Figure I.5).[6]

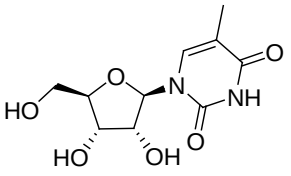

1.13

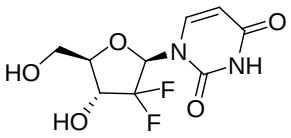

1.14

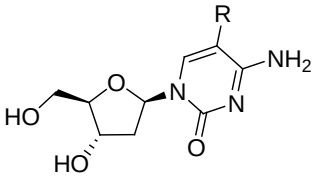

1.15: R = 2-chloroethyl
1.16: R = 2-bromovinyl

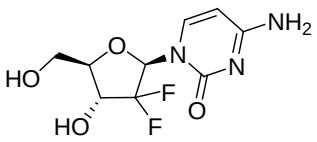

1.17

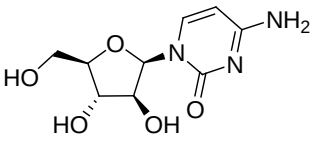

1.18

Figure I.5

1.3.2.2 Thymidine Kinase 1

The substrate specificity of TK-1 is mainly restricted to thymidine (**1.1**) and deoxyuridine (**1.3**), but some modifications are allowed at the 5 position of the pyrimidine ring and the 3' position of the deoxyribose.[19] ATP (**1.4**) and dATP (**1.19**) are the preferred phosphate donors (Figure I.6).

Several 5-substituted dUrd analogs are accepted by TK-1, e.g., 5-fluoro, 5-chloro, 5- iodo, 5-bromo and 5-ethyl dUrd, while bulkier substitutions, such as 5-propenyl, 5-(2-chloroethyl) and 5-(2-bromovinyl), are not recognized as substrates.[20] A number of large substitutions at the N3 position, e.g., *o*-carboranylalkyl dThd, have been shown to be good substrates for TK-1.[21]

Examples of clinically important 3'-modified nucleoside analogues phosphorylated by TK-1 are the anti-HIV agents AZT (**1.6**), 3'-deoxythymidine (ddT, **1.20**), 3'-deoxy-3'-fluoro-β-D-thymidine (**1.7**) and 2',3'-didehydro-3'-deoxythymidine (d4T, **1.21**) (Figure I.6).[22,23]

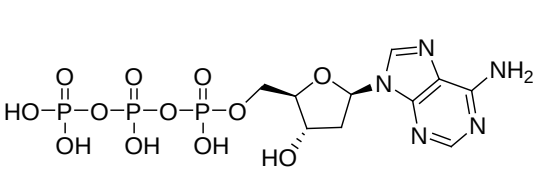

1.19

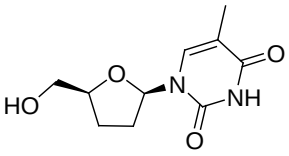

1.20

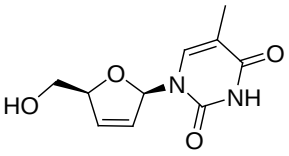

1.21

Figure I.6

1.3.3 Structure

1.3.3.1 Thymidine Kinase 2

Human thymidine kinase 2 was cloned in the 1990s by two independent research groups.[8] It is a dimer of 58 kDa compromising a mitochondrial targeting signal. On the basis of its amino acid sequence, TK-2 belongs to a large group of dNKs that includes other human enzymes such as deoxycytidine kinase and deoxyguanosine kinase, together with other dNKs of different origins, such as the multisubstrate dNK of the fruitfly, *Drosophila melanogaster*, and to a lesser extent, the thymidine kinase of herpes simplex virus type 1 (HSV-1 TK).[6] The amino acid sequence identity between human TK-2 and *Dm*-dNK is about 40% and there are no long insertions or deletions in their genes.

There are no crystal structures reported for TK-2. Therefore, efforts have been made to build a reliable model of the enzyme. Because of its high sequence identity with TK-2, *Dm*-dNK has been used as a template to construct a homology model of TK-2 (Figure I.7).[6,24,25,26]

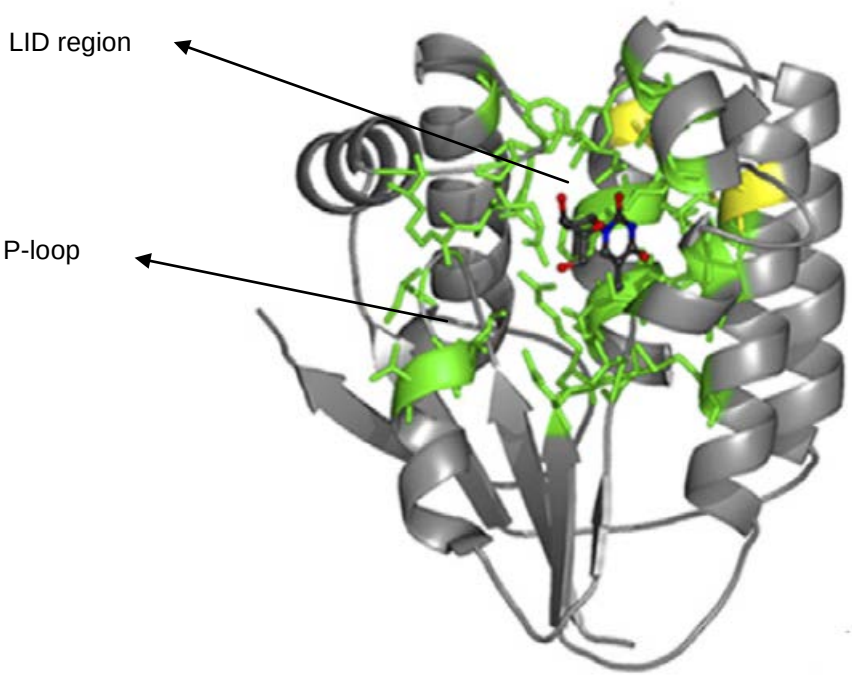

Figure I.7. Homology model of TK-2 monomeric subunit. Active-site residues are shown as sticks and colored green.[26]

Two amino acid sequence motifs that are common to several nucleotide kinases of the same family are present in TK-2:

- a conserved -GXXGXGKS/TT- sequence that corresponds to a glycine-rich loop found among ATP/GTP binding proteins. This motif forms a turn without hydrogen bonds, also known as the P-loop, which accommodates the γ-phosphate of ATP,

- an arginine rich region that function as a LID for the active site cleft. The consensus sequence -RXXXRXRXXE- forms a turn with several hydrogen bonds.

1.3.3.2 Thymidine Kinase 1

Thymidine kinase 1 is a tetramer of ~100 kDa.[27,28] It only shares significant sequence similarity with other deoxyribonucleoside kinases at the N-terminus within the P-loop, which binds the phosphate donor. The recently determined structure reveals that tetrameric TK-1 has a completely different overall monomer structure than other dNKs (Figure. I.8).

Figure I.8. Overall monomer structure of human TK-1 with dTTP.[29]

1.3.4 Mechanism of Action

The generally accepted mechanism for the phosphorylation reaction catalyzed by dNK is depicted in figure I.9. Activation of the 5'-OH of the deoxyribose is required in order to make a nucleophilic attack on the γ-phosphate of the phosphate donor. The Glu carboxylate close to the 5'-OH in the active site was suggested to act as a base in this deprotonation reaction. The transition state may be stabilized by a Mg^{2+}-ion and arginines and lysines that commonly occur at the catalytic sites of dNKs.[30,31,32]

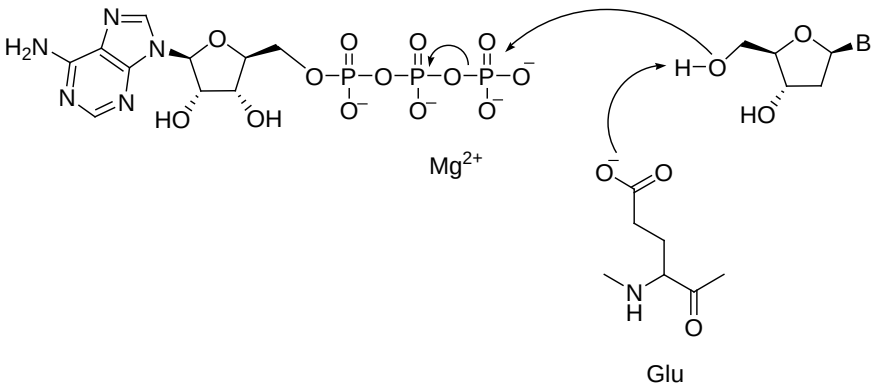

Figure I.9. General reaction mechanism for phosphate transfer as catalyzed by dNKs. Because of its high abundance ATP is considered as the preferred biological phosphate donor.[6]

1.4 THE ROLE OF TK-2

1.4.1 mtDNA Synthesis

The synthesis of DNA requires a supply of deoxyribonucleotides. In eukaryotic cells the bulk of DNA is located in the nucleus and is replicated once during the S phase. Terminally differentiated cells or resting cells in culture only rarely or never replicate DNA and their *de novo* synthesis of dNTPs is shut down. In addition to nuclear DNA, eukaryotic cells also contain mitochondrial DNA (mtDNA) that represents ~ 5% of the total cellular DNA.[33] mtDNA replication occurs during all phases of the cell cycle, even in postmitotic cells in which nuclear DNA synthesis has ceased. The measured half-life of mtDNA in mammalian cells is 10-30 days.[34] Without the ongoing process of mitochondrial DNA replication, mtDNA depletion occurs rapidly, eventually disrupting the production of ATP and causing failure of cell function.

A mitochondrion is surrounded by a double membrane defining two separate compartments within the organelle: the intermembrane space between the outer and inner membranes and the matrix space within the inner membrane. The mtDNA molecules are located within the matrix space. The outer membrane is highly porous to all nucleosides and nucleotides. Therefore, it is considered that the intermembrane space is in equilibrium with the cell cytoplasm. The mitochondrial inner membrane is highly impermeable to solutes, but it contains specific transporters to provide the precursors needed for mtDNA synthesis (Figure I.10). The inner membrane contains at least two proteins that transport DNA precursors into the mitochondrial matrix: the deoxynucleotide carrier (DNC) and an equilibrative nucleoside transporter (ENT). ENT carries nucleosides where DNC transports deoxynucleoside diphosphates into the mitochondrial matrix in exchange for ADP or ATP.[35] The DNC also transports deoxynucleoside triphosphates, but less efficiently than dNDPs.[36]

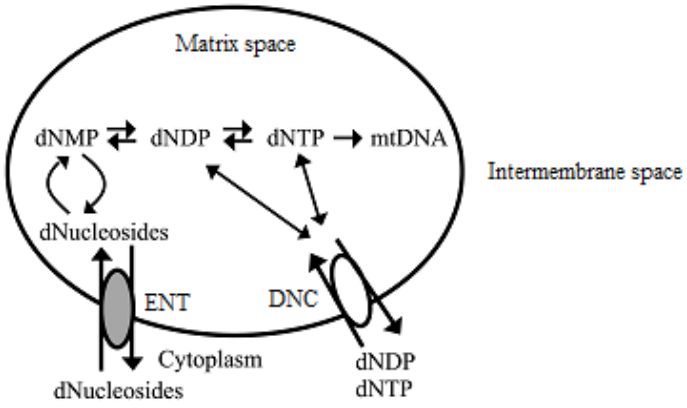

Figure I.10. General deoxynucleotide metabolism in a mitochondrion.[36]

So, the mitochondrial deoxynucleotide metabolism is connected to cytoplasmic deoxynucleotide metabolism at both ends of the phosphorylation process: at the deoxynucleoside level (via ENT) and at the diphosphate and triphosphate levels (via DNC).

Once transported into the mitochondrial matrix space, deoxynucleosides must be phosphorylated to the triphosphate form to be incorporated into mtDNA. Two irreversible enzymes, deoxyguanosine kinase for purines and TK-2 for pyrimidines, catalyze the first phosphorylation step.[6] In addition, mitochondrial nucleotidase enzymes remove the phosphate group form dNMP molecules. Separate reversible nucleoside monophosphate kinases for dAMP, dCMP, dGMP and dTMP are believed to exist to catalyze the second phosphorylation step. The final phosphorylation uses the reversible nucleoside diphosphate kinase enzymes for all dNDP.

After phosphorylation, dNTPs will be incorporated into a growing mtDNA strand. Synthesis of mtDNA is catalyzed by DNA polymerase γ. The action of Pol-γ occurs in two stages. The polymerase inserts a nucleotide into the growing mtDNA strand followed by proofreading in which incorrect nucleotides can be excised by the exonuclease domain of Pol-γ. This exonuclease activity is important to ensure the fidelity of mtDNA replication.[36,37]

1.4.2 TK-2 Deficiency

1.4.2.1 General

In healthy tissues, mitochondria contain two separate potential pathways to provide thymidine triphosphate for mtDNA replication: (1) deoxynucleotide transporters in the membrane introduce dTDP and dTTP from the cytosol and (2) equilibrative nucleoside transporters bring thymidine into the matrix. Phosphorylation of thymidine using TK-2 will provide dTMP which is further phosphorylated to dTTP using NMPK and NDPK (Figure I.11).[38,39]

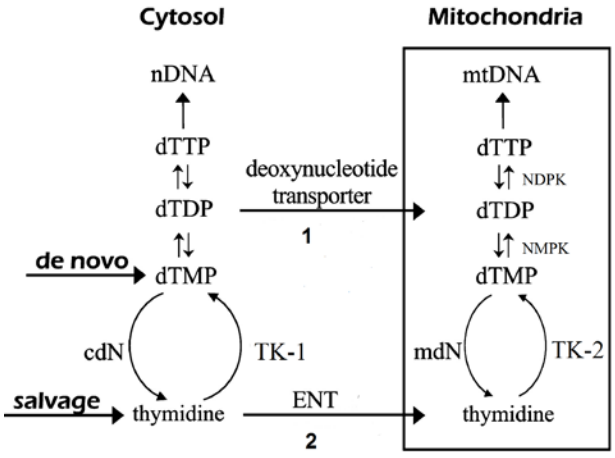

Figure I.11. Two pathways for dTTP: 1) import of nucleotides synthesized in the cytosol; 2) import of thymidine followed by intra-mitochondrial phosphorylation. cdN = cytosolic 5'-deoxyribonucleotidase, mdN = mitochondrial 5'-deoxyribonucleotidase.

Depending on the cell type and the cell cycle phase, one or both pathways will occur. In replicating cells both processes exist and as a result, a dysfunction of TK-2 will not necessarily cause a lot of damage because mitochondria can use cytosolic dTDP/dTTP for the synthesis of mtDNA.

In non-replicating cells, cytosolic dNTP synthesis is down regulated, and substrates for mtDNA synthesis should normally derive from the mitochondrial salvage pathway in which TK-2 plays an important role (pathway 2). In this case, TK-2 defiency will lead to a decreased level of mtDNA causing fatal myopathy due to impaired respiratory chain function.

1.4.2.2 Mitochondrial Depletion Syndrome (MDS)

Mitochondrial DNA depletion syndrome is a devastating disorder that was first described in 1991.[40] Unlike other mitochondrial diseases, MDS is characterized by a quantitative, rather than qualitative, defect of mtDNA. Affected tissues have a markedly reduced number of mtDNA copies which impairs the synthesis of respiratory chain components. MDS can be tissue-specific or multisystemic,[41] and is inherent as an autosomal recessive trait. In late 2001, mutations in 2 nuclear genes were identified in patients with MDS: changes in the deoxyguanosine kinase gene were identified in patients with the hepatocerebral form,[42] and changes in the thymidine kinase 2 gene were associated with the myopathic form.[43]

Patients with the myopathic form of MDS usually suffer from progressive weakness, hypotonia and areflexia soon after birth and die before 10 years of age as a result of decreased mtDNA levels. In tissues of patients with TK-2 mutations, the combined activities of the cytoplasmic TK-1 and dCK could normally compensate for the loss of TK-2. However, TK-1 is down regulated in non-replicative tissues and dCK has been reported to be low in liver and brain, rendering these tissues to the deleterious effect of TK-2 deficiency.[44]

Intact mitochondrial DNA is required for the production of the key catalytic subunits for the mitochondrial respiratory chain complexes and therefore is essential for oxidative ATP-production. The energy metabolism during fetal life relies heavily on glycolysis, and even the severest functional defects of mitochondria typically manifest only after birth. The decrease in mtDNA inhibits the synthesis of adequate proteins that are essential for oxidative phosphorylation (OXPHOS). A disruption of OXPHOS leads to energy (ATP) loss and an increase in electron leakage from the electron-transport chain, which increases the production of reactive oxygen species. This increase damages proteins, lipids and mtDNA, setting off a cascade of further oxidative damage.[45,46]

1.4.2.3 AZT Toxicity

mtDNA depletion may also occur as a secondary, iatrogenic phenomenon. For example, antiretroviral therapy with nucleoside analogues can affect the mtDNA synthesis, since these analogues may serve as a substrate for the host polymerases. This kind of mtDNA depletion, however, is transient and mtDNA levels recover to normal level upon termination of the treatment.[45]

AZT (**1.6**) was the first nucleoside analogue approved to combat HIV, and continues to be a major component of HAART (highly active antiretroviral therapy), the currently accepted treatment for HIV infection.[47] AZT is an analogue of the natural nucleoside thymidine, whereby the 3'-OH has been replaced by an azido group. AZT typically interacts with the same enzymes as dThd and follows the same metabolic pathways in the cell although with radically altered kinetic parameters. AZT itself is a prodrug. The pharmaceutically active form is the triphosphate, AZTTP. This can interact with DNA polymerases and can be incorporated into a replicating DNA strand in the place of thymidine triphosphate. The azido group prevents further replication of the DNA molecule, causing chain termination. The use of AZT and other nucleoside analogues does not completely destroy HIV, so life-long HAART is mandated.[37]

Specific tissue toxicities are associated with the prolonged use of AZT and other nucleoside analogues. Symptoms of AZT toxicity often include mitochondrial myopathy and cardiomyopathy with mtDNA depletion in patients, but other symptoms may occur. AZT also causes increased oxidative stress that may lead to mtDNA mutations. The exact mechanism by which AZT causes toxicity is not known.[47]

It has been proposed that the AZT-related toxicities are the consequence of mitochondrial damage due to mitochondrial DNA depletion. Different mechanisms of AZT-related mitochondrial damage may be involved.[48] The initial hypothesis postulated that the inhibition of DNA polymerase γ by AZT-triphosphate leads to depletion of mtDNA and consequently to depletion of mitochondrial RNA and polypeptides involved in oxidative phosphorylation ('DNA pol-γ hypothesis').[46,48] However, recently, some investigators disagree with this explanation, since they believe that the concentration of AZTTP required for efficiently inhibiting DNA polymerase γ is very difficult to achieve under physiological conditions.[49,50] Therefore, it was proposed that the mechanism underlying mitochondrial toxicity may instead be related to the inhibition exerted by AZT on thymidine phosphorylation by TK-2. In non-mitotic tissues like heart and liver, TK-2 is virtually the only enzyme able to phosphorylate thymidine. Studies performed in isolated heart and liver mitochondria have indeed shown that AZT exerts a competitive inhibition of thymidine phosphorylation by TK-2. Since TK-2 is the only TK enzyme in these organs and thymidine phosphorylation is competitively inhibited in the presence of AZT, dTTP pools are depleted resulting in a decrease of mtDNA. This mechanism of toxicity also provides a possible solution to overcoming AZT toxicity, namely by raising thymidine levels in the AZT-treated patient through exogenous dThd administration.[50]

1.5 TK-2 INHIBITORS

1.5.1 Role of TK-2 Inhibitors

From the above described features, it should be clear that TK-2 is implicated in the phosphorylation of pyrimidine nucleosides needed for mtDNA synthesis and could also be involved in the mitochondrial toxicity associated to antiviral nucleoside analogues. However, there are still many open questions related to the real contribution of TK-2 to these issues. Potent and selective TK-2 inhibitors could be valuable tools to unravel the role of TK-2 in mitochondrial dNTP pools and homeostasis, and may help to clarify the contribution of TK-2 catalyzed phosphorylation of antiviral drugs to the mitochondrial toxicity of these agents. Such inhibitors could also be helpful to investigate the activity of TK-1 and TK-2 in different cell types.[51]

On the other hand, potent and selective TK-2 inhibitors may become of potential practical use when added at subtoxic concentrations (that partially suppress TK-2 activity) in combination with antiviral and anticancer agents that display toxic side effects consequent to their activation by TK-2 in the mitochondrial environment.[52]

1.5.2 Structure of TK-2 Inhibitors

1.5.2.1 Ara-, Ribo- and 2'-Deoxyribonucleoside Analogues

In 1999, several nucleoside analogues modified at the sugar moiety, including *O*-alkyl analogues were tested as substrates or inhibitors of TK-1 and TK-2.[53] It was found that 3'-*O*-methyl- and 3'-*O*-ethyl-2'-deoxyuridine (**1.22** and **1.23**) were between 20 and 100-fold more inhibitory to TK-2 than to TK-1, with K_i values of 15 and 10 µM, respectively. Even more pronounced was the inhibitory effect of 3'-hexanoylamino-3'-deoxythymidine (**1.24**), with a more than 1000-fold higher affinity for TK-2 and a K_i value of 0.15 µM (Figure I.12).

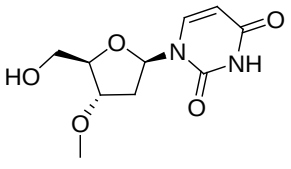

1.22

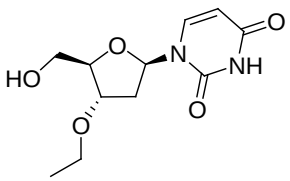

1.23

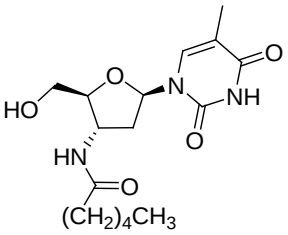

1.24

Figure I.12

In 2000, several ribofuranosyl nucleosides were examined for TK-2 inhibition.[52] In contrast to BVDU (**1.10**), which is an excellent substrate for TK-2, its ribo analogue (5-(*E*)-(2-bromovinyl)uridine, **1.25**) was found to be an inhibitor of thymidine phosphorylation. Also, the 3'-spironucleoside **1.26** inhibited dThd phosphorylation by TK-2 with an IC_{50} of 4.6 µM (Figure I.13). Despite the presence of a free 5'-OH, no phosphoryl transfer from [γ-^{32}P]ATP to the 5'-position of these ribonucleosides was observed, confirming a direct inhibitory activity rather than an alternative substrate behavior of these compounds.

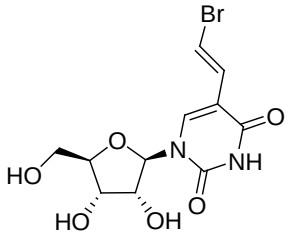

1.25

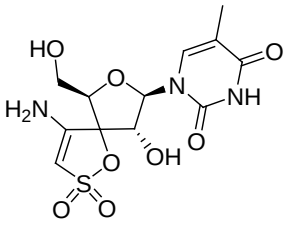

1.26

Figure I.13

Arabinofuranosyl nucleosides have also been explored as TK-2 inhibitors. In 2001 Manfredini *et al*.[54] communicated the first compounds within this series, and a full report on these derivatives has recently been published.[55] While Ara-T (**1.8**) is a good substrate for TK-2, introduction of a long chain acyl substituent (i.e., the decanoyl and dodecanoyl esters **1.27** and **1.28)** at the 2'-OH shifted the nucleosides from substrates to inhibitors. By shortening the 2'-*O*-acyl chain to a pentanoyl moiety, or by replacing the acyl chain by an alkyl moiety, an important decrease in the inhibitory activity was observed.[54,55] A similar approach has been applied to BVAraU (**1.11**) derivatives **1.29-1.30** (Figure I.14).

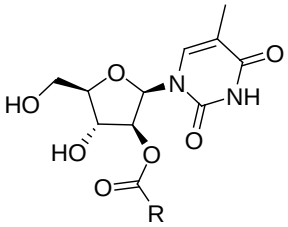

1.27: R = $(CH_2)_8CH_3$
1.28: R = $(CH_2)_{10}CH_3$

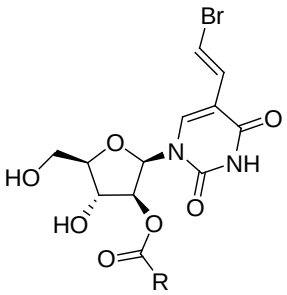

1.29: R = $(CH_2)_6CH_3$
1.30: R = $(CH_2)_8CH_3$

Figure I.14

Interestingly, the above described 2'-*O*-acylderivatives are highly selective in inhibiting TK-2 catalyzed dThd-phosphorylation, while no inhibitory effect was detected against HSV-1 TK or *Dm*-dNK.

1.5.2.2 Acyclic Nucleoside Analogues

This line of research started with the observation that 5'-*O*-(4,4'-dimethoxytrityl)thymidine (**1.31**) showed inhibitory activity against HSV-1 TK-catalyzed dThd phosphorylation (IC_{50} = 14 μM), while inhibition of TK-2 could only be achieved at a higher concentration (IC_{50} = 468 μM). Replacement of the acid labile dimethoxytrityl group by the more stable trityl analogue resulted in 5'-*O*-Tr-thymidine (**1.32**) (Figure I.15) that was a markedly more potent inhibitor against both enzymes, particularly against TK-2 (IC_{50} = 33 μM). In both compounds, the presence of the dimethoxytrityl group at the 5'-position of thymidine converted the thymidine substrate into an inhibitor since both compounds lack a free available 5'-OH group susceptible of being phosphorylated by TK-2.[56]

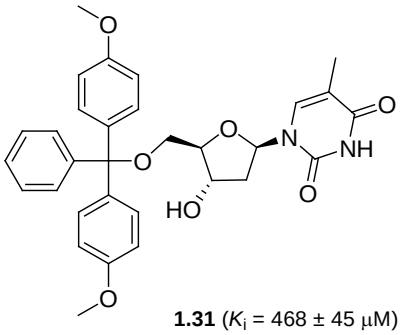

1.31 (K_i = 468 ± 45 μM)

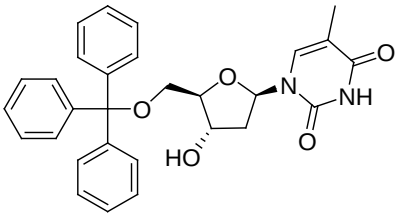

1.32 (K_i = 33 ± 20 μM)

Figure I.15

On the basis of this observation, it was hypothesized that the role of the 2'-deoxyribose moiety in compounds **1.31** and **1.32** was to locate the thymine base and the trityl substituents in the right way to interact with the enzyme, which encouraged Pérez-Pérez *et al.* to replace the sugar moiety by acyclic spacers.[56] These modifications were further accompanied by replacement of the thymine base by structurally related analogues and by exploration of the distal site with lipophilic groups different from the trityl present in the lead compounds **1.31** and **1.32**.[8]

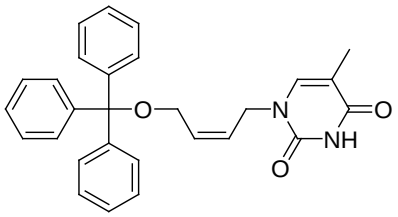

1.33 (K_i = 1.5 ± 0.2 μM)

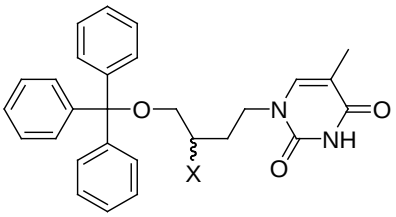

1.34: X = H (K_i = 3.3 ± 1.2 μM)
1.35: X = OH (K_i = 3.6 ± 0.4 μM)

Figure I.16

Replacement of the 2'-deoxyribose moiety of 5'-*O*-trityl-β-D-thymidine (**1.32**) by a (*Z*)-butenyl spacer, as in compound **1.33**, allowed a significant increase in the inhibitory activity against TK-2.[56] However other spacers like (*E*)-butenyl or butynyl led to considerably less active molecules against TK-2.

Compounds with a four-member spacer but with increased conformational freedom as in **1.34** or **1.35**, also showed potent TK-2 inhibition but were less selective vs. HSV-1 TK and *Dm*-dNK (Figure I.16). Therefore, the (*Z*)-butenyl spacer was kept present in most of the synthesized structures.[51]

It was observed that, concerning the base part, the thymine base can be replaced by structurally related analogues like 5-iodouracil (**1.36**) without compromising the inhibitory activity. Interestingly, the 5-(*E*)-(2-bromovinyl)uracil derivative (**1.37**) was equipotent with the thymine analogue against TK-2, but showed no inhibition of TK-1, HSV-1 TK or *Dm*-dNK, therefore becoming the most selective compound against TK-2 in this series (Figure I.17).[57]

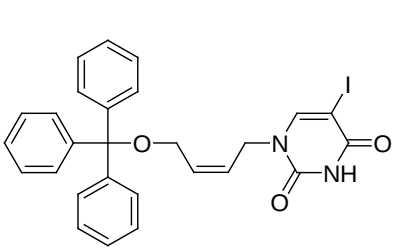

1.36 (K_i = 4.6 ± 0.4 μM)

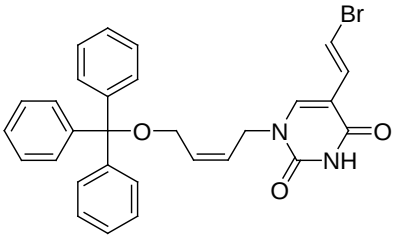

1.37 (K_i = 1.3 ± 1.1 μM)

Figure I.17

When considering the distal substituent, alternatives to the trityl group have been explored including acyl groups, amines and carboxamides. The most potent molecules are presented in Figure I.18. Compound **1.41** emerged as the most potent TK-2 inhibitor in a series of thymine derived carboxamides with cyano and/or phenyl groups at the distal site.[58]

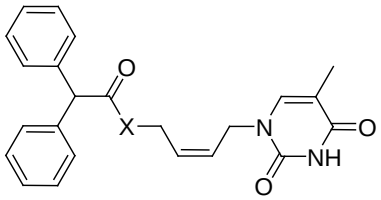

1.38: X = O (K_i = 4.6 ± 0.5 μM)
1.39: X = NH (K_i = 27 ± 1 μM)

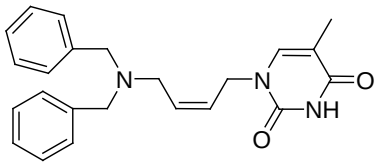

1.40 (K_i = 3.5 ± 0.5 μM)

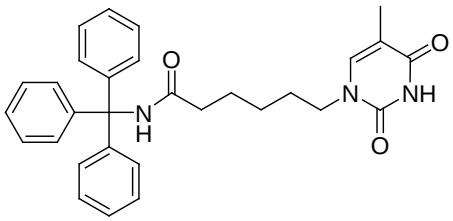

1.41 (K_i = 19 ± 2 μM)

Figure I.18

In a last series of acyclic TK-2 inhibitors the thymine base is kept intact to allow interaction with the substrate binding site and connected to an *O*-trityl moiety via more flexible spacers of different lengths (e.g., -$(CH_2)_3$-, -$(CH_2)_5$-, -$(CH_2)_6$-, -$(CH_2)_7$-, -$(CH_2)_8$-, -$(CH_2)_3$-O-$(CH_2)_3$-). These modifications have been combined with the incorporation of small substituents at position 4 of one of the phenyl rings of the trityl moiety as depicted in Figure I.19. It is interesting to note the strong relationship between the length of the spacer and the inhibitory activity against TK-2. Derivatives with short linkers afford TK-2 inhibition at an IC_{50} around 45 μM, while those with intermediate length linkers afforded at least 10-fold better inhibitory values. The hexamethylene linker gave the highest inhibitory potency against TK-2 with an IC_{50} of 0.50 μM. By replacement of one of the phenyl rings of the trityl by other aryl moieties, it is interesting to note that the 4-pyridyl derivatives keep similar activity as the parent trityl.[24]

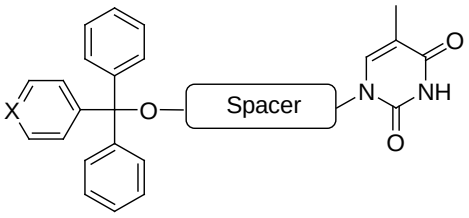

1.42

Figure I.19

2 SYNTHESIS AND BIOLOGICAL EVALUATION OF 3'-TRIAZOLE-SUBSTITUTED THYMIDINE AND BVDU DERIVATIVES

2.1 OBJECTIVES

Two series of thymidine analogues that were originally designed as TMPKmt inhibitors, were evaluated for their inhibitory activity against a panel of other nucleoside kinases (TK-1, TK-2, herpes simples virus 1 and varicella zoster virus (VZV) TK). Several substituted 3'-thiourea derivatives of β-dThd proved highly inhibitory to and selective for human mitochondrial TK-2 compared to related kinases. Compound **1.43** (Figure I.20), which emerged as the most potent analogue of this series, inhibited TK-2 at concentrations 2100-fold lower than those required to inhibit cytosolic TK-1 (IC_{50} for TK-1 = 316 μM; IC_{50} for TK-2 = 0.15 μM).[59]

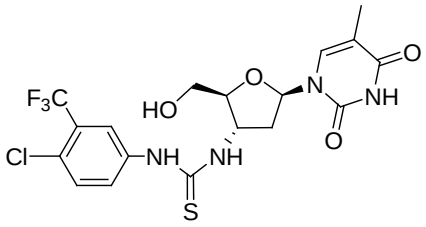

1.43

Figure I.20

Kinetic experiments indicated that this inhibitor specifically binds to the enzyme-ATP complex, and in consonance with this finding, molecular modeling studies suggested that the nitrogen atoms of the thiourea group of **1.43** could interact favorably with the oxygens of the γ-phosphate of the cosubstrate ATP. As it was demonstrated that the 3'-substituent of **1.43** and related analogues was responsible for extra interactions with TK-2 (after binding of the ATP phosphoryl donor), we decided to investigate if the thiourea moiety, earlier described as the perpetrator of toxicity,[60] could be replaced by alternative linkages to connect the C-3' atom of the deoxyribose moiety to several substituents.

In this chapter, we explore thymidine analogues containing a triazole ring instead of the thiourea moiety. Because of its synthetic convenience and the accessibility of AZT as the azide precursor, we decided to apply "click chemistry" reactions to synthesize a series of 3'-(1,2,3-triazol-1-yl) analogues of dThd. It should be noted that, in search for new antivirals resembling AZT, Wigerinck *et al*. already reported 3'-triazole thymidine analogues in 1989.[61] However, at that time, these were obtained by

classical (thermal) Huisgen reaction conditions[62] (i.e., in the absence of a Cu^{+} catalyst), which generally resulted in mixtures of the 1,4- and the 1,5-regioisomers that are not always easy to separate by classical chromatographic procedures.

As a further extension of this study, we also wanted to explore the effect of analogues that combined a favorable 3'-(4-substituted-1,2,3-triazole) moiety with a (*E*)-5-(2-bromovinyl)-substituent, known as a privileged scaffold for TK-2 binding (cf. infra).

2.2 CHEMISTRY

2.2.1 Synthesis of 3'-Triazole-Substituted Thymidine Analogues

The synthesis of 3'-triazole-substituted thymidine analogues is based on the Huisgen [3+2] cycloaddition of an organic azide and a terminal alkyne.[63,64] Although AZT (**1.6**), acting as azide precursor, is commercially available, it can be synthesized quite easily and in a minimum of steps starting form β-D-thymidine (**1.1**). We adapted Glinski's synthetic procedure[65] which started with the protection of 5'-OH followed by mesylation of the 3' hydroxyl group as depicted in Scheme I.1. Treatment of the 5'-tritylated derivative of 3'-*O*-mesyl-thymidine (**1.45**) with DBU and opening of the anhydro derivative **1.46** with NaN_3 in DMF afforded azidonucleoside **1.47**, which was deprotected under acidic conditions.[66]

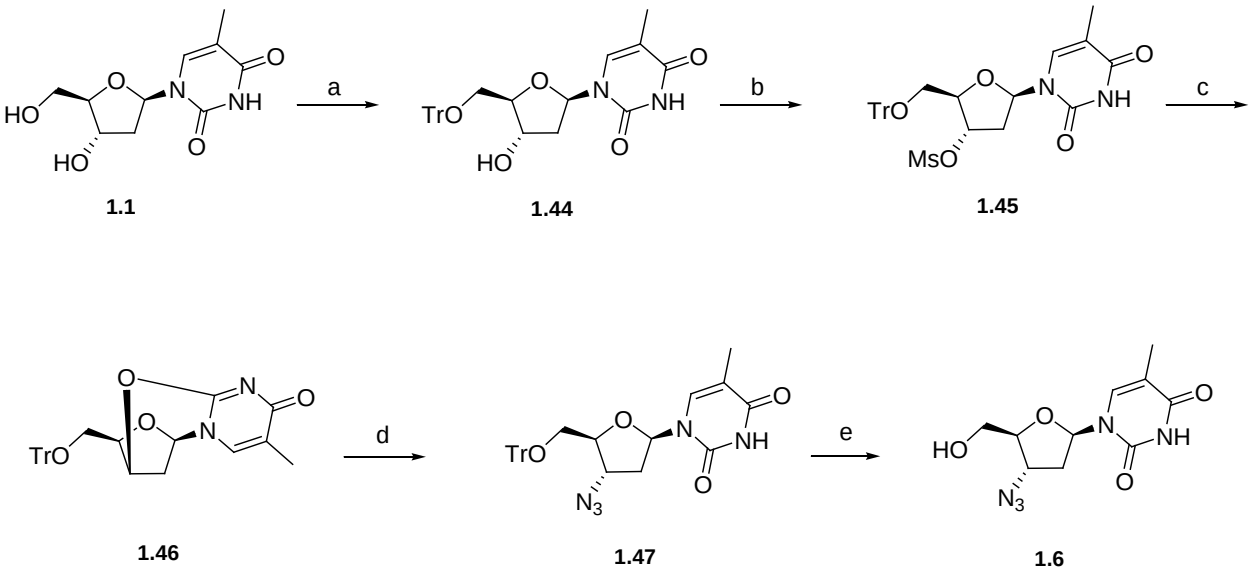

Scheme I.1. Reagents and conditions: (a) trityl chloride, pyridine, 65 °C, overnight, 100%; (b) MsCl, pyridine, 0 °C, 3 h; (c) DBU, CH_3CN, reflux, overnight, 88% over 2 steps; (d) NaN_3, DMF, reflux, overnight, 87%; (e) CH_3COOH 80%, 90 °C, 25 min, 62%.

AZT (**1.6**) was converted into the 1,4-disubstituted 1,2,3-triazoles **1.48-1.55** using different alkynes in the presence of copper(II) sulfate and sodium ascorbate.[67] The isomeric 1,5-disubstituted 1,2,3-triazoles **1.56** and **1.57** were obtained in moderate yield upon reaction of AZT with the appropriate alkynes in the presence of $[Cp^*RuCl(PPh_3)_2]$.[68]

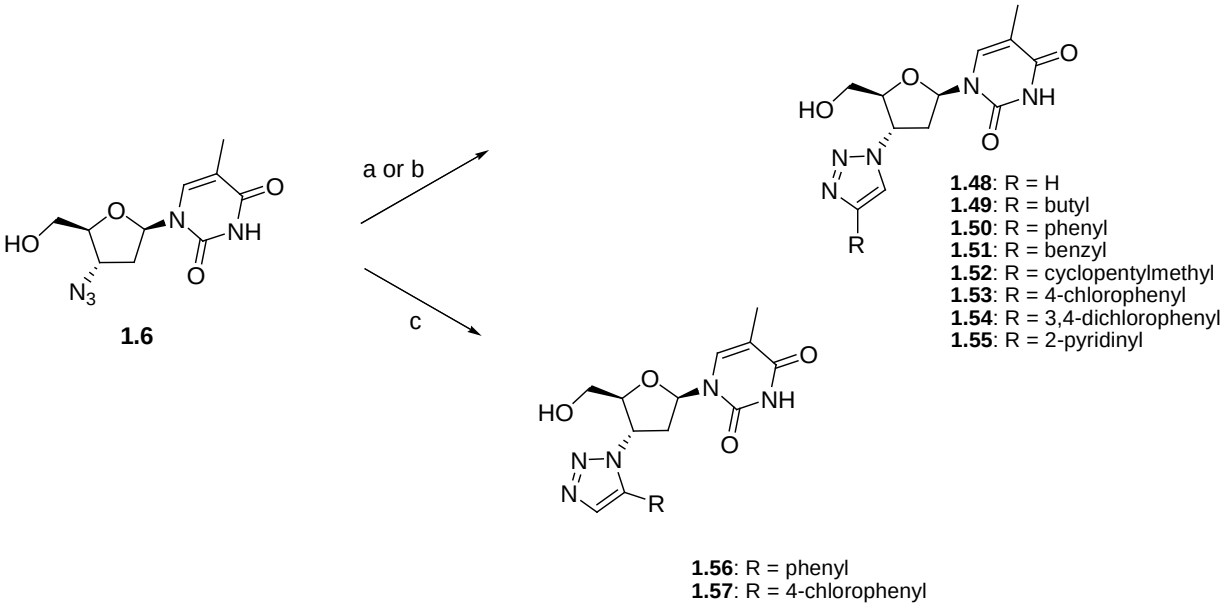

Scheme I.2. Reagents and conditions: (a) (i) trimethylsilylacetylene, $CuSO_4.5H_2O$, sodium ascorbate, H_2O/*t*BuOH (1:1), 45 °C, 24 h; (ii) 1M TBAF in THF, rt, overnight, 40% over 2 steps; (b) appropriate alkyne, $CuSO_4.5H_2O$, sodium ascorbate, H_2O/*t*BuOH (1:1), rt, 24 h, 14-69%; (c) appropriate alkyne, $Cp^*RuCl(PPh_3)_2$, THF, 65 °C, 8 h, 20-29%.

Unambiguous assignment of the substitution pattern of the triazole moiety of isomers **1.50** and **1.56** could be inferred from comparison of their ^{13}C NMR spectra with that of the monosubstituted triazole **1.48** (Table I.1). In the case of **1.50**, the largest resonance shift is found for the C-4" (13.0 ppm), while the shift for C-5" is relatively weak and has the sign changed (-3.5 ppm). An opposite phenomenon is observed for **1.56**, where these shifts are 4.7 ppm for C-4" and 8.7 ppm for C-5". The observed downfield shifts of the substituted carbon atoms is expected given the electron withdrawing nature of the phenyl ring.

Table I.1. ^{13}C-NMR data of the triazole moieties of **1.48, 1.50** and **1.56**.

Compound	C-4"	C-5"
1.48	133.57	124.49
1.50	146.57	121.01
1.56	138.22	133.16

2.2.2 Synthesis of 5'-*O*-Protected Isothiocyanate Analogue **1.59**

5'-*O*-Protected isothiocyanate **1.59** was prepared from its 3'-azido counterpart **1.47** by catalytic hydrogenation of the azido group in the presence of Pd/C, followed by treatment with 4-chloro-3-(trifluoromethyl)phenyl isothiocyanate in DMF (Scheme I.3).[69]

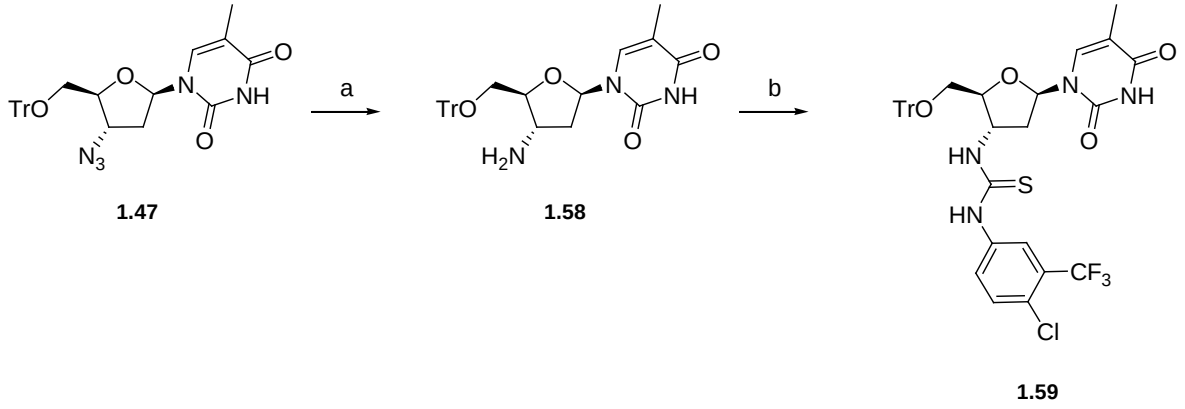

1.47 **1.58** **1.59**

Scheme I.3. Reagents and conditions: (a) H_2, Pd/C, MeOH, rt, 5 h, 73%; (b) 4-chloro-3-(trifluoromethyl)phenyl isothiocyanate, DMF, 0 °C, 3 h, 98%.

2.2.3 Synthesis of 3'-Triazole-Substituted BVDU Analogues

The synthesis of the 5-(*E*)-(2-bromovinyl) analogues is depicted in Scheme I.4. After tritylation of the 5' hydroxyl group of BVDU (**1.10**), the corresponding 2,3'-*O*-anhydro intermediate **1.62** was prepared by consecutive mesylation and treatment of the mesylate with Et_3N in EtOH. Treatment of **1.62** with sodium azide in the presence of *p*-nitrophenol[70] and detritylation afforded azido derivative **1.64**, which was converted to the 1,4-triazoles **1.65-1.66** under "click" conditions.

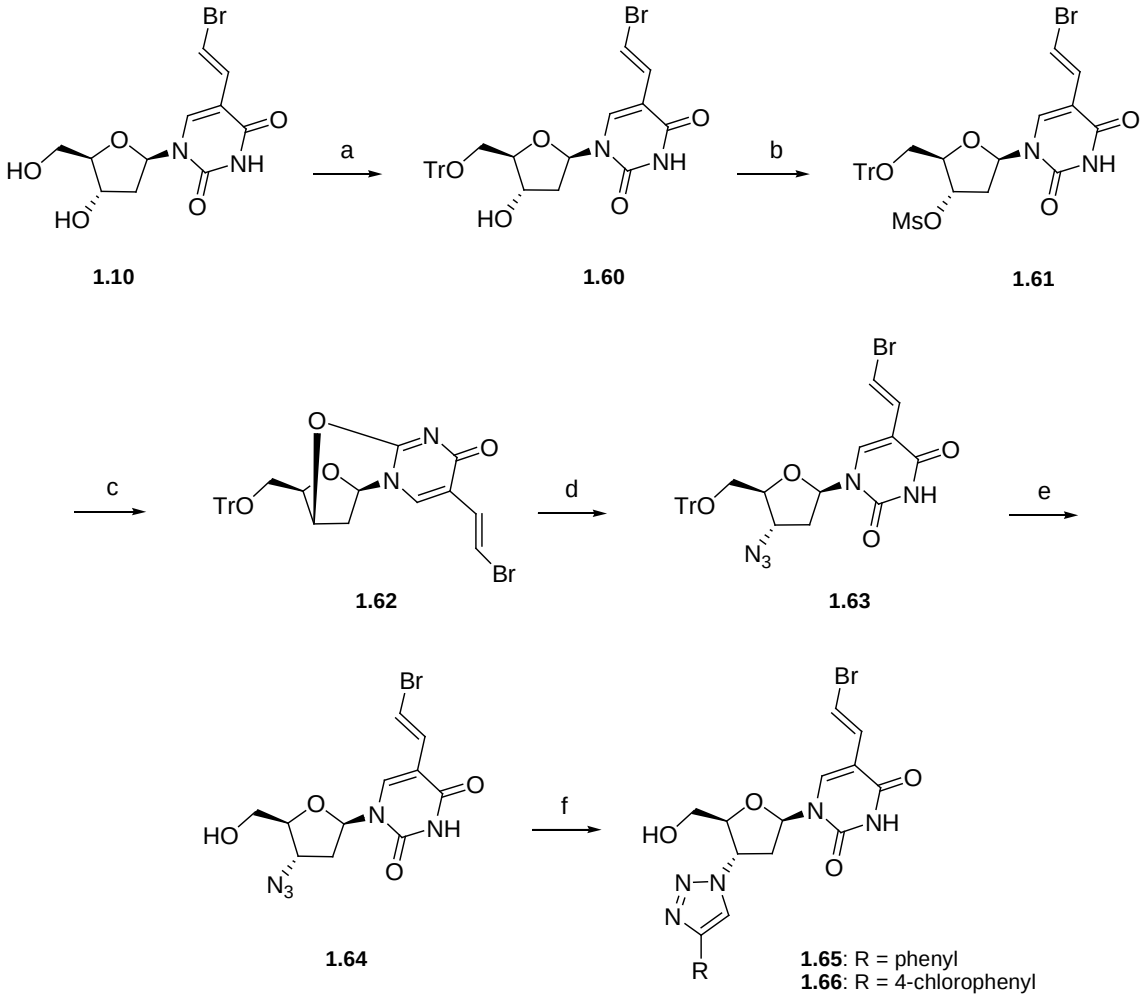

Scheme I.4. Reagents and conditions: (a) TrCl, pyridine, 65 °C, overnight, 65%; (b) MsCl, pyridine, 0 °C, 2 h; (c) Et_3N, EtOH, reflux, overnight, 75% over 2 steps; (d) NaN_3, *p*-NO_2-phenol, DMF, 110 °C, 7 h, 79%; (e) $ZnBr_2$, CH_2Cl_2/*i*PrOH (85:15), rt, overnight, 90%; (f) appropriate alkyne, $CuSO_4{\cdot}5H_2O$, sodium ascorbate, H_2O/*t*BuOH (1:1), rt, 24 h, 6%.

Conversion of **1.62** into the corresponding azide using the same conditions as described for the synthesis of the 3'-triazole-substituted dThd analogs (NaN_3, DMF, reflux, overnight) resulted in a new derivative, which was identified as **1.67** (Scheme I.5). The structural assignment of this compound. was based on a downfield shift of the ^{13}C NMR resonance signal from C-8 (110 → 145 ppm) which was in agreement with the reported signal of a similar reported derivative.[71] Mass spectroscopy confirmed the absence of the bromine atom by the disappearance of the typical 1:1 isotope peaks of Br as seen in compound **1.62**.

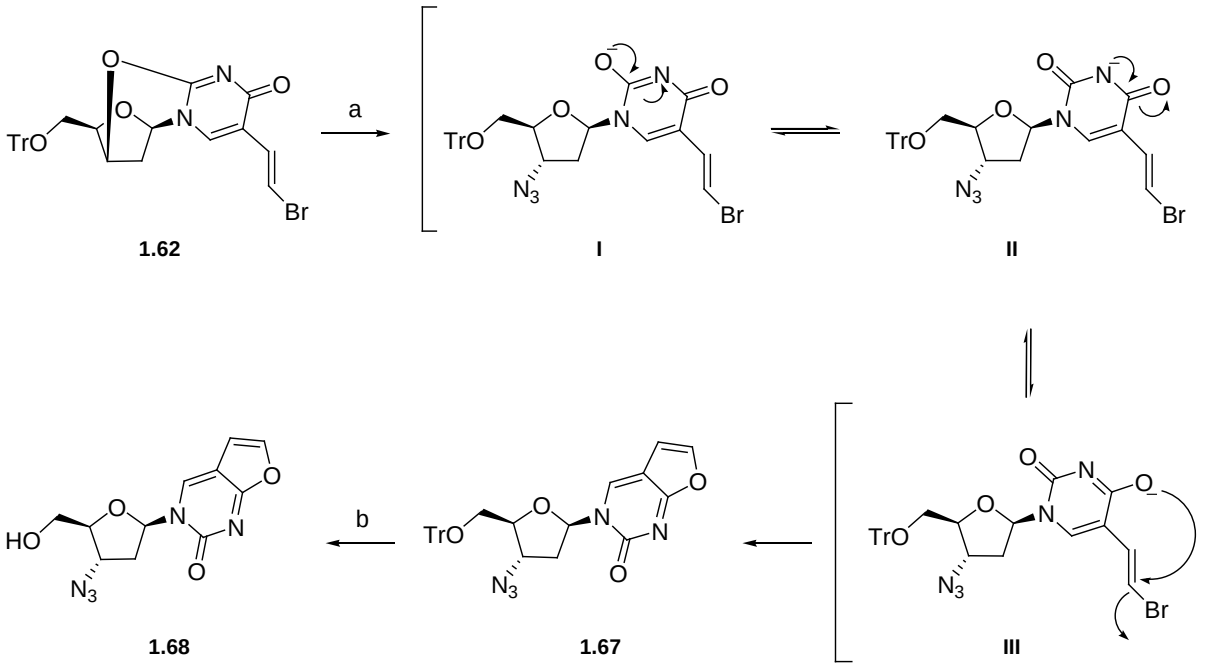

Scheme I.5. Reagents and conditions: (a) NaN_3, DMF, reflux, overnight, 54%; (b) $ZnBr_2$, CH_2Cl_2/*i*PrOH (85:15), rt, overnight, 39%.

Compound **1.67** appeared to be formed by the nucleophilic displacement of bromine by a negatively charged oxygen at the C-4 of the pyrimidine ring (intermediate **III**, Scheme I.5). This nucleophilic displacement has been previously observed by Jones and coworkers in the treatment of 5-(2-bromovinyl)uracil with potassium *tert*-butoxide.[71] To avoid the formation of **1.67**, stabilization of the negative charge at N3 was necessary (intermediate **II**). Therefore a compound with a pK_a lower than the pyrimidine base (pK_a between 9-10) was added to the reaction mixture. Opening of anhydro **1.62** in the presence of NaN_3 and *p*-nitrophenol (pK_a 7.15) successfully prevented formation of **1.67** and gave azide **1.63** in good yield.[70]

2.3 BIOLOGICAL EVALUATION

The 3'-triazole-substituted dThd and BVDU derivatives were evaluated for their inhibitory activity against dThd phosphorylation by recombinant purified human cytosolic TK-1, human mitochondrial TK-2, HSV-1 TK, VZV TK, and *Dm*-dNK under the guidance of Prof. Dr. Jan Balzarini at the Laboratory of Virology and Chemotherapy, Rega Institute, K.U.Leuven.

Table I.2. Inhibitory effects of thymidine and BVDU analogues on 1 μM [CH_3-^{3}H]dThd phosphorylation by deoxyribonucleoside kinases from different origins

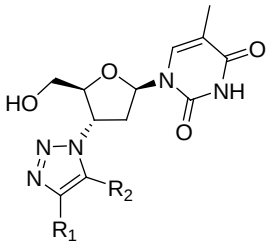

1.48-1.57

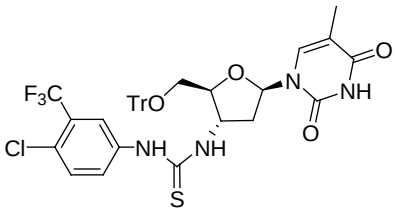

1.59

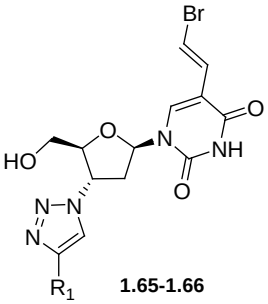

1.65-1.66

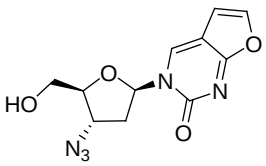

1.68

Compd	R_1	R_2	IC_{50}[a] (μM)				
			TK-1	TK-2	HSV-1 TK	VZV TK	*Dm*-dNK
1.48	H	H	≥ 500	4.7 ± 2.1	212 ± 17	15 ± 5	40 ± 1
1.49	*n*-Bu	H	366 ± 4	0.23 ± 0.05	95 ± 1	4.3 ± 0.3	4.1 ± 0.8
1.50	Ph	H	54 ± 16	0.32 ± 0.01	28 ± 6	2.5 ± 0.3	2.2 ± 0.8
1.51	-CH_2-Ph	H	318 ± 110	0.30 ± 0.12	158 ± 42	6.4 ± 4.0	3.9 ± 0.6
1.52	-CH_2-c-pentyl	H	177 ± 182	0.15 ± 0.02	48 ± 2	3.1 ± 0.2	3.0 ± 0.4
1.53	4-Cl-Ph	H	71 ± 0	**0.046 ± 0.002**	27 ± 5	3.3 ± 0.2	1.8 ± 0.9
1.54	3,4-diCl_2Ph	H	75 ± 49	**0.042 ± 0.008**	30 ± 2	2.7 ± 0.3	0.99 ± 0.53
1.55	2-pyridinyl	H	316 ± 17	1.3 ± 0.4	46 ± 1	3.1 ± 0.2	3.8 ± 0.1
1.56	H	Ph	≥ 500	1.1 ± 0.6	445 ± 78	19 ± 3	17 ± 0
1.57	H	4-Cl-Ph	109 ± 79	4.0 ± 0.0	392 ± 18	30 ± 0	30 ± 4
1.59	-	-	> 500	> 500	> 500	> 500	> 500
1.65	Ph	-	> 500	0.25 ±0.09	36 ± 6	3.7 ± 0.5	2.9 ± 0.8
1.66	4-Cl-Ph	-	> 500	**0.036 ± 0.003**	4.5 ± 0.6	1.7 ± 0.4	0.46 ± 0.06
1.68	-	-	> 500	354 ± 11	> 500	162 ± 81	107 ± 65
1.43			316 ± 1.2	0.15 ± 0.01	195 ± 54	24 ± 3.0	-
1.6			52	4	-	-	1.1 ± 0.3[7,23]

[a]IC_{50} is the 50% inhibitory concentration of the test compounds, which was measured as the concentration required to inhibit 1 μM [CH_3-^{3}H]dThd phosphorylation by 50%. The K_m values of TK-1, TK-2, HSV-1 TK, VZV TK, and *Dm*-dNK for the natural substrate dThd were 2.3, 1.1, 1.44, 3.4, and 3.5 μM, respectively.

Compound **1.43** and AZT (**1.6**), were included as references. In the 1,4-triazole series, the anti-TK-2 activity was clearly influenced by the nature of the substituent at C-4 of the triazole. Both a *n*-butyl (**1.49**) or phenyl (**1.50**) substituent gave submicromolar inhibition. Introduction of a -CH_2- group between the triazole and the phenyl (**1.51**) did not drastically alter the IC_{50} value, while replacement of the benzyl by a cyclopentylmethyl substituent (**1.52**) caused a 2-fold drop in IC_{50}. Introduction of an electron-withdrawing Cl in the para position of the phenyl (**1.53**) significantly improved the inhibitory activity. A similar effect had previously been observed in the thiourea series.[59] Remarkably, this increased activity could not be obtained with an electron-deficient pyridin-2-yl substituent (**1.55**). With analogues **1.56** and **1.57**, which are regioisomers of **1.50** and **1.53**, we could infer that the 4-position is the preferred site for triazole derivatization.

Introduction of an additional 5-(2-bromovinyl) group, known to be a privileged substituent for TK-2 binding, only slightly improved the inhibitory activity but caused a significant increase in the selectivity for TK-2 versus TK-1 as seen from the complete lack of inhibitory effect against TK-1-catalyzed dThd phosphorylation. Compound **1.66** showed an outstanding selectivity against TK-2 when compared to TK-1 (SI ≥ 14000), and is one of the most potent inhibitor of TK-2 (IC_{50} of 0.036 µM) reported so far. Because the K_m values of the natural substrate dThd for TK-1 (2.3 µM) and TK-2 (1.1 µM) were very similar and the IC_{50} values of the inhibitors were determined in the presence of 1 µM dThd, the IC_{50} values of the different inhibitors fairly reflect the degree of affinity of these compounds for both enzymes. In addition, **1.66** showed relatively poor inhibitory activity against the closely related HSV-1 and VZV TKs.

The mode of TK-2 inhibition by **1.66** was investigated (Figure I.21). First, its K_i value was determined in the presence of a fixed saturating concentration of ATP and variable concentrations of the dThd substrate. This revealed that **1.66** inhibited the enzyme in a purely competitive fashion and had K_i values as low as 0.012 µM. Its K_i/K_m ratios were markedly lower than 1 (0.011), pointing to an affinity for the enzyme that largely exceeds the affinity of the natural substrate. Second, the K_i values of this inhibitor were also determined in the presence of a fixed saturating concentration of dThd and variable concentrations of the cosubstrate ATP. Compound **1.66** showed a K_i value that was higher (0.41 µM) than that observed in the presence of dThd as the variable substrate. However, the K_i/K_m ratio was again much lower than 1 (0.019). Interestingly, under these conditions, **1.66** behaved kinetically differently and displayed an uncompetitive mechanism of enzyme inhibition, as revealed by the (virtually) parallel kinetic lines in the Lineweaver-Burk plots. These features point toward a specific binding of the inhibitor to an enzyme-ATP complex. Compound **1.59** was synthesized to assess the compatibility of combining the thiourea moiety of **1.43** with a 5'-*O*-trityl group. Combination of the 3'-modification and the 5'-*O*-trityl substituent led, as expected, to an analogue that was completely devoid of affinity for TK-2. Also for compound **1.68**, a very weak inhibitory activity was observed (IC_{50} = 354 ± 11 µM).

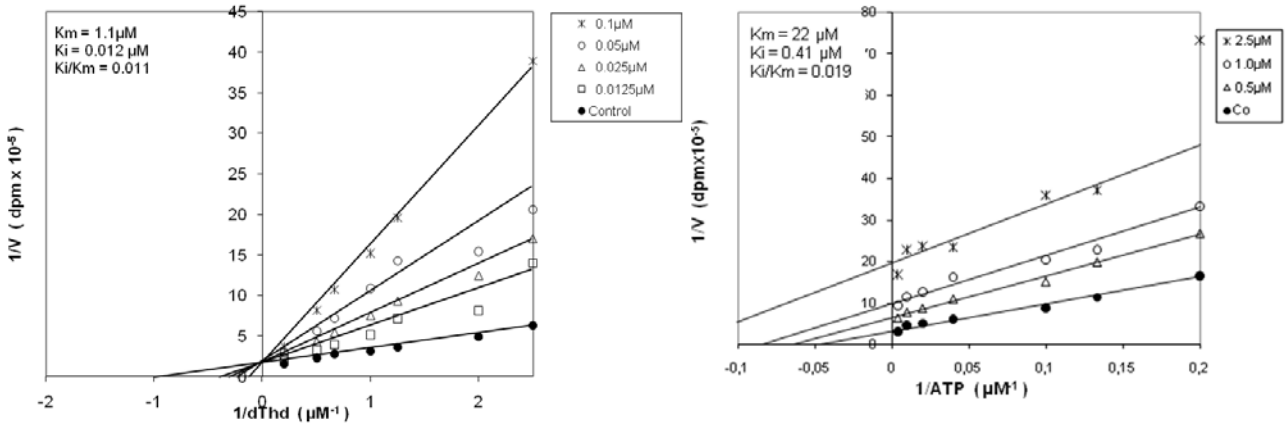

Figure I.21. Kinetics of **1.66** against purified recombinant mitochondrial TK-2.

2.4 MOLECULAR MODELING AND STRUCTURE-ACTIVITY RELATIONSHIP

To gain insight into the mode of binding of this new class of inhibitors, docking experiments were performed under the supervision of Prof. Dr. Federico Gago at the Centre for Computational Drug Discovery in Madrid, using a previously reported homology-based model of TK-2 as the target.[59] This model is largely, but not exclusively, based on many similarities with the well-characterized structure of *Dm*-dNK although relatively major uncertainties remain.

As previously proposed for **1.43** and related thiourea derived inhibitors,[59] the thymine ring of β-thymidine containing compounds can stack on the phenyl ring of Phe143, whereas O4 and N3 atoms are held in place by virtue of two highly directional hydrogen bonds with the carboxamide group of Gln110 (equivalent to Gln81 in *Dm*-dNK). On the other hand, a free 5'-hydroxyl of a nucleosidic ligand can be hydrogen bonded by the guanidinium nitrogen of Arg134 and the carboxylate of Glu81, whose equivalent residues in *Dm*-dNK have been shown to be crucial for the phosphoryl transfer reaction.[72] Thus, on the basis of the results from multiple sequence alignments (Figure I.22) and the homology-built model presented herein, Glu81 in TK-2 most likely acts as the base that deprotonates the 5'-OH of thymidine, whereas Arg134 plays a crucial role in the stabilization of the transition state during the phosphoryl transfer reaction.

Taking all TK-2's conformational features into account, the best docking solution for **1.53**, supported and refined by subsequent molecular dynamics (MD) simulation in water, suggests that the thymidine moiety of this inhibitor fills the same volume that is usually occupied by the substrate thus giving rise to the same interactions as reported for thymidine (Figure I.23).[73]

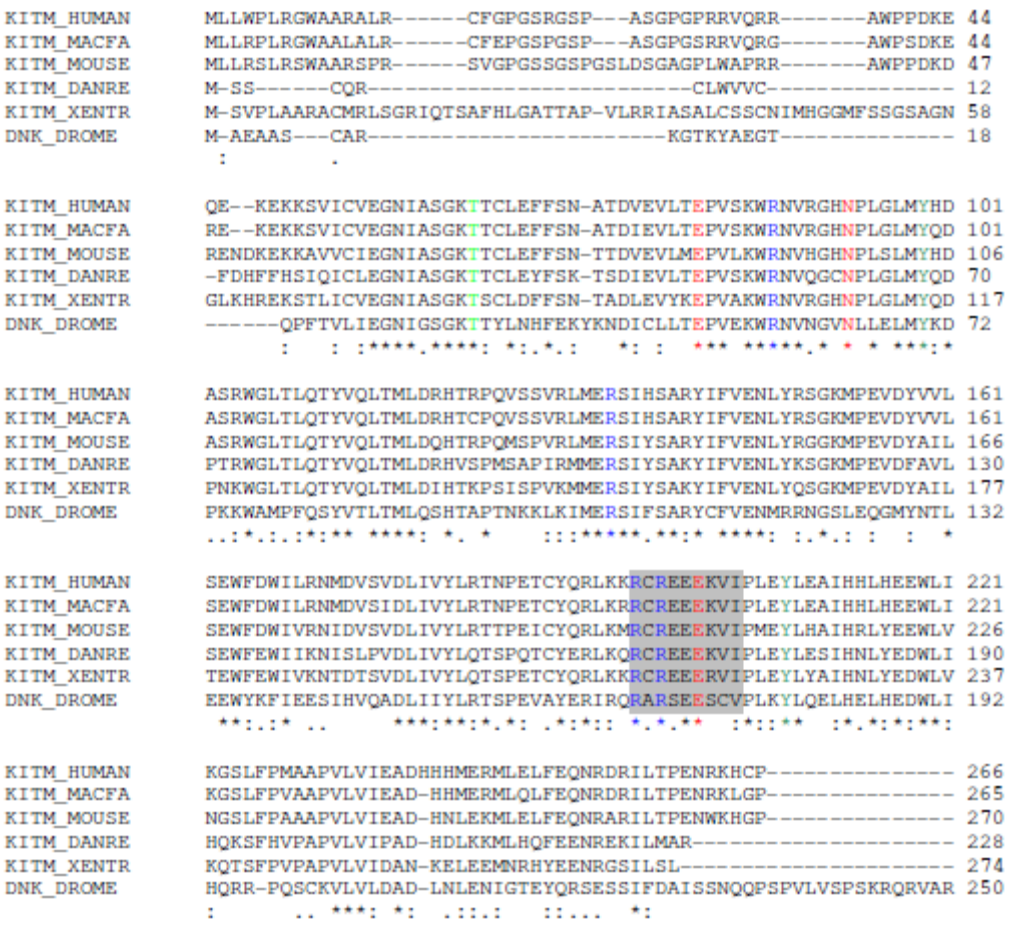

Figure I.22. Multiple sequence alignment (Clustal 2.0.10) and numbering of human TK-2 (KITM_HUMAN), related mitochondrial kinases and *Dm*-dNK (DNK_DROME). Residues discussed in the text are colored. Highlighted in grey is the LID loop region.

The direct interaction between the triazole moiety and the γ-phosphate group of ATP that was envisioned at the outset of this project was not supported by the docking and simulation studies. Instead, the results strongly suggest that the triazole appears to displace the side chain of a tyrosine residue (Tyr99) that is involved in anchoring the 3'-OH of the substrate in the thymidine binding pocket. Relatively small readjustments allow the triazole N-2 atom to hydrogen bond the carboxylate of Glu200 from the LID loop through the intervention of a bridging water molecule that is also hydrogen-bonded to the side chain of Arg198. This orientation allows the phenyl ring attached at position 4 of the triazole to occupy a hydrophobic cavity and increase the binding affinity. At this point it is worth noting that a 180 rotation of the triazole ring relative to the sugar would lead to a steric clash of the attached phenyl ring with the LID loop and also that this model does not favor substitution at position 5 of the triazole ring, in good agreement with the much lower inhibitory activity measured for the 1,5-substituted derivatives **1.56** and **1.57**. On the contrary, this binding orientation is fully compatible with the modulation of the inhibitory activity upon introduction of substituents at position 4.

Interestingly, interaction with the carboxylate of Glu200 happens to be mediated by a bridging water molecule that is also bonded to Arg198. As these two residues are part of the LID loop, this arrangement can account for the fact that the loop is closed over the active site and therefore the ATP molecule can get trapped.

It is important to highlight that the model provides an explanation to the 10-fold improvement in activity that is achieved upon incorporation of the phenyl ring to the unsubstituted triazole derivative **1.48**. The phenyl ring in **1.53** is proposed to make van der Waals interactions with Val203 and Ile204 within the VIPLEY sequence that immediately follows the LID loop so that these hydrophobic contacts can contribute to stabilization of the closed form of the enzyme. We are also aware that these proposed interactions are more favorable in TK-2 than those possible with the Cys and Val of CVPLKY in *Dm*-dNK. Taken together, sequence differences at these positions can account for the better inhibition of human TK-2 relative to *Dm*-dNK by the title compounds. It is also interesting to note that **1.65** and **1.66**, both containing a BVDU moiety in place of the thymine, are only marginally more potent than **1.50** and **1.53**, respectively, an observation that is in line with the facts that (i) the K_m value of BVDU when used as a substrate for *Dm*-DNK is only ~ 4-fold lower than that of AZT,[68] (ii) the nucleobases binding site in *Dm*-DNK and human TK-2 are highly comparable, and (iii) AZT and BVDU binding to *Dm*-dNK show similar characteristics, as inferred from comparison of PDB structures 2JJ8 and 2VQS. Finally, our finding that a 5'-*O*-trityl substituent renders the inhibitors in the present series inactive is also consistent with the proposed binding mode insofar as the 5'-hydroxyl is used, as described above and reported previously for thiourea-derived inhibitors,[59] to anchor the inhibitor in the substrate binding site through hydrogen bonding interactions with the catalytically important Arg134 and Glu81.

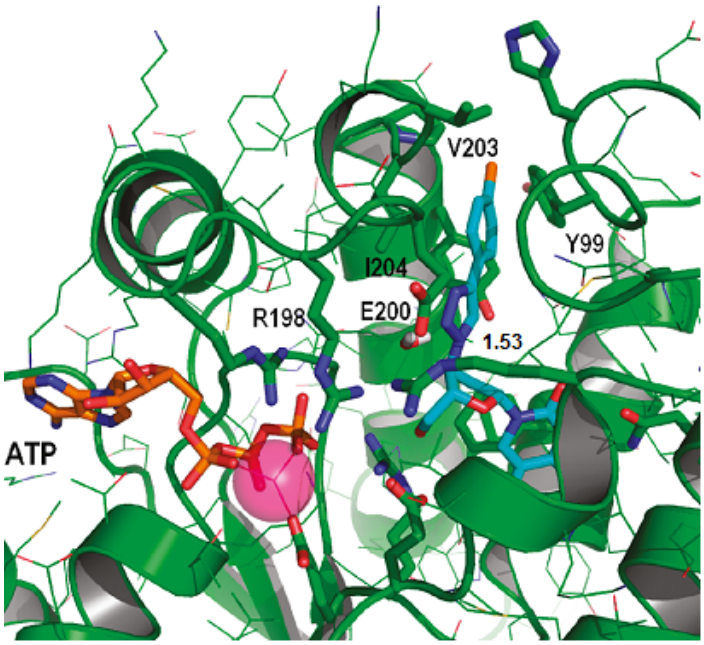

Figure I.23. Proposed binding mode for inhibitor **1.53** (C atoms in cyan), in the active site of human TK-2 (green ribbon). ATP is shown as sticks, with C atoms colored in orange, and Mg^{2+} is displayed as a semitransparent sphere colored in magenta. Some of the protein side-chains relevant to the discussion are labeled and shown as sticks. Note the "close" conformation of the lid loop that normally covers the substrate-binding cleft during catalysis and the water molecule that bridges the interaction between the triazole of the inhibitor and the carboxylate of Glu200.

To reveal whether the TK-2 inhibitors are able to be taken up by the cells, Balzarini *et al*. chose the most active compound **1.66** for further studies. Because of the lack of TK-2 gene-transduced tumor cells, human osteosarcoma cells (OST TK$^-$) were used that were transfected with the *Drosophila melanogaster* multifunctional deoxynucleoside kinase gene (OST TK$^-$/*Dm*-dNK$^+$). Alike TK-2, the *Dm*-dNK enzyme is sensitive to the inhibitory activity of compound **1.66** at an IC_{50} of 0.46 μM (Table I.2). The cytostatic agents (*E*)-5-(2-bromovinyl)-2'-deoxyuridine (BVDU, **1.10**) and 5-fluoro-2'-deoyxuridine (5FdUrd, **1.69**, Figure I.24) were exposed to these cell cultures in the presence or absence of **1.66** (used at subtoxic concentrations (10 μM and 4 μM)) (Table I.3). Whereas BVDU and 5FdUrd were cytostatic at an IC_{50} of 0.76 and 0.066 μM, respectively, their antiproliferative effect was significantly (4-fold) decreased in the presence of **1.66** at 10 μM (IC_{50}: 2.95 and 0.263 μM, respectively) and at 4 μM (IC_{50}: 1.64 and 0.110 μM, respectively). The conversion of BVDU and 5FdUrd to their toxic metabolites by *Dm*-dNK could be dose-dependently blocked by 80% in the presence of the TK-2 (*Dm*-dNK) inhibitor under the experimental conditions. These data revealed that the TK-2 inhibitors such as **1.66** can enter the intact tumor cells and be inhibitory to the nucleoside kinase present in the cytosol. It would now be imperative to investigate whether these compounds are also taken up by mitochondria after their penetration into the intact cells, enabling targeting TK-2 in the mitochondrial environment.

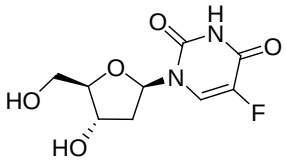

1.69

Figure I. 24

Table I.3. Cytostatic Activity of BVDU and 5FdUrd against *Dm*-dNK expressing OST TK$^-$/*Dm*-dNK$^+$ cells in the absence or presence of compound **1.66**.

Compound	IC_{50}[a] (μM)		
		Compound **1.66**	
	As such	4 μM	10 μM
BVDU (**1.10**)	0.76 ± 0.001	1.64 ± 0.07	2.95 ± 0.96
5FdUrd (**1.69**)	0.066 ± 0.003	0.110 ± 0.035	0.263 ± 0.104

[a]50% Inhibitory concentration or compound concentration required to inhibit OST TK$^-$/dNK$^+$ cell proliferation by 50%. Data are the mean ± SD of two independent experiments. The IC_{50} of compound **1.66** as such is 23 ± 15 μM.

2.5 PHOTOPHYSICAL EVALUATION

In 2004, Berry and co-workers reported a series of pyrimidines fused to furano and pyrrolo moieties to produce fluorescent analogs of thymidine and 2'-deoxycytidine to study DNA structure.[74] Additionally, Li *et al*. reported the synthesis of fluorescent nucleoside analogs with modified sugar moieties (e.g., sugars other than ribose and 2'-deoxyribose).[75] All these compounds represent promising tools for studying nucleoside metabolism inside living cells, including cellular uptake and phosphorylation (Figure I.25).

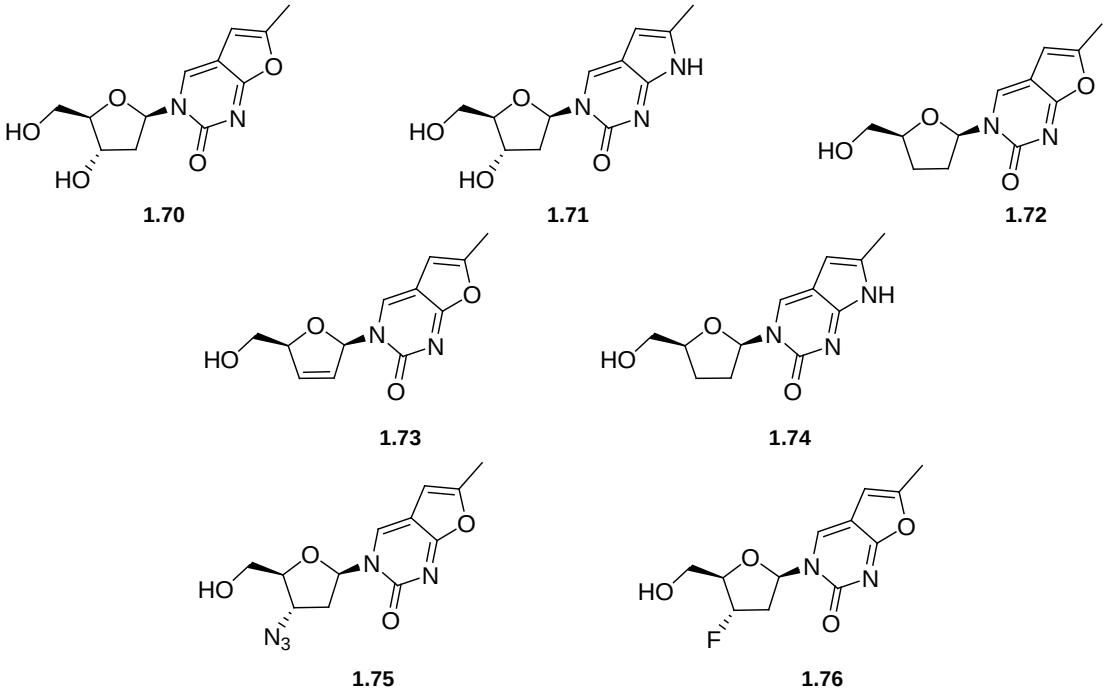

Figure I.25. Nucleoside analogs with fluorescent properties

Based on the structural similarity between compound **1.68** and the reported nucleoside analogs **1.70-1.76**, the fluorescence properties of azide **1.68** were determined at the Laboratory of General Biochemistry and Physical Pharmacy (UGent) and found to be similar to previously reported analogs having excitation wavelengths of 322 ± 2 nm and emission maxima ranging from 413 - 415 nm (Figure I.26).

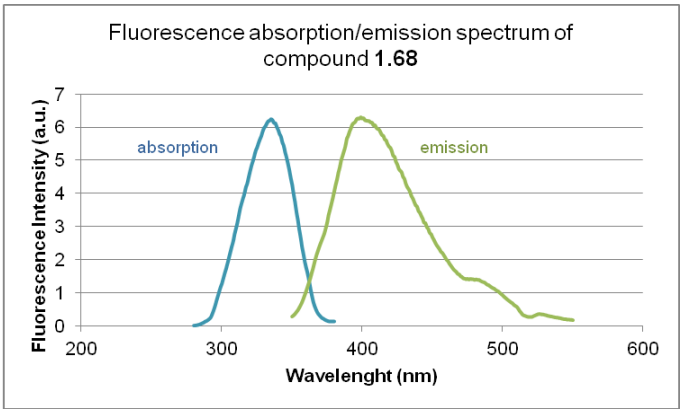

Figure I.26. Excitation and emission spectrum of compound **1.68**.

2.6 CONCLUSIONS

Cycloaddition of organic azides and alkynes is the most direct route to 1,2,3-triazoles. In this chapter, we used two different catalysts to achieve this reaction: the Cu(I) catalyst, which provided the 1,4-disubstituted 1,2,3-triazole regioisomers, and the [Cp*RuClP(Ph_3)$_2$] catalyst, which has recently been described for regioselective synthesis of 1,5-disubstituted 1,2,3-triazole systems. By replacing the thiourea linker of an earlier identified TK-2 inhibitor **1.43** by a 1,4-substituted triazole ring, we successfully generated a new generation of very potent TK-2 inhibitors. Combining such a favorable sugar modification with a bromovinyl substituent at position 5 of the pyrimidine moiety further enhanced the selectivity vis-à-vis TK-1. The direct interaction between the triazole moiety and the γ-phosphate group of ATP that was envisioned at the outset of this project was not supported by the docking and simulation studies. Instead, it is proposed that the best inhibitors in this series stabilize, through a well-defined set of interactions, a closed conformation of the enzyme that traps an ATP molecule in the cofactor binding site. This binding mode provides a rationale to the biochemical evidence and an explanation to the structure-activity relationship in atomic detail.

2.7 EXPERIMENTAL PART

2.7.1 Synthesis

General

All reagents were from standard commercial sources and of analytical grade. Precoated Merck silica gel F254 plates were purchased for TLC, spots were examined under ultraviolet light at 254 nm and further visualized by sulfuric acid-anisaldehyde spray. Column chromatography was performed on silica gel (63-200 µm, 60 Å, Biosolve, Valkenswaard, The Netherlands). NMR spectra were determined using a Varian Mercury 300 MHz spectrometer. Chemical shifts are given in ppm (δ) relative to the residual solvent signals, which in the case of DMSO-d_6 were 2.54 ppm for ^{1}H and 40.5 ppm for ^{13}C. Structural assignment was confirmed with COSY and DEPT. All signals assigned to hydroxyl groups were exchangeable with D_2O. Exact mass measurements were performed on a Waters LCT Premier XETM Time of flight (TOF) mass spectrometer equipped with a standard electrospray ionization (ESI) and modular LockSpray TM interface. Samples were infused in a CH_3CN/water (1:1) mixture at 10 µL/min.

5'-*O*-Triphenylmethyl-β-D-thymidine (1.44)

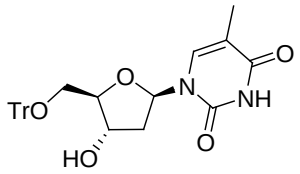

To a solution of β-D-thymidine (2.50 g, 10.32 mmol) in anhydrous pyridine (24 mL) was added trityl chloride (3.37 g, 12.11 mmol). The mixture was heated to 65 °C and stirred overnight. Then it was diluted with CH_2Cl_2 (25 mL), washed with saturated aqueous $NaHCO_3$ (3 x 50 mL), and dried over anhydrous $MgSO_4$. The solvent was removed under reduced pressure and the resulting residue was purified by column chromatography (CH_2Cl_2/MeOH 98:2), affording compound **1.44** (5.27 g, 100%) as a white foam.

^{1}H NMR (300 MHz, DMSO-d_6): δ 1.47 (3H, d, *J*= 0.9 Hz, 5-CH_3), 2.11-2.18 (1H, m, H-2'a), 2.21-2.30 (1H, m, H-2'b), 3.17 (1H, dd, *J*= 3.0 Hz, *J*= 10.5 Hz, H-5'a), 3.24 (1H, dd, *J*= 4.8 Hz, *J*= 10.8 Hz, H-5'b), 3.87 (1H, app q, *J*= 4.2 Hz, H-4'), 4.32 (1H, s, H-3'), 5.33 (1H, app s, 3'-OH), 6.21 (1H, app t, *J*= 7.2 Hz, H-1'), 7.25-7.41 (15H, m, Tr), 7.49 (1H, d, *J*= 0.9 Hz, H-6), 11.33 (1H, s, 3-NH).

^{13}C NMR (75 MHz, DMSO-d_6): δ 12.45 (5-CH_3), (C-2' under DMSO-signal), 4.67 (C-5'), 71.12 (C-3'), 84.40 (C-1'), 86.05 (C-4'), 87.07 (Tr), 110.25 (C-5), 127.86, 128.67 and 128.94 (Tr), 136.37 (C-6), 144.17 (Tr), 151.06 (C-2), 164.34 (C-4).
Exact Mass (ESI-MS) for $C_{29}H_{29}N_2O_5$ $[M+H]^+$ found: 485.2054, calcd: 485.2071.

2,3'-*O*-Anhydro-5'-*O*-triphenylmethyl-β-D-thymidine (1.46)

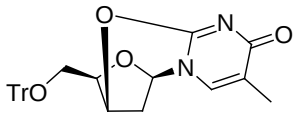

To an ice-cooled solution of compound **1.44** (2.80 g, 5.79 mmol) in pyridine (15.5 mL) was added methanesulfonyl chloride (0.90 mL, 11.57 mmol). The reaction mixture was stirred for 3 hours at room temperature, quenched with $NaHCO_3$ and extracted with CH_2Cl_2 (3 x 20 mL). The combined organic layers were dried over $MgSO_4$ and evaporated to dryness. The residue was dissolved in 26 mL CH_3CN and DBU (1.00 mL, 11.95 mmol) was added. After refluxing overnight, the mixture was evaporated to dryness and extracted with CH_2Cl_2 (3 x 25 mL). The combined organic layers were dried over $MgSO_4$ and evaporated to dryness. Further purification by column chromatography (CH_2Cl_2/MeOH 97:3) gave 2.38 g of compound **1.46** as a yellow, brownish foam (88%).

^{1}H NMR (300 MHz, DMSO-d_6): δ 1.77 (3H, d, *J*= 1.2 Hz, 5-CH_3), 2.47-2.60 (2H, m, H-2'a and H-2'b), 3.06-3.16 (2H, m, H-5'a and H-5'b), 4.40-4.46 (1H, m, H-4'), 5.32 (1H, app s, H-3'), 5.88 (1H, app d, *J*= 3.5 Hz, H-1'), 7.21-7.39 (15H, m, Tr), 7.61 (1H, d, *J*= 1.2 Hz, H-6).

^{13}C NMR (75 MHz, DMSO-d_6): δ 13.70 (5-CH_3), 33.39 (C-2'), 63.19 (C-5'), 77.73 (C-3'), 84.12 (C-1'), 87.03 (C-4'), 87.50 (Tr), 116.81 (C-5), 127.74, 128.59 and 128.86 (Tr), 137.36 (C-6), 143.95 (Tr), 153.95 (C-2), 171.40 (C-4).

Exact Mass (ESI-MS) for $C_{29}H_{29}N_2O_4$ $[M+H]^+$ found: 467.1926, calcd: 467.1965.

3'-Azido-3'-deoxy-5'-*O*-triphenylmethyl-β-D-thymidine (1.47)

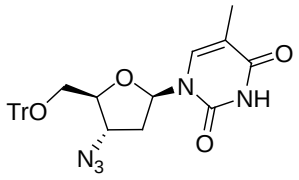

A mixture of compound **1.46** (2.38 g, 5.10 mmol) and NaN_3 (1.66 g, 25.50 mmol) was dissolved in DMF (8.5 mL) and heated to 150 °C. The reaction was refluxed overnight and then quenched with water (5 ml). The reaction mixture was extracted with CH_2Cl_2 (3 x 10 mL) and the combined organic

layers were dried over $MgSO_4$ and evaporated to dryness. The residue was purified by column chromatography (CH_2Cl_2/MeOH 93:7), affording compound **1.47** as a yellow oil (87%, 2.80 g).

^{1}H NMR (300 MHz, DMSO-d_6): δ 1.56 (3H, d, *J*= 0.9 Hz, 5-CH_3), 2.31-2.40 (1H, m, H-2'a), 2.46-2.55 (1H, m, H-2'b), 3.25 (2H, d, *J*= 3.6 Hz, H-5'a and H-5'b), 3.85-3.90 (1H, m, H-4'), 4.55-4.62 (1H, m, H-3'), 6.13 (1H, dd, *J*= 5.7 Hz en *J*= 7.2 Hz, H-1'), 7.23-7.42 (15H, m, Tr), 7.52 (1H, d, *J*= 1.2 Hz, H-6), 11.36 (1H, s, 3-NH). The spectrum is accordance with the literature report.[76]

^{13}C NMR (75 MHz, DMSO-d_6): δ 12.57 (5-CH_3), 36.66 (C-2'), 60.41 (C-3'), 63.82 (C-5'), 82.63 (C-1'), 83.99 (C-4'), 87.19 (Tr), 110.42 (C-5), 127.91, 128.70 and 128.94 (Tr), 136.56 (C-6), 144.06 (Tr), 151.05 (C-2), 164.35 (C-4).

Exact Mass (ESI-MS) for $C_{29}H_{28}N_5O_4$ $[M+H]^+$ found: 210.2138, calcd: 210.2136.

3'-Azido-3'-deoxy-β-D-thymidine (1.6)

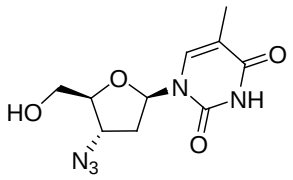

A suspension of compound **1.47** (1.13 g, 2.21 mmol) in 23 mL of 80% aqueous acetic acid was heated at 90 °C with stirring for 25 minutes. The solution was evaporated *in vacuo* and the residue was purified on a silica column (CH_2Cl_2/MeOH 95:5) affording 364 mg of crude **1.6** as light brown crystals (62%).

^{1}H NMR (300 MHz, DMSO-d_6): δ 1.87 (3H, s, 5-CH_3), 2.19-2.38 (2H, m, H-2'a and H-2'b), 3.36-3.63 (2H, m, H-5'a and H-5'b), 3.79 (1H, app q, *J*= 4.2 Hz, H-4'), 4.32-4.38 (1H, m, H-3'), 5.26 (1H, t, *J*= 6.0 Hz, 5'-OH), 6.05 (1H, t, *J*= 6 Hz, H-1'), 7.91 (1H, s, H-6), 11.29 (1H, s, 3-NH). The spectrum is accordance with the literature report.[76]

^{13}C NMR (75 MHz, DMSO-d_6): δ 12.85 (CH_3), 36.51 (C-2'), 55.48 (C-3'), 60.84 (C-5'), 84.09 (C-4'), 84.61 (C-1'), 110.26 (C-5), 136.79 (C-6), 163.17 (C-2), 172.80 (C-4).

Exact Mass (ESI-MS) for $C_{10}H_{14}N_5O_4$ $[M+H]^+$ found: 268.1028, calcd: 268.10403.

3'-Deoxy-3'-(1,2,3-triazol-1-yl)-β-D-thymidine (1.48)

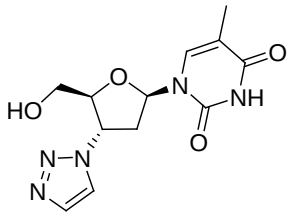

To a solution of trimethylsilylacetylene (85 µL, 0.59 mmol) in 3 mL of a H_2O/*t*BuOH (1:1; v:v) mixture, was added sodium ascorbate (18 mg, 0.089 mmol) and $CuSO_4 \cdot 5H_2O$ (11 mg, 0.044 mmol). The mixture was stirred for 15 min. Compound **1.6** (80 mg, 0.30 mmol) was added, and the resulting mixture was stirred at 45 °C for 24 h. The reaction mixture was washed with EtOAc (3 x 5 mL), and the combined organic phases were washed with water, dried over anhydrous Na_2SO_4, and evaporated to dryness. Without further purification, 1M TBAF in THF was added (1.2 mL) and the mixture was stirred at room temperature. After 16 h, TLC analysis revealed almost complete disappearance of all starting material. The solvent was evaporated and the mixture purified by column chromatography (EtOAc/MeOH, 100:0 → 95:5) yielding compound **1.48** as a white powder (35 mg, 40%).

^{1}H NMR (300 MHz, DMSO-d_6): δ 1.79 (3H, d, *J*=0.9 Hz, 5-CH_3), 2.63-2.72 (2H, m, H-2'a and H-2'b), 3.58-3.71 (2H, m, H-5'a and H-5'b), 4.17-4.21 (1H, m, H-4'), 5.21-5.32 (1H, m, 5'-OH), 5.37-5.39 (1H, m, H-3'), 6.41 (1H, app t, *J*= 6.3 Hz, H-1'), 7.78 (1H, d, *J*= 0.9 Hz, H-4"), 7.81 (1H, d, *J*= 1.2 Hz, H-6), 8.30 (1H, d, *J*= 0.9 Hz, H-5"), 11.33 (1H, s, 3-NH).

^{13}C NMR (75 MHz, DMSO-d_6): δ 12.27 (5-CH_3), 37.22 (C-2'), 58.97 (C-5'), 60.72 (C-3'), 83.89 (C-1'), 84.52 (C-4'), 109.63 (C-5), 124.49 (C-5"), 133.57 (C-4"), 136.26 (C-6), 150.45 (C-2), 163.74 (C-4).

Exact Mass (ESI-MS) for $C_{12}H_{16}N_5O_4$ $[M+H]^+$ found: 350.1820, calcd: 350.1823.

General procedure for the synthesis of 4"-substituted 3'-deoxy-3'-(1,2,3-triazol-1-yl)-β-D-thymidine derivatives 1.49-1.55

Compound **1.6** (1 mmol, 1 equiv), sodium ascorbate (0.05 equiv), and $CuSO_4 \cdot 5H_2O$ (0.04 equiv) were suspended in 10 mL of H_2O/*t*BuOH (1:1). The appropriate alkyne (2 equiv) was added after 15 min, and the mixture was stirred at room temperature for 24 h. The reaction mixture was washed with CH_2Cl_2, and the combined organic phases were washed with water, dried over anhydrous $MgSO_4$, and evaporated to dryness. The crude product was purified by column chromatography, affording the triazole in moderate yield.

3'-(4-Butyl-1,2,3-triazol-1-yl)-3'-deoxy-β-D-thymidine (1.49)

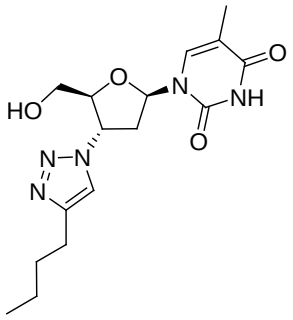

Reaction of compound **1.6** (66 mg, 0.24 mmol) with 1-hexyne (60 µL, 0.49 mmol) following the general procedure for the synthesis of 4"-substituted 3'-deoxy-3'-(1,2,3-triazol-1-yl)-β-D-thymidine derivatives gave compound **1.49** (47 mg, 55%) as a white powder.

^{1}H NMR (300 MHz, DMSO-d_6): δ 0.90 (3H, t, *J*= 7.2 Hz, butyl), 1.24-1.40 (2H, m, butyl), 1.54-1.64 (2H, m, butyl), 1.79 (3H, d, *J*= 0.9 Hz, 5-CH_3), 2.58-2.77 (4H, m, H-2'a, H-2'b and butyl), 3.53-3.72 (2H, m, H-5'a and H-5'b), 4.14-4.18 (1H, m, H-4'), 5.26-5.31 (2H, m, H-3' and 5'-OH), 6.40 (1H, app t, *J*= 6.6 Hz, H-1'), 7.81 (1H, d, *J*= 1.2 Hz, H-6), 8.04 (1H, s, H-5"), 11.33 (1H, s, 3-NH).

^{13}C NMR (75 MHz, DMSO-d_6): δ 12.26 (5-CH_3), 13.71, 22.71, 24.70, and 31.03 (butyl), 37.12 (C-2'), 58.95 (C-5'), 60.76 (C-3'), 83.88 (C-1'), 84.51 (C-4'), 109.63 (C-5), 121.39 (C-5"), 136.27 (C-6), 147.22 (C-4"), 150.46 (C-2), 163.76 (C-4).

Exact Mass (ESI-MS) for $C_{16}H_{24}N_5O_4$ $[M+H]^+$ found: 350.1820, calcd: 350.1823.

3'-Deoxy-3'-(4-phenyl-1,2,3-triazol-1-yl)-β-D-thymidine (1.50)

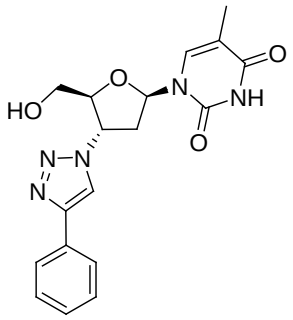

Reaction of compound **1.6** (50 mg, 0.19 mmol) with phenylacetylene (41 µL, 0.37 mmol) following the general procedure for the synthesis of 4"-substituted 3'-deoxy-3'-(1,2,3-triazol-1-yl)-β-D-thymidine derivatives afforded compound **1.50** in 72% yield (49 mg).

^{1}H NMR (300 MHz, DMSO-d_6): δ 1.82 (3H, d, *J*= 0.9 Hz, 5-CH_3), 2.65-2.86 (2H, m, H-2'a and H-2'b), 3.61-3.77 (2H, m, H-5'a and H-5'b), 4.27-4.31 (1H, m, H-4'), 5.31 (1H, app br s, 5'-OH), 5.38-5.45 (1H, m, H-3'), 6.46 (1H, app t, *J*= 6.3 Hz, H-1'), 7.33-7.38 (1H, m, Ph), 7.44-7.49 (2H, m, Ph), 7.85-7.88 (3H, m, Ph and H-6), 8.78 (1H, s, H-5"), 11.36 (1H, s, 3-NH).

^{13}C NMR (75 MHz, DMSO-d_6): δ 12.27 (5-CH_3), 37.15 (C-2'), 59.37 (C-5'), 60.76 (C-3'), 83.90 (C-1'), 84.43 (C-4'), 109.65 (C-5), 121.01 (C-5"), 125.17, 128.00, 128.95 and 130.58 (Ph), 136.26 (C-6), 146.57 (C-4"), 150.46 (C-2), 163.75 (C-4).

Exact Mass (ESI-MS) for $C_{18}H_{20}N_5O_4$ $[M+H]^+$ found: 370.1517, calcd: 370.1510.

3'-(4-Benzyl-1,2,3-triazol-1-yl)-3'-deoxy-β-D-thymidine (1.51)

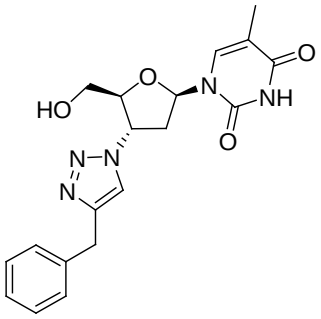

Reaction of compound **1.6** (50 mg, 0.19 mmol) with 3-phenyl-1-propyne (58 µL, 0.47 mmol) following the general procedure for the synthesis of 4"-substituted 3'-deoxy-3'-(1,2,3-triazol-1-yl)-β-D-thymidine derivatives gave compound **1.51** (42 mg, 59%) as a white powder.

^{1}H NMR (300 MHz, DMSO-d_6): δ 1.80 (3H, d, *J*= 1.2 Hz, 5-CH_3), 2.56-2.75 (2H, m, H-2'a and H-2'b), 3.53-3.64 (2H, m, H-5'a and H-5'b), 4.00 (2H, s, Bn), 4.16-4.20 (1H, m, H-4'), 5.24-5.34 (2H, m, 5'-OH and H-3'), 6.40 (1H, app t, *J*= 6.6 Hz, H-1'), 7.18-7.33 (5H, m, Bn), 7.80 (1H, d, *J*= 1.2 Hz, H-6), 8.03 (1H, s, H-5"), 11.33 (1H, s, 3-NH).

^{13}C NMR (75 MHz, DMSO-d_6): δ 12.24 (5-CH_3), 31.28 (Bn), 37.08 (C-2'), 59.05 (C-5'), 60.75 (C-3'), 83.83 (C-1'), 84.43 (C-4'), 109.60 (C-5), 122.15 (C-5"), 126.20, 128.44, and 128.56 (Bn), 136.23 (C-6), 139.41 (Bn), 146.34 (C-4"), 150.43 (C-2), 163.72 (C-4).

Exact Mass (ESI-MS) for $C_{19}H_{22}N_5O_4$ $[M+H]^+$ found: 384.1672, calcd: 384.1666.

3'-(4-Cyclopentylmethyl-1,2,3-triazol-1-yl)-3'-deoxy-β-D-thymidine (1.52)

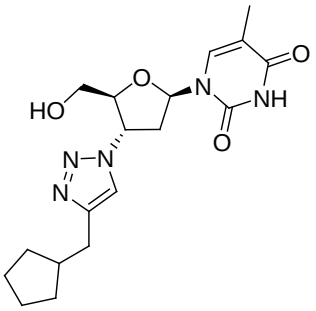

Reaction of compound **1.6** (89 mg, 0.33 mmol) with 3-cyclopentyl-1-propyne (88 µL, 0.66 mmol) following the general procedure for the synthesis of 4"-substituted 3'-deoxy-3'-(1,2,3-triazol-1-yl)-β-D-thymidine derivatives yielded compound **1.52** (86 mg, 69%) as a white powder.

^{1}H NMR (300 MHz, DMSO-d_6): δ 1.16-1.23 (2H, m, cyclopentyl), 1.46-1.59 (4H, m, cyclopentyl), 1.76-1.76 (2H, m, cyclopentyl), 1.81 (3H, d, *J*= 1.2 Hz, 5-CH_3), 2.06-2.16 (1H, m, cyclopentyl), 2.44-2.63 (4H, m, H-2'a, H-2'b and CH_2), 3.60-3.63 (2H, m, H-5'a and H-5'b), 4.14-4.21 (1H, m, H-4'), 5.22-5.35 (2H, m, H-3' and 5'-OH), 6.40 (1H, app t, *J*= 6.6 Hz, H-1'), 7.81 (1H, d, *J*= 1.2 Hz, H-6), 8.04 (1H, s, H-5"), 11.33 (1H, s, 3-NH).

^{13}C NMR (75 MHz, DMSO-d_6): δ 12.24 (5-CH_3), 24.61 (cyclopentyl), 31.07 (CH_2), 31.91 (cyclopentyl), 37.06 (C-2'), 58.88 (C-5'), 60.90 (C-3'), 83.83 (C-1'), 84.47 (C-4'), 109.60 (C-5), 121.63 (C-5"), 136.25 (C-6), 146.71 (C-4"), 150.43 (C-2), 163.72 (C-4).

Exact Mass (ESI-MS) for $C_{18}H_{26}N_5O_4$ $[M+H]^+$ found: 376.1975, calcd: 376.1979.

3'-[4-(*p*-Chlorophenyl)-1,2,3-triazol-1-yl]-3'-deoxy-β-D-thymidine (1.53)

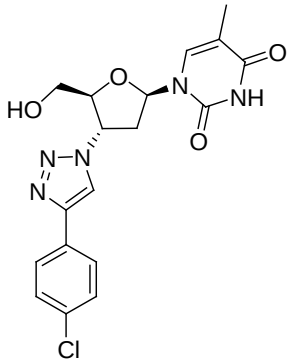

Reaction of compound **1.6** (70 mg, 0.26 mmol) with 1-chloro-4-ethynylbenzene (72 mg, 0.52 mmol) following the general procedure for the synthesis of 4"-substituted 3'-deoxy-3'-(1,2,3-triazol-1-yl)-β-D-thymidine derivatives yielded compound **1.53** (15 mg, 14%) as a light-gray powder.

^{1}H NMR (300 MHz, DMSO-d_6): δ 1.82 (3H, d, *J*= 1.2 Hz, 5-CH_3), 2.63-2.85 (2H, m, H-2'a and H-2'b), 3.60-3.74 (2H, m, H-5'a and H-5'b), 4.22-4.32 (1H, m, H-4'), 5.28-5.34 (1H, m, 5'-OH), 5.36-5.44 (1H, m, H-3'), 6.42 (1H, app t, *J*= 6.6 Hz, H-1'), 7.52-7.56 (2H, m, Ph), 7.83 (1H, d, *J*= 1.2 Hz, H-6), 7.86-7.91 (2H, m, Ph), 8.83 (1H, s, H-5"), 11.33 (1H, s, 3-NH).

^{13}C NMR (75 MHz, DMSO-d_6): δ 12.26 (5-CH_3), 37.13 (C-2'), 59.47 (C-5'), 60.76 (C-3'), 83.89 (C-1'), 84.41 (C-4'), 109.71 (C-5), 121.38 (C-5"), 126.86, 128.81, 129.03, 129.33, 129.49, and 132.42 (4-chlorophenyl), 136.25 (C-6), 145.49 (C-4"), 150.44 (C-2), 163.73 (C-4).

Exact Mass (ESI-MS) for $C_{18}H_{19}ClN_5O_4$ $[M+H]^+$ found: 404.1129, calcd: 404.1120.

3'-[4-(3,4-Dichlorophenyl)-1,2,3-triazol-1-yl]-3'-deoxy-β-D-thymidine (1.54)

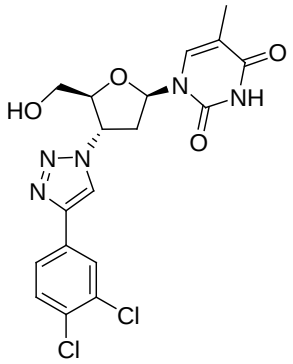

Reaction of compound **1.6** (67 mg, 0.25 mmol) with 3,4-dichlorophenylacetylene (88 mg, 0.50 mmol) following the general procedure for the synthesis of 4"-substituted 3'-deoxy-3'-(1,2,3-triazol-1-yl)-β-D-thymidine derivatives afforded compound **1.54** (25 mg, 25%) as a white powder.

^{1}H NMR (300 MHz, DMSO-d_6): δ 1.82 (3H, d, *J*= 0.9 Hz, 5-CH_3), 2.71-2.80 (2H, m, H-2'a and H-2'b), 3.64-3.77 (2H, m, H-5'a and H-5'b), 4.25-4.29 (1H, m, H-4'), 5.32 (1H, t, *J*= 5.1 Hz, 5'-OH), 5.37-5.43 (1H, m, H-3'), 6.42 (1H, app t, *J*= 6.9 Hz, H-1'), 7.72 (1H, d, *J*= 8.7 Hz, 3,4-dichlorophenyl), 7.82-7.87 (2H, m, 3,4-dichlorophenyl), 8.08 (1H, d, *J*= 1.8 Hz, H-6), 8.93 (1H, s, H-5").

^{13}C NMR (75 MHz, DMSO-d_6): δ 12.26 (5-CH_3), 37.06 (C-2'), 59.60 (C-5'), 60.76 (C-3'), 83.89 (C-1'), 84.43 (C-4'), 109.66 (C-5), 122.08 (C-5"), 125.18, 126.78, 130.26, 131.27, 131.32, and 131.77 (3,4-dichlorophenyl), 136.23 (C-6), 144.37 (C-4"), 150.44 (C-2), 163.73 (C-4).

Exact Mass (ESI-MS) for $C_{18}H_{18}Cl_2N_5O_4$ $[M+H]^+$ found: 438.0745, calcd: 438.0730.

3'-Deoxy-3'-[4-(pyridin-2-yl)-1,2,3-triazol-1-yl]-β-D-thymidine (1.55)

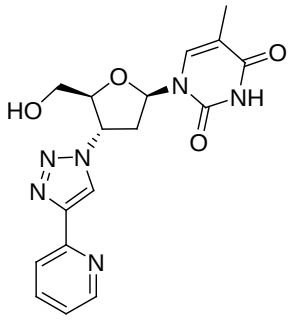

Reaction of compound **1.6** (74 mg, 0.28 mmol) with 2-ethynylpyridine (57 mg, 0.55 mmol) following the general procedure for the synthesis of 4"-substituted 3'-deoxy-3'-(1,2,3-triazol-1-yl)-β-D-thymidine derivatives gave compound **1.55** (22 mg, 21%) as a light gray powder.

^{1}H NMR (300 MHz, DMSO-d_6): δ 1.82 (3H, d, *J*= 1.2 Hz, 5-CH_3), 2.64-2.73 (1H, m, H-2'a), 2.79-2.88 (1H, m, H-2'b), 3.64-3.80 (2H, m, H-5'a and H-5'b), 4.27-4.32 (1H, m, H-4'), 5.34-5.25 (1H, m, 5'-OH), 5.43-5.52 (1H, m, H-3'), 6.46 (1H, app t, *J*= 6.9 Hz, H-1'), 7.34-7.39 (1H, m, pyridin-2-yl), 7.84 (1H, d, *J*=1.2 Hz, H-6), 7.88-7.94 (1H, m, pyridin-2-yl), 8.04-8.07 (1H, m, pyridin-2-yl), 8.60-8.63 (1H, m, pyridin-2-yl), 8.83 (1H, s, H-5"), 11.31 (1H, s, 3-NH).

^{13}C NMR (75 MHz, DMSO-d_6): δ 12.26 (5-CH_3), 37.14 (C-2'), 59.46 (C-5'), 60.73 (C-3'), 83.88 (C-1'), 84.40 (C-4'), 109.65 (C-5), 119.47 (pyridin-2-yl), 122.94 (C-5"), 123.11 (pyridin-2-yl), 136.30 (C-6), 137.27 (pyridin-2-yl), 147.46 (C-4"), 149.72 (pyridin-2-yl), 150.45 (C-2), 163.74 (C-4).

Exact Mass (ESI-MS) for $C_{17}H_{19}N_6O_4$ $[M+H]^+$ found: 371.1461, calcd: 371.1462.

General procedure for the synthesis of 5"-substituted 3'-deoxy-3'-(1,2,3-triazol-1-yl)-β-D-thymidine derivatives 1.56-1.57

The appropriate alkyne (2 equiv) and Cp*RuCl(PPh_3)$_2$ (0.02 equiv) were added to a solution of compound **1.6** (1 mmol, 1 equiv) in THF. The mixture was stirred at 65 °C, and after 24 hours the reaction was stopped. The solvent was removed and the residue dissolved in CH_2Cl_2, washed with water (3 x 10 mL), dried over $MgSO_4$, and evaporated *in vacuo*. Purification with column chromatography afforded the corresponding 5-substituted triazole.

3'-Deoxy-3'-(5-phenyl-1,2,3-triazol-1-yl)-β-D-thymidine (1.56)

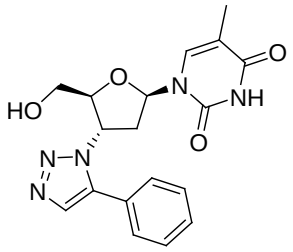

Reaction of compound **1.6** (66 mg, 0.25 mmol) with phenylacetylene (50 µL, 0.50 mmol) following the general procedure for the synthesis of 5"-substituted 3'-deoxy-3'-(1,2,3-triazol-1-yl)-β-D-thymidine derivatives afforded compound **1.56** (26 mg, 29%) as a white powder.

^{1}H NMR (300 MHz, DMSO-d_6): δ 1.77 (3H, d, *J*= 1.2 Hz, 5-CH_3), 2.56-2.63 (2H, m, H-2'a and H-2'b), 3.47-3.53 (1H, m, H-5'a), 3.54-3.64 (1H, m, H-5'b), 4.39 (1H, app dt, *J*= 3.6 Hz, H-4'), 5.14-5.19 (1H, m, H-3), 5.22-5.27 (1H, m, 5'-OH), 6.56 (1H, app t, *J*= 6.3 Hz, H-1'), 7.53-7.63 (5H, m, Ph), 7.77 (1H, d, *J*= 1.2 Hz, H-6), 7.92 (1H, s, H-4"), 11.35 (1H, s, 3-NH).

^{13}C NMR (75 MHz, DMSO-d_6): δ 12.45 (5-CH_3), 38.00 (C-2'), 58.57 (C-5'), 61.50 (C-3'), 84.97 (C-1'), 85.12 (C-4'), 110.03 (C-5), 126.49, 129.44, and 129.90 (Ph), 133.16 (C-5"), 136.45 (C-6), 138.22 (C-4"), 150.65 (C-2), 163.96 (C-4).

Exact Mass (ESI-MS) for $C_{18}H_{20}N_5O_4$ $[M+H]^+$ found: 370.1512, calcd: 370.1510.

3'-[5-(*p*-Chlorophenyl)-1,2,3-triazol-1-yl]-3'-deoxy-β-D-thymidine (1.57)

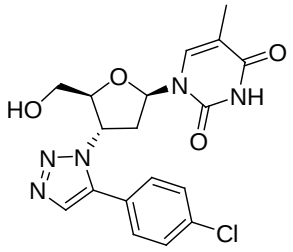

The reaction of compound **1.6** (52 mg, 0.19 mmol) with 1-chloro-4-ethynylbenzene (55 mg, 0.40 mmol) following the general procedure for the synthesis of 5"-substituted 3'-deoxy-3'-(1,2,3-triazol-1-yl)-β-D-thymidine derivatives yielded compound **1.57** (19 mg, 20%) as a white solid.

^{1}H NMR (300 MHz, DMSO-d_6): δ 1.78 (3H, app s, 5-CH_3), 2.44-2.65 (2H, m, H-2'a and H-2'b), 3.46-3.52 (1H, m, H-5'a), 3.57-3.63 (1H, m, H-5'b), 4.37-4.41 (1H, m, H-4'), 5.11-5.14 (1H, m, H-3'), 5.19-5.25 (1H, m, 5'-OH), 6.54 (1H, app t, *J*= 6.6 Hz, H-1'), 7.56-7.66 (4H, m, Ph), 7.76 (1H, app s, H-6), 7.95 (1H, s, H-4"), 11.35 (1H, s, 3-NH).

^{13}C NMR (75 MHz, DMSO-d_6): δ 12.94 (5-CH_3), 38.41 (C-2'), 59.06 (C-5'), 62.03 (C-3'), 85.33 (C-1'), 85.51 (C-4'), 110.39 (C-5), 125.98, 129.86, and 131.83 (4-chlorophenyl), 133.84 (C-5"), 135.22 (C-4"), 136.80 (C-6), 137.53 (4-chlorophenyl), 151.13 (C-2), 164.34 (C-4).

Exact Mass (ESI-MS) for $C_{18}H_{19}ClN_5O_4$ $[M+H]^+$ found: 404.1120, calcd: 404.1120;

3'-Amino-3'-deoxy-5'-*O*-triphenylmethyl-β-D-thymidine (1.58)

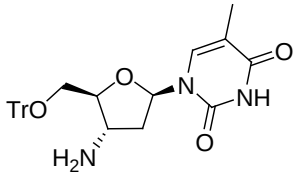

A solution of compound **1.47** (113 mg, 0.22 mmol) in methanol (6 mL) was hydrogenated under atmospheric pressure for 5 h in the presence of 10% Pd/C. The catalyst was removed by filtration through Celite and the filtrate was evaporated *in vacuo*. The residue was mixed with water and extracted with CH_2Cl_2 (3 x 10 mL). The combined organic layers were dried with $MgSO_4$ and evaporated under reduced pressure. The resulting residue was purified by column chromatography (CH_2Cl_2/MeOH 95:5) to obtain pure compound **1.58** (79 mg, 73%) as a white solid.

^{1}H NMR (300 MHz, DMSO-d_6): δ 1.49 (3H, app s, 5-CH_3), 1.90-2.08 (1H, m, H-2'a), 2.17-2.52 (1H, m, H-2'b), 3.22-3.27 (2H, m, H-5'a and H-5'b), 3.47-3.53 (1H, app dd, *J*= 6.6 Hz, *J*= 13.5 Hz, H-3'), 3.67-3.70 (1H, m, H-4'), 6.14 (1H, dd, *J*= 5.4 Hz, *J*= 6.8 Hz, H-1'), 7.25-7.42 (15H, m, Tr), 7.49 (1H, d, *J*= 0.9 Hz, H-6).

^{13}C NMR (75 MHz, DMSO-d_6): δ 12.56 (5-CH_3), 41.34 (C-2'), 52.23 (C-3'), 64.55 (C-5'), 84.28 (C-1'), 86.21 (C-4'), 86.92 (Tr), 109.97 (C-5), 127.81, 128.64 and 128.97 (Tr), 136.51 (C-6), 144.30 (Tr), 151.05 (C-2), 164.42 (C-4).

Exact Mass (ESI-MS) for $C_{29}H_{29}N_3NaO_4$ $[M+Na]^+$ found: 506.2050, calcd: 506.2057.

_N_-(3'-Deoxy-5'-_O_-triphenylmethyl-β-D-thymidin-3'-yl)-_N'_-(4-chloro-3-(trifluoromethyl)phenyl)-thiourea (1.59)

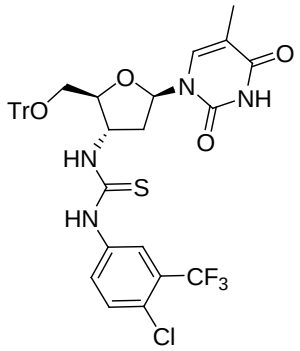

To a suspension of compound **1.58** (2.36 g, 4.88 mmol) in DMF (44 mL) was added 4-chloro-3-(trifluoromethyl)phenyl isothiocyanate (1.0 mL, 6.35 mmol) in 58 mL DMF at 0 °C. The reaction was stirred at room temperature for 3 h. The solvent was evaporated to dryness and the residue purified by column chromatography (CH_2Cl_2/MeOH 97:3) affording thiourea **1.59** as a white foam (3.44 g, 98%).

^{1}H NMR (300 MHz, DMSO-d_6): δ 1.46 (3H, d, *J*= 0.9 Hz, 5-CH_3), 2.26-2.34 (1H, m, H-2'a), 2.48-2.58 (1H, m, H-2'b), 3.18 (2H, d, *J*= 4.8 Hz, H-5'a and H-5'b), 4.07-4.12 (1H, m, H-4'), 5.21 (1H, app br s, H-3'), 6.28 (1H, app t, *J*= 6.6 Hz, H-1'), 7.24-7.44 (15H, m, Tr), 7.60-7.71 (3H, m, subs Ph), 8.03 (1H, s, H-6), 8.62 (1H, d, *J*= 6.3 Hz, 3'-NH), 9.84 (1H, s, N'H), 11.37 (1H, s, 3-NH).

^{13}C NMR (75 MHz, DMSO-d_6): δ 12.45 (5-CH_3), 37.52 (C-2'), 54.98 (C-5'), 64.69 (C-3'), 83.67 (C-1'), 84.31 (C-4'), 87.20 (Tr), 110.36 (C-5), 121.57 (CF_3), 125.19 (subs Ph), 126.78, 127.19, 127.59, 127.85, 128.40, 128.65, 128.80, and 128.99 (subs Ph and Tr), 132.37 and 136.24 (subs Ph), 139.71 (C-6), 144.13 (Tr), 151.06 (C-2), 164.35 (C-4), 181.32 (C=S).

Exact Mass (ESI-MS) for $C_{37}H_{32}ClF_3N_4NaO_4S$ $[M+Na]^+$ found: 743.1677, calcd: 743.1675.

(_E_)-5-(2-Bromovinyl)-2'-deoxy-5'-_O_-triphenylmethyl-β-D-uridine (1.60)

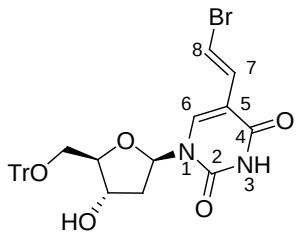

To a solution of (*E*)-5-(2-bromovinyl)-2'-deoxyuridine (BVDU, **1.10**) (467 mg, 1.40 mmol) in anhydrous pyridine (3 mL) was added trityl chloride (0.460 g, 1.65 mmol). The mixture was heated to 65 °C and stirred overnight. The reaction mixture was then diluted with CH_2Cl_2 (3 mL), washed with saturated aqueous $NaHCO_3$ (3 x 10 mL), and dried over anhydrous $MgSO_4$. The solvent was removed under

reduced pressure, and the resulting residue was purified by column chromatography (CH_2Cl_2/MeOH 94:6), affording **1.60** as a white foam (482 mg, 65%).

^{1}H NMR (300 MHz, DMSO-d_6): δ 2.12-2.31 (2H, m, H-2'a and H-2'b), 3.13-3.24 (2H, m, H-5'a and H-5'b), 3.86-3.90 (1H, m, H-4'), 4.24-4.27 (1H, m, H-3'), 5.32 (1H, d, *J*= 4,7 Hz, 3'-OH), 6.16 (1H, app t, *J*= 6,7 Hz, H-1'), 6.45 (1H, d, *J*= 13,5 Hz, H-8), 7.18 (1H, d, *J*= 13,5 Hz, H-7), 7.22-7.38 (15H, m, Tr), 7.72 (1H, s, H-6) 11.60 (1H, br s, 3-NH).

^{13}C NMR (75 MHz, DMSO-d_6): δ 38.69 (C-2'), 64.00 (C-5'), 70.06 (C-3'), 84.36 (C-1'), 85.47 (C-4'), 86.24 (Tr), 106.97 (C-5), 109.95 (C-8), 123.91, 127.16, 127.97, 128.56, and 128.26 (Tr), 129.68 (C-7), 139.32 (C-6), 148.52 (Tr), 149.26 (C-2), 161.68 (C-4).

Exact Mass (ESI-MS) for $C_{30}H_{28}BrN_2O_5$ $[M+H]^+$ found: 575.1118, calcd: 575.1176.

2,3'-*O*-Anhydro-(*E*)-5-(2-bromovinyl)-2'-deoxy-5'-*O*-triphenylmethyl-β-D-uridine (1.62)

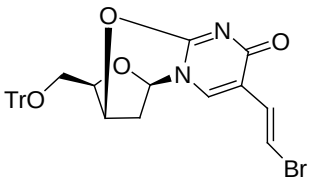

To an ice-cooled solution of compound **1.60** (482 mg, 0.84 mmol) in pyridine (3 mL) was added methanesulfonyl chloride (0.20 mL, 2.51 mmol). The reaction mixture was stirred for 2 h, quenched with $NaHCO_3$, and extracted with EtOAc (3 x 10 mL). The combined organic layers were dried over $MgSO_4$ and evaporated to dryness. The residue was dissolved in 10 mL of ethanol and dry Et_3N (0.68 mL, 4.88 mmol) was added. The mixture was heated, under reflux, for 18 h. The reaction was cooled, extracted with CH_2Cl_2 (3 x 10 mL), and the combined organic layers were dried over $MgSO_4$ and evaporated to dryness. The resulting residue was purified by column chromatography (CH_2Cl_2/MeOH 96:4), yielding compound **1.62** as a white foam (351 mg, 75%).

^{1}H NMR (300 MHz, DMSO-d_6): δ 2.43-2.67 (2H, m, H-2'a and H-2'b), 3.11-3.13 (2H, m, H-5'a and H-5'b), 4.43-4.49 (1H, m, H-4'), 5.38 (1H, app s, H-3'), 5.92 (1H, app d, *J*= 3.5 Hz, H-1'), 6.86 (1H, d, *J*= 13.5 Hz, H-8), 7.20-7.41 (15H, m, Tr), 7.54 (1H, d, *J*= 13.5 Hz, H-7), 7.96 (1H, s, H-6).

^{13}C NMR (75 MHz, DMSO-d_6): δ 32.73 (C-2'), 62.32 (C-5'), 77.55 (C-3'), 83.57 (C-1'), 86.39 (Tr), 87.57 (C-4'), 109.31 (C-5), 115.17 (C-8), 127.06, 127.92, and 128.16 (Tr), 130.17 (C-7), 139.62 (C-6), 143.22 (Tr), 152.29 (C-2), 168.07 (C-4).

Exact Mass (ESI-MS) for $C_{30}H_{26}BrN_2O$ $[M+H]^+$ found: 557.1061, calcd: 557.1070.

3'-Azido-(*E*)-5-(2-bromovinyl)-2',3'-dideoxy-5'-*O*-triphenylmethyl-β-D-uridine (1.63)

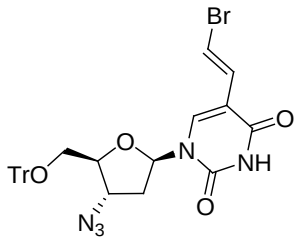

p-Nitrophenyl alcohol (114 mg, 0.82 mmol) first and then NaN_3 (267 mg, 4.12 mmol) were added to a suspension of anhydronucleoside **1.62** (229 mg, 0.41 mmol) in dry DMF (5 mL) under N_2. The solution was stirred for 7 h at 110 °C. The reaction was quenched with 5 mL water and extracted with CH_2Cl_2 (3 x 5 mL). The combined organic layers were dried over $MgSO_4$ and evaporated to dryness. The resulting residue was purified by column chromatography (CH_2Cl_2/MeOH 96:4), affording compound **1.63** as a yellow oil (195 mg, 79%).

^{1}H NMR (300 MHz, DMSO-d_6): δ 2.35-2.58 (2H, m, H-2'a and H-2'b), 3.25-3.40 (2H, m, H-5'a and H-5'b), 3.85-3.92 (1H, m, H-4'), 4.58 (1H, dt, *J*= 7.5 Hz, H-3'), 6.15 (1H, dd, *J*= 4.5 Hz, *J*= 7.2 Hz, H-1'), 6.64 (1H, d, *J*= 13.5 Hz, H-8), 7.23-7.44 (16H, m, H-7 and Tr), 7.79 (1H, s, H-6).

^{13}C NMR (75 MHz, DMSO-d_6): δ 35.90 (C-2'), 59.16 (C-5'), 62.81 (C-3'), 82.11 (C-1'), 83.79 (C-4'), 86.37 (Tr), 110.12 (C-5), 115.79 (C-8), 126.19, 127.05, 127.20, 127.86, 127.99, and 128.22 (Tr), 129.71 (C-7), 139.59 (C-6), 143.38 (Tr), 149.23 (C-2), 161.63 (C-4).

Exact Mass (ESI-MS) for $C_{30}H_{27}BrN_5O_4$ $[M+H]^+$ found: 600.1274, calcd: 600.1241.

3'-Azido-(*E*)-5-(2-bromovinyl)-2',3'-dideoxy-β-D-uridine (1.64)

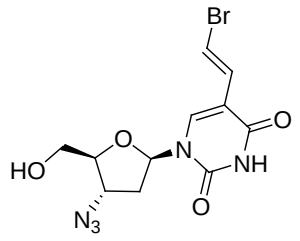

Compound **1.63** (260 mg, 0.43 mmol) was dissolved in a mixture of $ZnBr_2$ (1.59 g, 7.05 mmol) in CH_2Cl_2/*i*PrOH (7 mL, 85:15) and stirred overnight at room temperature. The reaction was quenched with water and extracted with CH_2Cl_2 (3 x 10 mL). The combined organic layers were dried over $MgSO_4$ and evaporated to dryness. The resulting residue was purified by column chromatography (CH_2Cl_2/MeOH 98:2), affording compound **1.64** (139 mg, 90%) as a yellow-brown oil.

^{1}H NMR (300 MHz, DMSO-d_6): δ 2.31-2.44 (2H, m, H-2'a and H-2'b), 3.60-3.71 (2H, m, H-5'a and H-5'b), 3.80-3.86 (1H, m, H-4'), 4.38-4.44 (1H, m, H-3'), 5.30 (1H, app s, 5'-OH), 6.05-6.09 (1H, m, H-1'), 6.84 (1H, d, *J*= 13.8 Hz, H-8), 7.25 (1H, d, *J*= 13.5 Hz, H-7), 8.04 (1H, s, H-6).

^{13}C NMR (75 MHz, DMSO-d_6): δ 36.67 (C-2'), 54.92 (C-5'), 60.36 (C-3'), 84.12 (C-1'), 84.37 (C-4'), 106.60 (C-5), 109.71 (C-8), 129.83 (C-7), 139.38 (C-6), 149.24 (C-2), 168.25 (C-4).

Exact Mass (ESI-MS) for $C_{11}H_{13}BrN_5O_4$ $[M+H]^+$ found: 358.0119, calcd: 358.0145.

(*E*)-5-(2-Bromovinyl)-2',3'-dideoxy-3'-(4-phenyl-1,2,3-triazol-1-yl)-β-D-uridine (1.65)

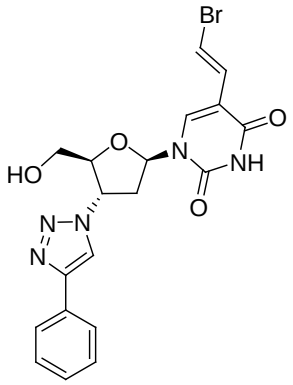

Reaction of compound **1.64** (64 mg, 0.18 mmol) with phenylacetylene (39 µL, 0.36 mmol) was performed as described in the general procedure for the synthesis of 4"-substituted 3'-deoxy-3'-(1,2,3-triazol-1-yl)-β-D-thymidine derivatives. Compound **1.65** was obtained as a white solid in 6% yield (5 mg).

^{1}H NMR (300 MHz, DMSO-d_6): δ 2.73-2.80 (1H, m, H-2'a), 2.86-2.95 (1H, m, H-2'b), 3.66-3.70 (1H, m, H-5'a), 3.76-3.80 (1H, m, H-5'b), 4.32-4.34 (1H, m, H-4'), 5.34-5.48 (2H, m, 5'-OH and H-3'), 6.42 (1H, app t, *J*= 6.9 Hz, H-1'), 6.90 (1H, d, *J*= 13.2 Hz, H-8), 7.28 (1H, d, *J*= 13.5 Hz, H-7), 7.33-7.38 (1H, m, Ph), 7.44-7.50 (2H, m, Ph), 7.85 (2H, d, *J*= 5.1 Hz, Ph), 8.25 (1H, s, H-6), 8.77 (1H, s, H-5").

^{13}C NMR (75 MHz, DMSO-d_6): δ 39.95 (C-2'), 55.47 (C-5'), 63.77 (C-3'), 84.66 (C-1'), 4.80 (C-4'), 108.00 (C-5), 109.92 (C-8), 122.28 (C-5"), 126.89 (Ph), 129.77 (C-7), 130.87, 131.58, and 133.20 (Ph), 139.02 (C-6), 144.25 (C-4"), 148.71 (C-2), 160.16 (C-4).

Exact Mass (ESI-MS) for $C_{19}H_{19}BrN_5O_4$ $[M+H]^+$ found: 460.0637, calcd: 460.0615.

(*E*)-5-(2-Bromovinyl)-3'-[4-(*p*-chlorophenyl)-1,2,3-triazol-1-yl]-2',3'-dideoxy-β-D-uridine (1.66)

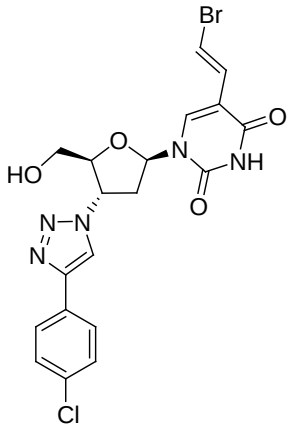

Reaction of compound **1.65** (69 mg, 0.19 mmol) with 1-chloro-4-ethynylbenzene (52 mg, 0.38 mmol) was performed as described in the general procedure for the synthesis of 4"-substituted 3'-deoxy-3'-(1,2,3-triazol-1-yl)-β-D-thymidine derivatives, affording compound **1.66** (6 mg) in a 6% yield.

^{1}H NMR (300 MHz, DMSO-d_6): δ 2.73-2.80 (1H, m, H-2'a), 2.85-2.94 (1H, m, H-2'b), 3.64-3.71 (1H, m, H-5'a), 3.75-3.81 (1H, m, H-5'b), 4.32-4.35 (1H, m, H-4'), 5.36-5.46 (2H, m, 5'-OH and H-3'), 6.41 (1H, app t, *J*= 6.9 Hz, H-1'), 6.89 (1H, d, *J*= 13.5 Hz, H-8), 7.28 (1H, d, *J*= 13.5 Hz, H-7), 7.52-7.56 (2H, m, Ph), 7.86-7.90 (2H, m, Ph), 8.21 (1H, s, H-6), 8.82 (1H, s, H-5"), 11.65 (1H, s, 3-NH).

^{13}C NMR (75 MHz, DMSO-d_6): δ 37.18 (C-2'), 55.73 (C-5'), 61.79 (C-3'), 84.59 (C-1'), 84.83 (C-4'), 107.44 (C-5), 109.90 (C-8), 121.37 (C-5"), 126.89, 129.06, and 129.47 (4-chlorophenyl), 129.83 (C-7), 132.461 (4-chlorophenyl), 139.54 (C-6), 145.51 (C-4"), 149.32 (C-2), 160.16 (C-4).

Exact Mass (ESI-MS) for $C_{19}H_{18}BrClN_5O_4$ $[M+H]^+$ found: 494.0219, calcd: 494.0225.

3-[3-Azido-2,3-dideoxy-5-*O*-triphenylmethyl-β-D-ribofuranosyl)]-2,3-dihydrofuro-[2,3-*d*]pyrimidin-2-one (1.67)

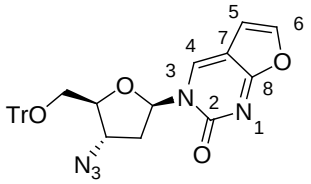

NaN_3 (1.21 g, 18.57 mmol) was added to a suspension of anhydronucleoside **1.62** (1.04 g, 1.86 mmol) in dry DMF (25 mL) under N_2. The solution was stirred overnight at 110 °C. The reaction was quenched with 25 mL water and extracted with CH_2Cl_2 (3 x 25 mL). The combined organic layers were dried over $MgSO_4$ and evaporated to dryness. The resulting residue was purified by column chromatography (CH_2Cl_2/MeOH 97:3), affording compound **1.67** as a brown foam (600 mg, 54 %).

^{1}H NMR (300 MHz, DMSO-d_6): δ 2.53-2.65 (2H, m, H-2'a and H-2'b), 3.30-3.40 (2H, m, H-5'a and H-5'b), 4.02-4.08 (1H, m, H-4'), 4.56 (1H, app dd, *J*= 7.2 Hz, *J*= 14.1 Hz, H-3'), 6.09-6.14 (2H, m, H-1' and H-5), 7.23-7.43 (15H, m, Tr), 7.71 (1H, d, *J*= 3.0 Hz, H-6), 8.71 (1H, s, H-4).

^{13}C NMR (75 MHz, DMSO-d_6): δ 37.77 (C-2'), 58.40 and 62.13 (C-3' and C-5'), 83.08 (C-4'), 86.83 (Tr), 87.08 (C-1'), 104.63 and 104.70 (C-5 and C-7), 127.30, 128.11 and 128.24 (Tr), 138.67 (C-4), 143.78 (Tr), 145.00 (C-6), 153.63 (C-2), 171.33 (C-8).

Exact Mass (ESI-MS) for $C_{30}H_{25}N_5NaO_4$ $[M+Na]^+$ found: 542.1792, calcd: 542.1799.

3-[3-Azido-2,3-dideoxy-β-D-ribofuranosyl]-2,3-dihydrofuro-[2,3-*d*]pyrimidin-2-one (1.68)

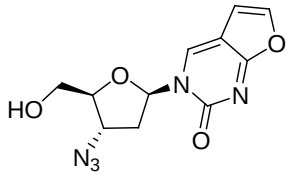

Compound **1.67** (98 mg, 0.19 mmol) was dissolved in a mixture of $ZnBr_2$ (678 mg, 3.01 mmol) in CH_2Cl_2/*i*PrOH (3 mL, 85:15) and stirred overnight at room temperature. The reaction was quenched with water and extracted with CH_2Cl_2 (3 x 5 mL). The combined organic layers were dried over $MgSO_4$ and evaporated to dryness. The resulting residue was purified by column chromatography (CH_2Cl_2/MeOH 95:5) yielding compound **1.68** (20 mg, 39%) as a yellow powder.

^{1}H NMR (300 MHz, DMSO-d_6): δ 2.37-2.45 (1H, m, H-2'a), 2.53-2.60 (1H, m, H-2'b), 3.64-3.78 (2H, m, H-5'a and H-5'b), 3.97-4.01 (1H, m, H-4'), 4.35 (1H, app dd, *J*= 6.3 Hz, *J*= 12.6 Hz, H-3'), 5.38 (1H, app br s, 5'-OH), 6.08-6.12 (1H, m, H-1'), 6.82 (1H, d, *J*= 2.7 Hz, H-5), 7.75 (1H, d, *J*= 2.7 Hz, H-6), 8.88 (1H, s, H-4).

^{13}C NMR (75 MHz, DMSO-d_6): δ 37.95 (C-2'), 58.78 and 60.03 (C-3' and C-5'), 85.17 (C-4'), 87.16 (C-1'), 104.71 and 105.26 (C-5 and C-7), 139.04 (C-4), 144.88 (C-6), 153.74 (C-2), 171.35 (C-8).

Exact Mass (ESI-MS) for $C_{11}H_{11}N_5NaO_4$ $[M+Na]^+$ found: 300.0713, calcd: 300.0703.

2.7.2 Experimental Assays

Radiochemicals

The radiolabeled substrate [CH_3-^{3}H]dThd (70 Ci/mmol) was obtained from Moravek Biochemicals (Brea, CA).

Thymidine Kinase Assay Using [CH_3-^{3}H]dThd as the Natural Substrate

The activity of recombinant TK-1, TK-2, herpes simplex virus-1 TK, varicella zoster virus TK, and the multifunctional deoxynucleoside kinase of *Drosophila melanogaster* and the 50% inhibitory concentration of the test compounds were assayed in a 50 µL reaction mixture containing 50 mM Tris/HCl, pH 8.0, 2.5 mM $MgCl_2$, 10 mM dithiothreitol, 0.5 mM CHAPS, 3 mg/mL bovine serum albumin, 2.5 mM ATP, 1 µM [methyl-^{3}H]dThd, and enzyme. The samples were incubated at 37 °C for 30 min in the presence or absence of different concentrations (5-fold dilutions) of the test compounds. At this time point, the enzyme reaction still proceeded linearly. Aliquots of 45 µL of the reaction mixtures were spotted on Whatman DE-81 filter paper disks (Whatman, Clifton, NJ). The filters were washed three times for 5 min each in 1 mM ammonium formate, once for 1 min in water, and once for 5 min in ethanol. The radioactivity was determined by scintillation counting. To determine the K_m (for dThd or ATP) and K_i values (for the inhibitors), varying concentrations of dThd (ranging between 0.4 and 5 µM) were used at saturating concentrations of ATP (2.5 mM) or varying concentrations of ATP (ranging between 5 and 100 µM) at saturating concentrations of dThd (20 µM). The kinetic values were derived from Lineweaver-Burk plots.

Cytostatic Assay

Human osteosarcoma cells (OST TK$^-$) that had been transduced by the *Drosophila melanogaster* deoxynucleoside kinase gene were seeded in 48-well plates at 20000 cells/1 mL well in DMEM supplemented with 10% fetal calf serum, 10 mM HEPES, 1 mM Na pyruvate, and 2 mM L-glutamine. The cells were incubated at 37 °C in the presence of 10 or 4 µM compound **1.66**. One day later, serial dilutions of BVDU (**1.10**) and 5FdUrd (**1.69**) were added to the cell cultures. At day 4, cell number was counted using a Coulter particle counter model Z1, enabling the calculation of the 50% inhibitory concentrations of BVDU and 5FdUrd in the presence or absence of compound **1.66**.

Molecular Modeling

The thymine ring of compound **1.53** was manually docked into the substrate-binding site of the previously reported[59] homology-based model of human TK-2 in complex with ATP and Mg^{2+}, and the two alternative locations for the phenyl triazole substituent were explored. Energy refinement of the resulting complexes and subsequent molecular dynamics simulations were carried out essentially as described[59] using the AMBER 10.0 suite of programs.[77]

3 SYNTHESIS AND BIOLOGICAL EVALUATION OF 3'-GUANIDINE-SUBSTITUTED THYMIDINE AND BVDU DERIVATIVES

3.1 OBJECTIVES

Modeling studies on the binding of compound **1.43** to human TK-2 suggested that the nitrogen atoms of the thiourea urea group of **1.43** could interact favorably with the oxygens of the γ-phosphate of the co-substrate ATP,[59] whereas for **1.53** a binding mode involving a water-mediated interaction with the side chain of the central glutamate in the EEE LID region of the enzyme was proposed (Figure I.27).[73] To further expand the array of hydrogen-bonding functionalities at the 3' position and to identify those that are optimal for TK-2 inhibition, we decided to synthesize a series of novel thymidine and BVDU analogues containing a substituted amine or guanidine group instead of a thiourea at the 3' position or a 1,5-disubstituted tetrazole linker.

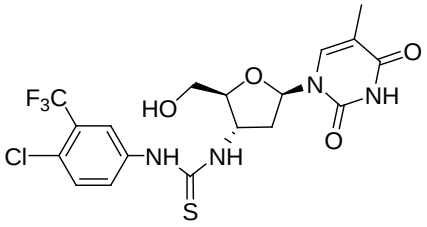

1.43

TK-2: IC_{50} = 0.15 μM
TK-1: IC_{50} = 316 μM

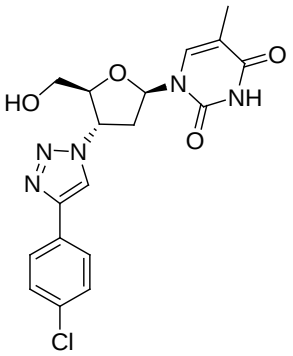

1.53

TK-2: IC_{50} = 46 nM
TK-1: IC_{50} = 71 μM

Figure I.27

3.2 CHEMISTRY

3.2.1 Synthesis of 3'-Benzylamino Analogues of Thymidine

A small series of 3'-benzylamino analogues of thymidine (**1.80-1.82**) was synthesized by treatment of amine **1.58** with different aldehydes followed by in situ reduction of the resulting imines with $NaBH_4$ and final detritylation (Scheme I.6).[78]

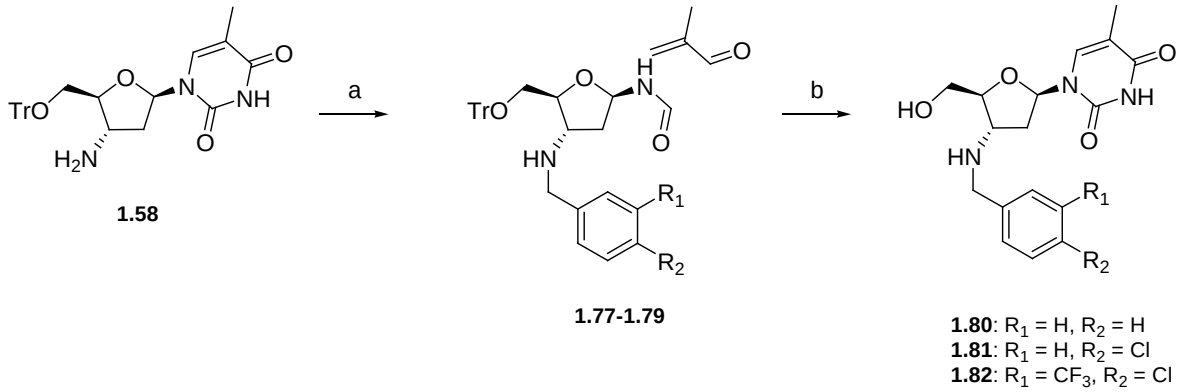

Scheme I.6. Reagents and conditions: a) (i) suitable benzaldehyde, dry MeOH, rt, 24 h; (ii) $NaBH_4$, rt, 30 min, 16-88% over 2 steps; b) $ZnBr_2$, CH_2Cl_2/*i*PrOH 85:15, rt, overnight, 34-58%.

3.2.2 Synthesis of 3'-Guanidine and 3'-Aminotetrazole Analogues of Thymidine

The guanidine analogues **1.86-1.88** were synthesized by an $HgCl_2$-promoted guanylation[79] of the 3'-thiourea precursor **1.59** which was prepared from the 3'-amino analogue **1.58**, followed by final detritylation (Scheme I.7).

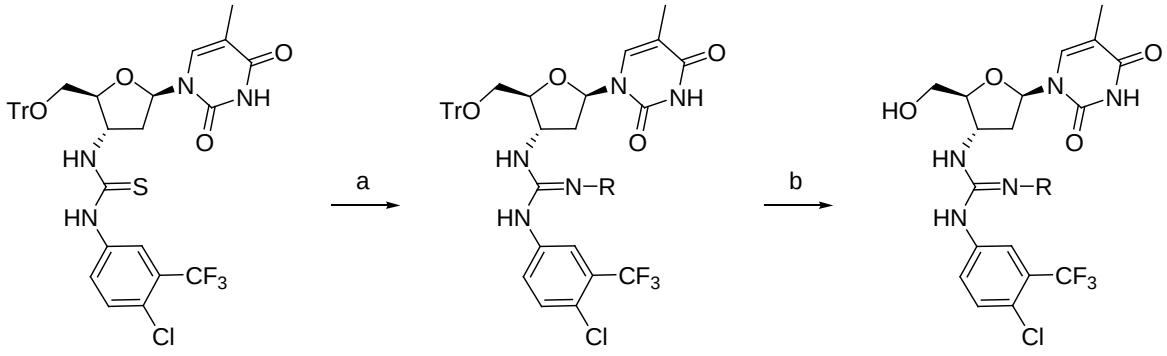

Scheme I.7. Reagents and conditions: a) suitable amine or 7N NH_3, Et_3N, $HgCl_2$, DMF, 0 °C → rt, 20 h, 56-57%; b) HCOOH/Et_2O 7:3, rt, 1 h, 64–71%.

Interestingly, upon replacement in the above mentioned guanylation conditions of the amine by sodium azide, thiourea **1.59** was converted into 5-aminotetrazole **1.89** by spontaneous electrocyclization of an intermediate guanyl azide (Scheme I.8).[80] The observed selectivity of the electrocyclization step is in accordance with earlier results, leading to the regioisomer in which the tetrazole is conjugated with the phenyl ring.[81] Two typical methods for the removal of the trityl protecting group of **1.89** were explored.[66,82] Surprisingly, treatment with $ZnBr_2$ resulted in a 9:1-mixture of both tetrazole isomers **1.90** and **1.91**, which were separated using preparative HPLC. In our view, $ZnBr_2$ may promote the observed isomerization by catalyzing opening of the tetrazole ring followed by a non-specific ring closure. This isomerization could be prevented by performing the deprotection with formic acid in ether (Scheme I.8).

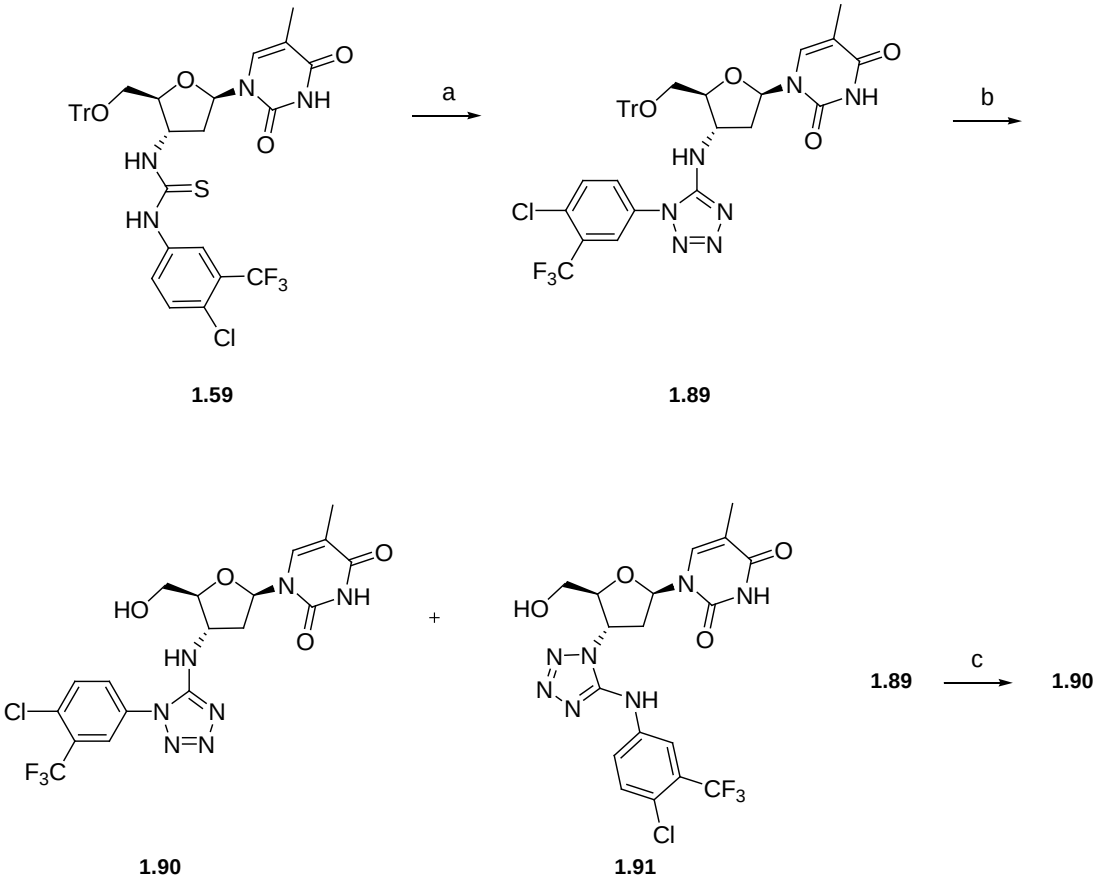

1.59 **1.89**

1.90 **1.91**

Scheme I.8. Reagents and conditions: a) NaN_3, DMF, Et_3N, $HgCl_2$, 0 °C → rt, 6 h, 31%; b) $ZnBr_2$, CH_2Cl_2/*i*PrOH (85:15), rt, overnight, 32%; c) HCOOH/Et_2O 7:3, rt, 1 h, 45%.

A possible mechanism for the formation of compound **1.89** is depicted in Scheme I.9, displacement by sodium azide of a mercury(II)-activated thiourea **I** generates an intermediate guanyl azide **II**, which upon electrocyclization, forms the corresponding 5-aminotetrazole **1.89**.[80]

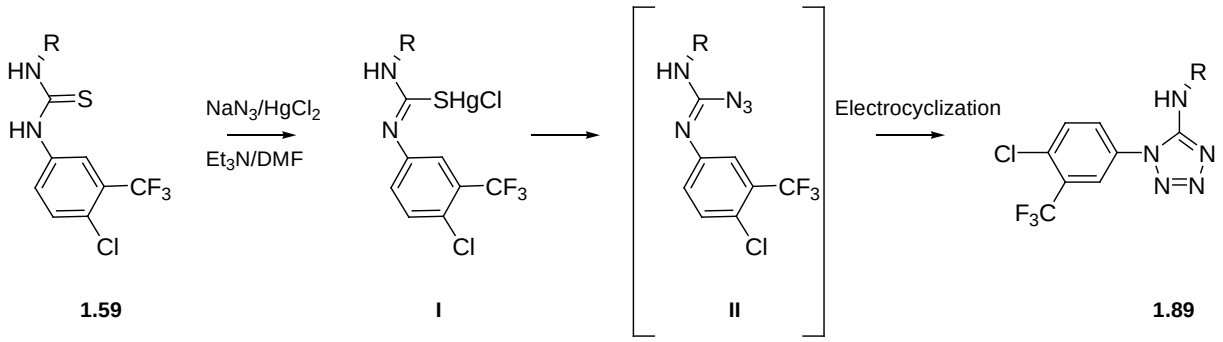

Scheme I.9. Mechanism for the formation of aminotetrazole analogue **1.89** starting from thiourea **1.59**.

An IR spectrum (performed at the Laboratory of Drug Quality and Registration, UGent) of compound **1.90** proved that the molecule represented the 1,5-aminotetrazole and not the uncyclisized azide form. Absorption in the 2100-2270 cm^{-1} region, due to azide stretching, is not present whereas the emergence of peaks in the 1400-1500 cm^{-1} region confirms the formation of a tetrazole ring (Figure I.28).

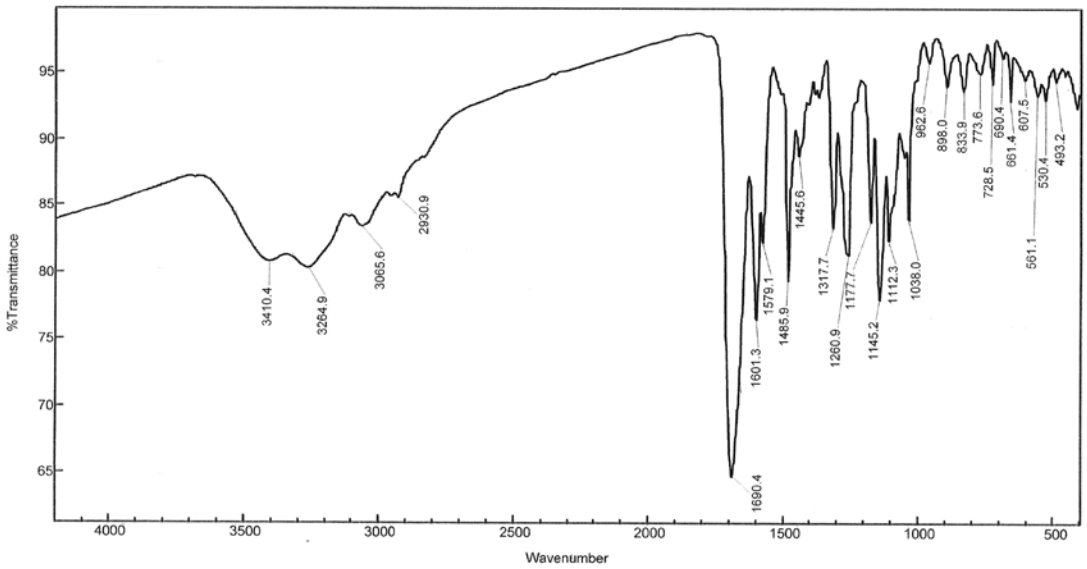

Figure I.28. IR spectra of compound **1.90**

In the case of the benzylthiourea analogue **1.92**, competitive cyclization of the guanyl azide afforded a 1:2.2-mixture of the tetrazoles **1.93** and **1.94**. This isomer ratio was only slightly affected after further trityl deprotection with $ZnBr_2$ (1:2.6-mixture of isomers **1.95** and **1.96**). Identification of each isomer was based on the multiplicity of 3'-NH and 5''-NH (e.g., **1.95**: 3'-NH, d, *J*= 6.9 Hz; **1.96**: 5''-NH, t, *J*= 5.7 Hz) (Scheme I.10).

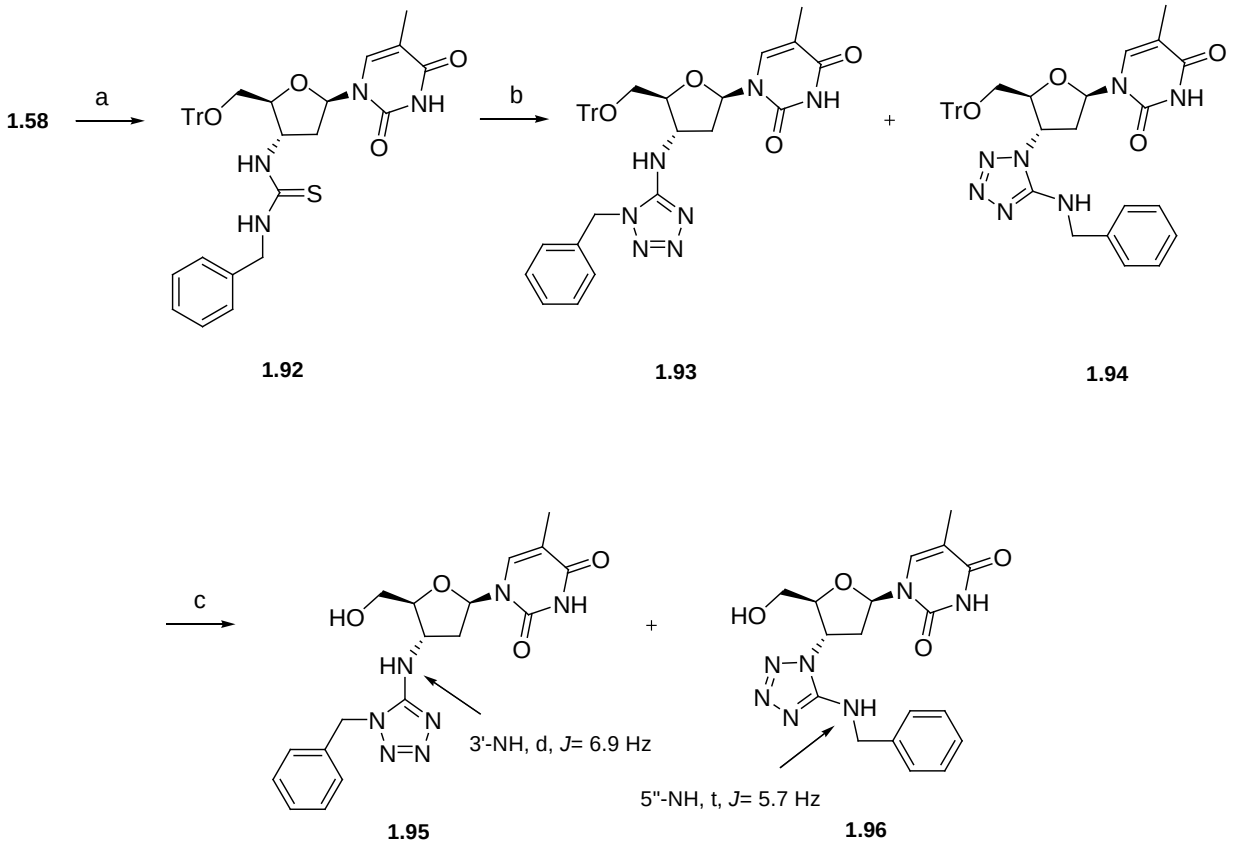

Scheme I.10. Reagents and conditions: a) benzyl isothiocyanate, DMF, 0 °C → rt, 3 h, 99%; b) NaN_3, DMF, Et_3N, $HgCl_2$, 0 ℃ → rt, 6 h, 52%; c) $ZnBr_2$, CH_2Cl_2/*i*PrOH (85:15), rt, overnight, 54%.

3.2.3 Synthesis of 3'-Aminotetrazole Analogues of BVDU

Application of an identical reaction sequence used for **1.59** on the BVDU thiourea analogue **1.98** afforded **1.100** and **1.101** (3:1) in moderate yields (Scheme I.11).

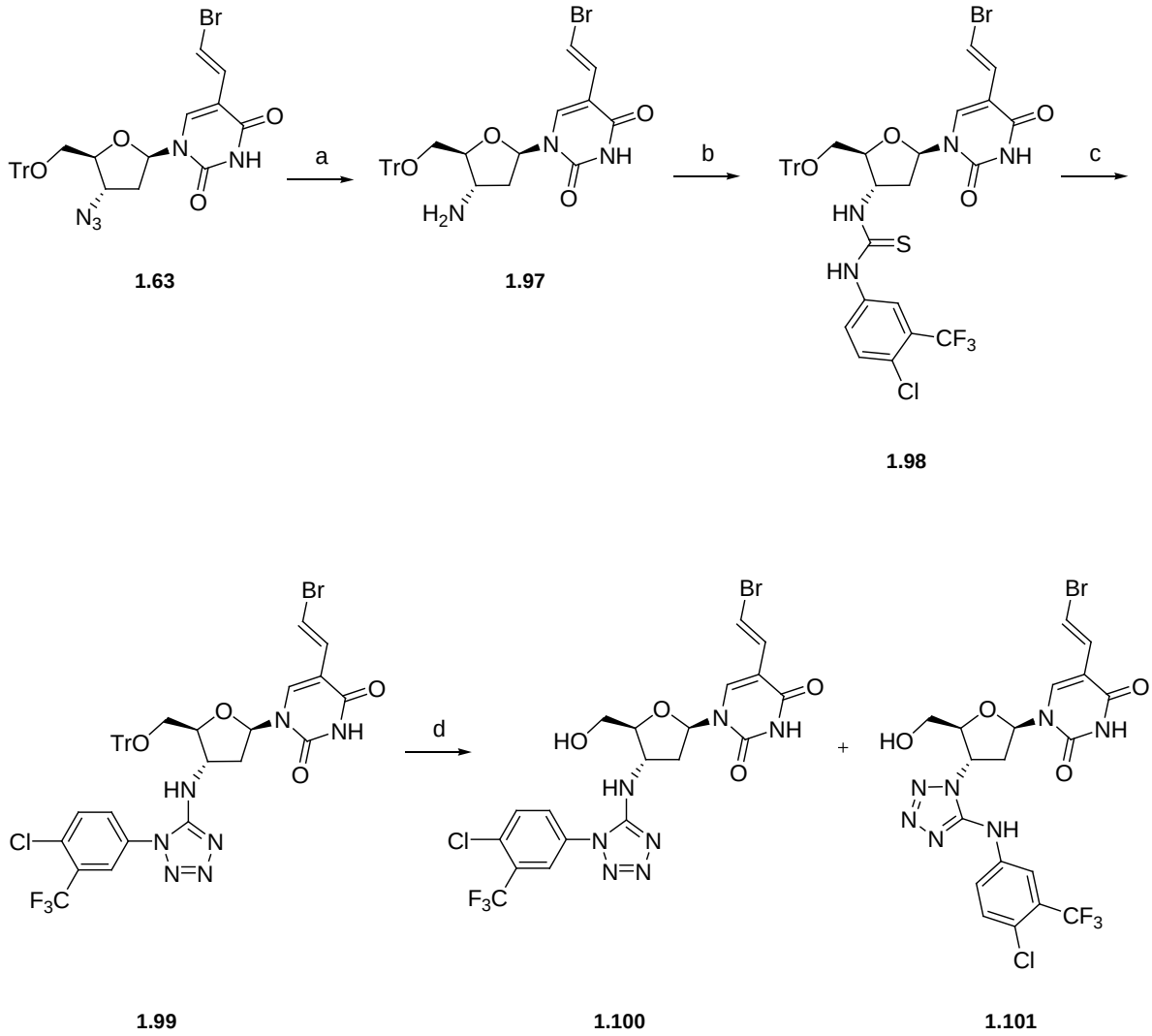

Scheme I.11. Reagents and conditions: a) PPh_3, THF, H_2O, rt, overnight, 71%; b) 4-chloro-3-(trifluoromethyl)phenyl isothiocyanate, DMF, 0 °C → rt, 3 h, 82%; c) NaN_3, $HgCl_2$, Et_3N, DMF, 0 °C → rt, 6 h, 75%; d) $ZnBr_2$, CH_2Cl_2/*i*PrOH (85:15), rt, overnight, 32%.

3.3 BIOLOGICAL EVALUATION

All compounds were evaluated for their ability to inhibit dThd phosphorylation by recombinant purified human cytosolic TK-1, human mitochondrial TK-2, HSV-1 TK, VZV-TK and *Dm*-dNK under the guidance of Prof. Dr. Jan Balzarini at the Laboratory of Virology and Chemotherapy, Rega Institute, K.U.Leuven (Table I.4). The 3'-benzylamino analogues demonstrated modest inhibitory activity on TK-2. This activity was influenced by the nature of the substituents at the phenyl ring. Derivatives containing either the unsubstituted (**1.80**) or a 4-chloro-substituted (**1.81**) phenyl gave micromolar inhibition, while the analogue possessing a 3-CF_3-4-Cl-substituted phenyl (**1.82**) displayed significantly improved TK-2 inhibitory activity. In addition, all the 3'-aminobenzyl derivatives showed poor inhibitory activity against TK-1 (IC_{50} values, 442 to ≥ 500 µM). dThd phosphorylation by TK-2 was also inhibited by the substituted guanidine analogues (compounds **1.86-1.88**), which yielded IC_{50} values ranging from 0.43 to 1.3 µM. The anti-TK-2 activity was influenced by the nature of the third substituent on the guanidine moiety. The "unsubstituted" analogue **1.86** and the *i*Pr-substituted analogue **1.88** afforded appreciable potency and excellent selectivity over TK-1 (Table I.4). In the 1,5-aminotetrazole series, the anti-TK-2 activity was clearly influenced by a) the type of isomer, b) the substituent at position N-1 of the tetrazole ring, and c) the substituent on position 5 of the base. In all cases, the isomer in which the tetrazole ring is attached to C-3' via a NH bridge (**1.90, 1.95** and **1.100**), showed the best inhibitory activity against TK-2 (IC_{50}s in the 0.014-0.90 mM range). The benzyl substituted analogue **1.95** gave submicromolar inhibition, while introduction of an electron-withdrawing 3-CF_3-4-Cl phenyl substituent significantly improved the inhibitory activity (**1.90**), which matches with that of the earlier described 3'-(4-(3,4-dichlorophenyl)-1,2,3-triazol-1-yl) analogue. Combination of this favorable 3'-modification with a 5'-*O*-trityl substituent led, as expected,[73] to an analogue (**1.89**) that was completely devoid of TK-2 inhibitory activity (IC_{50}s > 500 µM for all kinases tested). On the other hand, introduction of an additional 5-(2-bromovinyl) group (**1.100**), known to be a privileged substituent for TK-2 recognition, proved to be compatible with the 3'-modification (IC_{50} TK-2: 0.014 µM). This 5-(2-bromovinyl) substituent improved the TK-2 inhibitory activity by 2- to 3-fold, and it further caused an increase in the selectivity for TK-2 versus TK-1, resulting in the complete lack of inhibitory effect against TK-1-catalyzed dThd phosphorylation. A similar effect had previously been observed in the triazole series.[73] To the best of our knowledge, compound **1.100** is the most potent and selective inhibitor of TK-2 reported to date. The isomeric aminotetrazole analogues in which the similar substituted tetrazole group is connected directly to the sugar ring were markedly less inhibitory to TK-2 activity: **1.101** showed an IC_{50} value of 0.40 µM, that is, at least 25-fold higher than the IC_{50} value observed for **1.100** (Table I.4).

Table I.4. Inhibitory effects of thymidine and BVDU analogues on 1 µM [CH_3-^{3}H]dThd phosphorylation by deoxyribonucleoside kinases from different origins.

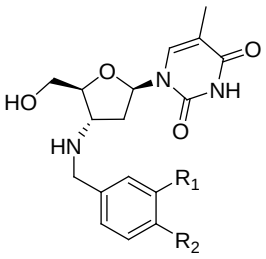

1.80-1.82

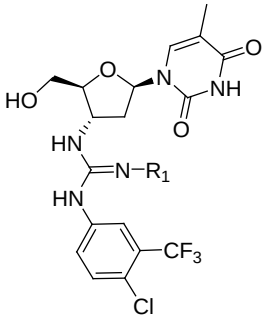

1.86-1.88

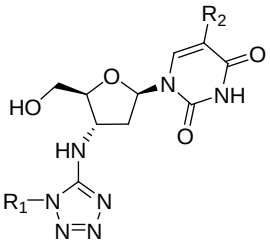

1.90, 1.95 and **1.100**

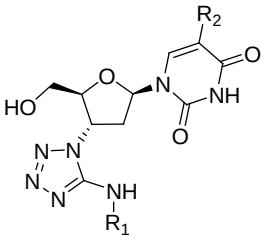

1.91, 1.96 and **1.101**

Cmpd	R_1	R_2	IC_{50}[a] (µM)				
			TK-1	TK-2	HSV-1 TK	VZV TK	*Dm*-dNK
1.80	H	H	> 500	4.6 ± 0.3	> 500	99 ± 74	48 ± 3
1.81	H	Cl	≥ 500	3.3 ± 0.2	> 500	35 ± 5	41 ± 4
1.82	CF_3	Cl	442 ± 37	0.33 ± 0.04	492 ± 12	28 ± 1	4.8 ± 0.2
1.86	H	-	355 ± 69	0.43 ± 0.02	> 500	41 ± 3	11 ± 6
1.87	Bn	-	468 ± 12	1.3 ± 0.5	372 ± 39	41 ± 1	7.7 ± 4.1
1.88	*i*Pr	-	≥ 500	0.58 ± 0.29	> 500	277 ± 35	12 ± 4
1.90	**3-CF_3,4-ClPh**	**CH_3**	**382 ± 52**	**0.035 ± 0.007**	**316 ± 39**	**63 ± 26**	**1.2 ± 0.0**
1.91	3-CF_3, 4-ClPh	CH_3	29 ± 1	0.59 ± 0.19	40 ± 0	5.5 ± 2.3	3.6 ± 0.7
1.95	Bn	CH_3	> 500	0.90 ± 0.01	> 500	144 ± 42	10 ± 6
1.96	Bn	CH_3	222 ± 112	2.6 ± 1.2	39 ± 1	3.2 ± 0.5	31 ± 4
1.100	**3-CF_3, 4-ClPh**	**Bromovinyl**	**> 500**	**0.014 ± 0.001**	**34 ± 3**	**26 ± 3**	**0.41 ± 0.04**
1.101	3-CF_3, 4-ClPh	Bromovinyl	> 500	0.40 ± 0.04	26 ± 4	6.1 ± 1.6	3.6 ± 0.2

[a]IC_{50} is the 50% inhibitory concentration of the test compounds, which was measured as the concentration required to inhibit 1 µM [CH_3-^{3}H]dThd phosphorylation by 50%. Data are the mean of at least 2 to 3 independent experiments (± S.D.).

Interestingly, a close relationship for the inhibitory concentration of the test compounds was observed between TK-2 and *Dm*-dNK (r = 0.951) but not between TK-2 and HSV-1 TK (r = -0.229) (Table I.4, Figure I.29).

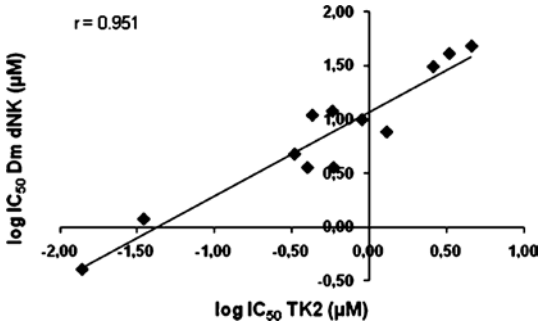

Figure I.29. Correlation between the IC_{50} values of the inhibitors shown in Table I.4 against TK-2 and *Dm*-dNK.

3.4 MOLECULAR MODELING

Gago *et al*. used the previously reported homology-built model of ATP-bound TK-2 (Part I, chapter 2) and the same methodology[59,73] to provide a rationale for the present findings in atomic detail. In the case of **1.90**, the tetrazole moiety is proposed to establish a non-water mediated interaction with the guanidinium of Arg167 whereas the amino group can establish a hydrogen bond with the hydroxyl group of Tyr177 (Figure. I.30). Interestingly, whereas Arg167 in TK-2 is positionally equivalent to Arg169 in *Dm*-dNK and Arg222 in HSV-1 TK, the structural equivalent of Tyr177 in TK-2 is also a tyrosine (Tyr179) in *Dm*-dNK but a methionine (Met231) in HSV-1 TK. This latter amino acid cannot establish a hydrogen bond with the amino group of **1.90** and this may contribute to the fact that these compounds are much better inhibitors against TK-2 and *Dm*-dNK than against HSV-1 TK.

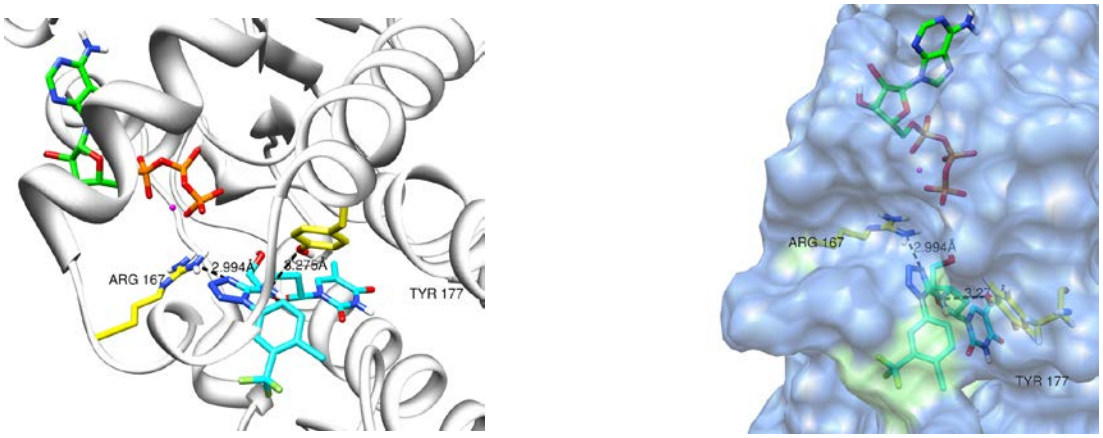

Figure I.30. (left) Detail of the substrate binding site in the refined complex of **1.90** with ATP-bound human TK-2. Inhibitor, protein and ATP carbon atoms are colored blue, grey and green, respectively. The magenta sphere represents the catalytic Mg^{2+} ion. Some of the protein side-chains relevant to the discussion are labeled and shown as sticks. Note the non-water mediated interaction between the tetrazole moiety and the guanidinium of Arg167 and the hydrogen bond between the amino group and the hydroxyl group of Tyr177. (right) Contact surface of the enzyme with inhibitor **1.90** (colored in green).

3.5 CONCLUSIONS

Our ongoing efforts to identify potent and selective inhibitors of mitochondrial thymidine kinase 2, led us to synthesize new 3'-modified thymidines related to the recently discovered 3'-[4-aryl-(1,2,3-triazol-1-yl)]-3'-deoxythymidine analogues. Replacement of the triazole linkage by a basic amine or guanidine, as possible interaction partners of the γ-phosphate group of the ATP cosubstrate, generally led to a drop in inhibitory activity. Interestingly, treatment of a 3'-arylthiourea-substituted 5'-*O*-tritylated thymidine precursor with $HgCl_2$ and sodium azide exclusively afforded tetrazole **1.89** containing an amino group between C-3' of the deoxyribose and the tetrazole, while the same reaction performed on a 3'-benzylthiourea congener mainly gave rise to the regioisomer with the tetrazole ring directly connected to the sugar. In the resulting 1,5-aminotetrazole series, the isomers in which the tetrazole ring is attached to C-3' via a NH bridge exhibit the best anti-TK-2 activity, with a 3-CF_3-4-Cl phenyl substituent at position N-1 of the tetrazole ring affording the best TK-2-inhibition profile. Further introduction of a 5-(2-bromovinyl) substituent gave derivative **1.100**, which emerged as the most potent and selective TK-2 inhibitor reported so far. A TK-2 homology model allowed to assess the binding mode of both tetrazole isomers. In the case of regioisomer **1.90**, modeling studies indicated a contributing role of the tetrazole ring and the amino bridge to the overall affinity for TK-2.

3.6 EXPERIMENTAL PART

3.6.1 Synthesis

General procedure for the synthesis of substituted 3'-benzylamino-3'-deoxy-5'-*O*-triphenylmethyl-β-D-thymidine analogues 1.77-1.79

To a suspension of amine **1.58** (1.0 equiv.) in dry MeOH was added a suitable benzaldehyde (1.05 equiv.). After 24 h stirring at room temperature, $NaBH_4$ (1.5 equiv.) was added and 30 min later the mixture was quenched with 1M NaOH. The reaction mixture was extracted with CH_2Cl_2 and the organic layer washed with brine and dried over $MgSO_4$, filtered and evaporated to dryness. The residue was purified by column chromatography affording 3'-benzylamino analogues **1.77-1.79** in moderate yield.

3'-Benzylamino-3'-deoxy-5'-*O*-triphenylmethyl-β-D-thymidine (1.77)

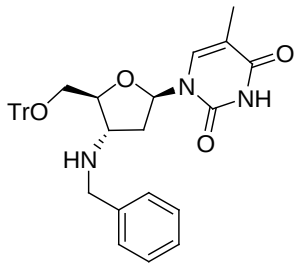

Reaction of compound **1.58** (88 mg, 0.18 mmol), benzaldehyde (17 mL, 0.17 mmol) in 0.7 mL MeOH was performed as described in the general procedure for the synthesis of 3'-benzylamino-3'-deoxy-5'-*O*-triphenylmethyl-β-D-thymidine analogues affording **1.77** as a colourless solid (17 mg, 16%).

^{1}H NMR (300 MHz, $CDCl_3$): δ 1.47 (3H, d, *J*= 1.2 Hz, 5-CH_3), 2.29 (2H, app t, *J*= 6.0 Hz, H-2'a and H-2'b), 3.33-3.47 (2H, m, H-5'a and H-5'b), 3.57 (1H, app dd, *J*= 6.3 Hz, *J*= 12.3 Hz, H-3'), 3.74 (2H, app q, *J*= 13.2 Hz, Bn), 3.91-3.93 (1H, m, H-4'), 6.26 (1H, app t, *J*= 6.0 Hz, H-1'), 7.20-7.40 (20H, m, Tr and Bn), 7.52 (1H, d, *J*= 0.9 Hz, H-6).

^{13}C NMR (75 MHz, $CDCl_3$): δ 12.10 (5-CH_3), 39.60 (C-2'), 52.29 (Bn), 57.53 (C-3'), 63.80 (C-5'), 84.68 (C-1'), 85.11 (C-4'), 87.45 (Tr), 110.96 (C-5), 127.42, 127.51, 128.15, 128.71, 128.81 (Bn and Tr), 135.70 (C-6), 139.60 (Bn), 143.50 (Tr), 150.29 (C-2), 163.77 (C-4).

Exact Mass (ESI-MS) for $C_{36}H_{36}N_3O_4$ $[M+H]^+$ found: 574.2770, calcd: 574.2700.

3'-(4-Chlorobenzylamino)-3'-deoxy-5'-*O*-triphenylmethyl-β-D-thymidine (1.78)

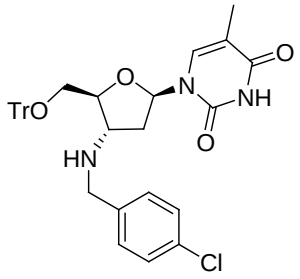

Reaction of compound **1.58** (82 mg, 0.17 mmol), 4-chlorobenzaldehyde (23 mg, 0.16 mmol) in 0.6 mL MeOH was performed as described in the general procedure for the synthesis of 3'-benzylamino-3'-deoxy-5'-*O*-triphenylmethyl-β-D-thymidine analogues affording **1.78** as a colourless solid (91 mg, 88%).

^{1}H NMR (300 MHz, DMSO-d_6): δ 1.43 (3H, d, *J*= 0.9 Hz, 5-CH_3), 2.13-2.27 (2H, m, H-2'a and H-2'b), 3.16-3.24 (2H, m, H-5'a and H-5'b), 3.39 (1H, app dt, *J*= 5.7 Hz, H-3'), 3.67 (2H, app q, *J*= 14.1 Hz, subs Bn), 3.87-3.91 (1H, m, H-4'), 6.19 (1H, app t, *J*= 6.3 Hz, H-1'), 7.24-7.37 (19H, m, Tr and subs Bn), 7.51 (1H, d, *J*= 0.9 Hz, H-6), 11.32 (1H, s, 3-NH).

^{13}C NMR (75 MHz, DMSO-d_6): δ 11.75 (5-CH_3), 37.44 (C-2'), 49.98 (subs Bn), 56.83 (C-3'), 64.04 (C-5'), 83.26 (C-1'), 83.91 (C-4'), 86.30 (Tr), 109.38 (C-5), 127.14, 127.93, 128.01, 128.24, 129.70, 131.06 (Tr and subs Bn), 135.66 (C-6), 139.60 (subs Bn), 143.48 (Tr), 150.34 (C-2), 163.67 (C-4).

Exact Mass (ESI-MS) for $C_{36}H_{35}ClN_3O_4$ $[M+H]^+$ found: 608.2357, calcd: 608.2311.

3'-[4-Chloro-(3-trifluoromethyl)benzylamino]-3'-deoxy-5'-*O*-triphenylmethyl-β-D-thymidine (1.79)

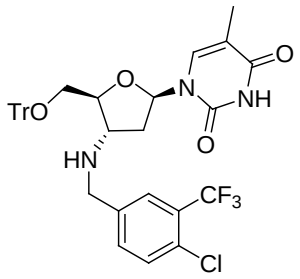

Reaction of compound **1.58** (108 mg, 0.22 mmol), 4-chloro-3-(trifluoromethyl)benzaldehyde (51 mg, 0.24 mmol) in 0.8 mL MeOH was performed as described in the general procedure for the synthesis of 3'-benzylamino-3'-deoxy-5'-*O*-triphenylmethyl-β-D-thymidine analogues affording **1.79** as a colourless solid (103 mg, 68%).

^{1}H NMR (300 MHz, DMSO-d_6): δ 1.44 (3H, d, *J*= 0.9 Hz, 5-CH_3), 2.18-2.26 (2H, m, H-2'a and H-2'b), 3.19 (2H, d, *J*= 3.6 Hz, H-5'a and H-5'b), 3.30-3.38 (1H, m, H-3'), 3.74 (2H, app q, *J*= 14.1 Hz, Bn), 3.88-3.89 (1H, m, H-4'), 6.18 (1H, app t, *J*= 6.6 Hz, H-1'), 7.24-7.34 (15H, m, Tr), 7.50 (1H, d, *J*= 1.5 Hz, H-6), 7.55-7.63 (2H, m, Bn), 7.76 (1H, d, *J*= 1.5 Hz, Bn), 11.31 (1H, s, 3-NH).

^{13}C NMR (75 MHz, DMSO-d_6): δ 11.79 (5-CH_3), 37.29 (C-2'), 49.49 (Bn), 57.09 (C-3'), 59.74 (C-5'), 83.22 (C-1'), 83.87 (C-4'), 86.28 (Tr), 109.38 (C-5), 121.15, 124.77, 126.93-128.22, 128.63 (Tr and subs Bn), 131.28 and 133.47 (subs Bn), 135.70 (C-6), 140.99 (subs Bn), 143.49 (Tr), 150.34 (C-2), 163.67 (C-4).

Exact Mass (ESI-MS) for $C_{37}H_{34}ClF_3N_3O_4$ $[M+H]^+$ found: 676.2194, calcd: 676.2184.

3'-Benzylamino-3'-deoxy-β-D-thymidine (1.80)

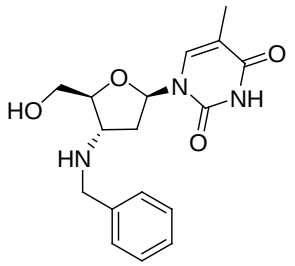

Compound **1.77** (94 mg, 0.16 mmol) was dissolved in a mixture of $ZnBr_2$ (592 mg, 2.63 mmol) in CH_2Cl_2/*i*PrOH (2.6 mL, 85:15) and stirred overnight at room temperature. The reaction was quenched with water and extracted with CH_2Cl_2 (3 x 5 mL). The combined organic layers were dried over $MgSO_4$ and evaporated to dryness. The resulting residue was purified by column chromatography (CH_2Cl_2/MeOH 95:5), to yield compound **1.80** (18.2 mg, 34%) as a colourless oil.

^{1}H NMR (300 MHz, DMSO-d_6): δ 1.77 (3H, m, 5-CH_3), 1.99-2.14 (2H, m, H-2'a and H-2'b), 3.27-3.33 (1H, m, H-3'), 3.53-3.71 (4H, m, H-5'a, H-5'b and Bn), 3.76-3.80 (1H, m, H-4'), 4.10 (1H, app br s, 3'-NH), 5.01 (1H, app br s, 5'-OH), 6.15 (1H, app t, *J*= 6.3 Hz, H-1'), 7.19-7.32 (5H, m, Bn), 7.74 (1H, d, *J*= 1.2 Hz, H-6), 11.25 (1H, s, 3-NH).

^{13}C NMR (75 MHz, DMSO-d_6): δ 12.27 (5-CH_3), 37.55 (C-2'), 51.10 (Bn), 57.39 (C-3'), 61.75 (C-5'), 83.96 (C-1'), 85.32 (C-4'), 109.14 (C-5), 126.56, 127.96 and 128.09 (Bn), 136.25 (C-6), 140.78 (Bn), 150.42 (C-2), 163.77 (C-4).

Exact Mass (ESI-MS) for $C_{17}H_{22}N_3O_4$ $[M+H]^+$ found: 332.1613, calcd: 332.1605.

3'-(4-Chlorobenzylamino)-3'-deoxy-β-D-thymidine (1.81)

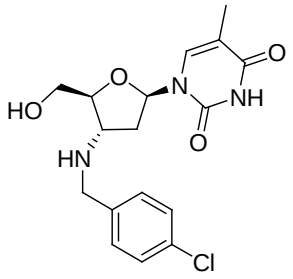

Compound **1.81** (14 mg, 56%, colourless solid) was synthesized from compound **1.78** (40 mg, 0.066 mmol) using the same procedure as described for the synthesis of **1.80**.

^{1}H NMR (300 MHz, DMSO-d_6): δ 1.76 (3H, d, *J*= 1.0 Hz, 5-CH_3), 2.04-2.10 (2H, m, H-2'a and H-2'b), 3.24-3.40 (1H, m, H-3'), 3.51-3.66 (2H, m, H-5'a and H-5'b), 3.69 (2H, d, *J*= 3.3 Hz, subs Bn), 3.75-3.79 (1H, m, H-4'), 5.02 (1H, app br s, 5'-OH), 6.14 (1H, app t, *J*= 6.5 Hz, H-1'), 7.37 (4H, app s, subs Bn), 7.73 (1H, d, *J*= 1.3 Hz, H-6), 11.25 (1H, s, 3-NH).

^{13}C NMR (75 MHz, DMSO-d_6): δ 12.35 (5-CH_3), 37.58 (C-2'), 50.30 (subs Bn), 57.33 (C-3'), 61.77 (C-5'), 84.03 (C-1'), 85.35 (C-4'), 109.27 (C-5), 128.12, 129.88 and 131.12 (subs Bn), 136.35 (C-6), 139.95 (subs Bn), 150.51 (C-2), 163.90 (C-4).

Exact Mass (ESI-MS) for $C_{17}H_{21}ClN_3O_4$ $[M+H]^+$ found: 366.1215, calcd: 366.1215.

3'-[4-Chloro-3-(trifluoromethyl)benzylamino]-3'-deoxy-β-D-thymidine (1.82)

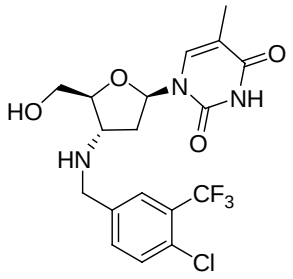

Compound **1.82** (80 mg, 58%, colourless solid) was synthesized from compound **1.79** (97 mg, 0.14 mmol) using the same procedure as described for the synthesis of **1.80**.

^{1}H NMR (300 MHz, DMSO-d_6): δ 1.77 (3H, d, *J*= 1.2 Hz, 5-CH_3), 2.05-2.12 (2H, m, H-2'a and H-2'b), 3.25-3.33 (1H, m, H-3'), 3.52-3.67 (2H, m, H-5'a and H-5'b), 3.73-3.84 (3H, m, H-4' and subs Bn), 4.07 (1H, app br s, 3'-NH), 5.01 (1H, app br s, 5'-OH), 6.15 (1H, app t, *J*= 6.3 Hz, H-1'), 7.67 (2H, app s, subs Bn), 7.73 (1H, d, *J*= 0.9 Hz, H-6), 7.84 (1H, app s, subs Bn), 11.25 (1H, s, 3-NH).

^{13}C NMR (75 MHz, DMSO-d_6): δ 12.25 (5-CH_3), 37.43 (C-2'), 49.63 (subs Bn), 57.24 (C-3'), 61.62 (C-5'), 83.88 (C-1'), 85.22 (C-4'), 109.15 (C-5), 124.83, 126.06-128.57, 131.30 and 133.59 (subs Bn), 136.21 (C-6), 141.23 (subs Bn), 150.41 (C-2), 163.76 (C-4).

Exact Mass (ESI-MS) for $C_{18}H_{20}ClF_3N_3O_4$ $[M+H]^+$ found: 434.1114, calcd: 434.1089.

General procedure for the synthesis of *N*-(3'-deoxy-5'-*O*-triphenylmethyl-β-D-thymidin-3'-yl)-*N*'-(4-chloro-3-(trifluoromethyl)phenyl)guanidine analogues 1.83-1.85

To a solution of thiourea **1.59** (1.0 equiv.) in dry DMF were added the appropriate amine (1.0 equiv.), Et_3N (2.0 equiv.) and $HgCl_2$ (1.0 equiv.) at 0 °C under N_2 atmosphere. The resulting black reaction mixture was stirred for several hours at room temperature until TLC indicated complete consumption of starting material. The suspension was filtered through a pad of Celite, washing with CH_2Cl_2. The filtrate was diluted with water and extracted with CH_2Cl_2. The combined organic layers were dried over $MgSO_4$, filtered and concentrated under reduced pressure. The resulting residue was purified by silica gel chromatography (CH_2Cl_2/MeOH 90:10 or 80:20) to give the appropriate guanidine in moderate yield.

***N*-(3'-Deoxy-5'-*O*-triphenylmethyl-β-D-thymidin-3'-yl)-*N*'-[4-chloro-3-(trifluoromethyl)phenyl]-guanidine (1.83)**

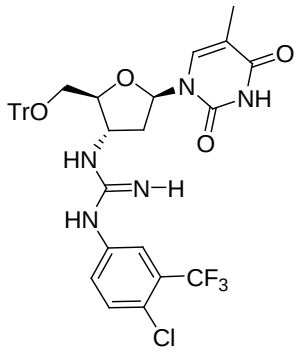

Reaction of compound **1.59** (232 mg, 0.32 mmol) with 10 mL 7N NH_3 following the procedure as described above, yielded compound **1.83** (128 mg, 57%) as a white powder.

^{1}H NMR (300 MHz, DMSO-d_6): δ 1.50 (3H, app s, 5-CH_3), 2.29-2.34 (1H, m, H-2'a), 2.49-2.52 (1H, m, H-2'b), 3.26-3.39 (2H, m, H-5'a and H-5'b), 4.00-4.02 (1H, m, H-4'), 4.64-4.66 (1H, m, H-3'), 6.21 (1H, app t, *J*= 5.7 Hz, H-1'), 7.23-7.61 (19H, m, Tr, subs Ph and H-6), 11.34 (1H, s, 3-NH).

^{13}C NMR (75 MHz, DMSO-d_6): δ 11.87 (5-CH_3), 37.24 (C-2'), 50.90 (C-3'), 62.94 (C-5'), 82.65 (C-1'), 83.35 (C-4'), 86.39 (Tr), 109.50 (C-5), 122.39, 124.59, 125.95, 126.73, 127.05, 127.16, 127.90, 127.97, 128.29, 132.21 (CF_3, subs Ph and Tr), 135.79 (C-6), 143.46 (Tr), 150.37 (C-2), 153.18 (C=N), 163.74 (C-4).

Exact Mass (ESI-MS) for $C_{37}H_{34}ClF_3N_5O_4$ $[M+H]^+$ found: 704.2241, calcd: 704.2246.

***N*-(3'-Deoxy-5'-*O*-triphenylmethyl-β-D-thymidin-3'-yl)-*N*'-[4-chloro-3-(trifluoromethyl)phenyl]-benzylguanidine (1.84)**

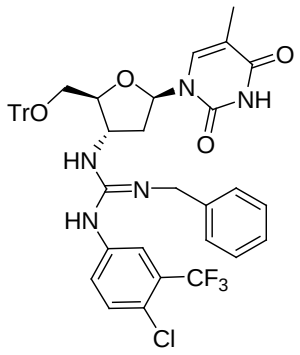

Reaction of compound **1.59** (87 mg, 0.12 mmol) with benzylamine (13 µL, 0.12 mmol) following the procedure as described above, afforded compound **1.84** (54 mg, 56%) as a white solid.

^{1}H NMR (300 MHz, DMSO-d_6): δ 1.43 (3H, d, *J*= 0.9 Hz, 5-CH_3), 2.20-2.28 (1H, m, H-2'a), 2.31-2.41 (1H, m, H-2'b), 3.23-3.32 (2H, m, H-5'a and H-5'b), 3.92-3.95 (1H, m, H-4'), 4.26 (2H, d, *J*= 5.7 Hz, Bn), 4.60-4.63 (1H, m, H-3'), 6.13-6.26 (3H, m, H-1' and Bn), 6.73 (1H, d, *J*= 8.4 Hz, 3'-NH), 6.91 (1H, s, N'H), 7.19-7.41 (21H, m, Tr, Bn and subs Ph), 7.54 (1H, d, *J*= 0.9 Hz, H-6).

^{13}C NMR (75 MHz, DMSO-d_6): δ 11.81 (5-CH_3), 37.32 (C-2'), 44.48 (Bn), 54.91 (C-3'), 63.42 (C-5'), 83.46 (C-1'), 86.26 (C-4' and Tr), 109.31 (C-5), 119.81, 126.63, 127.02, 127.06, 127.89, 128.11, 128.26, 131.62 (CF_3, subs Ph, Tr and Bn), 135.73 (C-6), 140.03 (Bn), 143.56 (Tr), 151.33 (C-2), 151.49 (C=N), 163.70 (C-4).

Exact Mass (ESI-MS) for $C_{44}H_{40}ClF_3N_5O_4$ $[M+H]^+$ found: 794.2727, calcd: 794.2715.

***N*-(3'-Deoxy-5'-*O*-triphenylmethyl-β-D-thymidin-3'-yl)-*N*'-[4-chloro-3-(trifluoromethyl)phenyl]-isopropylguanidine (1.85)**

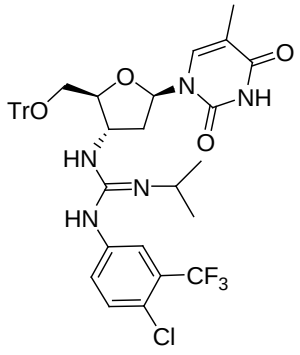

Reaction of compound **1.59** (232 mg, 0.32 mmol) with isopropylamine (27 µL, 0.32 mmol) following the procedure as described above, afforded compound **1.85** (128 mg, 57%) as a white powder.

^{1}H NMR (300 MHz, DMSO-d_6): δ 0.97-1.06 (6H, m, *i*Pr), 1.42 (3H, s, 5-CH_3), 2.26-2.35 (2H, m, H-2'a and H-2'b), 3.24-3.35 (2H, m, H-5'a and H-5'b), 3.66 (1H, app sex, *J*= 6.9 Hz, *i*Pr), 3.95-3.96 (1H, m, H-4'), 4.64 (1H, app d, *J*= 5.4 Hz, H-3'), 5.29 (1H, d, *J*= 5.4 Hz, 3'-NH), 6.08 (1H, br s, N'H), 6.20 (1H, app t, *J*= 6.3 Hz, H-1'), 6.76 (1H, d, *J*= 8.7 Hz, subs Ph), 6.94 (1H, s, subs Ph), 7.21-7.42 (16H, m, Tr and subs Ph), 7.56 (1H, d, *J*= 1.2 Hz, H-6), 11.32 (1H, s, 3-NH).

^{13}C NMR (75 MHz, DMSO-d_6): δ 11.74 (5-CH_3), 22.65 (*i*Pr), 37.20 (C-2'), 42.73 (*i*Pr), 50.48 (C-3'), 63.51 (C-5'), 83.48 (C-1'), 83.75 (C-4'), 86.27 (Tr), 109.34 (C-5), 119.34, 121.30, 124.92, 126.42, 126.81, 127.07, 127.42, 127.87, 128.27, 128.54, 131.63 (CF_3, subs Ph and Tr), 135.72 (C-6), 143.54 (Tr), 150.33 (C-2), 151.32 (C=N), 163.68 (C-4).

Exact Mass (ESI-MS) for $C_{40}H_{40}ClF_3N_5O_4$ $[M+H]^+$ found: 746.2717, calcd: 746.2715.

***N*-(3'-Deoxy-β-D-thymidin-3'-yl)-*N*'-[4-chloro-3-(trifluoromethyl)phenyl]guanidine (1.86)**

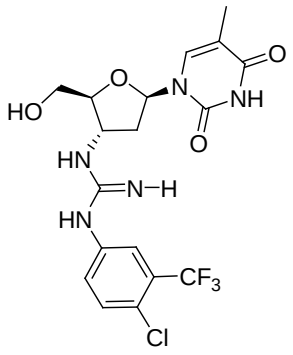

A solution of compound **1.83** (108 mg, 0.15 mmol) in 3.0 mL HCOOH/Et_2O 7:3 (v:v) reacted for 45 min at room temperature. The reaction was quenched with EtOAc and water, washed with sat. $NaHCO_3$ and extracted with EtOAc (3 x 5mL). The combined organic layers were dried over $MgSO_4$ and the solvent evaporated. The residue was purified by column chromatography (CH_2Cl_2/MeOH 80:20) to yield compound **1.86** (50 mg, 71%) as a yellow/brown solid. Treatment with a 4N HCl solution in 1,4-dioxane gave the appropriate salt.

^{1}H NMR (300 MHz, DMSO-d_6): δ 1.78 (3H, d, *J*= 0.9 Hz, 5-CH_3), 2.16-2.36 (2H, m, H-2'a and H-2'b), 3.59-3.72 (2H, m, H-5'a and H-5'b), 3.81-3.84 (1H, m, H-4'), 4.29 (1H, app dd, *J*= 6.0 Hz, *J*= 12.9 Hz, H-3'), 5.76 (1H, app br s, 5'-OH), 6.16 (1H, app t, *J*= 6.3 Hz, H-1'), 7.12 (1H, d, *J*= 7.5 Hz, subs Ph), 7.25 (1H, s, subs Ph), 7.50 (1H, d, *J*= 8.4 Hz, subs Ph), 7.75 (1H, d, *J*= 1.2 Hz, H-6).

^{13}C NMR (75 MHz, DMSO-d_6): δ 12.29 (5-CH_3), 37.33 (C-2'), 50.93 (C-3'), 61.17 (C-5'), 83.34 (C-1'), 85.37 (C-4'), 109.26 (C-5), 126.65, 127.06, 128.26 and 131.97 (subs Ph), 136.08 (C-6), 147,39 (C-2), 150.42 (C=N), 163.76 (C-4).

Exact Mass (ESI-MS) for $C_{18}H_{20}ClF_3N_5O_4$ $[M+H]^+$ found: 462.1132, calcd: 462.1150.

***N*-(3'-Deoxy-β-D-thymidin-3'-yl)-*N*'-[4-chloro-3-(trifluoromethyl)phenyl]benzylguanidine (1.87)**

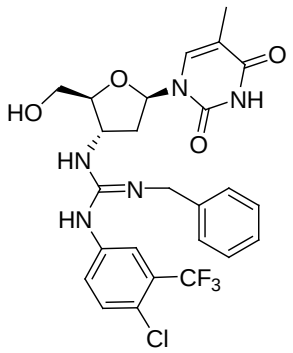

Compound **1.87** (15 mg, 68%) was synthesized from compound **1.84** (33 mg, 0.041 mmol) using the same procedure as described for the synthesis of **1.86**. Treatment with a 4N HCl solution in 1,4-dioxane gave the appropriate salt.

^{1}H NMR (300 MHz, DMSO-d_6): δ 1.76 (3H, d, *J*= 0.6 Hz, 5-CH_3), 2.23 (2H, app t, *J*= 6.9 Hz, H-2'a and H-2'b), 3.51-3.3.57 (1H, m, H-5'a), 3.62-3.67 (1H, m, H-5'b), 3.77-3.81 (1H, m, H-4'), 4.27-4.32 (3H, m, H-3' and Bn), 6.14 (1H, app t, *J*= 6.3 Hz, H-1'), 6.35 (1H, app br s, 5'-OH), 6.93 (1H, app dd, *J*= 2.4 Hz, *J*= 8.7 Hz, subs Ph), 7.02-7.03 (1H, m, subs Ph), 7.20-7.35 (5H, m, Bn), 7.41 (1H, d, *J*= 8.7 Hz, subs Ph), 7.73 (1H, d, *J*= 1.2 Hz, H-6).

^{13}C NMR (75 MHz, DMSO-d_6): δ 12.27 (5-CH_3), 37.32 (C-2'), 44.59 (Bn), 51.01 (C-3'), 60.98 (C-5'), 83.32 (C-1'), 85.17 (C-4'), 109.18 (C-5), 120.07, 121.28, 121.52, 121.60, 124.90, 126.56, 126.70, 126.96, 127.13, 127.86, 128.18, 131.82, (CF_3, subs Ph and Bn), 136.18 (C-6), 140.01 (Bn), 150.40 (C-2), 152.17 (C=N), 163.77 (C-4).

Exact Mass (ESI-MS) for $C_{25}H_{26}ClF_3N_5O_4$ $[M+H]^+$ found: 552.1620, calcd: 552.1620.

_N_-(3'-Deoxy-β-D-thymidin-3'-yl)-_N'_-[4-chloro-3-(trifluoromethyl)phenyl]isopropylguanidine (1.88)

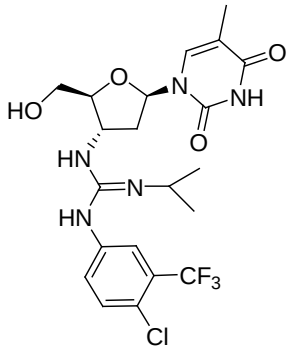

Compound **1.88** (54 mg, 0.11 mmol, 64%) was synthesized from compound **1.85** (123.7 mg, 0.17 mmol) using the same procedure as described for the synthesis of **1.86**. Treatment with a 4N HCl solution in 1,4-dioxane gave the appropriate salt.

^{1}H NMR (300 MHz, DMSO-d_6): δ 1.07-1.09 (6H, m, *i*Pr), 1.77 (3H, d, *J*= 1.2 Hz, 5-CH_3), 2.28 (2H, app t, *J*= 7.2 Hz, H-2'a and H-2'b), 3.56-3.84 (4H, m, H-4', H-5'a, H-5'b and *i*Pr), 4.32 (1H, app dd, *J*= 6.6 Hz, *J*= 12.3 Hz, H-3'), 5.90 (1H, app br s, 5'-OH), 6.18 (1H, app t, *J*= 6.6 Hz, H-1'), 7.06 (1H, app dd, *J*= 2.4 Hz, *J*= 8.7 Hz, subs Ph), 7.19 (1H, d, *J*= 2.1 Hz, subs Ph), 7.47 (1H, d, *J*= 8.7 Hz, subs Ph), 7.71 (1H, d, *J*= 1.2 Hz, H-6).

^{13}C NMR (75 MHz, DMSO-d_6): δ 12.25 (5-CH_3), 22.59 (*i*Pr), 36.96 (C-2'), 43.23 (*i*Pr), 51.64 (C-3'), 61.14 (C-5'), 83.30 (C-1'), 85.08 (C-4'), 109.36 (C-5), 120.86, 121.21, 121.41, 124.83, 126.64, 127.05, 127.57, 131.97 (CF_3 and subs Ph), 136.13 (C-6), 150.42 (C-2), 152.10 (C=N), 163.74 (C-4).

Exact Mass (ESI-MS) for $C_{21}H_{26}ClF_3N_5O_4$ $[M+H]^+$ found: 504.1644, calcd: 504.1620.

General procedure for the synthesis of substituted 1,5-aminotetrazole analogues 1.89, 1.93, 1.94 and 1.99

To a suspension of a suitable thiourea (1.0 equiv.), sodium azide (3.0 equiv.) and $HgCl_2$ (1.1 equiv.) in dry DMF was added Et_3N (3.0 equiv.) at 0 °C under N_2 atmosphere. The resulting suspension was stirred for several hours at room temperature until TLC indicated complete consumption of starting material. The suspension was filtered through a pad of Celite, washing with CH_2Cl_2. The filtrate was diluted with water and extracted with CH_2Cl_2. The combined organic layers were dried over $MgSO_4$, filtered and concentrated under reduced pressure. The resulting residue was purified by silica gel chromatography (EtOAc/hexane 95:5 or CH_2Cl_2/MeOH 98:2) to give the appropriate tetrazole.

5-(3'-Amino-3'-deoxy-5'-*O*-triphenylmethyl-β-D-thymidin-3'*N*-yl)-1-(4-chloro-3-(trifluoromethyl)-phenyl)tetrazole (1.89)

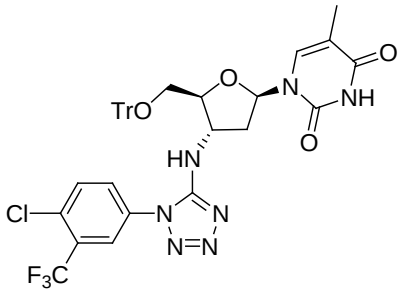

Reaction of compound **1.59** (189 mg, 0.26 mmol), NaN_3 (51 mg, 0.79 mmol), $HgCl_2$ (78 mg, 0.29 mmol) and Et_3N (105 µL, 0.76 mmol) yielded compound **1.89** (58 mg, 31%) as a yellow/brown solid.

^{1}H NMR (300 MHz, DMSO-d_6): δ 1.51 (3H, s, 5-CH_3), 2.33-2.42 (1H, m, H-2'a), 2.46-2.53 (1H, m, H-2'b), 3.27-3.33 (1H, m, H-5'a), 3.41-3.46 (1H, m, H-5'b), 4.09-4.13 (1H, m, H-4'), 4.55-4.60 (1H, m, H-3'), 6.31 (1H, app t, *J*= 6.6 Hz, H-1'), 7.23-7.42 (15H, m, Tr), 7.50 (1H, d, *J*= 7.2 Hz, 3'-NH), 7.60 (1H, d, *J*= 1.2 Hz, H-6), 7.90-8.05 (3H, subs Ph), 11.36 (1H, s, 3-NH).

^{13}C NMR (75 MHz, DMSO-d_6): δ 11.82 (5-CH_3), 36.68 (C-2'), 59.74 (C-3'), 64.09 (C-5'), 82.60 (C-1'), 83.70 (C-4'), 86.44 (Tr), 109.73 (C-5), 120.36, 123.99, 124.96, 125.03, 127.17-127.67, 127.95-128.27, 128.51, 130.86, 131.90, 132.21, 133.21 (CF_3, subs Ph and Tr), 135.83 (C-6), 143.49 (Tr), 150.39 (C-2), 154.54 (C=N), 163.66 (C-4).

Exact Mass (ESI-MS) for $C_{37}H_{31}ClF_3N_7O_4Na$ $[M+Na]^+$ found: 752.006, calcd: 752.1970.

5-(3'-Amino-3'-deoxy-β-D-thymidin-3'*N*-yl)-1-(4-chloro-3-(trifluoromethyl)phenyl)tetrazole (1.90)

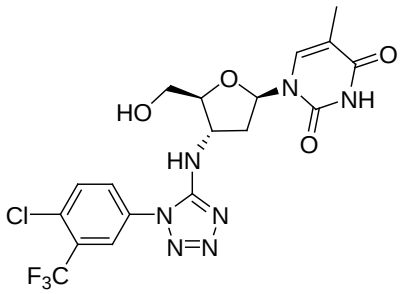

A solution of compound **1.89** (34 mg, 0.047 mmol) in 1.0 mL HCOOH/Et_2O 7:3 (v:v) reacted for 45 min. EtOAc and water were added to the mixture which was then washed with saturated $NaHCO_3$ and extracted with EtOAc (3 x 5 mL). The combined organic layers were dried over $MgSO_4$ and the solvent evaporated. The residue was purified by column chromatography (CH_2Cl_2/MeOH 95:5) to yield compound **1.90** (10.0 mg, 0.021 mmol, 45%) as a white solid.

^{1}H NMR (300 MHz, DMSO-d_6): δ 1.80 (3H, s, 5-CH_3), 2.29-2.34 (2H, m, H-2'a and H-2'b), 3.65-3.73 (2H, m, H-5'a and H-5'b), 3.97-4.01 (1H, m, H-4'), 4.35-4.41 (1H, m, H-3'), 5.19 (1H, app br s, 5'-OH), 6.25 (1H, app t, *J*= 6.9 Hz, H-1'), 7.81 (1H, d, *J*= 0.9 Hz, H-6), 7.96-8.03 (2H, m, subs Ph), 8.17 (1H, s, subs Ph).

^{13}C NMR (75 MHz, DMSO-d_6): δ 12.30 (5-CH_3), 37.05 (C-2'), 54.46 (C-3'), 61.51 (C-5'), 83.63 (C-1'), 84.66 (C-4'), 109.45 (C-5), 124.06-133.14 (subs Ph), 136.18 (C-6), 150.49 (C-2), 154.84 (C=N), 163.79 (C-4).

Exact Mass (ESI-MS) for $C_{18}H_{18}ClF_3N_7O_4$ $[M+H]^+$ found: 488.1070, calcd: 488.1055.

5-(3'-Amino-3'-deoxy-β-D-thymidin-3'*N*-yl)-1-(4-chloro-3-(trifluoromethyl)phenyl)tetrazole (1.90) and 5-[(4-chloro-3-(trifluoromethyl)phenyl)amino]-1-(3'-deoxy-β-D-thymidin-3'-yl)tetrazole (1.91)

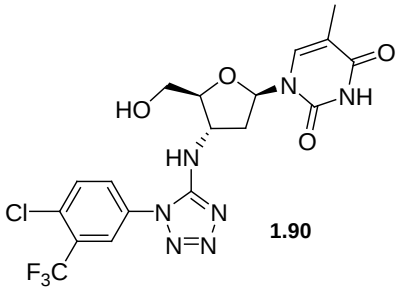

1.90

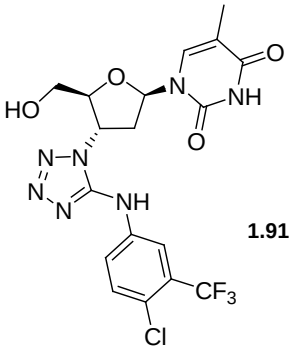

1.91

Compound **1.89** (80 mg, 0.11 mmol) was dissolved in a mixture of $ZnBr_2$ (394 mg, 1.75 mmol) in CH_2Cl_2/*i*PrOH (1.8 mL, 85:15) and stirred overnight at room temperature. The reaction was quenched with water and extracted with CH_2Cl_2 (3 x 5 mL). The combined organic layers were dried over $MgSO_4$ and evaporated to dryness. The resulting residue was purified using RP-HPLC (Phenomenex Luna C-18, 250 x 21.10 mm 5 mm, H_2O-CH_3CN, 90:10 → 0:100 in 29 min, flow: 17.5 mL min^{-1}), affording isomers **1.90** and **1.91** as white powders (17 mg, 32%, 9:1).

Compound **1.91**:

^{1}H NMR (300 MHz, DMSO-d_6): δ 1.83 (3H, app s, 5-CH_3), 2.50-2.2.62 (2H, m, H-2'a and H-2'b), 3.65-3.76 (3H, m, H-4', H-5'a and H-5'b), 4.25 (1H, app s, H-3'), 5.43 (1H, br s, 5'-OH), 6.46 (1H, app t, *J*= 6.6 Hz, H-1'), 7.55-7.58 (1H, d, *J*= 8.1 Hz, subs Ph), 7.80-7.96 (2H, m, subs Ph), 8.15 (1H, app s, H-6).

^{13}C NMR (175 MHz, DMSO-d_6): δ 12.73 (5-CH_3), 61.68 (C-5'), 84.32 and 84.54 (C-1' and C-4'), 110.20 (C-5), 127.97-134.08 (subs Ph), 136.59 (C-6), 150.94 (C-2), (C=N not visible), 164.19 (C-4).

Exact Mass (ESI-MS) for $C_{18}H_{18}ClF_3N_7O_4$ $[M+H]^+$ found: 488.1063, calcd: 488.1055.

***N*-(3'-Deoxy-5'-*O*-triphenylmethyl-β-D-thymidin-3'-yl)-*N*'-benzylthiourea (1.92)**

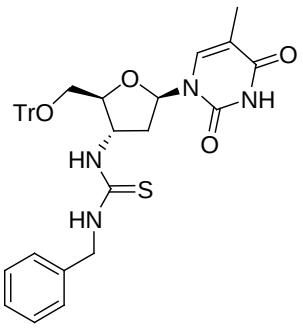

Reaction of compound **1.58** (364 mg, 0.75 mmol) with benzyl isothiocyanate (114 mg, 0.75 mmol) was performed as described for the synthesis of compound **1.59** affording compound **1.92** in a 99% yield (471 mg, white foam).

^{1}H NMR (300 MHz, DMSO-d_6): δ 1.42 (3H, s, 5-CH_3), 2.18-2.26 (1H, m, H-2'a), 2.45-2.55 (1H, m, H-2'b), 3.18-3.22 (1H, m, H-5'a), 3.38-3.43 (1H, m, H-5'b), 4.03 (1H, app s, H-4'), 4.68 (2H, app s, Bn), 5.10 (1H, app br s, H-3'), 6.21 (1H, app t, *J*= 6.6 Hz, H-1'), 7.21-7.42 (20H, m, Tr and Bn), 7.55 (1H, app s, 6-H), 7.80-7.92 (1H, m, 3'-NH), 8.02 (1H, m, N'H), 11.35 (1H, s, 3-NH).

^{13}C NMR (75 MHz, DMSO-d_6): δ 11.79 (5-CH_3), 30.80 (Bn), 35.81 (C-2'), 47.04 (C-3'), 63.76 (C-5'), 83.63 (C-1' and C-4'), 86.51 (Tr), 109.55 (C-5), 126.86, 127.17, 127.23, 128.01, 128.27, 128.32 (Tr and Bn), 135.51 (Bn), 139.13 (C-6'), 143.47 (Tr), 150.38 (C-2), 162.34 (C-4).

Exact Mass (ESI-MS) for $C_{37}H_{37}N_4O_4S$ $[M + H]^+$ found: 633.2505, calcd: 633,2530.

5-(3'-Amino-3'-deoxy-5'-*O*-triphenylmethyl-β-D-thymidin-3'*N*-yl)-1-benzyltetrazole (1.93) and 5-(benzylamino)-1-(3'-deoxy-5'-*O*-triphenylmethyl-β-D-thymidin-3'-yl)tetrazole (1.94)

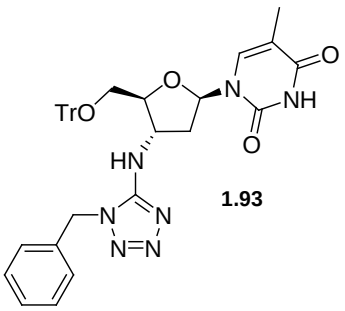

1.93

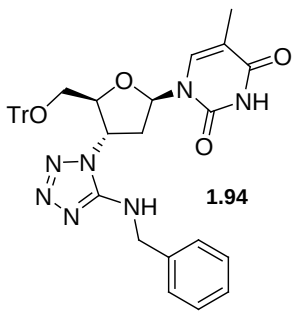

1.94

Reaction of compound **1.92** (207 mg, 0.33 mmol), NaN_3 (64 mg, 0.98 mmol), $HgCl_2$ (98 mg, 0.36 mmol) and Et_3N (136 µL, 0.98 mmol) in 1.3 mL DMF was performed as described in the general

synthesis of substituted 1,5-aminotetrazole analogues. A mixture of compounds **1.93** and **1.94** (1:2.2) was obtained as a white solid (108 mg, 52%).

^{1}H NMR (300 MHz, $CDCl_3$): δ 1.33 (isomer 1: 5-CH_3, s), 1.49 (isomer 2: 5-CH_3, s), 2.40-2.50 (isomer 1: H-2'a and H-2'b, m), 2.79-2.88 (isomer 2: H-2'a and H-2'b, m), 3.34-3.45 (isomer 2: H-5'a and H-5'b, m), 3.48-3.54 (isomer 1: H-5'a and H-5'b, m), 4.07-4.10 (isomer 1:H-4', m), 4.33-4.47 (isomer 2: CH_2Ph, m), 4.51-4.56 (isomer 2: H-4', m), 4.69-4.71 (isomer 1: H-3', m), 5.07-5.15 (isomer 2: H-3', m), 5.32 (isomer 1: Bn, s), 6.09 (isomer 2: H-1', app t, *J*= 5.4 Hz), 6.18 (isomer 1: H-1' and isomer 2: N'H, app t, *J*= 6.0 Hz), 6.57 (isomer 1: 3'-NH, d, *J*= 7.2Hz), 7.07-7.56 (20H, m, Tr, Bn & 6-H), 10.15 (isomer 1: 3-NH, s), 10.27 (isomer 2: 3-NH, s).

^{13}C NMR (75 MHz, $CDCl_3$): δ 11.72 and 12.13 (5-CH_3), 37.66 (C-2'), 48.15 and 48.72 (Bn), 54.31 and 55.24 (C-3'), 62.59 (C-5'), 82.25 (C-1'), 84.17 (C-4'), 87.48 and 87.69 (Tr), 110.69 and 111.54 (C-5), 127.36-128.90 (Tr), 133.91 (Bn), 135.75 and 136.72 (C-6), 137.86 (Bn), 143.15 and 143.34 (Tr), 150.70 and 151.04 (C-2), 154.92 and 155.81 (C=N), 164.04 (C-4).

Exact Mass (ESI-MS) for $C_{37}H_{36}N_7O_4$ $[M + H]^+$ found: 642.2827, calcd: 642,2823.

5-(3'-Amino-3'-deoxy-β-D-thymidin-3'*N*-yl)-1-(benzyl)tetrazole (1.95) and 5-(benzylamino)-1-(3'-deoxy-β-D-thymidin-3'-yl)tetrazole (1.96)

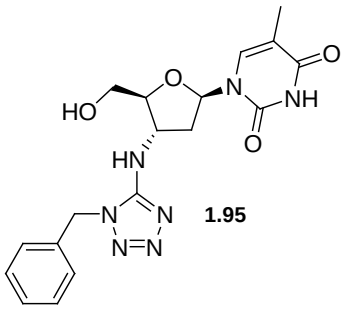

1.95

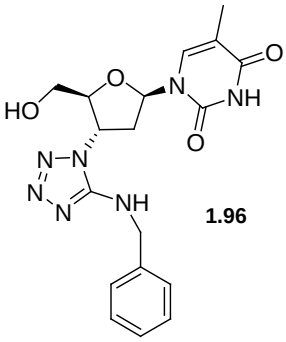

1.96

Reaction of a mixture of compounds **1.93** and **1.94** (199 mg, 0.31 mmol) under the same conditions as described for the synthesis of **1.90** and **1.91** and purification on a RP-HPLC (Phenomenex Luna C-18, H_2O/0.1% HCOOH in CH_3CN, 90:10 → 0:100 in 29 min, flow: 17.5 mL min^{-1}) afforded compounds **1.95** and **1.96** as white powders (17 mg, 54%, 1:3).

Compound **1.95**:

^{1}H NMR (300 MHz, DMSO-d_6): δ 1.79 (3H, d, *J*= 0.9 Hz, 5-CH_3), 2.22-2.40 (2H, m, H-2'a and H-2'b), 3.62-3.72 (2H, m, H-5'a and H-5'b), 3.97 (1H, app dt, *J*= 3.3 Hz, H-4'), 4.30-4.36 (1H, m, H-3'), 5.19 (1H, app br s, 5'-OH), 5.43 (2H, s, Bn), 6.29 (1H, t, *J*= 6.9 Hz, H-1'), 7.22-7.25 (2H, m, Bn), 7.30-7.41 (3H, m, Bn), 7.51 (1H, d, *J*= 6.9 Hz, 3'-NH), 7.81 (1H, d, *J*= 0.9 Hz, 6-H).

^{13}C NMR (75 MHz, DMSO-d_6): δ 12.30 (5-CH_3), 37.08 (C-2'), 47.66 (Bn), 54.26 (C-3'), 61.56 (C-5'), 83.62 (C-1'), 84.89 (C-4'), 109.48 (C-5), 127.42, 127.97, 128.77 and 135.30 (Bn), 136.09 (C-6), 150.53 (C-2), 154.95 (C=N), 163.82 (C-4).

Exact Mass (ESI-MS) for $C_{18}H_{22}N_7O_4$ $[M + H]^+$ found: 400.1738, calcd: 400,1728.

Compound **1.96**:

^{1}H NMR (300 MHz, DMSO-d_6): δ 1.81 (3H, d, *J*= 0.9 Hz, 5-CH_3), 2.52-2.60 (2H, m, H-2'a and H-2'b), 3.68 (2H, app dq, *J*= 3.0 Hz, *J*= 11.9 Hz, H-5'a and H-5'b), 4.32 (1H, app q, *J*= 3.6 Hz, H-4'), 4.51 (2H, d, *J*= 5.7 Hz, Bn), 5.10-5.16 (1H, m, H-3'), 5.39 (1H, app br s, 5'-OH), 6.39 (1H, t, *J*= 6.6 Hz, H-1'), 7.23-7.40 (5H, m, Bn), 7.60 (1H, t, *J*= 5.7 Hz, 5''-NH), 7.81 (1H, d, *J*= 1.5 Hz, 6-H), 11.35 (1H, s, 3-NH).

^{13}C NMR (75 MHz, DMSO-d_6): δ 12.36 (5-CH_3), 36.66 (C-2'), 46.87 (Bn), 55.04 (C-3'), 60.90 (C-5'), 83.60 (C-4'), 84.03 (C-1'), 109.51 (C-5), 127.08, 127.40 and 128.32 (Bn), 136.05 (C-6), 138.92 (Bn), 150.45 (C-2), 155.40 (C=N), 163.76 (C-4).

Exact Mass (ESI-MS) for $C_{18}H_{22}N_7O_4$ $[M + H]^+$ found: 400.1709, calcd: 400.1728.

3'-Amino-(*E*)-5-(2-bromovinyl)-2',3'-dideoxy-5'-*O*-triphenylmethyl-β-D-uridine (1.97)

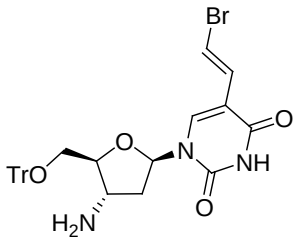

Water (40 µL) and triphenylphosphine (318 mg, 1.21 mmol) were added to a solution of compound **1.63** (154 mg, 0.26 mmol) in THF (6.6 mL). The solution was stirred for 24 h at room temperature. Then the solvent was evaporated and the crude residue was purified by column chromatography (CH_2Cl_2/MeOH 93:7) affording compound **1.97** as a yellow solid (104 mg, 71%).

^{1}H NMR (300 MHz, DMSO-d_6): δ 2.03-2.12 (1H, m, H-2'a), 2.21-2.29 (1H, m, H-2'b), 3.17-3.29 (2H, m, H-5'a and H-5'b), 3.46 (1H, app dt, *J*= 7.2 Hz, H-3'), 3.69-3.74 (1H, m, H-4'), 4.09 (1H, br s, 3'-NH), 6.13 (1H, dd, *J*= 4.5 Hz, *J*= 6.9 Hz, H-1'), 6.53 (1H, d, *J*= 13.2 Hz, H-8), 7.19-7.42 (16H, m, H-7 and Tr), 7.74 (1H, s, 6-H).

^{13}C NMR (75 MHz, DMSO-d_6): δ 51.34 (C-3'), 63.94 (C-5'), 84.20 (C-1'), 85.70 (C-4'), 86.11 (Tr), 106.80 (C-8), 109.73 (C-5), 127.09, 127.93, 128.27, 129.85 (C-7 and Tr), 139.45 (C-6), 143.63 (Tr), 149.23 (C-2), 161.70 (C-4).

Exact Mass (ESI-MS) for $C_{30}H_{28}BrN_3NaO_4$ $[M+Na]^+$ found: 596.1162, calcd: 596.1155.

***N*-[(*E*)-5-(2-Bromovinyl)-2',3'-dideoxy-5'-*O*-triphenylmethyl-β-D-uridin-3'-yl]-*N*'-[4-chloro-3-(trifluoromethyl)phenyl]thiourea (1.98)**

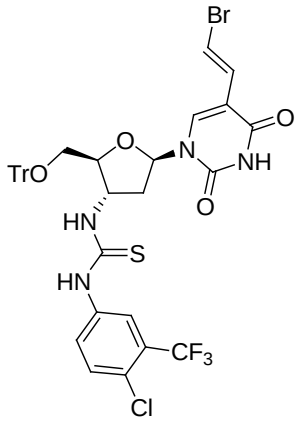

Reaction of compound **1.97** (104 mg, 0.18 mmol) with 4-chloro-3-(trifluoromethyl)phenyl isothiocyanate (37 µL, 0.24 mmol) was performed as described for the synthesis of compound **1.58** affording compound **1.98** in a 82% yield (119 mg, colourless solid).

^{1}H NMR (300 MHz, DMSO-d_6): δ 2.27-2.33 (1H, m, H-2'a), 2.49-2.60 (1H, m, H-2'b), 3.27-3.32 (1H, m, H-5'a), 3.41-3.46 (1H, m, H-5'b), 4.12-4.13 (1H, m, H-4'), 5.08 (1H, app br s, H-3'), 6.25 (1H, app t, *J*= 6.6 Hz, H-1'), 6.41 (1H, d, *J*= 13.8 Hz, H-8), 7.19-7.42 (16H, m, H-7 and Tr), 7.63-7.70 (2H, m, subs Ph), 7.85 (1H, s, 6-H), 8.02 (1H, s, subs Ph), 8.62 (1H, m, 3'-NH), 9.94 (1H, s, N'H), 11.65 (H, s, 3-NH).

^{13}C NMR (75 MHz, DMSO-d_6): δ 36.83 (C-2'), 54.23 (C-3'), 64.18 (C-5'), 83.07 (C-1'), 84.35 (C-4'), 86.40 (Tr), 107.12 (C-8), 110.02 (C-5), 120.88, 121.60, 124.50, 124.74, 125.29, 126.56, 127.17, 127.96, 128.28, 129.51, 130.42, 131.67 (CF_3, C-7, subs Ph and Tr), 139.14 (C-6), 143.39 (Tr), 149.24 (C-2), 161.67 (C-4), 180.57 (C=S).

Exact Mass (ESI-MS) for $C_{38}H_{31}BrClF_3N_4NaO_4S$ $[M + H]^+$ found: 833.0752, calcd: 833.0782.

5-(3'-Amino-(*E*)-5-(2-bromovinyl)-2',3'-dideoxy-5'-*O*-triphenylmethyl-β-D-uridin-3'*N*-yl)-1-[4-chloro-3-(trifluoromethyl)phenyl]tetrazole (1.99)

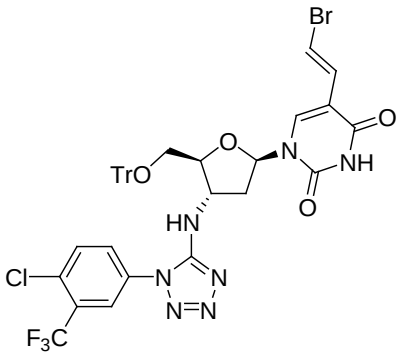

Reaction of compound **1.98** (90 mg, 0.11 mmol), NaN_3 (22 mg, 0.34 mmol), $HgCl_2$ (33 mg, 0.12 mmol) and Et_3N (45 µL, 0.32 mmol) in 0.5 mL DMF was performed as described in the general synthesis of substituted 1,5-aminotetrazole analogues. Compound **1.99** was obtained as white foam (68 mg, 75%).

^{1}H NMR (300 MHz, DMSO-d_6): δ 2.36-2.45 (1H, m, H-2'a), 2.49-2.58 (1H, m, H-2'b), 3.27-3.32 (1H, m, H-5'a), 3.43-3.48 (1H, m, H-5'b), 4.14 (1H, ddd, *J*= 2.7 Hz, *J*= 5.4 Hz, *J*= 5.4 Hz, H-4'), 4.43-4.55 (1H, m, H-3'), 6.29 (1H, app t, *J*= 6.9 Hz, H-1'), 6.50 (1H, m, *J*= 13.5 Hz, H-8), 7.21-7.46 (17H, m, H-7 and 3'-NH and Tr), 7.87-7.91 (2H, m, subs Ph), 8.00 (1H, s, 6-H), 8.03-8.04 (1H, subs Ph), 11.65 (1H, s, 3-NH).

^{13}C NMR (75 MHz, DMSO-d_6): δ 36.65 (C-2'), 54.40 (C-3'), 64.28 (C-5'), 82.75 (C-1'), 84.35 (C-4'), 86.36 (Tr), 107.11 (C-8), 110.13 (C-5), 120.36, 123.98, 124.93, 127.15, 127.68, 127.93-128.26, 129.53, 130.83, 131.89, 132.19 and 133.23 (CF_3, C-7, subs Ph and Tr), 139.42 (C-6), 143.49 (Tr), 149.24 (C-2), 154.48 (C=N), 161.63 (C-4).

Exact Mass (ESI-MS) for $C_{38}H_{30}BrClF_3N_7NaO_4$ $[M + Na]^+$ found: 842.1042, calcd: 842.1076.

5-(3'-Amino-(*E*)-5-(2-bromovinyl)-2',3'-dideoxy-β-D-uridin-3'*N*-yl)-1-[4-chloro-3-(trifluoromethyl)phenyl]tetrazole (1.100) and 5-[(4-chloro-3-(trifluoromethyl)phenyl)amino]-1-[(*E*)-5-(2-bromovinyl)-2',3'-dideoxy-β-D-uridin-3'-yl]tetrazole (1.101)

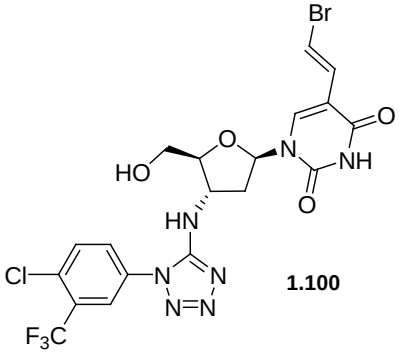

1.100

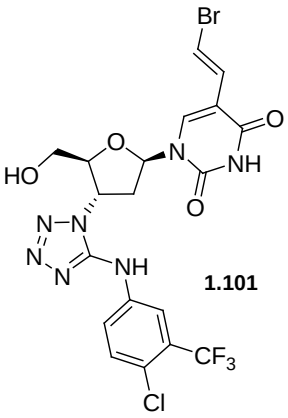

1.101

Reaction of compound **1.99** (80 mg, 0.11 mmol) under the same conditions as described for the synthesis of **1.90** and **1.91** and purification on a RP-HPLC (Phenomenex Luna C-18, H_2O/0.1% HCOOH in CH_3CN, 90:10 → 0:100 in 29 min, flow: 17.5 mL min^{-1}) afforded compounds **1.100** and **1.101** as white powders (17 mg, 32%, 3:1).

Compound **1.100**:

^{1}H NMR (300 MHz, DMSO-d_6): δ 2.38 (2H, app t, *J*= 6.6 Hz, H-2'a and H-2'b), 3.67-3.77 (2H, m, H-5'a and H-5'b), 4.02-4.06 (1H, m, H-4'), 4.40 (1H, app dd, *J*= 5.7 Hz, *J*= 6.0 Hz, H-3'), 5.23 (1H, app br s, 5'-OH), 6.22 (1H, app t, *J*= 6.9 Hz, H-1'), 6.86 (1H, d, *J*= 13.5 Hz, H-8), 7.26 (1H, d, *J*= 13.5 Hz, H-7), 7.95-8.09 (2H, m, subs Ph), 8.13-8.14 (1H, m, subs Ph), 8.19 (1H, s, H-6).

^{13}C NMR (75 MHz, DMSO-d_6): δ 37.36 (C-2'), 54.06 and 61.27 (C-3' and C-5'), 84.43 (C-1'), 84.91 (C-4'), 106.59 (C-5), 109.79 (C-8), 124.03-133.20 (CF_3, C-7 and subs Ph), 139.49 (C-6), 149.29 (C-2), 154.67 (C=N), 161.68 (C-4).

Exact Mass (ESI-MS) for $C_{19}H_{17}BrClF_3N_7O_4$ $[M+H]^+$ found: 578.0168, calcd: 578,0161.

Compound **1.101**:

^{1}H NMR (300 MHz, DMSO-d_6): δ 2.65-2.71 (2H, m, H-2'a and H-2'b), 3.70-3.3.74 (2H, m, H-5'a and H-5'b), 3.90-4.03 (1H, m, H-4'), 4.34-4.40 (1H, m, H-3'), 5.55-5.57 (1H, m, 5'-OH), 6.42 (1H, app t, *J*= 6.3 Hz, H-1'), 6.93 (1H, d, *J*= 13.8 Hz, H-8), 7.29 (1H, d, *J*= 13.5 Hz, H-7), 7.69 (2H, d, *J*= 8.7 Hz, subs Ph), 7.99-8.01 (1H, m, subs Ph), 8.22 (1H, s, H-6).

^{13}C NMR (175 MHz, DMSO-d_6): δ 56.70 and 61.46 (C-3' and C-5'), 84.80 (C-1'), 85.25 (C-4'), 110.49 (C-5), 116.92-132.73 (CF_3, C-7, C-8 and subs Ph), 139.91 (C-6), 149.78 (C-2), 162.16 (C-4).

Exact Mass (ESI-MS) for $C_{19}H_{17}BrClF_3N_7O_4$ $[M+H]^+$ found: 578.0173, calcd: 578,0161.

PART II

FURTHER EXPLORATION OF THE S.A.R. OF SUBSTRATE-BASED *M. tuberculosis* TMPK INHIBITORS

1 INTRODUCTION

Tuberculosis (TB), a contagious infection caused by *Mycobacterium tuberculosis*, has troubled humankind since its inception. It has been a leading cause of death throughout the world (± 2 million people annually), mainly in developing and underdeveloped countries. Currently, one third of the world population is latently infected. In 2009, there were an estimated 9.4 million incident cases of TB globally, with much of the burden falling on the young and middle aged between 15-49 years old.[83] Most occur in Asia (55%) and Africa (30%), smaller proportions in the Eastern Mediterranean Region (7%), the European Region (4%) and the Region of the Americas (3%) (Figure II.1).[84]

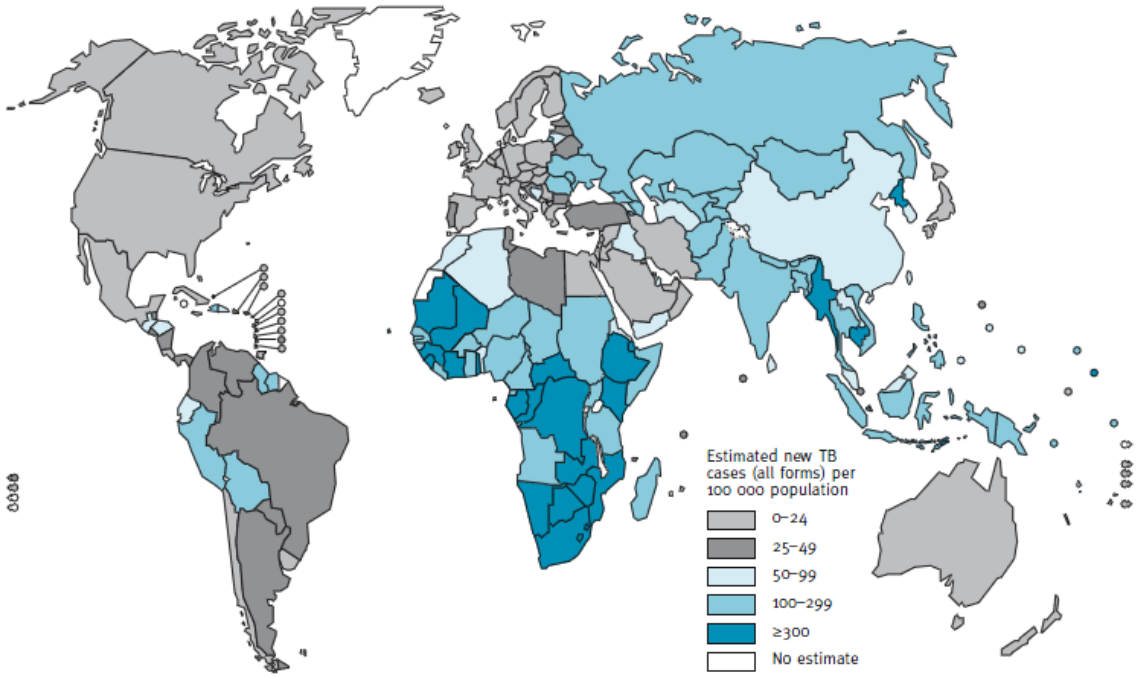

Figure II.1. Estimated TB incidence rates by country, 2009[84]

HIV infection accounts for much of the recent increase in the global tuberculosis burden. In 2009, an estimated 12% of the 9.4 million incident cases were HIV-positive. Of these HIV-positive TB cases, approximately 80% were in the African Region. HIV-associated TB (HIV-TB) remains a major challenge to global health, and the epidemic is one of the major hurdles to attain the 2015 Millennium Development Goals for TB control (United Nations 2008).[84]

In the early 1980's, the great majority of patients with tuberculosis could be cured by treatment with short-course curative chemotherapy that was possible as a consequence of several newly introduced anti-TB drugs. Unfortunately, the huge success of this drug treatment has been the catalyst for the emergence of a new wave of drug resistance. While wealthy industrialized countries with good public health care systems are expected to keep TB under control, in much of the developing world a catastrophe awaits. To avoid the risk of losing the battle against TB, it is crucially important to support research efforts devoted to (i) developing an effective TB vaccine, (ii) improving the diagnosis of TB and (iii) creating new, highly effective anti-TB medications.

1.1 TUBERCULOSIS

1.1.1 Causative Organisms

Human tuberculosis is an infection caused by the rod-shaped, Gram positive, aerobic bacterium *Mycobacterium tuberculosis.* Other human pathogens belonging to the *Mycobacterium* genus and causing TB include *Mycobacterium bovis* (usually in cows and rarely in humans) and *Mycobacterium avium*. Mycobacteria typically have a unique cell wall structure crucial to their survival. The well developed cell wall contains a considerable amount (± 50%) of a fatty acid, mycolic acid, covalently attached to the underlying peptidoglycan-bound polysaccharide arabinogalactan, providing an extraordinary lipid barrier (Figure II.2). This unique hydrophobic layer is an extremely efficient permeability barrier protecting the cell from toxic compounds and is generally thought to be the major determinant of the intrinsic resistance of mycobacteria to most common antibiotics, chemotherapeutic agents and chemical disinfectants.[85]

One of the major hurdles in the search for new anti-TB agents is their uptake into the bacillus. So far, a few pathways for transport across the cell wall are suggested: (i) penetration of hydrophobic compounds by temporarily dissolving in the lipid bilayer and (ii) diffusion through water-filled protein channels (= porins) for small and hydrophilic compounds.[85] Nevertheless, further research is indispensable to facilitate the development of new antituberculosis drugs.

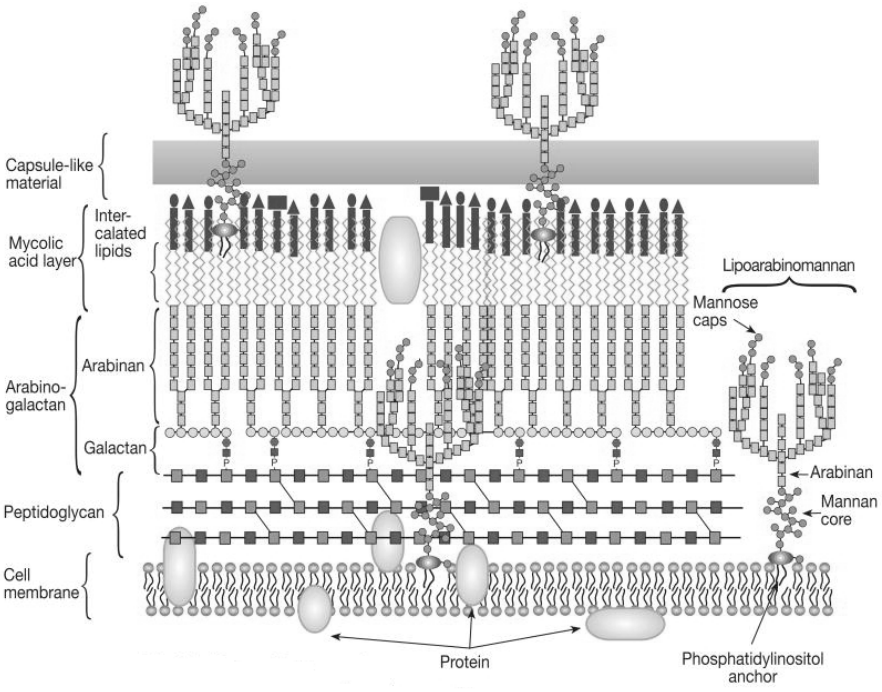

Figure II.2. Schematic representation of the cell envelope of *Mycobacterium tuberculosis*.[86,87]

1.1.2 Transmission

Mycobacterium tuberculosis is spread by small airborne droplets, generated by the coughing, sneezing, talking or singing of a person with pulmonary or laryngeal tuberculosis. Because of their small size, 1-5 µm in diameter, these particles can remain airborne for minutes to hours after expectoration.[88] Introduction of *M. tuberculosis* into the lungs can lead to infections of the respiratory system, however, the organism can spread to other organs, such as the lymphatics, pleura, bones/joints, or meninges, and cause extrapulmonary tuberculosis.[89] The risk of infection following exposure depends on several factors, including the concentration of bacteria in the air, the duration of exposure, the virulence of the organism and the immunocompetence of the exposed individual.[90]

1.1.3 Pathophysiology

Once inhaled, the infectious droplets settle throughout the airways. The majority of the bacilli are trapped in the upper parts of the airways where the mucus-secreting goblet cells exist. The mucus produced catches foreign substances, and the cilia on the surface of the cells constantly beat the mucus and its entrapped particles upwards for removal. This system provides the body with an initial physical defense that prevents infection in most persons exposed to TB.[89]

Bacteria in droplets that bypass the mucociliary system and reach the alveoli are quickly surrounded and engulfed by alveolar macrophages, the most abundant immune effector cells present in alveolar spaces. The macrophages, are part of the innate immune system and provide an opportunity for the body to destroy the invading mycobacteria and prevent infection. The subsequent phagocytosis by macrophages initiates a cascade of events resulting in either successful control of the infection, followed by latent tuberculosis, or progression to active disease, called primary progressive tuberculosis. The risk of development of active disease varies according to time since infection, age and host immunity.[88]

After being ingested by alveolar macrophages, *M. tuberculosis* replicates slowly but continuously and spreads via the lymphatic system to the hilar lymph nodes. In most infected individuals, cell-mediated immunity develops 2-8 weeks after infection. For persons with intact cell-mediated immunity, the next defensive step is the formation of granulomas around *M. tuberculosis* organisms. These nodular-type of lesions, coming from an accumulation of macrophages and lymphocytes, create a micro-environment that limits replication and the spread of the mycobacteria. This environment destroys macrophages and produces early solid necrosis at the center of the lesion, however, the bacilli are able to survive. By 2 or 3 weeks, the necrotic environment resembles cheese, often referred to caseous necrosis, and is characterized by low oxygen levels, low pH and limited nutrients restricting further growth, thereby establishing latency. Lesions in persons with an adequate immune system generally undergo fibrosis and calcification, successfully controlling the infection. For less immunocompetent persons, granuloma formation is unsuccessful in capturing the bacilli. The necrotic

tissue undergoes liquefaction, and the fibrous wall loses structural integrity. The semi-liquid material can then drain into a bronchus or nearby blood vessel. If discharge into a vessel occurs, extrapulmonary tuberculosis is likely to occur. Bacilli can also drain into the lymphatic system and collect in the tracheobronchial lymph nodes of the affected lung, where the organism can form new caseous granulomas.[89]

Although, an effective host immune response can initially suppress *M. tuberculosis*, several factors can trigger subsequent development of active disease from reactivation of the latent infection. HIV is the greatest single risk factor for progression to active disease in adults. Other medical conditions that can compromise the immune system and predispose to development of active disease include poorly controlled diabetes mellitus, renal failure, chemotherapy, extensive corticosteroid therapy and malnutrition.[88]

1.1.4 Symptoms

Tuberculosis, although quite a serious disease, does not produce any symptoms in most of the cases where the infection has entered the body. Many individuals may host the bacteria but remain unaffected by their presence. Persons with latent tuberculosis have no signs or symptoms and are not infectious.

Primary pulmonary tuberculosis is often asymptomatic, so that the results of diagnostic tests are the only evidence of the disease. In some cases patients suffer from fever, paratracheal lymphadenopathy or dyspnea. In this stage the infection may be only subclinical and may not advance to active disease.

Primary progressive TB develops in 5-10% of persons exposed to *M. tuberculosis*. When a patient progresses to active tuberculosis, early signs and symptoms are often nonspecific including progressive fatigue, malaise, weight loss and a low-grade fever accompanied by chills and night sweats. Other symptoms of active TB involve wasting, finger clubbing, coughing, hemoptysis, pleuritic chest pain and dyspnea or orthopnea.

Although the pulmonary system is the most common location for tuberculosis, extrapulmonary disease occurs in more than 20% of immunocompetent patients and the risk for extrapulmonary disease increases with immunosuppression. Most devastating is TB of the central nervous system, where infection may result in meningitis or space-occupying tuberculomas. If not treated, tubercular meningitis is fatal in most cases.

Another fatal form of extrapulmonary TB is infection of the bloodstream by mycobacteria (= disseminated or miliary tuberculosis). The bacilli can then spread throughout the body, leading to multi-organ involvement. Miliary TB progresses rapidly and can be difficult to diagnose because of its systemic and nonspecific signs and symptoms such as fever, weight loss and weakness. Lymphatic

TB is the most common extrapulmonary tuberculosis. Other possible locations include bones, joints, pleura and genitourinary system.[89]

1.1.5 Diagnosis

People who are suspected of having active TB may be given a number of different tests to confirm the damage caused by the infection or to identify the organisms responsible for the infection.

1.1.5.1 Microscopy

Worldwide, the most common diagnostic test used to detect tuberculosis is the microscopic examination of sputum or other clinical materials. For the smear, the sample is spread thinly onto a glass slide, treated with Ziehl-Neelsen stain, decolorized using acid alcohol and counterstained with methylene blue. Acid-fast organisms appear to be red, other tissue elements will be blue.

Microscopy is cheap to perform, specific enough to indicate treatment in countries where TB is prevalent and can be completed within hours if necessary. However, microscopy requires a large number of bacilli (5000 - 10 000 per mL sputum) to be present in order for the result to be positive.[90]

1.1.5.2 Culture

Bacteriological culture, considered as a the diagnostic gold standard, can identify the *M. tuberculosis* organism in >80% of TB cases with a specificity of >98%. As few as 10 - 100 viable bacilli per mL may be detected, although the sensitivity of cultures varies substantially depending on the specimen-processing method and the culture medium used.

Compared to the smear microscopy method, culture technique is more sensitive but its also more expensive and requires highly trained personnel. Nevertheless, it allows detection of more forms of disease, including less advanced cases. As *M. tuberculosis* grows slowly, conventional culture with visual detection of bacterial colony formation usually requires 2 to 6 weeks.[90]

1.1.5.3 Tuberculin Skin Test (= Mantoux test)

This method has been used in the clinic for many years primarily to detect latent infection, although it has also been applied inappropriately for detecting active disease in adults. Tuberculin or purified protein derivative (PPD) is composed of proteins from heat killed *M. tuberculosis*. Injection of PPD under the forearm skin will cause a hypersensitivity reaction in people with prior TB infection. This reaction presents as skin thickening at the site of injection after 24-48 hours. Unfortunately, its application is problematic due to the frequency of false-positive (e.g., BCG vaccine) and false negative (e.g., immunodefiency) skin reactions. Despite these shortcomings, the test is manufactured around the globe and applied broadly in almost all countries.[89,90]

1.1.5.4 Radiographic Methods

It is still widely believed that tuberculosis of the lung can be diagnosed by chest X-ray. However, practical experience and numerous studies have shown that no radiographic pattern is diagnostic of tuberculosis. Many diseases of the lung have a similar radiographic appearance that can easily mimic TB. Similarly, the lesions of pulmonary tuberculosis can take almost any form on a radiographic picture. In developed countries where facilities and resources permit, patients with signs and symptoms of pulmonary TB are screened by chest X-ray. However, to establish the tubercular etiology of an abnormality, further examination is necessary and only bacteriology can provide the necessary proof.[90]

1.1.5.5 NAATs

Nucleic acid amplification tests constitutes a rapidly evolving improvement in the detection and identification of *M. tuberculosis*. Bacterial DNA (or ribosomal RNA transcribed into DNA) is enzymatically amplified and detected with an appropriate reading system via a signal-generating probe. Although the test can provide rapid confirmation of *M. tuberculosis* in sputum specimens positive for acid-fast bacilli, it has limitations including high cost, low sensitivity in smear-negative, culture positive specimens and low availability.[90]

1.1.6 Prevention and Control

The fundamental strategies for the prevention and control of TB include:[91]

- early and accurate detection, diagnosis, and reporting of TB cases, leading to initiation and completion of treatment,
- identification of contacts of patients with infectious TB and treatment of those at risk with an effective drug regimen,
- identification of other persons with latent TB infection at risk for progression to TB disease, and treatment of those persons with an effective drug regimen,
- identification of settings in which a high risk exists for transmission of *M. tuberculosis* and application of effective infection control measures.

Interestingly, BCG vaccination is not recommended world wide as a routine strategy for TB control.

1.1.6.1 DOTS

To control tuberculosis, WHO and IUATLD (International Union Against Tuberculosis and Lung Diseases) recommend the DOTS strategy. Directly Observed Treatment Short course is a highly efficient and cost-effective strategy which is based on a five point policy package: political commitment, diagnosis primarily by sputum-smear microcopy, short-course anti-TB treatment, regular

drug supply and systematic monitoring to assess outcomes of every treated patient. Standard short-course regimens can cure more than 95% of cases of new, drug-susceptible tuberculosis.[88]

DOTS produces superior treatment completion rates to those achieved by non-supervised interventions (DOTS: 79-81% vs. non-supervised: 61%). When implemented over a long period, there will be a huge reduction in sources of infection and transmission.[92]

1.1.6.2 BCG Vaccination

BCG (Bacille Calmette-Guérin) was developed at the start of this century and is the most widely used vaccine in the world. It was developed by attenuation of *M. bovis*, which is closely related to *M. tuberculosis* (> 90% DNA homology). It is given in a single dose following a negative tuberculin skin test. The most controversial aspect of BCG is the variable efficacy found in different clinical trials. Generally speaking, trials conducted in the 1940s and 1950s in developed countries such as the UK, Denmark and North America demonstrated the vaccine to be highly efficient (70-80%), whereas more recent trials demonstrated no detectable protection against pulmonary TB. Several explanations for this variation in protective efficacy have been suggested, such as differences in strains and doses, genetic variability in the population studied, … . The most accepted hypothesis attributes this variation to higher levels of exposure to environmental mycobacteria in the areas where the vaccine affords no protection. Nevertheless, based on available information concerning the effectiveness of BCG vaccine in preventing serious forms of TB in children, WHO recommends BCG vaccination of children as soon as possible after birth in countries with a high TB prevalence.[93,94]

1.1.7 Treatment

1.1.7.1 Chemotherapy

Mycobacteria are intrinsically resistant to most antibiotics due to several reasons (e.g., slow growth dormant stage, lipid-rich mycobacterial cell wall, …). Normally, the response of mycobacterial infections to chemotherapy is slow, and treatment must be administered for months to years, depending on which drugs are used. According to their therapeutic relevance and side effects, one can distinguish primary and second-line drugs. First-line drugs are common for patients without drug resistance strains or strains resistant to one or two drugs (other than isoniazid and rifampicin) and second line drugs are used in cases of multi-drug resistant infections, in combination with first-line drugs. These second line drugs are often less effective, have more side effects and are more expensive compared to the standard drugs.

a) First-line antituberculosis drugs (Table II.1).

Table II.1 First-line anti-tuberculosis drugs

	Isoniazid[95,96]	**Rifampicin**[96,97]	**Pyrazinamide**[96,98]	**Ethambutol**[98,99]	**Streptomycin**[96,98]
Structure	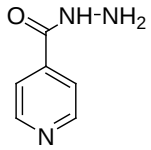	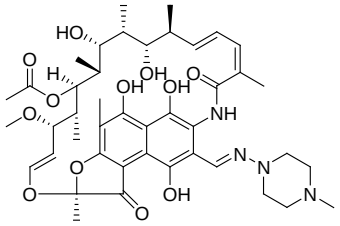	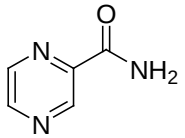	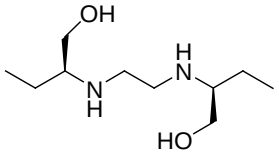	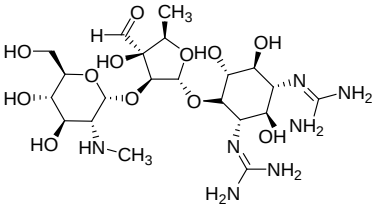
Mechanism of action	Inhibition of mycolic acid biosynthesis	Inhibition of protein synthesis	Unknown	Inhibition of arabinosyl transferases involved in cell wall biosynthesis	Inhibitors of protein synthesis
Activity	Bactericidal in high concentration	Bactericidal	Alkaline or neutral: ineffective Acidic: effective Bactericidal against 'semi dormant bacilli'	Bacteriostatic	Bactericidal
Administration	Oral	Oral	Oral	Oral	Parenteral
Drawback	Limited efficacy against metabolically less active bacilli	Hepatotoxicity, resistance is developed with high frequency	Resistance is developed with high frequency	Vision impairment	Ototoxic, given by injection
Resistance	Mutations in gene encoding for katG and *inh*A	Mutation in gene for RNA-polymerase β-subunit	Mutations in gene encoding for pyrazinamidase	Mutations in gene encoding for arabinosyl transferases	Mutation in genes encoding for bacterial ribosomes

b) Second-line antituberculosis drugs (Table II.2)

Table II.2 Second-line anti-tuberculosis drugs

	Thioamides[96,100] (e.g., ethionamide, prothionamide)	**Aminoglycosides**[96] (kanamycin, amikacin)	**Peptides**[96,98,101] (capreomycin, viomycin)	**Fluoroquinolones**[96,98] (ciprofloxacin, ofloxacin)	**D-Cycloserine**[98]	***p*-Amino-salicylic acid**[102]
Structure	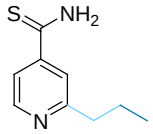	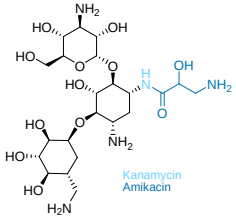	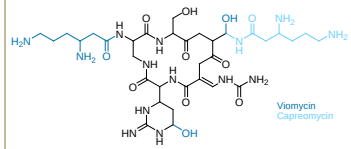	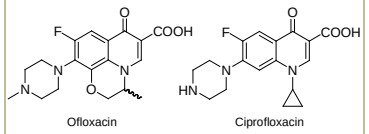	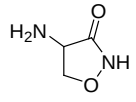	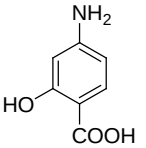
Mechanism of action	Inhibition of mycolic acid biosynthesis	Inhibitors of protein synthesis	Inhibitors of protein synthesis	Inhibition of DNA-gyrase	Inhibition of peptidoglycan involved in cell wall biosynthesis	Inhibition of folate and mycobactin biosynthesis
Administration	Oral	Parenteral	Parenteral or intramuscular	Oral or parenteral	Oral	Oral
Side effects	Gastric irritation, neurologic symptoms, hepatotoxic	Irreversible ototoxicity, nephrotoxic effects	Nephrotoxic and ototoxic	Gastrointestinal disturbance and neurologic effects	Central nervous system dysfunction	Gastro-intestinal irritations and hepatotoxic effects
Resistance	Mutation in gene encoding for *inh*A	Mutation in gene encoding for 16S RNA	Mutations in gene encoding for 16S RNA	Mutations in genes encoding for DNA-gyrase	Mutation on gene encoding for D-alanine racemase	Mutations on gene encoding for *thy*A

c) WHO recommended regimens

According to the World Health Organization, treatment of active tuberculosis is dependent on whether the disease has become drug resistant or not.

- Standard first-line TB treatment requires a patient to take a combination of four drugs (isoniazid, rifampicin, pyrazinamide and ethambutol or streptomycin) for a minimum of six months. An unfinished treatment course can lead to treatment failure and the emergence of drug resistance.[88,103]

- TB patients returning after defaulting or relapsing from their first treatment course may receive the retreatment regimen combining five drugs for a period of 8 months. During the whole period, isoniazid, rifampicine and ethambutol are administered, combined with pyrazinamide during the first three months and streptomycin during the first two months. The vast majority of the patients will be cured with this retreatment regimen. Failures are generally due to the use of an incorrect regimen and/or failure to ensure that the regimen is fully administered and directly observed.[103]

- Multidrug resistance makes regimens with first-line drugs much less effective. Initiation of MDR treatment with second-line drugs gives a better chance of cure and prevents the development and spread of further resistance. Unfortunately, these agents are more expensive and cause more side effects compared to the standard drugs. Treatment regimens should consist of at least four drugs with either certain, or almost certain, effectiveness.[103]

1.1.7.2 Surgery

Surgery is rarely used to treat tuberculosis (TB), although it may be used to treat extensively drug-resistant TB (XDR-TB) or to treat complications of an infection in the lungs or other parts of the body.

1.1.8 Resistance

1.1.8.1 Drug Resistant Tuberculosis

Resistance to anti-TB drugs arises as a result of spontaneous mutations in the genome of *M. tuberculosis.* These mutations occur at predictable rates for each anti-tuberculosis drug (e.g., isoniazid 10^{-6}, rifampicin 10^{-8}). Thus, in patients with active tuberculosis disease, subpopulations of resistant mycobacteria spontaneously arise, and can emerge as the dominant strain in the presence of drug-selection pressure. Resistance to additional tuberculosis drugs can be added in a step-wise manner to create tuberculosis strains that are resistant to several drugs. This process is referred to as acquired resistance (= secondary resistance, figure II.3) and is the rationale for the adage “never add a single drug to a failing regimen”.[104]

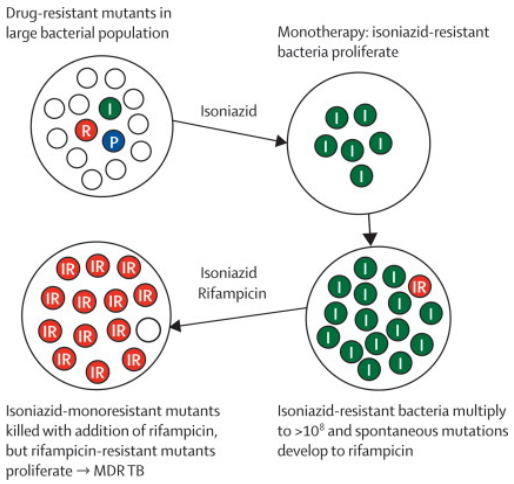

Figure II.3. Acquisition of resistance[104]

Once created, drug-resistant strains can be transmitted, giving rise to drug-resistant tuberculosis in individuals never previously exposed to anti-TB drugs (= primary resistance, Figure II.4). The global epidemic of drug-resistant tuberculosis is due to a combination of acquired resistance and primary transmission.

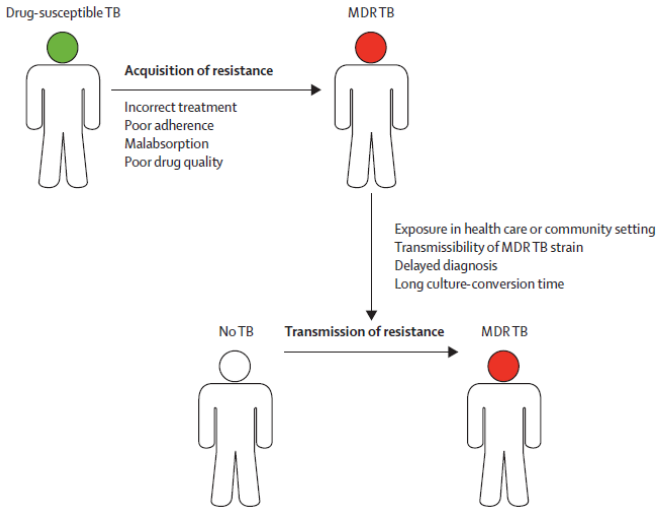

Figure II.4. Mechanisms in the development of resistance.[104]

1.1.8.2 Multidrug Resistant (MDR) - Extensively Drug Resistant (XDR) Tuberculosis

A particularly dangerous form of drug-resistant TB is multidrug-resistant TB, which is defined as the disease caused by TB bacilli resistant to at least isoniazid and rifampicin, the two most powerful anti-TB drugs. MDR-TB is not limited to the developing world. During the late 1980s and early 1990s, outbreak of MDR-TB in North America and Europe killed more than 80% of those who contracted the disease. In 2008, an estimated 440 000 cases of multidrug-resistant TB emerged. The WHO estimates that MDR-TB makes up greater than 10 percent of all new TB cases in Eastern Europe, the region most affected by the disease.[84,104] Nevertheless, drug-resistant TB is generally treatable although it requires extensive chemotherapy (up to two years of treatment) with second-line anti-TB drugs, which are more costly than first-line drugs and which produce adverse drug reactions that are more severe, though manageable.

Extensively drug resistant is emerging as an even more ominous threat. XDR-TB is caused by *M. tuberculosis* that is resistant to rifampicin and isoniazid, any fluoroquinolone, and one of the three injectable drugs, capreomycin, kanamycin and amikacyn. In March 2006, the Centers for Disease Control and Prevention (CDC) released the first known data on XDR-TB. The CDC and the WHO surveyed TB strains from a global network of TB laboratories and identified XDR-TB cases in all regions of the world. In the worst affected areas, an average of 10% of MDR-TB cases were found to be XDR-TB.[105]

1.2 THYMIDINE MONOPHOSPHATE KINASE (TMPK)

Thymidine monophosphate kinase (TMPK, also called ATP:dTMP phosphotransferase or thymidylate kinase) belongs to the nucleoside monophosphate kinase (NMPKs) family.[106] It catalyses the reversible phosphorylation of thymidine monophosphate (dTMP) to thymidine diphosphate (dTDP) utilizing ATP as its preferred phosphoryl donor.

$$dTMP + ATP \xrightleftharpoons{TMPKmt} dTDP + ADP$$

TMPK lies at the junction of the *de novo* and salvage pathway for the synthesis of thymidine triphosphate (dTTP). Because its crucial role in thymidine metabolism and in view of its low (22%) sequence identity with the human isoenzym (TMPKh), it represents an attractive target for blocking mycobacterial DNA synthesis.

1.2.1 Structure of TMPKmt

In 2001, de la Sierra *et al*. reported the X-ray structure of TMPK from *M. tuberculosis* (TMPKmt) bound to its natural substrate.[107] TMPKmt has a molecular mass of 24 kDa and consists of 214 amino acid residues. It is a homodimer, each monomer being composed of nine α-helices surrounding a five-stranded β-sheet core. This global folding is similar to that of other TMPKs, despite the low similarity of their primary sequences: 26%, 25% and 22% sequence identity over about 200 aligned residues with TMPKec (*E. coli*), TMPKy (yeast) and TMPKh respectively.

The essential residues for the function of the enzyme can be found in three regions:

- The P-loop, a highly conserved motif, controls the positioning of the phosphoryl groups of the phosphate donor. It binds and positions the α- and β-phosphoryl groups of ATP through interactions with amide backbone hydrogens. Unique for TMPKs is an interaction between the P-loop and the phosphoryl acceptor dTMP achieved through interaction between the 3'-hydroxyl group of dTMP and a carboxylic acid residue at position X_2 of the P-loop motif (Asp9 in TMPKmt). Although the exact function of Asp9 is still unclear, it seems to play a key role in the catalytic mechanism of TMPK as any mutation of this residue in either the yeast, human or *E. coli* enzyme abolishes the phosphoryl transfer activity.[108]

- The DR(Y/H/F)-motif is a strictly conserved Arg residue acting as a clip to orient the phosphoryl donor and acceptor via an interaction with the phosphate group of dTMP and the γ-phosphate of ATP.

- The LID region closes as a flexible stretch upon binding of the phosphoryl donor to the enzyme. Phosphoryl groups of both substrates interact with Arg side chains of the LID region, revealing the importance of these amino acids in catalyzing phosphoryl transfer.[107]

NMPKs, including TMPKmt, are highly flexible molecules that undergo large conformational changes upon substrate binding. One can distinguish between (i) the open conformation, observed without substrate, (ii) the partially closed conformation with a single substrate and (iii) the fully closed and active conformation, observed in the presence of both substrates (dTMP and ATP).[107]

Another unique feature of TMPKmt is that, for catalysis, it requires the transient binding of a magnesium ion to coordinate the phosphate acceptor. The observed Mg^{2+} is not reported for the yeast or *E. coli* enzyme and for the human enzyme, one magnesium binding site has been reported but is located further away along the ATP-binding site, between the β- and γ-phosphate groups. Three water molecules, an oxygen atom from the phosphoryl of dTMP and the carboxylate oxygen atoms of Asp9 and Glu166 coordinate the Mg^{2+} in an octahedral configuration.[107] Fioravanti *et al*. suggest that this cation neutralizes the electrostatic repulsion between the anionic substrates and optimizes their proper alignment.[109]

1.2.1.1 The dTMP-binding Site

Examination of the X-ray structure of TMPKmt reveals that the main binding forces between dTMP (**2.1**) and the enzyme are (Figure II.5):[110]

- a stacking interaction between the pyrimidine ring and Phe70,
- a hydrogen bond between *O*4 of thymidine and the Arg74 side-chain which results in a preference for thymidine over cytosine,
- a hydrogen bond between Asn100 and N3 of the thymidine ring,
- a hydrogen bond between the 3'-hydroxyl of dTMP and the terminal carboxyl of Asp9, that in turns interacts with Mg^{2+}, responsible for positioning the phosphate oxygen of dTMP,
- hydrogen bonds between the 5'-*O*-phosphoryl group and Tyr39 and Phe36,
- ionic interactions between the 5'-*O*-phosphoryl group and Arg95 and Mg^{2+}.

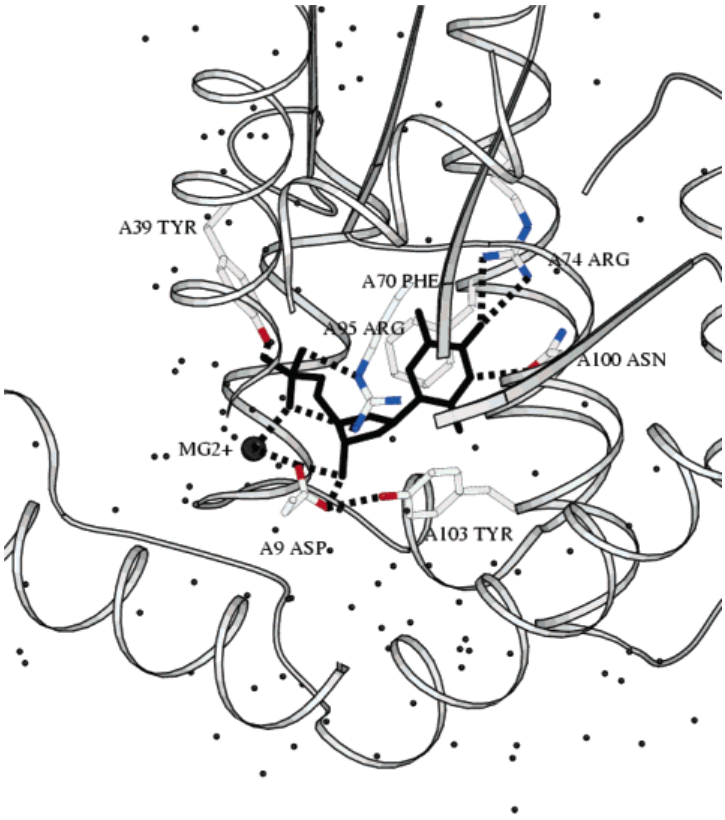

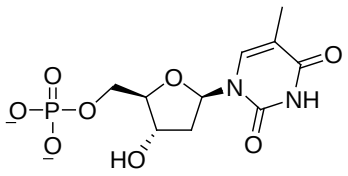

2.1 (dTMP)

Figure II.5. Schematic representation of the most important amino acid residues of TMPKmt interacting with dTMP (in black) + structure and atom numbering of dTMP[110]

1.2.2 Known TMPKmt Inhibitors

1.2.2.1 Close Analogues of the dTMP Substrate

Initially, effort were made to obtain TMPK inhibitors by modifying the structure of the substrate.[111]

- Base modifications

The 5-methyl group of dTMP was replaced by several halogen atoms. All these compounds behaved as substrates for TMPKmt, the best one being 5-Br-dUMP with a slight decrease in K_m and V_m compared to dTMP. Substitution by an iodine (5-I-dUMP) or a fluorine (5-F-dUMP) drastically decreased the affinity for the enzyme. Upon removal of the methyl group (dUMP), the affinity drastically decreased (50-fold) as well as the reaction rate (3-fold). Modification at the 2-position of the pyrimidine ring resulted in 5-methyl-iso-dCMP which acted as a competitive inhibitor with a K_i of 130 µM.[111]

Because a 5-bromine (5-Br-dUMP) was well accepted by the enzyme, analogs with sterically demanding substituents at the 5-position (e.g., hydroxymethyl, ethyl, bromovinyl, furanyl, thienyl or benzyloxymethyl) were investigated as TMPKmt inhibitors and found less potent indicating that the cavity near the 5-position cannot be stretched too much.[112]

- 3'-modifications

The first reported selective competitive inhibitor for TMPKmt is AZTMP in which the 3'-hydroxyl of the natural substrate is substituted by an azido group. While AZTMP behaves as a substrate for TMPKec and TMPKy, it showed a K_i of 20 µM for TMPKmt. X-ray structures of TMPKmt in complex with dTMP and AZTMP provide structural evidence that AZTMP inhibits TMPKmt by excluding the Mg^{2+} ion, essential for catalysis.[110]

Due to the unique behavior of AZTMP towards TMPKmt in comparison to other TMPKs, 3'-modifications in particular were considered to have potential for finding good and selective inhibitors. 3'-Amino-3'-deoxythymidine monophosphate, intended to establish an ionic interaction with Asp9, showed a 20-fold higher K_i value compared to AZTMP indicating that the 3'-amino group does not interact with Asp9 as strongly as AZTMP.[113]

In the X-ray structure, near the 3'-posititon, one could observe a cavity with the potential of accommodating larger substituents, which led Vanheusden *et al.* to prepare a series of 3'-*C*-branched-chain nucleotides (the 3'-*C*-hydroxymethyl (**2.2**), 3'-*C*-azidomethyl (**2.3**), 3'-*C*-aminomethyl (**2.4**) and 3'-*C*-fluoromethyl (**2.5**) derivatives of dTMP). 2'-Deoxy-3'-branched chain analogues proved to be potent inhibitors of TMPKmt: within the series 3'-CH_2NH_2 (**2.4**), 3'-CH_2N_3 (**2.3**) and 3'-CH_2F (**2.5**) nucleotides exhibited the highest affinities with K_i values of 10.5, 12 and 15 µM, respectively (Figure II.6).[110]

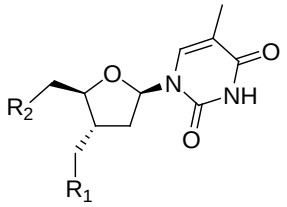

2.2: R_1 = OH, R_2 = OPO_3^{2-}
2.3: R_1 = N_3, R_2 = OPO_3^{2-}
2.4: R_1 = NH_2, R_2 = OPO_3^{2-}
2.5: R_1 = F, R_2 = OPO_3^{2-}

2.6: R_1 = OH, R_2 = OH
2.7: R_1 = N_3, R_2 = OH
2.8: R_1 = NH_2, R_2 = OH
2.9: R_1 = F, R_2 = OH

Figure II.6

Interestingly, the parent nucleosides (**2.6-2.9**) generally exhibited affinities for TMPKmt in the same order of magnitude and displayed a superior selectivity profile versus human TMPK.[110] A main disadvantage of 5'-*O*-phosphorylated analogues concerned their uptake in cells, generally accepted to be very difficult. Normally, nucleosides cross the cell membrane barrier in the non-phosphorylated form and are then phosphorylated by intracellular kinases. However, in this particular case, intracellular activation is not possible, as no gene coding for TK could be identified in the *M. tuberculosis* genome. The inhibitory activities of **2.6-2.9** indicated the possibility of the enzyme to accommodate non-phosphorylated thymidine analogues and directed further research toward the synthesis of non-phosphorylated TMPKmt inhibitors.

- Bicyclic and dimeric nucleoside inhibitors

In an effort to further optimize the inhibitory potency of 3'-*C*-branched-chain nucleosides, Vanheusden *et al*. serendipitously obtained 3 potent and selective TMPKmt inhibitors **2.10-2.12** (Figure II.7).[114]

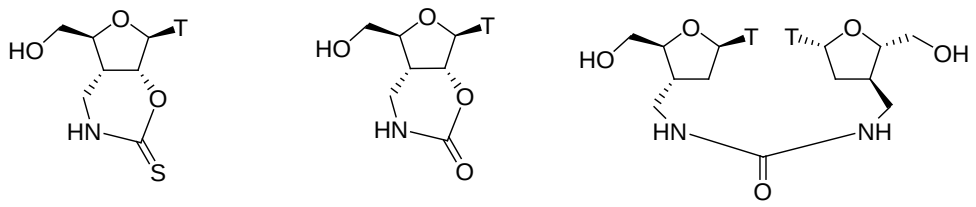

2.10 (K_i = 3.5 μM) **2.11** (K_i = 13.5 μM) **2.12** (K_i = 37 μM)

Figure II.7

1.2.2.2 Optimization of the Branched-Chain Nucleosides

Due to the lack of a binding site for a second nucleoside at the 3'-position, the K_i value of **2.12** (37 μM) was most unexpected. Modeling studies on the binding mode of dinucleoside **2.12** to its target suggested that the second monomer binds to the area where normally the phosphoryl donor binds, in this way forcing the sugar ring to tilt over 180° compared to the natural substrate dTMP (Figure II.8).[114]

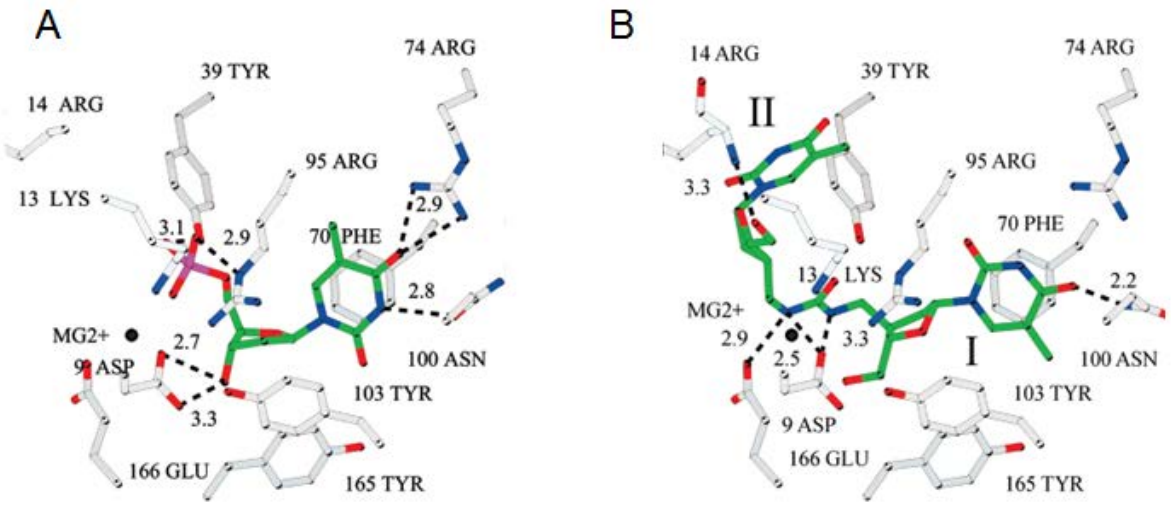

Figure II.8. Comparison of the binding mode of dTMP with the binding mode of compound **2.12**. (A) dTMP as observed in the X-ray structure with TMPKmt.[107] (B) Predicted binding mode of **2.12** with TMPKmt. Hydrogen bonds are drawn as dashed lines from **2.12** to residues Asp9, Arg14, Asn100 and Glu166. Residues whose atoms make hydrophobic contact with **2.12** are Lys13, Ala35, Tyr39, Phe36, Phe70, Arg95, Asn100, Tyr103 and Tyr165.[114]

These results encouraged Van Daele *et al*. to explore if the binding site, which accommodates the second thymidine residue of **2.12**, could be occupied with different aryl moieties connected to 3'-*C*-branched thymidine via a thiourea moiety.[69] This resulted in several analogs with excellent affinity for TMPKmt, e.g., **2.13** (K_i = 5 µM, Figure II.9).

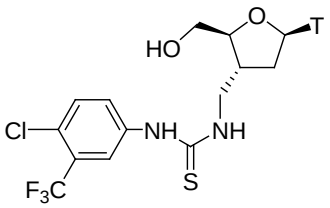

2.13

Figure II.9

In a next step, Van Daele *et al*. explored if an alternative sugar scaffold could be used to impose the favorable relative orientation of the thymine and the phenylthiourea moieties for TMPKmt inhibition.[69] It was hypothesized that an α-nucleoside in which the 5'-position served as the thiourea anchor might show potential towards this end (Figure II.10). This hypothesis was supported by the discovery that α-thymidine 5'-monophosphate (α-dTMP) was accepted by TMPKmt as a substrate (K_m = 15 µM), indicating that inversion of configuration at the anomeric position does not prevent the 5'-OP(O)(OH)$_2$ moiety from being favorably oriented in order to operate as a phosphate acceptor.[69]

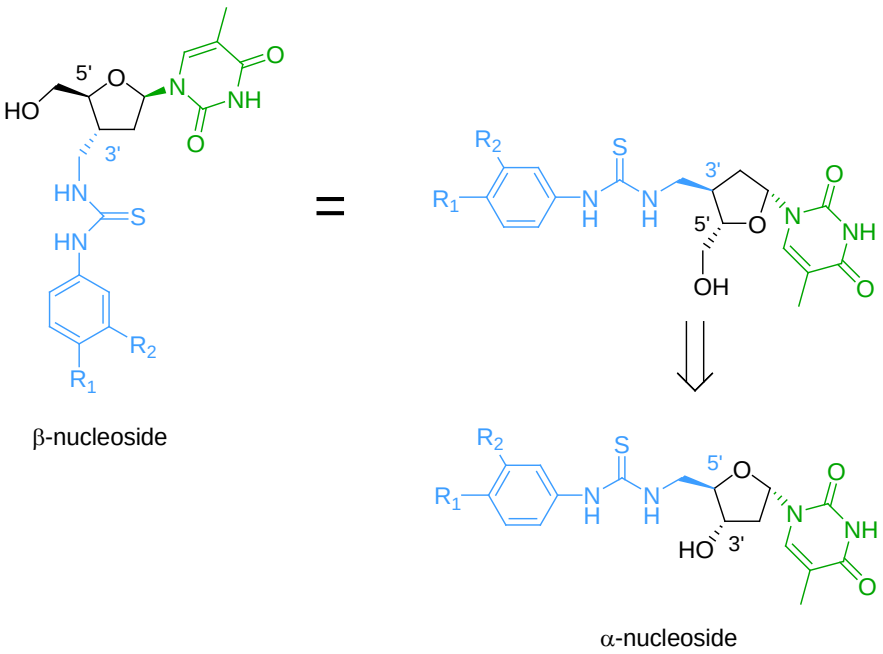

β-nucleoside

α-nucleoside

Figure II.10. Suggested inverse sugar binding of 3'-*C*-arylthiourea-modified β-thymidine and anticipated similar relative orientation of the colored moieties in 5'-deoxy-5'-arylthiourea modified α-thymidines.

From a small library of 5'-*N*-arylthiourea α-dT derivatives, compound **2.14** (Figure II.11) emerged as the most potent TMPKmt inhibitor (K_i = 0.6 µM).[69] Based on the observation that the 3'-deoxy and the 3'-deoxy-2',3'-didehydro analogs of **2.14** exhibit slightly higher K_i values (2.3 and 3.8 µM), the 3'-OH group is assumed to contribute to the overall affinity of **2.14** to TMPKmt.

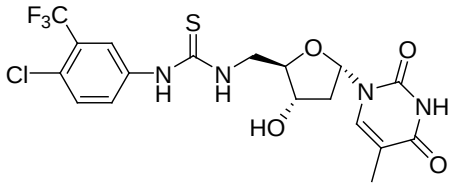

2.14

Figure II.11

2 SYNTHESIS AND INHIBITORY ACTIVITY OF THYMIDINE ANALOGUES TARGETING TMPKmt

2.1 OBJECTIVES

Based on the interesting TMPKmt inhibitory activities previously discovered in both series of thiourea-modified nucleosides represented by **2.13** and **2.14** (Figure II.12), the present synthetic work was directed towards structural variations of these compounds to gain further insight into the S.A.R.

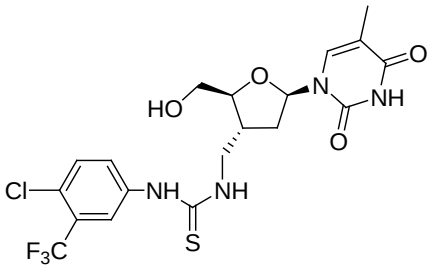

2.13 (K_i = 5 μM)

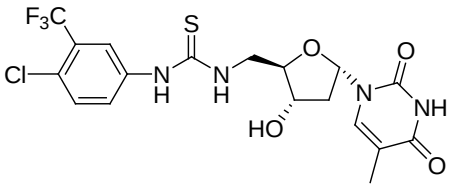

2.14 (K_i = 0.6 μM)

Figure II.12

First, we decided to investigate unbranched 3'-modified analogues of β-thymidine that are synthetically easier accessible than **2.13**. Analogues **1.43** and **2.15** represent close analogues of 3'-*C*-arylthiourea **2.13**, in which the methylene group between C-3' and the (thio)urea group has been omitted.[59] Analogues **1.50, 1.51,** and **1.53**, derived from AZT (**1.6**), were selected to investigate if a 1,4-disubstituted 1,2,3-triazole motif can act as a bioisostere for the 3'-*C*-thiourea linker of **2.13** as previously found to be the case for TK-2 inhibition.[73] The aminotetrazole isomers **1.90** and **1.96** were synthesized in the context of TK-2 inhibition[115] and are also characterized by the presence of a heterocyclic linker to connect the aromatic moiety to position 3 of the 2-deoxyribofuranose ring (Figure II.13).

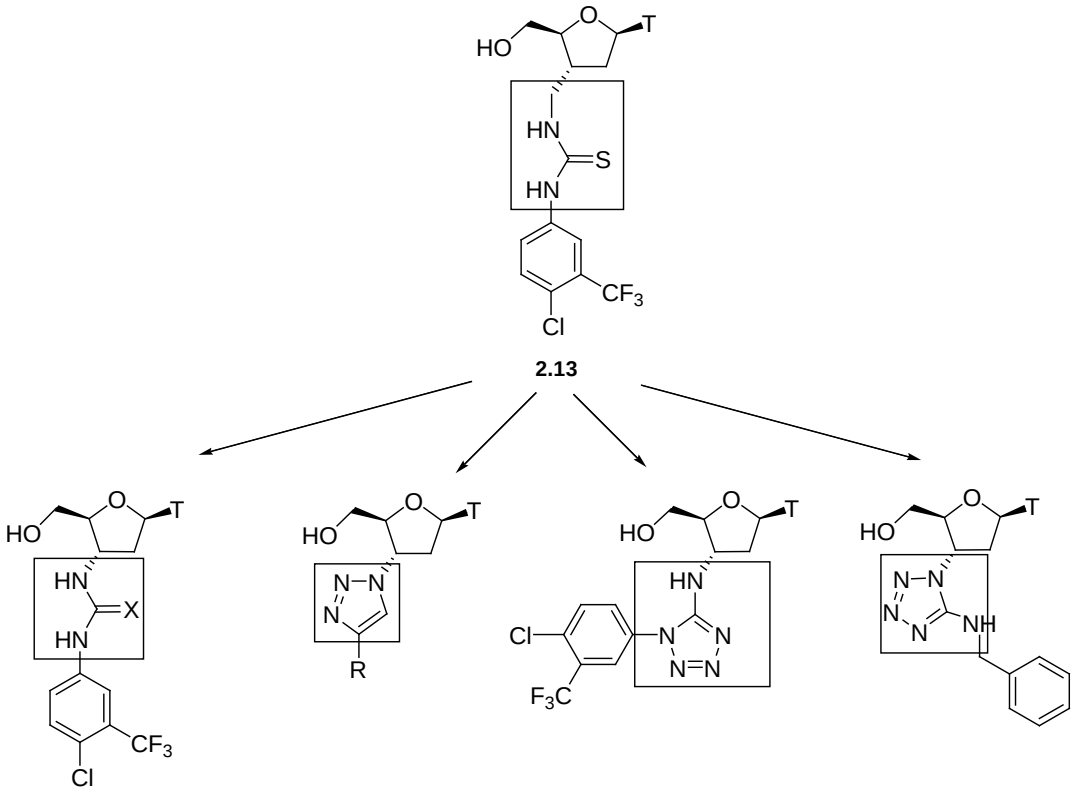

Figure II.13

Compounds **2.22-2.24** are derived from 5'-azido-5'-deoxy-α-D-thymidine (**2.21**) and synthesized in an effort to improve the activity of compound **2.14** (Figure II.14).

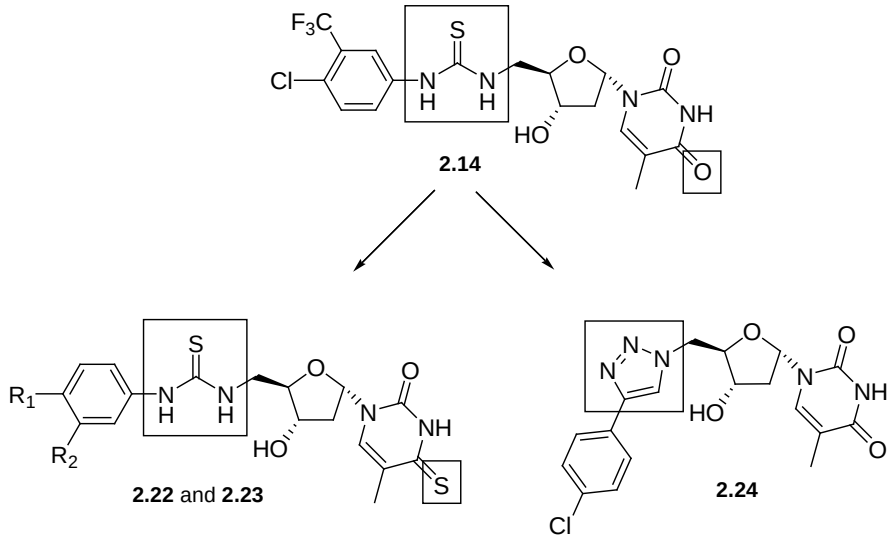

Figure II.14

To further investigate the influence of the relative orientation between the aryl moiety and the nucleobase, compound **2.26**, which is the α-analogue of **1.53**, was synthesized and evaluated (Figure II.15).

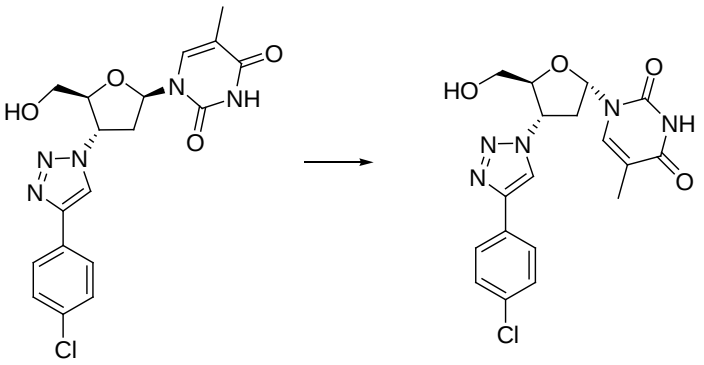

1.53 **2.26**

Figure II.15

To assess the inhibitory activity of anomeric variants of **2.14**, its β-anomer **2.18**, as well as two heterocyclic analogues, **2.19** and **2.20,** are included in this study (Figure II.16).

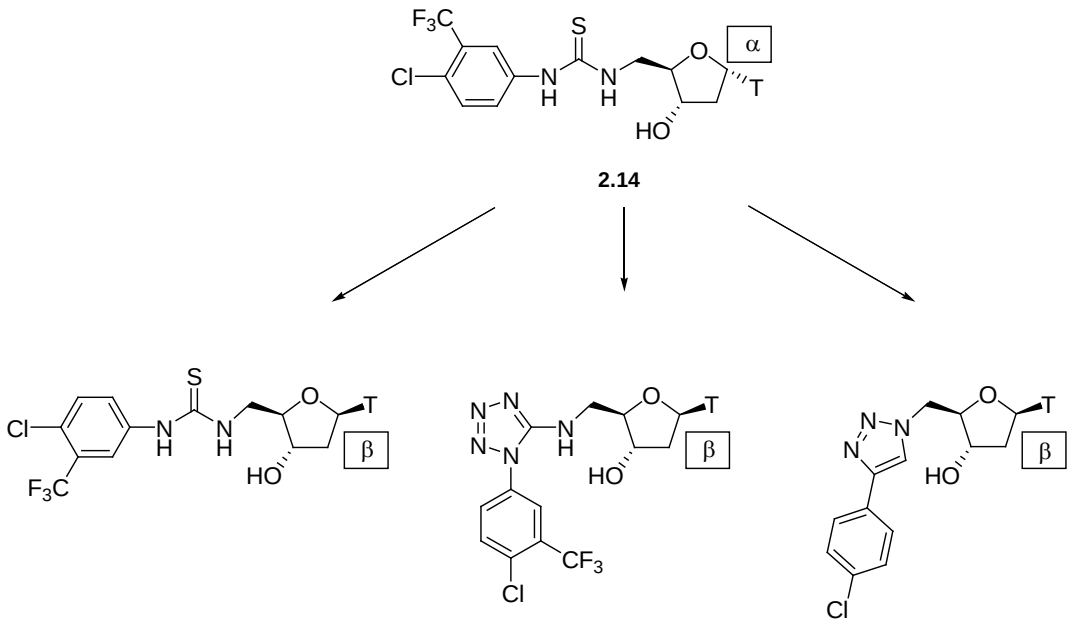

2.14

2.18 **2.19** **2.20**

Figure II.16

Based on earlier reports of 4-thiothymidine analogues showing promising antimycobacterial potency against *M. bovis* and *M. tuberculosis in vitro* and thus capable of entering the bacillus,[116] several analogues were synthesized in which the 4-oxygen of the thymine moiety was replaced by a more lipophilic sulfur atom (e.g., **2.16**, **2.17, 2.22** and **2.23**) to probe the influence of this modification on the inhibitor uptake in the bacillus.

2.2 CHEMISTRY

With the exception of compounds **2.16-20**, **2.22-24** and **2.26**, the chemical synthesis of all other final compounds has been reported before.[59,69,73,115,117]

2.2.1 Synthesis of 3'-Modified 4-Thio-β-Thymidine Analogues

For the preparation of 4-thio-AZT (**2.16**, Scheme II.1), AZT (**1.6**) was first protected using acetic anhydric.[117] Subsequent treatment of compound **2.27** with Lawesson's reagent[118] generated 4-thio pyrimidine **2.28** which was hydrolysed under basic conditions.[119]

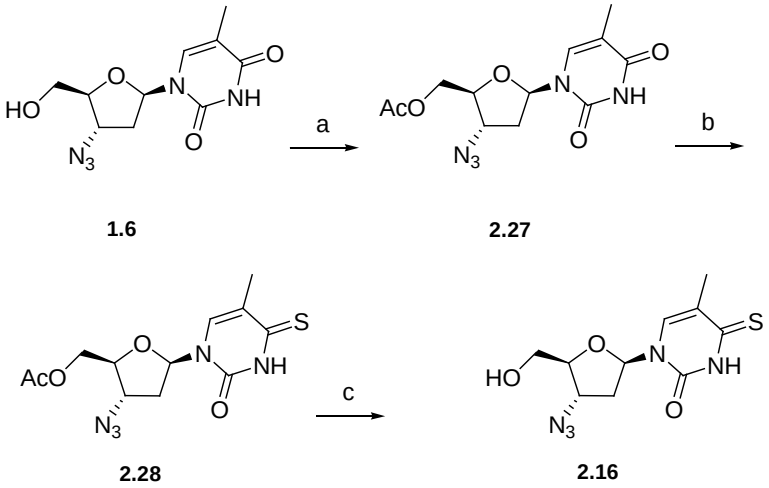

Scheme II.1. Reagents and conditions: (a) Ac_2O, DMAP, rt, 3 h, 99%; (b) Lawesson's reagent, toluene, 80 °C, overnight, 20%; (c) 7N NH_3 in MeOH, rt, 6 h, 42%.

A CuAAC reaction (see PART I - chapter 2) between **2.27** and 1-chloro-4-ethynylbenzene, followed by thionation of the resulting 1,4-disubstituted 1,2,3-triazole **2.29** gave analogue **2.17** after final deprotection (Scheme II.2).

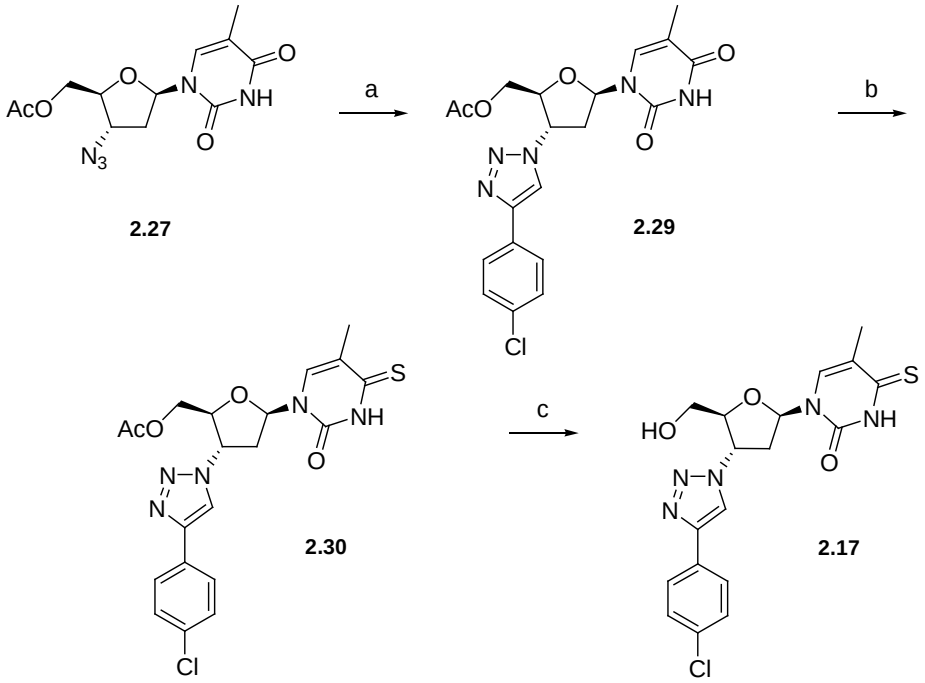

Scheme II.2. Reagents and conditions: (a) 1-chloro-4-ethynylbenzene, $CuSO_4 \cdot 5H_2O$, sodium ascorbate, H_2O/*t*-BuOH 2:1, rt, 24 h, 41%; (b) Lawesson's reagent, toluene, 80 °C, overnight, 49%; (c) 7N NH_3 in MeOH, rt, 6 h, 66%.

2.2.2 Synthesis of 5'-Modified β-Thymidine Analogues

The synthesis of a series of 5'-substituted thymidine analogues started from β-thymidine which was converted into 5'-azido-5'-deoxy **2.32** as depicted in Scheme II.3.[69] Protection of azide **2.32** followed by catalytic hydrogenation and coupling of amine **2.34** with 4-chloro-3-(trifluoromethyl)phenyl isothiocyanate gave thiourea derivative **2.35** which was deprotected using TBAF in THF.[120] A mercury(II)-promoted reaction of **2.35** with NaN_3 and Et_3N gave access to aminotetrazole **2.19** after final desilylation.

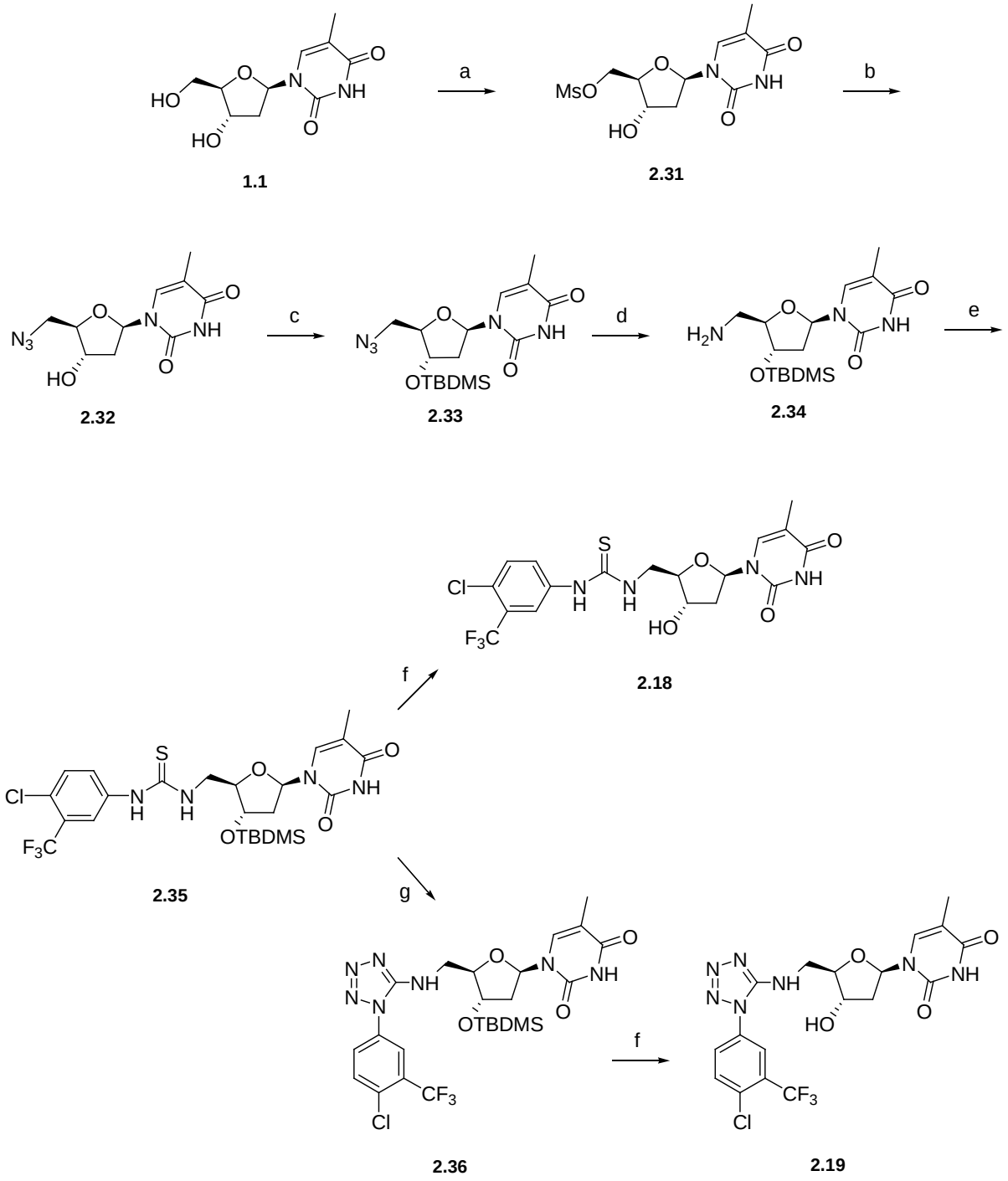

Scheme II.3. Reagents and conditions: (a) MsCl, pyridine, -78 °C → 0 °C, 1 h, 63%; (b) NaN_3, DMF, 60 °C, overnight, 38%; (c) TBDMSCl, imidazole, pyridine, rt, 1 h, 100%; (d) H_2, Pd/C, MeOH, rt, overnight, 95%; (e) 4-chloro-3-(trifluoromethyl)phenyl isothiocyanate, DMF, 0 °C → rt, 1 h, 76%; (f) 1M TBAF in THF, THF, rt, 1 h, 53-60%; (g) NaN_3, $HgCl_2$, Et_3N, DMF, 0 °C → rt, overnight, 83%.

"Click chemistry" followed by HPLC purification allowed to isolate enough pure material of **2.20** for testing (Scheme II.4).

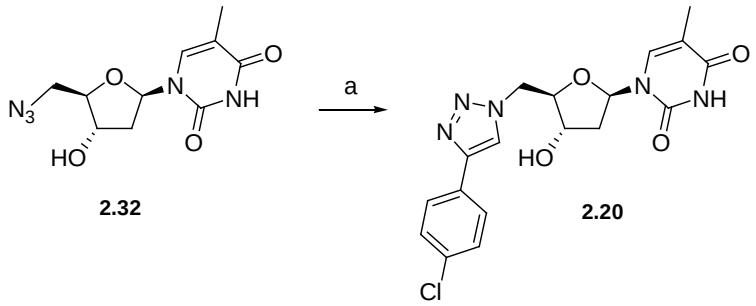

2.32 **2.20**

Scheme II.4. Reagents and conditions: (a) 1-chloro-4-ethynylbenzene, $CuSO_4 \cdot 5H_2O$, sodium ascorbate, H_2O/*t*-BuOH (1:2), rt, 7 d, 2%.

2.2.3 Synthesis of 5'-Modified (4-Thio-)α-Thymidine Analogues

For the synthesis of 5'-modified α-D-thymidine analogues **2.21-2.24**, 3',5'-*O*-diacetyl-β-D-thymidine **2.37** was first anomerized to its α-anomer according to the procedure of Ward *et al*.[121] (Scheme II.5). Compound **2.38** was then thionated using Lawesson's reagent followed by deprotection and conversion into the monomesylate ester **2.41**. Upon treatment with NaN_3, **2.41** was converted into azide **2.42**, which was reduced to afford 5'-amino-5'-deoxy-4-thio-α-D-thymidine **2.43**. Final treatment of this amine with the appropriate isothiocyanate analogues afforded derivatives **2.22** and **2.23**.

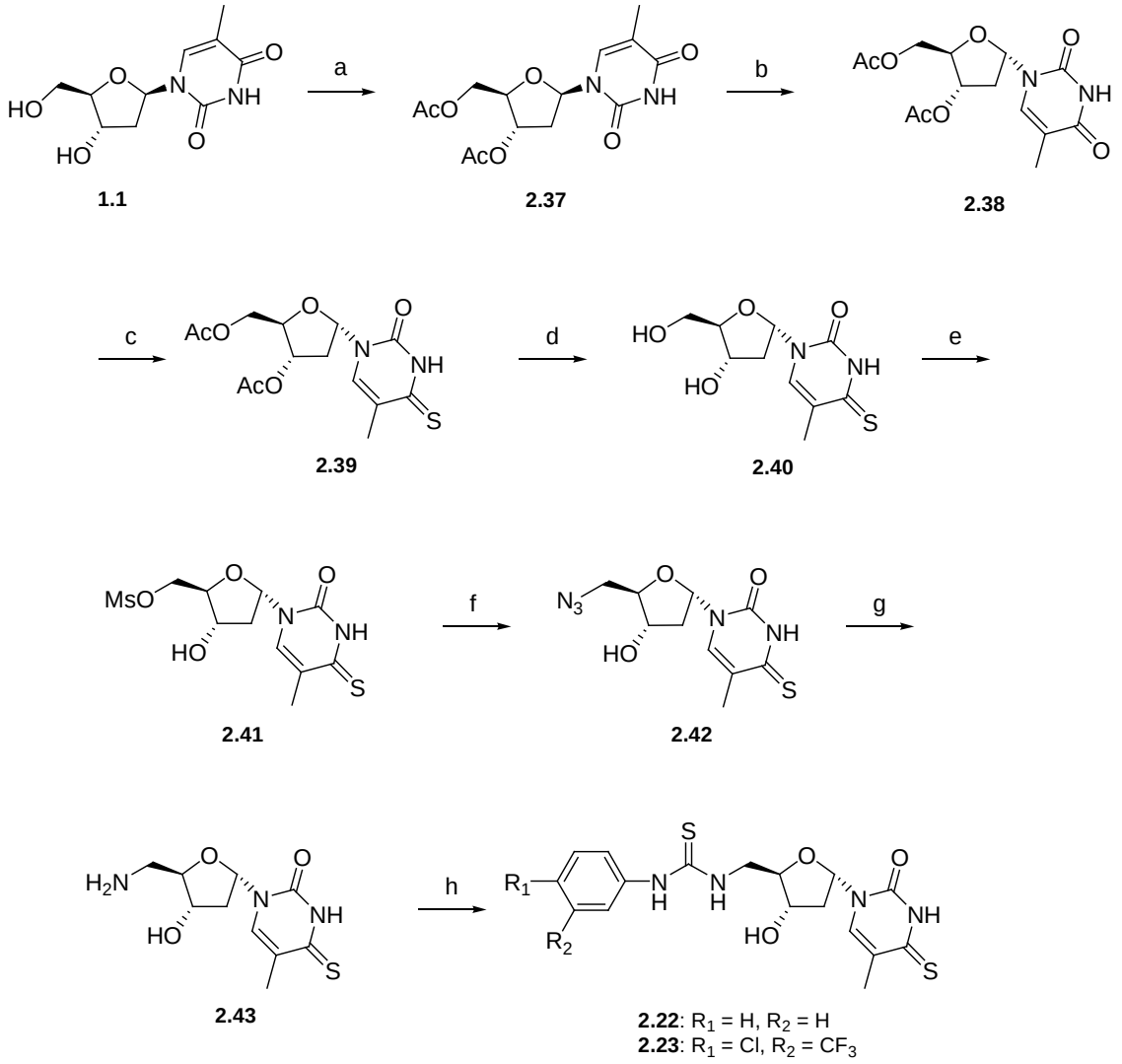

Scheme II.5. Reagents and conditions: (a) Ac_2O, pyridine, rt, 2 h, 98%; (b) H_2SO_4, Ac_2O, CH_3CN, rt, 2 h, 45%; (c) Lawesson's reagent, dry 1,4-dioxane, reflux, 4 h; (d) 7N NH_3 in MeOH, rt, 4 h, 37% over 2 steps; (e) MsCl, pyridine, -78 °C → 0 °C, 1 h, 70%; (f) NaN_3, DMF, 60 °C, overnight, 89%; (g) PPh_3, THF, H_2O, rt, 1 d, 89%; (h) suitable isothiocyanate, DMF, 0 °C → rt, 3 h, 42-69%.

After deprotection of compound **2.38** under basic conditions and conversion into azide **2.21**,[69] compound **2.24** was synthesized using the same method as described for triazole **2.20** (Scheme II.6)

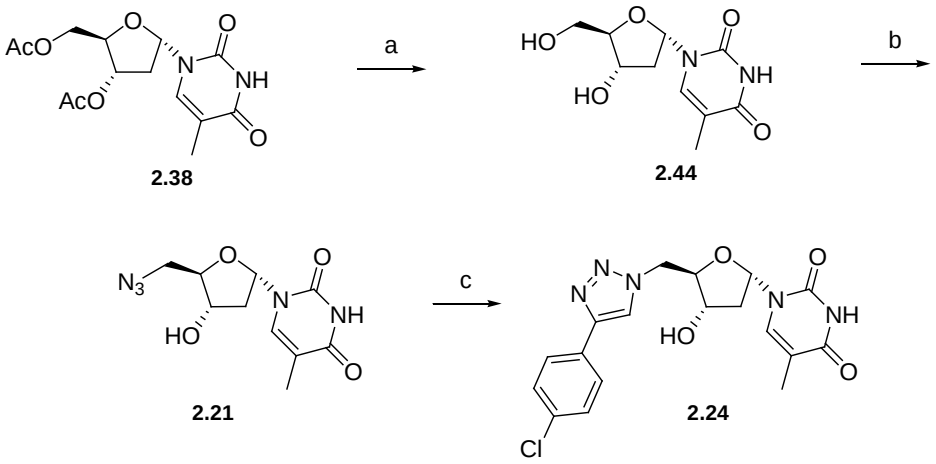

Scheme II.6. Reagents and conditions. (a) 7N NH_3 in MeOH, rt, 16 h, 90%; (b) (i) MsCl, Pyridine, 0 °C, 1 h, 62%; (ii) NaN_3, DMF, 60 °C, 16 h, 65%; (c) 1-chloro-4-ethynylbenzene, $CuSO_4 \cdot 5H_2O$, sodium ascorbate, H_2O/*t*-BuOH (2:1), rt, 4 d, 31%.

2.2.4 Synthesis of 3'-Modified α-Thymidine Analogues

The synthesis of 3'-modified α-D-thymidine analogues **2.25**[117] and **2.26** started with the anomerisation of 5'-*O*-acetylated AZT **2.27**. Deprotection of **2.45** followed by CuAAC with 1-chloro-4-ethynylbenzene afforded triazole **2.26** in moderate yield (Scheme II.7).

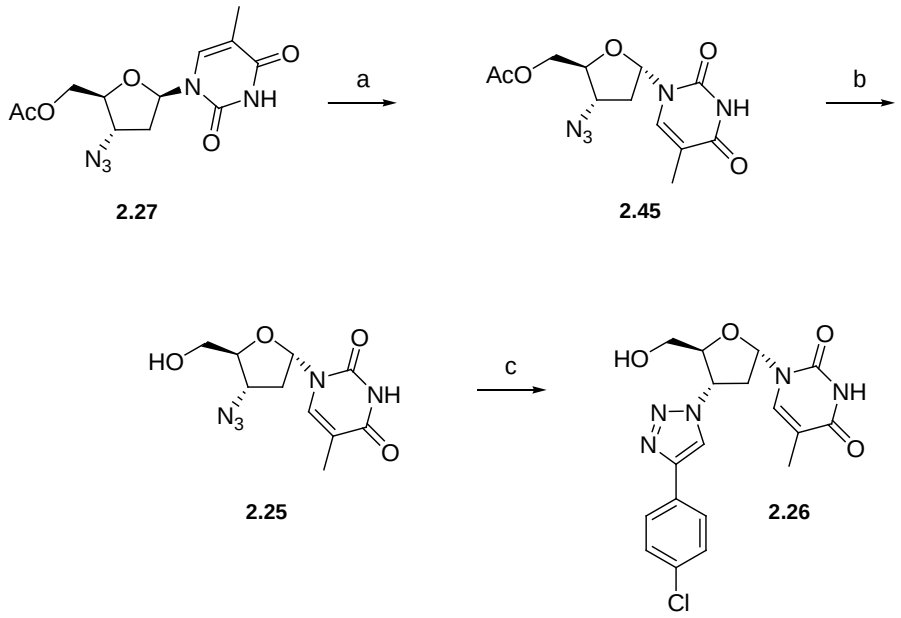

Scheme II.7. Reagents and conditions: (a) acetic anhydride, H_2SO_4, CH_2Cl_2, rt, 2 h, 20% (b) 7N NH_3 in MeOH, rt, overnight, 72%, (c) 1-chloro-4-ethynylbenzene, $CuSO_4 \cdot 5H_2O$, sodium ascorbate, H_2O/*t*-BuOH (1:3), rt, 24 h, 47%.

2.3 BIOLOGICAL EVALUATION

Table II.3. Kinetic parameters of TMPKmt with compounds **1.43**, **1.50, 1.51, 1.53, 1.90, 1.96** and **2.14-2.26**.

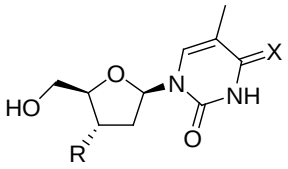

1.43, 1.50, 1.51, 1.53, 1.90, 1.96, 2.15-2.17

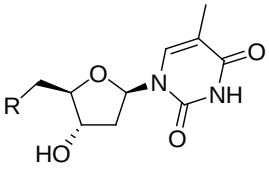

2.18-2.20

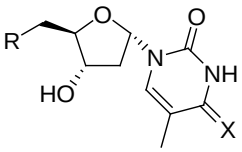

2.14, 2.21-2.24

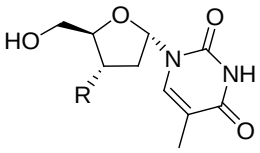

2.25-2.26

Compd	X	R	K_i (µM) TMPKmt	K_i (µM) TMPKh	SI[c]	MIC_{99} *M. Bovis* (µg/mL)
2.14	O	3-CF_3-4-Cl-phenylthiourea	0.6			
2.15	O	3-CF_3-4-Cl-phenylurea	2.8	95	34	
1.43	O	3-CF_3-4-Cl-phenylthiourea	9.9			
1.6	O	N_3	28			
2.16	S	N_3	>100			
1.50	O	4-(phenyl)-triazol-1-yl	4.2			
1.53	O	4-(*p*-chlorophenyl)-triazol-1-yl	2.1			
2.17	S	4-(*p*-chlorophenyl)-triazol-1-yl	15			
1.51	O	4-(benzyl)-triazol-1-yl	2.7	N.I.[b]	>100	
1.90	O	1-(3-CF_3-4-Cl-phenyl)-tetrazol-5-amine	45			
1.96	O	5-(aminobenzyl)-tetrazol-1-yl	2.3	N.I.[b]	>100	
2.18	O	3-CF_3-4-Cl-phenylthiourea	14.5			
2.19	O	1-(3-CF_3-4-Cl-phenyl)-tetrazol-5-amine	73			
2.20	O	4-(*p*-chlorophenyl)-triazol-1-yl	201			
2.21	O	N_3	26.5			
2.22	S	phenylthiourea	N.I.[a]			>>100
2.23	**S**	**3-CF_3-4-Cl-phenylthiourea**	**0.17**	N.I.[a]	>100	**25**
2.24	O	4-(*p*-chlorophenyl)-triazol-1-yl	9			
2.25	O	N_3	6			
2.26	O	4-(*p*-chlorophenyl)-triazol-1-yl	35			

N.I.: no inhibition detected at a final concentration of (a) 0.05 mM and (b) 1 mM.

SI[c]: K_i TMPKh/K_i TMPKmt

All compounds have been evaluated for TMPKmt inhibition under the supervision of Dr. Hélène Munier-Lehmann at the Institut Pasteur (Paris, France) as described in the Experimental Section. Replacement of the 3'-azido group of AZT (**1.6**) by a 3-CF_3-4-Cl-phenylurea substituent (**2.15**) resulted in a 10-fold increased activity, while this trend was less pronounced with the thiourea analogue **1.43**. In the 1,4-disubstituted 1,2,3-triazole series, the anti-TMPKmt activity was clearly influenced by the nature of the substituent at C-4 of the triazole. The click product of AZT and phenylacetylene (**1.50**) proved to be more potent than AZT itself. *p*-Chloro-substitution of the phenyl ring of **1.50** or introduction of a methylene between the triazole and the phenyl caused a moderate increase in activity (**1.51** and **1.53**). In this series of 3'-modified thymidine analogues, replacement of the oxygen at position 4 of the thymine moiety by a sulfur typically led to a significant drop in affinity for the target enzyme (compare couples **1.6**/**2.16** and **1.53**/**2.17**). Compounds **1.90** and **1.96**, both containing a 1,5-disubstituted tetrazole significantly differed in their capacity to inhibit TMPKmt. The aminotetrazole analogue **1.96**, in which the tetrazole ring is directly attached to the sugar ring, showed a significantly better activity compared to analogue **1.90** in which the tetrazole ring is connected to C-3' via a NH-bridge. Remarkably, an opposite trend was observed for these tetrazole analogues on mitochondrial thymidine kinase 2.

The inhibitory activity of a series of 5'-modified β-thymidine analogues appeared to be weak. Introduction of a 3-CF_3-4-Cl-phenylthiourea substituent (**2.18**) gave micromolar inhibition, while replacement of the thiourea by a 1-(3-CF_3-4-Cl-phenyl)-tetrazol-5-amine (**2.19**) or a 4-(*p*-chlorophenyl)-triazol-1-yl (**2.20**) caused a 5 and 14-fold drop in K_i value, respectively. Comparison of the anomeric couples **2.14**/**2.18** and **2.20**/**2.24** demonstrate that the α-anomers, which feature a trans orientation of the nucleobase and the 5'-substituent, exhibit superior TMPKmt inhibition compared to their β-epimers (factor 22-24).

The 5'-modified α-thymidine analogues (**2.14**, **2.21-2.24**) demonstrated moderate to excellent inhibitory activity for TMPKmt. Also in this small series, the activity is influenced by the nature of the substituent at the 5'-position. Derivative **2.21**, containing an azide function, gave moderate inhibition with a strikingly comparable K_i value (26.5 μM) as its AZT counterpart (28 μM). As observed in the 3'-modified series, conversion of the azide moiety by a 4-(4-chlorophenyl)-1,2,3-triazol-1-yl substituent improved the inhibitory activity, although to a lesser extent. Most interestingly and in contrast to what was observed in the 3'-modified series, substitution of the 4-oxygen of the original hit **2.14** by a 4-S, increased the activity by a factor 3, ranking it amongst the most potent TMPKmt inhibitor together with the (*Z*)-butenylthymines carrying a naphtholactam or naphthosultam moiety (K_i values of 0.42 and 0.27 μM, respectively).[122]

In addition, α-analogue **2.26**, which was synthesized to further assess the influence of the relative orientation between the aryl moiety and the nucleobases, showed poor inhibitory activity against TMPKmt, indicating that the preferred trans-orientation of the base and the aromatic substituent also holds for the 3'-modified analogues.

Compound **2.23** was evaluated for its *in vitro* inhibitory activity against *Mycobacterium bovis* BCG. It showed 100% inhibition of bacterial growth at a concentration of 25 μg/mL.

2.4 MOLECULAR DOCKING

In an effort to rationalize the threefold increase in affinity upon replacement of the 4-O of the original hit **2.14** by a 4-S (**2.23**), both compound were docked into the substrate binding site of the TMPKmt enzyme (Figure II.17). For inhibitor **2.14**, the interactions of the base moiety with the surrounding residues are similar to the ones with the natural substrate: a stacking with Phe70, a H-bond of base atom N3 with Asn100 and base atom O4 hydrogen bonding with Arg74. In compound **2.23** where the C(4)=O is replaced by a C(4)=S, the hydrogen bonds to Arg74 is lost. However, due to the bigger size of the sulfur atom, a better van der Waals interaction is seen with surrounding residues Phe70, Arg74 and Asn100 which may explain a higher affinity for this inhibitor.

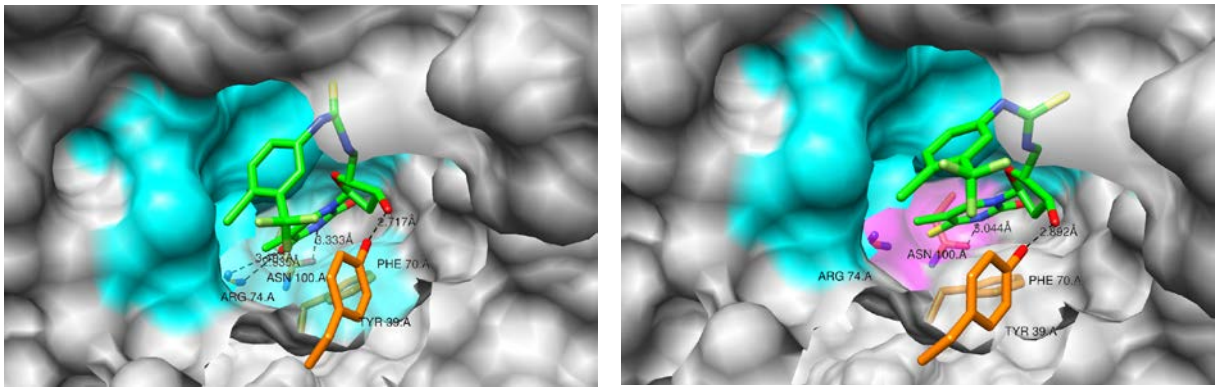

Figure II.17. Compound **2.14** (left) and compound **2.23** (right) docked in the substrate binding site of TMPKmt. The carbon atoms of both inhibitors are colored green. The enzyme contact surface is colored cyan, and the contact surface with the 4S atom is colored magenta.

2.5 CONCLUSIONS

On the basis of the structures of nucleosides **2.13** and **2.14**, which were identified earlier as potent TMPKmt inhibitors, this chapter described the synthesis and biological evaluation of a series of new thymidine analogues, including α- and β-derivatives. In both the 3'- and the 5'-derivatised analogues, the anomer that places the thymine base trans to the aromatic substituent showed the best TMPKmt inhibition. In addition, several analogues were synthesized in which the 4-oxygen was replaced by a more lipophilic sulfur atom to probe the influence of this modification on TMPKmt inhibitory activity. Remarkably, a 4-thio modification of the pyrimidine base was favorable for the 5'-modified α-analogues, while it caused an opposite effect on the 3'-modified β-analogues. Several compounds showed an inhibitory potency in the low micromolar range, with the 5'-arylthiourea 4-thio-α-thymidine analogue **2.23** being the most active one (K_i = 0.17 μM). This compound is capable of inhibiting mycobacterial growth at a concentration of 25 μg/mL, promoting TMPKmt as an attractive target for further inhibitor design.

2.6 EXPERIMENTAL PART

2.6.1 Synthesis

5'-*O*-Acetyl-3'-azido-3'-deoxy-β-D-thymidine (2.27)

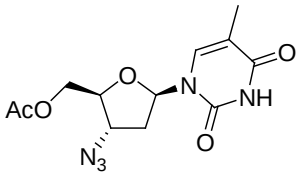

To a stirred suspension of 3'-azido-3'-deoxy-β-D-thymidine (**1.6**, AZT) (231 mg, 0.86 mmol) in acetic anhydride (5 mL), 4-dimethylaminopyridine (DMAP) (10 mg, 0.086 mmol) was added. The reaction mixture was stirred at room temperature for 3 h. Acetic anhydride was removed *in vacuo* and the residue was dissolved in EtOAc and washed with brine. The organic layer was dried over Na_2SO_4, evaporated and purified by column chromatography (CH_2Cl_2/MeOH 95:5) to afford compound **2.27** (264 mg, 99%) as a white foam.

^{1}H NMR (300 MHz, DMSO-d_6): δ 1.78 (3H, d, *J*= 1.5 Hz, 5-CH_3), 2.04 (3H, s, OAc), 2.27-2.36 (1H, m, H-2'a), 2.40-2.50 (1H, m, H-2'b), 3.95 (1H, app dd, *J*= 4.8 Hz, *J*= 10.2 Hz, H-4'), 4.22 (2H, app d, *J*= 4.8 Hz, H-5'a an H-5'b), 4.42-4.48 (1H, m, H-3'), 6.07-6.13 (1H, m, H-1'), 7.44 (1H, d, *J*= 1.2 Hz, H-6), 11.33 (1H, s, 3-NH).

^{13}C NMR (75 MHz, DMSO-d_6): δ 12.12 (5-CH_3), 20.57 (OAc), 35.61 (C-2'), 60.06 (C-3'), 63.24 (C-5'), 80.61 (C-4'), 83.60 (C-1'), 109.88 (C-5), 136.05 (C-6), 150.37 (C-2), 163.66 (C-4), 170.11 (OAc).

Exact mass (ESI-MS) for $C_{12}H_{16}N_5O_5$ $[M+H]^+$ found, 310.0837; calcd, 310.1146.

5'-*O*-Acetyl-3'-azido-3'-deoxy-4-thio-β-D-thymidine (2.28)

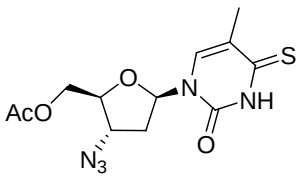

Lawesson's reagent (154 mg, 0.38 mmol) was added to a solution of compound **2.27** (111 mg, 0.36 mmol) in 10 mL dry toluene. The mixture was refluxed overnight and the solvent was removed *in vacuo*. The residue was purified by column chromatography (CH_2Cl_2/ MeOH 95:5) to give compound **2.28** as a brown-yellow solid (23 mg, 20%).

^{1}H NMR (300 MHz, DMSO-d_6): δ 1.99 (3H, d, *J*= 0.9 Hz, 5-CH_3), 2.06 (3H, s, OAc), 2.34-2.43 (1H, m, H-2'a), 2.53-2.57 (1H, m, H-2'b), 3.99-4.04 (1H, m, H-4'), 4.21-4.32 (2H, m, H-5'a an H-5'b), 4.44-4.50 (1H, m, H-3'), 6.07 (1H, dd, *J*= 5.7 Hz, *J*= 7.2 Hz, H-1'), 7.58 (1H, s, H-6), 12.75 (1H, s, 3-NH).

^{13}C NMR (75 MHz, DMSO-d_6): δ 16.78 (5-CH_3), 20.58 (OAc), 35.96 (C-2'), 59.81 (C-3'), 63.09 (C-5'), 81.10 (C-4'), 84.64 (C-1'), 117.95 (C-5), 133.32 (C-6), 147.67 (C-2), 171.92 (OAc), 190.95 (C-4).

Exact mass (ESI-MS) for $C_{12}H_{16}N_5O_4S$ $[M+H]^+$ found, 326.0941; calcd, 326.0918.

3'-Azido-3'-deoxy-4-thio-β-D-thymidine (2.16)

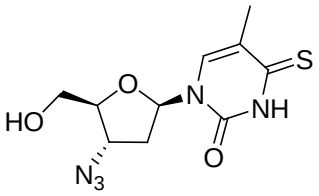

Compound **2.28** (16 mg, 0.050 mmol) was dissolved in a 7N NH_3 in MeOH solution (1 mL) and stirred at room temperature for 6 hours. The reaction mixture was concentrated *in vacuo* and the residue was purified on a silica gel column using CH_2Cl_2/MeOH (95:5) as the eluent to afford compound **2.16** as a yellow powder (6.0 mg, 42%). Spectroscopic data of **2.16** are in accordance with literature data.[123]

^{1}H NMR (300 MHz, DMSO-d_6): δ 1.97 (3H, d, *J*= 0.6 Hz, 5-CH_3), 2.29-2.38 (1H, m, H-2'a), 2.41-2.48 (1H, m, H-2'b), 3.59-3.71 (2H, m, H-5'a and H-5'b), 3.83-3.87 (1H, m, H-4'), 4.40 (1H, app dd, *J*= 6.0 Hz, *J*= 12.6 Hz, H-3'), 5.28 (1H, br s, 5'-OH), 6.04 (1H, app t, *J*= 5.7 Hz, H-1'), 7.86 (1H, s, H-6).

^{13}C NMR (75 MHz, DMSO-d_6): δ 16.90 (5-CH_3), 36.64 (C-2'), 59.44 (C-3'), 60.35 (C-5'), 84.32 and 84.44 (C-4' and C-1'), 117.63 (C-5), 133.34 (C-6), 147.71 (C-2), 190.76 (C-4).

Exact mass (ESI-MS) for $C_{10}H_{14}N_5O_3S$ $[M+H]^+$ found, 326.284.0813; calcd, 284.0812.

5'-*O*-Acetyl-3'-(4-(*p*-chlorophenyl)-1,2,3-triazol-1-yl)-3'-deoxy-β-D-thymidine (2.29)

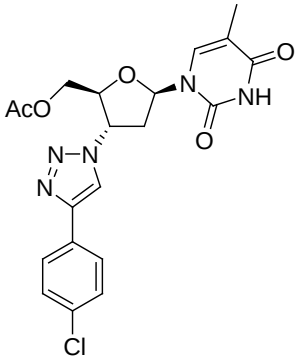

Compound **2.27** (146 mg, 0.47 mmol), sodium ascorbate (5 mg, 0.024 mmol) and $CuSO_4 \cdot 5H_2O$ (5 mg, 0.019 mmol) were suspended in 9 mL of H_2O/*t*-BuOH (2:1). 1-Chloro-4-ethynylbenzene (129 mg, 0.94 mmol) was added after 15 minutes and the mixture was stirred at room temperature for 24 h. The reaction mixture was extracted with EtOAc and the combined organic phases were dried over anhydrous $MgSO_4$ and evaporated to dryness. The crude product was purified using column chromatography (CH_2Cl_2/MeOH 95:5) to afford compound **2.29** (87 mg, 41 %) as a white powder.

^{1}H NMR (300 MHz, DMSO-d_6): δ 1.84 (3H, s, 5-CH_3), 2.04 (3H, s, OAc), 2.73-2.94 (2H, m, H-2'a and H-2'b), 4.27-4.37 (2H, m, H-5'a and H-5'b), 4.43-4.49 (1H, m, H-4'), 5.47-5.54 (1H, m, H-3'), 6.45 (1H, t, *J*= 7.2 Hz, H-1'), 7.52-7.57 (2H, m, subs Ph), 7.63 (1H, d, *J*= 1.2 Hz, H-6), 7.85-7.90 (2H, m, subs Ph), 8.86 (1H, s, H-5"), 11.41 (1H, s, 3-NH).

^{13}C NMR (75 MHz, DMSO-d_6): δ 12.14 (5-CH_3), 20.53 (OAc), 36.36 (C-2'), 59.50 and 63.29 (C-5' and C-3'), 80.85 (C-4'), 84.15 (C-1'), 110.00 (C-5), 121.34 (C-5"), 126.86, 129.07, 129.42 and 132.48 (subs Ph), 136.39 (C-6), 145.54 (C-4"), 150.44 (C-2), 163.74 (C-4), 170.08 (OAc).

Exact mass (ESI-MS) for $C_{20}H_{21}ClN_5O_5$ $[M+H]^+$ found, 446.1238; calcd, 446.1226.

5'-*O*-Acetyl-3'-(4-(*p*-chlorophenyl)-1,2,3-triazol-1-yl)-3'-deoxy-4-thio-β-D-thymidine (2.30)

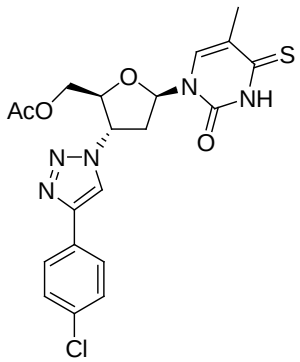

Lawesson's reagent (158 mg, 0.39 mmol) was added to a solution of compound **2.29** (87 mg, 0.20 mmol) in 10 mL dry toluene. The mixture was refluxed overnight and the solvent was removed *in vacuo*. The residue was purified by column chromatography (CH_2Cl_2/ MeOH 95:5) to give compound **2.30** as a brown-yellow solid (44 mg, 49%).

^{1}H NMR (300 MHz, $CDCl_3$): δ 2.00 (3H, s, 5-CH_3), 2.05 (3H, s, OAc), 2.86-2.94 (1H, m, H-2'a), 3.17-3.26 (1H, m, H-2'b), 4.35 (2H, d, *J*= 3.3 Hz, H-5'a and H-5'b), 4.59-4.65 (1H, m, H-4'), 5.49 (1H, app dd, *J*= 7.5 Hz, *J*= 15.3 Hz, H-3'),6.01-6.04 (1H, m, H-1'), 7.24 (1H, s, H-6), 7.32 (2H, d, *J*= 8.4 Hz, subs Ph), 7.68 (2H, d, *J*= 8.4 Hz, subs Ph), 7.93 (1H, s, H-5"), 11.10 (1H, s, 3-NH).

^{13}C NMR (75 MHz, $CDCl_3$): δ 17.41 (5-CH_3), 21.00 (OAc), 38.16 (C-2'), 60.31 and 63.45 (C-5' and C-3'), 82.99 (C-4'), 89.57 (C-1'), 120.21 and 120.71 (C-5 and C-5"), 127.23, 128.77, 129.39, 134.01 and 134.47 (C-6 and subs Ph), 147.20 and 148.49 (C-4" and C-2), 170.66 (OAc), 190.91 (C-4).

Exact mass (ESI-MS) for $C_{20}H_{21}ClN_5O_4S$ $[M+H]^+$ found, 462.1042; calcd, 462.0997.

3'-(4-(*p*-Chlorophenyl)-1,2,3-triazol-1-yl)-3'-deoxy-4-thio-β-D-thymidine (2.17)

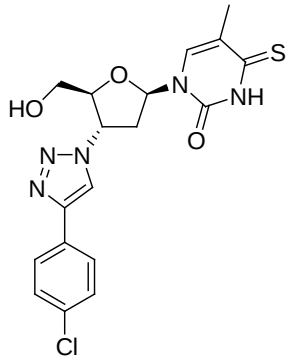

Compound **2.30** (42 mg, 0.090 mmol) was dissolved in a 7N NH_3 in MeOH solution (1 mL) and stirred at room temperature for 6 hours. The reaction mixture was concentrated *in vacuo* and the residue was purified on a silica gel column using CH_2Cl_2/MeOH (95:5) as the eluent to afford compound **2.17** as a yellow powder (25.2 mg, 66%).

^{1}H NMR (300 MHz, DMSO-d_6): δ 1.75 (3H, d, *J*= 0.9 Hz, 5-CH_3), 1.96 (1H, app dt, *J*= 3.6 Hz, *J*= 14.1 Hz, H-2'a), 2.45-2.55 (1H, m, H-2'b), 4.28 (1H, app s, H-3'), 4.47-4.64 (3H, m, H-4', H-5'a and H-5'b), 5.63 (1H, s, 5'-OH), 6.18 (1H, dd, *J*= 3.9 Hz, *J*= 7.5 Hz, H-1'), 7.49-7.54 (2H, m, subs Ph), 7.72 (1H, d, *J*= 1.2 Hz, H-6), 7.86-7.91 (2H, m, subs Ph), 8.62 (1H, s, H-5").

^{13}C NMR (75 MHz, DMSO-d_6): δ 16.94 (5-CH_3), 37.51 (C-2'), 59.02 (C-3'), 60.41 (C-5'), 84.80 and 84.90 (C-4' and C-1'), 117.81 (C-5), 121.40 (C-5"), 126.87, 129.03, 129.47, 132.44 and 133.50 (C-6 and subs Ph), 145.49 and 147.79 (C-4" and C-2), 190.90 (C-4).

Exact mass (ESI-MS) for $C_{18}H_{19}ClN_5O_3S$ $[M+H]^+$ found, 420.0915; calcd, 420.0892.

5'-*O*-Methanesulfonyl-β-D-thymidine (2.31)

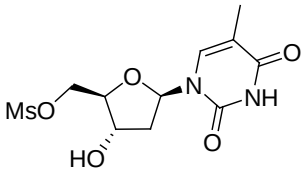

To a solution of β-thymidine (3 g, 12 mmol) in pyridine (45 mL) was added methanesulfonyl chloride (0.86 mL, 11 mmol) at -78 °C. The reaction mixture was stirred for 1 h at 0 °C. The reaction was quenched with saturated aq. $NaHCO_3$ and extracted with CH_2Cl_2 three times, dried over $MgSO_4$ and evaporated. The residue was purified by column chromatography (CH_2Cl_2/MeOH 95:5) to give compound **2.31** (2.5 g, 63%) as a white solid.

^{1}H NMR (300 MHz, DMSO-d_6): δ 1.78 (3H, d, *J*= 1.2 Hz, 5-CH_3), 2.10-2.20 (2H, m, H-2'a and H-2'b), 3.23 (3H, s, CH_3SO_2), 3.95-4.00 (1H, m, H-4'), 4.24-4.29 (1H, m, H-3'), 4.32-4.43 (2H, m, H-5'a and H-5'b), 6.23 (1H, app t, *J*= 7.5 Hz, H-1'), 7.48 (1H, d, *J*= 1.2 Hz, H-6).

^{13}C NMR (75 MHz, DMSO-d_6): δ 12.04 (5-CH_3), 36.73 (C-2'), (CH_3SO_2 under DMSO peak), 69.62 (C-5'), 70.14 (C-5'), 83.38 (C-4'), 83.98 (C-1'), 109.88 (C-5), 135.82 (C-6), 150.46 (C-2), 163.67 (C-4).

Exact mass (ESI-MS) for $C_{11}H_{17}N_2O_7S$ $[M+H]^+$ found, 321.0119; calcd, 321.0751.

5'-Azido-5'-deoxy-β-D-thymidine (2.32)

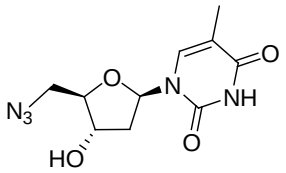

A solution of compound **2.31** (2.5 g, 7.8 mmol) and NaN_3 (5.07 g, 78 mmol) in DMF (140 mL) was stirred at 60 °C overnight. The reaction mixture was evaporated *in vacuo*. The residue was dissolved in CH_2Cl_2 and washed with H_2O. The organic layer was dried over $MgSO_4$, evaporated and purified by column chromatography (CH_2Cl_2/MeOH 95:5) to afford compound **2.32** (793 mg, 38%) as white crystals.

^{1}H NMR (300 MHz, DMSO-d_6): δ 1.77 (3H, d, *J*= 1.2 Hz, 5-CH_3), 2.03-2.10 (1H, m, H-2'a), 2.19-2.28 (1H, m, H-2'b), 3.54 (2H, app d, *J*= 5.1 Hz, H-5'a and H-5'b), 3.80-3.85 (1H, m, H-4'), 4.15-4.19 (1H, m, H-3'), 5.39 (1H, br s, 3'-OH), 6.18 (1H, app t, *J*= 6.9 Hz, H-1'), 7.47 (1H, d, *J*= 1.2 Hz, H-6), 11.30 (1H, s, 3-NH).

^{13}C NMR (75 MHz, DMSO-d_6): δ 12.10 (5-CH_3), 38.08 (C-2'), 51.70 (C-5'), 70.73 (C-3'), 83.87 (C-4'), 84.56 (C-1'), 109.82 (C-5), 136.08 (C-6), 150.49 (C-2), 163.67 (C-4).

Exact mass (ESI-MS) for $C_{10}H_{14}N_5O_4$ $[M+H]^+$ found, 268.1055; calcd, 268.1040.

5'-Azido-3'-*O*-*tert*-butyldimethylsilyl-5'-deoxy-β-D-thymidine (2.33)

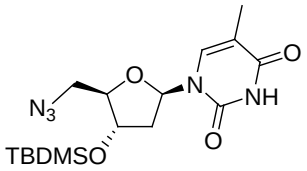

To a stirred solution of compound **2.32** (296 mg, 1.11 mmol) in anhydrous pyridine (16 mL), *tert*-butyldimethylsilyl chloride (627 mg, 4.16 mmol) and imidazole (359 mg, 5.27 mmol) were added. After stirring for 1 h at room temperature, solvents were removed under reduced pressure and the crude was purified over silica gel (CH_2Cl_2/MeOH 95:5) affording compound **2.33** (450 mg, 100%) as a brown solid.

^{1}H NMR (300 MHz, $CDCl_3$): δ 0.089 (6H, s, TBDMS), 0.89-0.91 (9H, m, TBDMS), 1.95 (3H, s, 5-CH_3), 2.15-2.29 (2H, m, H-2'a and H-2'b), 3.50 (1H, dd, *J*= 3.6 Hz, *J*= 13.5 Hz, H-5'a), 3.71 (1H, dd, *J*= 3.0 Hz, *J*= 13.2 Hz, H-5'b), 3.92-3.95 (1H, m, H-4'), 4.34-4.37 (1H, m, H-3'), 6.26 (1H, app t, *J*= 6.3 Hz, H-1'), 7.32 (1H, s, H-6), 9.46 (1H, s, 3-NH).

^{13}C NMR (75 MHz, $CDCl_3$): δ -4.65, -4.41 and -3.33 (TBDMS), 12.91 (5-CH_3), 18.17 (TBDMS), 25.93 (TBDMS), 40.91 (C-2'), 51.98 (C-5'), 71.90 (C-3'), 85.02 and 85.10 (C-4' and C-1'), 111.62 (C-5), 135.64 (C-6), 150.68 (C-2), 164.16 (C-4).

Exact mass (ESI-MS) for $C_{16}H_{28}N_5O_4Si$ $[M+H]^+$ found, 382.1879; calcd, 382.1905.

5'-Amino-3'-*O*-*tert*-butyldimethylsilyl-5'-deoxy-β-D-thymidine (2.34)

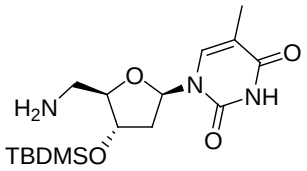

A solution of compound **2.33** (458 mg, 1.20 mmol) in methanol (5 mL) was hydrogenated under atmospheric pressure overnight in the presence of 10% Pd/C. The catalyst was removed by filtration through Celite and the filtrate was evaporated *in vacuo* to obtain pure compound **2.34** (403 mg, 95%) as a white foam.

^{1}H NMR (300 MHz, $CDCl_3$): δ 0.077 (6H, s, TBDMS), 0.89-0.91 (9H, m, TBDMS), 1.92 (3H, s, 5-CH_3), 2.10-2.30 (2H, m, H-2'a and H-2'b), 2.86 (1H, dd, *J*= 6.3 Hz, *J*= 13.8 Hz, H-5'a), 3.05 (1H, dd, *J*= 3.3 Hz, *J*= 13.5 Hz, H-5'b), 3.77-3.82 (1H, m, H-4'), 4.25-4.30 (1H, m, H-3'), 6.25 (1H, app t, *J*= 6.6 Hz, H-1'), 7.30 (1H, s, H-6).

^{13}C NMR (75 MHz, $CDCl_3$): δ -4.69, -4.45 and -3.38 (TBDMS), 12.83 (5-CH_3), 18.08 and 18.19 (TBDMS), 25.87 (TBDMS), 40.82 (C-2'), 43.42 (C-5'), 72.18 (C-3'), 84.67 (C-1'), 87.57 (C-4'), 111.37 (C-5), 135.74 (C-6), 151.40 (C-2), 165.16 (C-4).

Exact mass (ESI-MS) for $C_{16}H_{30}N_3O_4Si$ $[M+H]^+$ found, 356.2004; calcd, 356.2000.

***N*-(3'-*O*-*tert*-Butyldimethylsilyl-5'-deoxy-β-D-thymidin-5'-yl)-*N*'-(4-chloro-3-trifluoromethyl-phenyl)thiourea (2.35)**

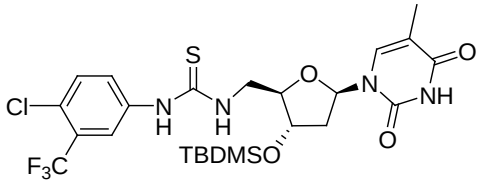

To a solution of compound **2.34** (403 mg, 1.13 mmol) in DMF (4 mL) was added a solution of 4-chloro-3-(trifluoromethyl)phenyl isothiocyanate (0.18 mL, 1.13 mmol) in DMF (2 mL) at 0 °C. The reaction mixture was stirred for 1 h. The solvents were evaporated to dryness and the residue was purified by column chromatography (CH_2Cl_2/MeOH 98:2) affording compound **2.35** as a colourless solid (510 mg, 76%).

^{1}H NMR (300 MHz, DMSO-d_6): δ 0.098 (6H, s, TBDMS), 0.87-0.88 (9H, m, TBDMS), 1.80 (3H, s, 5-CH_3), 2.02-2.10 (1H, m, H-2'a), 2.24-2.34 (1H, m, H-2'b), 3.55-3.65 (1H, m, H-4'), 3.98-3.99 (2H, m, H-5'a and H-5'b), 4.45-4.47 (1H, m, H-3'), 6.15-6.19 (1H, m, H-1'), 7.52 (1H, s, subs Ph), 7.62-7.72 (2H, m, subs Ph and H-6), 7.96 (1H, subs Ph), 8.12 (1H, s, 5'-NH), 9.93 (1H, s, N'H), 11.33 (1H, s, 3-NH).

^{13}C NMR (75 MHz, DMSO-d_6): δ -4.99 and -4.93 (TBDMS), 11.95 (5-CH_3), 17.57 (TBDMS), 25.57 (TBDMS), (C-2' under DMSO peak), 45.74 (C-5'), 72.80 (C-3'), 83.98 and 84.19 (C-1' and C-4'), 109.74 (C-5), 124.50-139.00 (subs Ph, CF_3 and C-6), 150.36 (C-2), 163.56 (C-4), 180.77 (C=S).

Exact mass (ESI-MS) for $C_{24}H_{33}ClF_3N_4O_4Si$ $[M+H]^+$ found, 593.1643; calcd, 593.1627.

***N*-(5'-Deoxy-β-D-thymidin-5'-yl)-*N*'-(4-chloro-3-trifluoromethylphenyl)thiourea (2.18)**

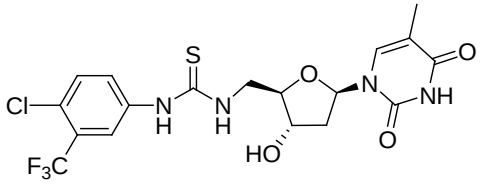

Compound **2.35** (84 mg, 0.14 mmol) was dissolved in THF (0.9 mL). A solution of 1M tetra-*n*-butylammonium fluoride in THF (0.31 mL) was added. After 1 h at room temperature the reaction was

completed. The solvent was evaporated and the dry residue was purified by column chromatography (CH_2Cl_2/MeOH 95:5) to give pure compound **2.18** (40 mg, white solid) in 60% yield.

^{1}H NMR (300 MHz, DMSO-d_6): δ 1.79 (3H, s, 5-CH_3), 2.05-2.13 (1H, m, H-2'a), 2.17-2.27 (1H, m, H-2'b), 3.59-3.66 (1H, m, H-4'), 3.87-3.96 (2H, m, H-5'a and H-5'b), 4.23-4.24 (1H, m, H-3'), 5.38 (1H, d, *J*= 4.2 Hz, 3'-OH), 6.18-6.22 (1H, m, H-1'), 7.51-7.7.75 (3H, m, subs Ph and H-6), 8.17-8.22 (2H, m, subs Ph and 5'-NH), 9.99 (1H, s, N'H), 11.32 (1H, s, 3-NH).

^{13}C NMR (75 MHz, DMSO-d_6): δ 12.73 (5-CH_3), (C-2' under DMSO peak), 46.95 (C-5'), 71.97 (C-3'), 84.56 and 84.69 (C-1' and C-4'), 110.54 (C-5), 121.59-139.91 (subs Ph, CF_3 and C-6), 151.18 (C-2), 164.38 (C-4), 181.44 (C=S).

Exact mass (ESI-MS) for $C_{18}H_{19}ClF_3N_4O_4$ $[M+H]^+$ found, 479.0778; calcd, 479.0762.

1-(4-Chloro-3-trifluoromethylphenyl)-5-(5'-amino-3'-*O*-*tert*-butyldimethylsilyl-5'-deoxy-β-D-thymidin-5'*N*-yl)tetrazole (2.36)

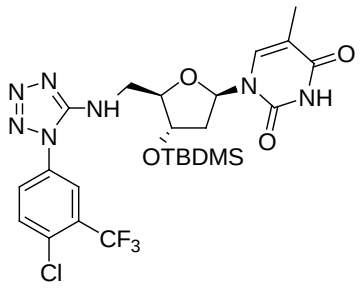

To a suspension of compound **2.35** (504 mg, 0.85 mmol), sodium azide (166 mg, 2.55 mmol) and $HgCl_2$ (253 mg, 0.93 mmol) in dry DMF (3.3 mL) was added Et_3N (0.36 mL, 2.55 mmol) under N_2 atmosphere. The resulting black suspension was stirred overnight at room temperature. The mixture was filtered through a pad of Celite, washing with CH_2Cl_2. The filtrate was diluted with water and extracted with CH_2Cl_2. The combined organic layers were dried over $MgSO_4$, filtered and concentrated under reduced pressure. The resulting residue was purified by silica gel chromatography (CH_2Cl_2/MeOH 98:2) affording compound **2.36** (424 mg, 83%) as a colourless solid.

^{1}H NMR (300 MHz, DMSO-d_6): δ 0.029-0.042 (6H, m, TBDMS), 0.84-0.86 (9H, m, TBDMS), 1.78 (3H, s, 5-CH_3), 2.00-2.07 (1H, m, H-2'a), 2.23-2.33 (1H, m, H-2'b), 3.48-3.62 (2H, m, H-5'a and H-5'b), 3.94-3.99 (1H, m, H-4'), 4.42-4.45 (1H, m, H-3'), 6.10-6.14 (1H, m, H-1'), 7.41 (1H, t, *J*= 6.0 Hz, 5'-NH), 7.53 (1H, d, *J*= 1.2 Hz, H-6), 7.88-8.03 (3H, m, subs Ph), 11.31 (1H, s, 3-NH).

^{13}C NMR (75 MHz, DMSO-d_6): δ -5.06 and -4.91 (TBDMS), 11.92 (5-CH_3), 17.56 (TBDMS), 25.56 (TBDMS), (C-2' under DMSO peak), 45.82 (C-5'), 72.90 (C-3'), 84.07 and 84.58 (C-1' and C-4'), 109.61 (C-5), 128.00-136.27 (subs Ph, CF_3 and C-6), 150.35 (C-2), 155.28 (C=N), 163.62 (C-4).

Exact mass (ESI-MS) for $C_{24}H_{32}ClF_3N_7O_4Si$ $[M+H]^+$ found, 602.1910; calcd, 602.1920.

1-(4-Chloro-3-trifluoromethylphenyl)-5-(5'-amino-5'-deoxy-β-D-thymidin-5'*N*-yl)tetrazole (2.19)

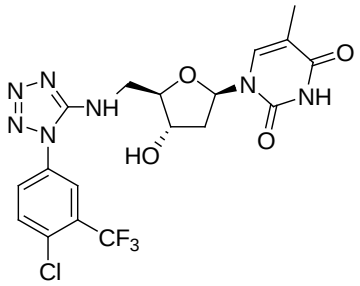

Compound **2.36** (241 mg, 0.400 mmol) was dissolved in THF (2.5 mL). A solution of 1M tetra-*n*-butylammonium fluoride in THF (0.88 mL) was added. After 1 h at room temperature the reaction was completed. The solvent was evaporated and the dry residue was purified by column chromatography (CH_2Cl_2/MeOH 95:5) to give pure compound **2.19** (104 mg, white solid) in 53% yield.

^{1}H NMR (300 MHz, DMSO-d_6): δ 1.76 (3H, d, *J*= 0.9 Hz, 5-CH_3), 2.04-2.11 (1H, m, H-2'a), 2.14-2.24 (1H, m, H-2'b), 3.49-3.65 (2H, m, H-5'a and H-5'b), 3.93-3.98 (1H, m, H-4'), 4.22-4.27 (1H, m, H-3'), 5.32 (1H, d, *J*= 4.5 Hz, 3'-OH), 6.12-6.17 (1H, m, H-1'), 7.39 (1H, t, *J*= 5.7 Hz, 5'-NH), 7.50 (1H, d, *J*= 1.5 Hz, H-6), 7.90-8.07 (3H, m, subs Ph), 11.29 (1H, s, 3-NH).

^{13}C NMR (75 MHz, DMSO-d_6): δ 12.02 (5-CH_3), (C-2' under DMSO peak), 46.16 (C-5'), 71.24 (C-3'), 83.91 (C-1'), 84.28 (C-4'), 109.73 (C-5), 124.95-136.26 (subs Ph, CF_3 and C-6), 150.47 (C-2), 155.42 (C=N), 163.76 (C-4).

Exact mass (ESI-MS) for $C_{18}H_{18}ClF_3N_7O_4$ $[M+H]^+$ found, 488.1052; calcd, 488.1055.

5'-(4-(*p*-Chlorophenyl)-1,2,3-triazol-1-yl)-5'-deoxy-β-D-thymidine (2.20)

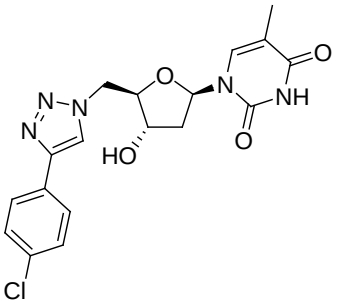

Compound **2.32** (56 mg, 0.21 mmol), sodium ascorbate (cat. amount) and $CuSO_4 \cdot 5H_2O$ (cat. amount) were suspended in 3 mL of H_2O/*t*-BuOH (1:2). 1-Chloro-4-ethynylbenzene (57 mg, 0.42 mmol) was added after 15 minutes and the mixture was stirred at room temperature for 7 days. The reaction

mixture was extracted with EtOAc and the combined organic phases were dried over anhydrous $MgSO_4$ and evaporated to dryness. Purification of the crude using RP-HPLC (Phenomenex Luna C-18, H_2O/0.1% HCOOH in CH_3CN, 90:10 → 0:100 in 23 min, flow 17.5 mL/min) afforded compound **2.20** (2.0 mg, 2%) as a white powder.

^{1}H NMR (300 MHz, DMSO-d_6): δ 1.68 (3H, s, 5-CH_3), 2.02-2.24 (2H, m, H-2'a and H-2'b), 4.09-4.14 (1H, m, H-4'), 4.28-4.31 (1H, m, H-3'), 4.64-4.80 (2H, m, H-5'a and H-5'b), 5.59 (1H, br s, 3'-OH), 6.18 (1H, app t, *J*= 6.9 Hz, H-1'), 7.23 (1H, d, *J*= 1.2 Hz, H-6), 7.49-7.53 (2H, m, subs Ph), 7.85-7.90 (2H, m, subs Ph), 8.62 (1H, s, H-5"), 11.30 (1H, s, 3-NH).

^{13}C NMR (75 MHz, DMSO-d_6): δ 11.96 (5-CH_3), 37.84 (C-2'), 51.13 (C-5'), 70.47 (C-3'), 83.66 (C-4'), 83.77 (C-1'), 109.79 (C-5), 122.53-132.25 (subs Ph and C-5"), 135.96 (C-6), 145.26 (C-4"), 150.37 (C-2), 163.56 (C-4).

Exact mass (ESI-MS) for $C_{18}H_{19}ClN_5O_4$ $[M+H]^+$ found, 404.1125; calcd, 404.1120.

3',5'-Di-*O*-acetyl-β-D-thymidine (2.37)

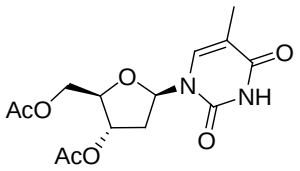

β-thymidine (2.50 g, 10.32 mmol) was dissolved in pyridine (40 mL) and acetic anhydride (40 mL). The reaction mixture was stirred at room temperature during 2 h, evaporated to dryness, and co-evaporated with toluene to obtain pure compound **2.37** in a 98% yield (3.30 g, white foam).

^{1}H NMR (300 MHz, $CDCl_3$): δ 1.94 (3H, d, *J*= 1.2 Hz, 5-CH_3), 2.11 (3H, s, OAc), 2.13 (3H, s, OAc), 2.12 (1H, dd, *J*= 6.6 Hz, *J*= 8.4 Hz, H-2'a), 2.43-2.51 (1H, m, H-2'b), 4.24-4.28 (1H, m, H-4'), 4.35-4.45 (2H, m, H-5'a and H-5'b), 5.21 (1H, dt, *J*= 2.1 Hz, *J*= 6.6 Hz, H-3'), 6.31 (1H, dd, *J*= 5.7 Hz, *J*= 8.7, H-1'), 7.29 (1H, d, *J*= 1.2 Hz, H-6), 8.62 (1H, br s, 3-NH).

Exact mass (ESI-MS) for $C_{14}H_{19}N_2O_7$ $[M+H]^+$ found, 327.1194; calcd, 327.1192.

3',5'-Di-*O*-acetyl-α-D-thymidine (2.38)

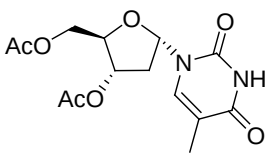

To a solution of compound **2.37** (3.30 g, 10.11 mmol) in 5 mL dry CH_3CN, was added a freshly prepared solution, containing 17 µL H_2SO_4 and 0.66 mL acetic anhydride in 5 mL dry CH_3CN. After 2 h, the mixture was quenched with saturated $NaHCO_3$-solution and extracted three times with EtOAc. After purification (CH_2Cl_2/MeOH 95:5), compound **2.38** was obtained in a 45% yield (1.51 g, white crystals).

^{1}H NMR (300 MHz, $CDCl_3$): δ 1.95 (3H, d, *J*= 1.2 Hz, 5-CH_3), 2.05 (3H, s, OAc), 2.12 (3H, s, OAc), 2.21-2.28 (1H, m, H-2'a), 2.81 (1H, dt, *J*= 6.9 Hz, *J*= 15.1 Hz, H-2'b), 4.19-4.25 (2H, m, H-5'a and H-5'b), 4.59-4.63 (1H, m, H-4'), 5.23 (1H, dt, *J*= 1.6 Hz, *J*= 6.4 Hz, H-3'), 6.26 (1H, dd, *J*= 2.4 Hz, *J*= 7.2 Hz, H-1'), 7.30 (1H, d, *J*= 1.2 Hz, H-6), 8.62 (1H, br s, 3-NH).

Exact mass (ESI-MS) for $C_{14}H_{19}N_2O_5$ $[M+H]^+$ found, 327.1195; calcd, 327.1192.

4-Thio-α-D-thymidine (2.40)

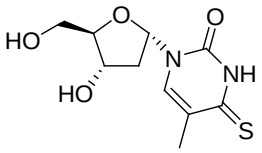

Lawesson's reagent (777 mg, 1.92 mmol) was added to a solution of compound **2.38** (519 mg, 1.59 mmol) in 15 mL dry 1,4-dioxane. The mixture was refluxed for 4 hours. After the reaction mixture had been cooled, the solvent was removed *in vacuo*. The crude product thus obtained (compound **2.39**) was treated with 8 mL of a 7N NH_3 in MeOH solution and stirred at room temperature for 4 hours. The reaction mixture was concentrated *in vacuo* and the residue was purified on a silica gel column using CH_2Cl_2/MeOH (94:6) as the eluent to afford compound **2.40** as a yellow foam (150 mg, 37%).

^{1}H NMR (300 MHz, DMSO-d_6): δ 1.75 (3H, s, 5-CH_3), 1.94-1.98 (1H, m, H-2'a), 2.51-2.57 (1H, m, H-2'b), 3.40 (2H, t, *J*= 5.2 Hz, H-5'a and H-5'b), 4.23-4.25 (2H, m, H-3' and H-4'), 4.86 (1H, t, *J*= 5.7 Hz, 5'-OH), 5.26 (1H, d, *J*= 2.7 Hz, 3'-OH), 6.04 (1H, dd, *J*= 2.7 Hz, *J*= 7.5 Hz, H-1'), 7.81 (1H, d, *J*= 0.9 Hz, H-6), 12.65 (1H, s, 3-NH).

Exact mass (ESI-MS) for $C_{10}H_{15}N_2O_4S$ $[M+H]^+$ found, 259.0753; calcd, 259.0747.

5'-*O*-Methanesulfonyl-4-thio-α-D-thymidine (2.41)

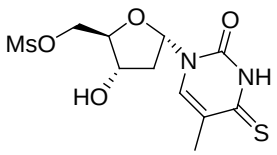

To a solution of 4-thio-α-D-thymidine **2.40** (146 mg, 0.57 mmol) in pyridine (5 mL) was added methanesulfonyl chloride (42 µL,0.54 mmol) at -78 °C. The reaction mixture was stirred for 1 h at 0 °C. The reaction was quenched with saturated aqueous $NaHCO_3$-solution and extracted with CH_2Cl_2 three times, dried over $MgSO_4$ and evaporated. The residue was purified by column chromatography (CH_2Cl_2/ MeOH 95:5) to give compound **2.41** as a yellow foam (133 mg, 70%).

^{1}H NMR (300 MHz, DMSO-d_6): δ 1.97 (3H, d, *J*= 0.6 Hz, 5-CH_3), 1.99-2.04 (1H, m, H-2'a), 2.53-2.30 (1H, m, H-2'b), 3.22 (3H, s, SO_2CH_3), 4.08-4.10 (2H, m, H-5'a and H-5'b), 4.16-4.30 (1H, m, H-3'), 4.40-4.46 (1H, m, H-4'), 5.55 (1H, br s, 3'-OH), 6.09 (1H, dd, *J*= 3.6 Hz, *J*= 7.5 Hz, H-1'), 7.69 (1H, s, H-6).

Exact mass (ESI-MS) for $C_{11}H_{17}N_2O_6S_2$ $[M+H]^+$ found, 337.0533; calcd, 337.0523.

5'-Azido-5'-deoxy-4-thio-α-D-thymidine (2.42)

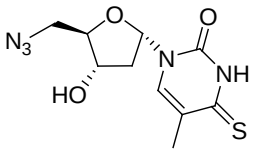

A solution of compound **2.41** (129 mg, 0.38 mmol) and NaN_3 (250 mg, 3.86 mmol) in DMF (7 mL) was heated overnight at 60 °C. The reaction mixture was evaporated *in vacuo*. The residue was dissolved in CH_2Cl_2 and washed with brine. The organic layer was dried over $MgSO_4$, evaporated and purified by column chromatography (CH_2Cl_2/MeOH 95:5) affording compound **2.42** (97 mg, 89%) as a yellow oil.

^{1}H NMR (300 MHz, DMSO-d_6): δ 1.98 (3H, d, *J*= 0.9 Hz, 5-CH_3), 2.04 (1H, t, *J*= 3.3 Hz, H-2'a), 2.56-2.65 (1H, m, H-2'b), 3.40-3.44 (2H, m, H-5'a and H-5'b), 4.14-4.17 (1H, m, H-3'), 4.34-4.39 (1H, m, H-4'), 5.47 (1H, br s, 3'-OH), 6.09 (1H, dd, *J*= 3.6 Hz, *J*= 7.5 Hz, H-1'), 7.78 (1H, s, H-6).

Exact mass (ESI-MS) for $C_{10}H_{14}N_5O_3S$ $[M+H]^+$ found, 284.0813; calcd, 284.0812.

5'-Amino-5'-deoxy-4-thio-α-D-thymidine (2.43)

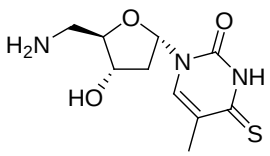

Compound **2.42** (97 mg, 0.34 mmol) and PPh_3 (187 mg, 0.71 mmol) were dissolved in THF (6 mL). After stirring for 10 minutes, H_2O was added (883 µL) and the mixture was stirred for 1 day. The

reaction mixture was extracted with CH_2Cl_2 and the water phase lyophilized to give amine **2.43** (78 mg, 89%).

^{1}H NMR (300 MHz, DMSO-d_6): δ 1.96 (3H, d, *J*= 0.6 Hz, 5-CH_3), 2.00 (1H, t, *J*= 3.6 Hz, H-2'a), 2.58-2.68 (1H, m, H-2'b), 2.76-2.87 (1H, m, H-5'a), 2.96-3.04 (1H, m, H-5'b), 4.18-4.20 (1H, m, H-3'), 4.32 (1H, dt, *J*= 3.3 Hz, *J*= 9.6 Hz, H-4'), 5.57 (1H, br s, 3'-OH), 6.15 (1H, dd, *J*= 3.3 Hz, *J*= 7.5 Hz, H-1'), 7.77 (1H, s, H-6).

Exact mass (ESI-MS) for $C_{10}H_{16}N_3O_3S$ $[M+H]^+$ found, 258.0907; calcd, 258.0907.

***N*-(5'-Deoxy-4-thio-α-D-thymidin-5'-yl)-*N*'-phenylthiourea (2.22)**

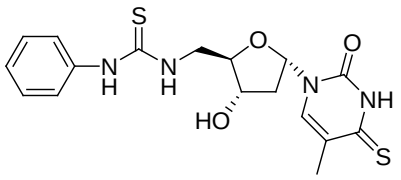

For the synthesis of compound **2.22**, amine **2.43** (26 mg, 0.10 mmol) was dissolved in DMF (1 mL). At 0 °C, phenyl isothiocyanate (16 mg, 0.12 mmol) was added and the reaction mixture was allowed to stir at room temperature during 3 h. After completion of the reaction, the reaction mixture was evaporated to dryness and the residue was purified by column chromatography (CH_2Cl_2/MeOH 95:5) to obtain final compound **2.22** (27.0 mg, 69%) as a yellow powder.

^{1}H NMR (300 MHz, DMSO-d_6): δ 1.97 (3H, d, *J*= 0.9 Hz, 5-CH_3), 2.01-2.03 (1H, m, H-2'a), 2.54-2.63 (1H, m, H-2'b), 3.53-3.70 (2H, m, H-5'a and H-5'b), 4.21-4.24 (1H, m, H-3'), 4.42-4.46 (1H, m, H-4'), 5.43 (1H, d, *J*= 2.7 Hz, 3'-OH), 6.12 (1H, dd, *J*= 2.7 Hz, *J*= 7.5 Hz, H-1'), 7.08-7.13 (1H, m, Ph), 7.29-7.34 (2H, m, Ph), 7.43-7.47 (2H, m, Ph), 7.80 (1H, s, H-6).

^{13}C NMR (75 MHz, DMSO-d_6): δ 17.03 (5-CH_3), (C-2' under DMSO peak), 45.49 (C-5'), 70.79 (C-3'), 86.08 (C-1'), 86.78 (C-4'), 117.22 (C-5), 123.22, 124.30, 128.63 and 134.25 (Ph), 139.13 (C-6), 147.87 (C-2), 180.74 (C=S), 190.56 (C-4).

Exact mass (ESI-MS) for $C_{17}H_{21}N_4O_3S_2$ $[M+H]^+$ found,393.1053; calcd, 393.1050.

***N*-(5'-Deoxy-4-thio-α-D-thymidin-5'-yl)-*N*'-(4-chloro-3-trifluoromethylphenyl)thiourea (2.23)**

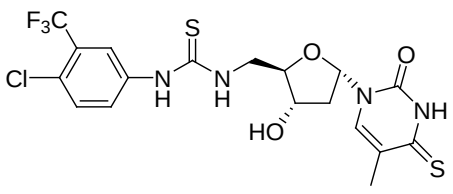

Compound **2.23** was synthesized from amine **2.43** (52 mg, 0.20 mmol) and 4-chloro-3-trifluoromethylphenyl isothiocyanate (57 mg,0.24 mmol) using the same procedure as described for the synthesis of compound **2.22**. After purification by column chromatography (CH_2Cl_2/MeOH 95:5), compound **2.23** (41.7mg, 42%) was obtained as a yellow powder.

^{1}H NMR (300 MHz, DMSO-d_6): δ 1.98 (3H, d, *J*= 0.6 Hz, 5-CH_3), 2.06 (1H, t, *J*= 2.1 Hz, H-2'a), 2.57-2.66 (1H, m, H-2'b), 3.56-3.59 (1H, m, H-5'a), 3.67-3.72 (1H, m, H-5'b), 4.25-4.26 (1H, m, H-3'), 4.44-4.48 (1H, m, H-4'), 5.47 (1H, d, *J*= 3.0 Hz, 3'-OH), 6.14 (1H, dd, *J*= 2.7 Hz, *J*= 7.5 Hz, H-1'), 7.64 (2H, d, *J*= 8.7 Hz, subs Ph), 7.74 (2H, dd; *J*= 2.1 Hz, *J*= 8.4 Hz, subs Ph), 7.83 (1H, d, *J*= 0.9 Hz, H-6).

^{13}C NMR (75 MHz, DMSO-d_6): δ 17,11 (5-CH_3), (C-2' under DMSO peak), 45.62 (C-5'), 70.95 (C-3'), 86.18 and 86.55 (C-4' and C-1'), 117.22 (C-5), 124.61, 127.50, 131.77 and 134.28 (CF_3 and subs Ph), 139.23 (C-6), 148.00 (C-2), 180.95 (C=S), 190.70 (C-4).

Exact mass (ESI-MS) for $C_{18}H_{19}ClF_3N_4O_3S_2$ $[M+H]^+$ found,495.0508; calcd, 495.0534.

α-D-Thymidine (2.44)

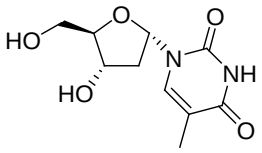

Compound **2.38** (1.1 g, 3.37 mmol) was dissolved in a 7N solution of NH_3 in MeOH (35 mL). The reaction mixture was stirred overnight at room temperature. The solvent was evaporated *in vacuo* and the residue was dissolved in EtOAc and extracted three times with water. The organic layer was dried over $MgSO_4$, filtered and concentrated under reduced pressure, yielding 0.73 g of pure compound **2.44** (90%).

^{1}H NMR (300 MHz, DMSO-d_6): δ 1.78 (3H, d, *J*= 1.2 Hz, 5-CH_3), 1.84-1.91 (1H, m, H-2'a), 2.48-2.60 (1H, m, H-2'b), 3.39 (2H, app t, *J*= 5.2 Hz, H-5'a and H-5'b), 4.13-4.17 (1H, m, H-3'), 4.23-4.26 (1H, m, H-4'), 4.81 (1H, t, *J*= 5.7 Hz, 5'-OH), 5.30 (1H, d, *J*= 3.0 Hz, 3'-OH), 6.12 (1H, dd, *J*= 3.3 Hz, *J*= 7.5 Hz, H-1'), 7.75 (1H, d, *J*= 1.2 Hz, H-6), 11.20 (1H, br s, 3-NH).

Exact mass (ESI-MS) for $C_{10}H_{15}N_2O_5$ $[M+H]^+$ found, 243.0975; calcd, 243.0981.

5'-Azido-5'-deoxy-α-D-thymidine (2.21)

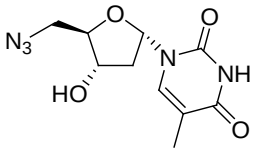

To a solution of α-D-thymidine **2.44** (0.45 g, 1.86 mmol) in pyridine (7 mL) was added methanesulfonyl chloride (130 µL, 0.21 mmol) at -78 °C. The reaction mixture was stirred for 1 h at 0 °C. The reaction was quenched with a saturated aqueous $NaHCO_3$-solution and extracted with CH_2Cl_2 three times, dried over $MgSO_4$ and evaporated. The residue was purified by column chromatography (CH_2Cl_2/MeOH 98:2) to give the mesylated compound as a white solid (0.37 g, 62%).

^{1}H NMR (300 MHz, DMSO-d_6): δ 1.75 (3H, s, 5-CH_3), 1.95-2.05 (1H, m, H-2'a), 2.55-2.68 (1H, m, H-2'b), 3.19 (3H, s, CH_3SO_2), 4.12-4.34 (3H, m, H-5'a, H-5'b and H-3'), 4.33-4.36 (1H, m, H-4'), 5.58 (1H, br s, 3'-OH), 6.12 (1H, dd, *J*= 4.4 Hz, *J*= 7.6 Hz, H-1'), 7.73 (1H, s, H-6), 11.27 (1H, br s, 3-NH).

Exact mass (ESI-MS) for $C_{11}H_{17}N_2O_7S$ $[M+H]^+$ found, 321.0759; calcd, 321.0756.

A solution of 5'-mesylated α-D-thymidine (370 mg, 1.16 mmol) and NaN_3 (755 g, 11.71 mmol) in DMF (20 mL) was stirred overnight at 60 °C. The reaction mixture was evaporated *in vacuo*. The residue was dissolved in CH_2Cl_2 and washed with H_2O. The organic layer was dried over $MgSO_4$, evaporated and purified by column chromatography (CH_2Cl_2/MeOH 95:5) to afford compound **2.21** as a white solid (200 mg, 65%). Spectroscopic data of **2.21** are in accordance with literature data.[69]

^{1}H NMR (300 MHz, DMSO-d_6): 1.76 (3H, s, 5-CH_3), 1.93-2.02 (1H, m, H-2'a), 2.51-2.60 (1H, m, H-2'b), 3.49-3.60 (2H, m, H-5'a and H-5'b), 4.12-4.16 (1H, m, H-3'), 4.24-4.27 (1H, m, H-4'), 5.50 (1H, br s, 3'-OH), 6.13 (1H, dd, *J*= 4.5 Hz, *J*= 7.5 Hz, H-1'), 7.72 (1H, s, H-6), 11.26 (1H, br s, 3-NH).

Exact mass (ESI-MS) for $C_{10}H_{14}N_5O_4$ $[M+H]^+$ found, 268.1045; calcd, 268.1046.

5'-(4-(*p*-Chlorophenyl)-1,2,3-triazol-1-yl)-5'-deoxy-α-D-thymidine (2.24)

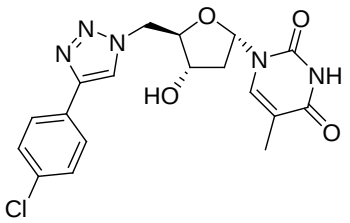

Compound **2.21** (85 mg, 0.32 mmol), sodium ascorbate (3 mg, 0.016 mmol) and $CuSO_4 \cdot 5H_2O$ (3 mg, 0.013 mmol) were suspended in 3 mL of H_2O/*t*-BuOH (2:1). 1-Chloro-4-ethynylbenzene (87 mg, 0.64 mmol) was added after 15 minutes and the mixture was stirred at room temperature for 4 days. Water was added and the triazole product precipitated. Filtration of the mixture afforded pure compound **2.24** (40.0 mg, 31%) as a white powder.

^{1}H NMR (300 MHz, DMSO-d_6): δ 1.75 (3H, d, *J*= 1.2 Hz, 5-CH_3), 1.94 (1H, app t, *J*= 3.9 Hz, H-2'a), 1.99 (1H, app t, *J*= 3.9 Hz, H-2'b), 4.22-4.32 (1H, m, H-4'), 4.43-4.66 (3H, m, H-3', H-5'a and H-5'b), 5.65 (1H, br s, 3'-OH), 6.18 (1H, dd, *J*= 4.2 Hz, *J*= 7.5 Hz, H-1'), 7.49-7.54 (2H, m, subs Ph), 7.72 (1H, d, *J*= 1.2 Hz, H-6), 7.86-7.91 (2H, m, subs Ph), 8.62 (1H, s, H-5"), 11.26 (1H, s, 3-NH).

^{13}C NMR (75 MHz, DMSO-d_6): δ 12.15 (5-CH_3), 51.20 (C-5'), 70.53 (C-4'), 84.72 (C-1'), 85.37 (C-3'), 108.81 (C-5), 122.41 (C-5"), 126.73, 128.83, 129.45 and 132.15 (subs Ph), 136.64 (C-6), 145.12 (C-4"), 150.29 (C-2), 163.65 (C-4).

Exact mass (ESI-MS) for $C_{18}H_{19}ClN_5O_4$ $[M+H]^+$ found, 404.1129; calcd, 404.1120.

5'-*O*-Acetyl-3'-azido-3'-deoxy-α-D-thymidine (2.45)

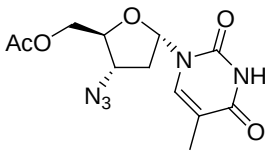

To a solution of compound **2.27** (642 mg, 2.08 mmol) in 1 mL dry CH_2Cl_2, was added a freshly prepared solution containing 34 µL H_2SO_4 and 140 µL acetic anhydride in 1 mL dry CH_2Cl_2. After 2 h, the mixture was quenched with a saturated $NaHCO_3$-solution and extracted three times with EtOAc. Purification of the crude on a silica gel column (EtOAc/hexane 9:1) yielded compound **2.45** as a white foam (126 mg, 20%).

^{1}H NMR (300 MHz, DMSO-d_6): δ 1.80 (3H, d, *J*= 0.9 Hz, 5-CH_3), 2.06 (3H, s, OAc), 2.15-2.22 (1H, m, H-2'a), 2.70-2.75 (1H, m, H-2'b), 4.11-4.14 (2H, m, H-5'a and H-5'b), 4.34-4.39 (1H, m, H-3'), 4.42-4.45 (1H, m, H-4'), 6.07 (1H, dd, *J*= 6.0 Hz, *J*= 6.9 Hz, H-1'), 7.59 (1H, d, *J*= 1.2 Hz, H-6), 11.32 (1H, s, 3-NH).

^{13}C NMR (75 MHz, DMSO-d_6): δ 12.15 (5-CH_3), 20.62 (OAc), 36.23 (C-2'), 60.43 (C-3), 63.68 (C-5'), 81.46 (C-4'), 84.93 (C-1'), 109.38 (C-5), 136.25 (C-6), 150.36 (C-2), 163.80 (C-4), 170.15 (OAc).

Exact mass (ESI-MS) for $C_{12}H_{16}N_5O_5$ $[M+H]^+$ found, 310.1164; calcd, 310.1146.

3'-Azido-3'-deoxy-α-D-thymidine (2.25)

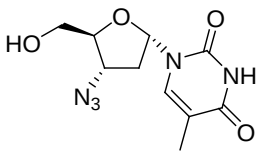

Compound **2.45** (146 mg, 0.47 mmol) was dissolved in a 7N NH_3 in MeOH solution (2.6 mL) and stirred at room temperature for 6 hours. The reaction mixture was concentrated *in vacuo* and the residue was purified on a silica gel column using EtOAc/hexane (8:2) as the eluent to afford compound **2.25** as a colourless solid (91 mg, 72%). Spectroscopic data of **2.25** are in accordance with literature data.[117]

^{1}H NMR (300 MHz, $CDCl_3$): δ 1.95 (3H, d, *J*= 0.9 Hz, 5-CH_3), 2.12-2.17 (1H, m, H-2'a), 2.82-2.91 (1H, m, H-2'b), 3.08 (1H, t, *J*= 5.4 Hz, 5'-OH), 3.65-3.72 (1H, m, H-5'a), 3.81-3.85 (1H, m, H-5'b), 4.27-4.35 (2H, m, H-3' and H-4'), 6.29 (1H, dd, *J*= 4.2 Hz, *J*= 6.9 Hz, H-1'), 7.32 (1H, d, *J*= 1.5 Hz, H-6), 9.48 (1H, s, 3-NH).

^{13}C NMR (75 MHz, $CDCl_3$): δ 12.67 (5-CH_3), 38.22 (C-2'), 60.83 (C-3), 62.62 (C-5'), 85.93 and 86.02 (C-4' and C-1'), 111.24 (C-5), 135.35 (C-6), 150.72 (C-2), 164.03 (C-4).

Exact mass (ESI-MS) for $C_{10}H_{14}N_5O_4$ $[M+H]^+$ found, 268.1020; calcd, 268.1040.

3'-(4-(*p*-Chlorophenyl)-1,2,3-triazol-1-yl)-3'-deoxy-α-D-thymidine (2.26)

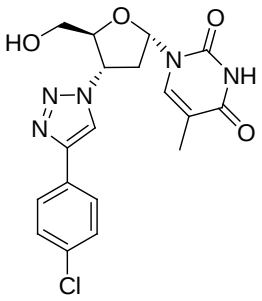

Compound **2.25** (72 mg, 0.27 mmol), sodium ascorbate (3 mg, 0.024 mmol) and $CuSO_4 \cdot 5H_2O$ (3 mg, 0.011 mmol) were suspended in 3 mL of a H_2O/*t*-BuOH (1:2) mixture. 1-Chloro-4-ethynylbenzene (74 mg, 0.54 mmol) was added after 15 minutes and the mixture was stirred at room temperature for 24 h. The reaction mixture was extracted with EtOAc and the combined organic phases were dried over $MgSO_4$ and evaporated to dryness. The crude product was purified using column chromatography (EtOAc/hexane 8:2) to obtain compound **2.26** (50.8 mg, 47%) as a white powder.

^{1}H NMR (300 MHz, DMSO-d_6): δ 1.75 (3H, s, 5-CH_3), 2.71-2.80 (1H, m, H-2'a), 2.98-3.07 (1H, m, H-2'b), 3.54-3.70 (2H, m, H-5'a and H-5'b), 4.65-4.70 (1H, m, H-4'), 5.12 (1H, t, *J*= 5.4 Hz, 5'-OH), 5.29-5.36 (1H, m, H-3'), 6.26 (1H, app t, *J*= 6.6 Hz, H-1'), 7.50-7.54 (2H, m, subs Ph), 7.63 (1H, d, *J*= 1.2 Hz, H-6), 7.84-7.87 (2H, m, subs Ph), 8.82 (1H, s, H-5"), 11.29 (1H, s, 3-NH).

^{13}C NMR (75 MHz, DMSO-d_6): δ 12.18 (5-CH_3), 37.12 (C-2'), 59.23 (C-3), 61.12 (C-5'), 83.89 (C-4'), 84.43 (C-1'), 109.58 (C-5), 121.38 (C-5"), 126.88-132.47 (subs Ph), 136.07 (C-6), 145.49 (C-4"), 150.46 (C-2), 163.78 (C-4).

Exact mass (ESI-MS) for $C_{18}H_{19}ClN_5O_4$ $[M+H]^+$ found, 404.1156; calcd, 404.1120.

2.6.2 Biological Assays

Spectrophotometric Binding Assay

TMPKmt activities were determined using the coupled spectrophotometric assay described by Blondin *et al*.[124] using an Eppendorf ECOM 6122 photometer and a wavelength of 334 nm. The reaction medium (0.5 mL final volume) contained 50 mM Tris-HCl, pH 7.4, 50 mM KCl, 2 mM $MgCl_2$, 0.2 mM NADH, 1 mM phosphoenol pyruvate, and 2 units each of lactate dehydrogenase, pyruvate kinase and nucleoside diphosphate kinase. The concentrations of ATP and dTMP were kept constant at 0.5 and 0.05 mM, respectively, whereas the concentrations of analogues varied between 0.01 and 2 mM.

Biological Assays on *Mycobacterium bovis* (BCG)

Compound **2.23** was assayed for its inhibitory potency on *Mycobacterium bovis* growth *in vitro*.[125] A micro-method of culture was performed in 7H9 Middlebrook broth medium containing 0.2% glycerol and 0.5% Tween-80. Serial 2-fold dilutions of each compound were prepared directly in 96-well plates. The bacterial inoculum was prepared previously at a concentration in the range of 10^7 bacteria (*M. bovis* BCG 1173P2) in 7H9 medium and stored at -80 °C until used. The bacteria, adjusted at 10^5 per mL, were delivered in 100 µL per well. The covered plates were sealed with parafilm and incubated at 37 °C in plastic boxes containing a humidified normal atmosphere. At day 8 of incubation, 30 µL of a resazurin (Sigma) solution at 0.01% (wt/vol) in water was added to each well. After an overnight incubation at 37 °C, the plates were assessed for color development using the optical density difference at 570 and 630 nm on a microplate reader. The change from blue to pink indicates reduction of resazurin and therefore bacterial growth. The lowest compound concentration that prevented the color change determined the MIC for the assayed compound.

PART III

5-SUBSTITUTED URIDINE-5'-PHOSPHONATE ANALOGUES AS $P2Y_2$ AGONISTS

1 INTRODUCTION

1.1 PURINERGIC RECEPTORS

Extracellular nucleotides, such as ATP, ADP, UTP and UDP are important signaling molecules that mediate diverse biological effects via cell-surface receptors termed purinergic receptors.[126] These receptors were first formally recognized by Burnstock in 1978, when he proposed that these could be divided into two classes termed “P1-purinoceptors”, at which adenosine is the principal natural ligand, and “P2-purinoceptors”, recognizing ATP, ADP, UTP and UDP.[127] Although P1 and P2 receptors are now characterized primarily according to their distinct molecular structures, supported by evidence of distinct effector systems, pharmacological profiles, and tissue distributions, this major division remains a fundamental part of purine receptor classification. In addition, receptors for pyrimidines are now included within the P2 receptor family.[128]

P1 receptors have been further subdivided, according to convergent molecular, biochemical, and pharmacological evidence into four subtypes: A_1, A_{2A}, A_{2B} and A_3.[126] All are members of the rhodopsin family of G protein-coupled receptors and are coupled principally to adenylate cyclase.[129]

Based on differences in molecular structure and signal transduction mechanisms, P2 receptors divide naturally into two families of ligand-gated ion channels and G protein-coupled receptors termed P2X and P2Y receptors, respectively. To date seven mammalian P2X receptors ($P2X_{1–7}$) and at least eight different P2Y receptor subtypes ($P2Y_1$, $P2Y_2$, $P2Y_4$, $P2Y_6$, $P2Y_{11}$, $P2Y_{12}$, $P2Y_{13}$ and $P2Y_{14}$) have been cloned, characterized and accepted as valid members of the P2 receptor family (Figure III.1).[130]

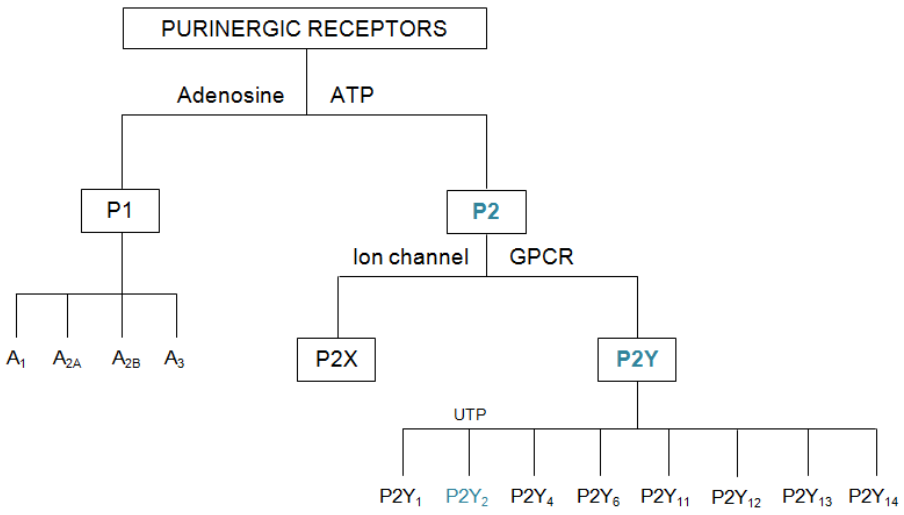

Figure III.1. Purinergic receptor superfamily tree.

1.2 THE P2Y RECEPTOR FAMILY

1.2.1 Biochemistry of P2Y Receptors

The cloning of the first two members of the P2Y receptor family, $P2Y_1$ and $P2Y_2$, has been reported in 1993[131,132] and up to now, eight distinct subtypes are cloned and pharmacologically characterized: $P2Y_{1,2,4,6,11,12,13,14}$. The missing numbers belong to non-mammalian receptors, which may be orthologs of mammalian subtypes, or receptors that do not appear to be bona-fide P2Y receptor family members.[130]

The P2Y receptors belong to the rhodopsin family of GPCRs and show the typical features of G-protein-coupled receptors consisting of seven hydrophobic transmembrane regions (TM) connected by three intracellular and three extracellular loops (EL) (Figure III.2). The peptides of the human P2Y receptors consist of 328 ($P2Y_6$) to 377 ($P2Y_2$) amino acids corresponding to a predicted molecular mass 41 to 53 kDa after glycosylation. The biochemical analysis of the P2Y-receptor proteins has shown that P2Y-receptors expressed at the level of the cell membrane are in fact modified by *N*-linked glycosylation. For the $P2Y_{12}$-receptor, it has recently been demonstrated that *N*-linked glycosylation of the receptor protein is essential for signal transduction, but not for ligand binding or cell surface expression.[133]

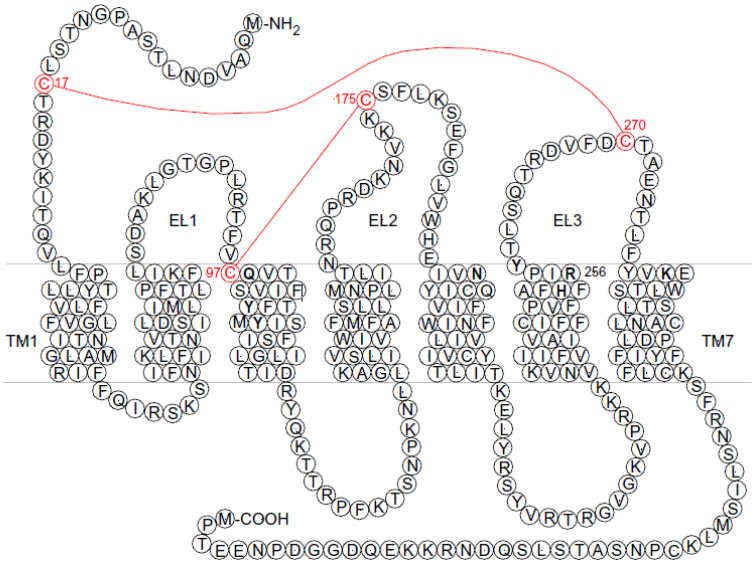

Figure III.2. Predicted secondary structure of the human $P2Y_{12}$ receptor. The dashed lines show predicted disulfide bridges. [134]

The degree of relationship among the members of human P2Y receptors is 20 to 50%, indicating a relative high diversity in the amino acid composition.[135] For comparison, the $hP2Y_1$ receptor and the $hP2Y_{2,4,6}$ receptors share 38, 44 and 46% sequence identity, respectively, and the $hP2Y_1$ receptor and the $hP2Y_{12}$ receptor, which have similarities in their pharmacological profile, share only 24%. 144

Interestingly, all known P2Y receptor subtypes possess at their extracellular domains 4 cysteine residues, which are likely to form 2 disulfide bridges, the first one between the N-terminal domain and EL3 and the second bridge between EL1 and EL2 (Figure III.2).[136,137]

1.2.2 P2Y Receptor Subtypes and Their Signaling

From a phylogenetic and structural point of view, two distinct P2Y receptor subgroups have been identified both characterized by a relatively high level of sequence divergence. The first subgroup includes the $P2Y_{1,2,4,6,11}$ receptors and the second group encompasses the $P2Y_{12,13,14}$ subtypes.

$P2Y_{1,2,4,6}$ receptors act via G_q proteins resulting in phospholipase C (PLC) stimulation leading to the formation of IP_3 and mobilization of intracellular Ca^{2+}. In addition, activation of the $P2Y_{11}$ receptor by ATP leads to a rise in both cAMP and IP_3, whereas activation by UTP produces calcium mobilization without IP_3 or cAMP increase.[129] The second group of P2Y receptors couples via G_i proteins leading to the inhibition of adenylate cyclase followed by a decrease in intracellular cAMP levels (Figure III.3).[130]

The response time of P2Y receptors is longer than the rapid responses mediated by P2X receptors because it involves second-messenger systems and/or ionic conductances mediated by G protein coupling.[126]

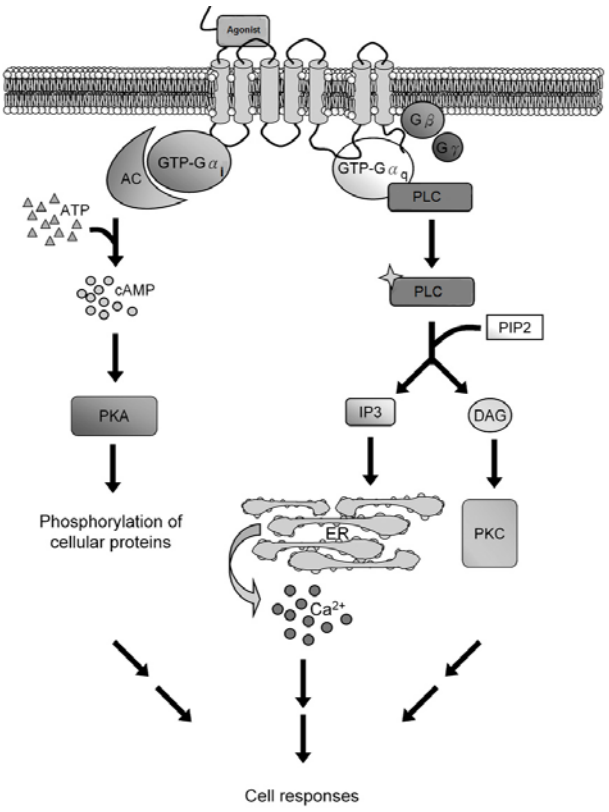

Figure III.3. Schematic diagram of the cAMP (left) and PLC (right) signal transduction pathways.[138]

1.3 THE $P2Y_2$ RECEPTOR

The $P2Y_2$ receptor is the most widely studied uracil nucleotide receptor. It is broadly distributed throughout the body and is most prominently expressed in the lung, heart, skeletal muscle, spleen, kidney and liver.[134,139,140]

$P2Y_2$ receptors have been cloned and pharmacologically characterized from human, rat, mouse, canine and porcine cells or tissues. The human receptor exhibits 89% identity in amino acid sequence to the mouse receptor.

As mentioned above, $P2Y_2$ receptor signaling is linked to PLC. Ligand and receptor binding triggers the GDP-GTP exchange of G_q proteins and the dissociation of the α-subunit. The latter activates phospholipase C which will hydrolyze phosphatidylinositol 4,5-bisphosphate (PIP_2) into inositol 1,4,5-triphosphate (IP_3) and diacylglycerol (DAG). Formation of IP_3 results in an intracellular Ca^{2+} mobilization from internal stores. Additionally, DAG activates protein kinase C which in turn phosphorylates cellular proteins.[138]

1.3.1 $P2Y_2$ Receptor Agonists

The $P2Y_2$ receptor is unique among the human pyrimidine nucleotide receptors in that it is activated by two structurally different nucleotides, ATP and UTP, which contain a different base moiety. Other naturally occurring bases, e.g., guanine and cytosine are not tolerated.

The $P2Y_2$ receptor is activated equipotently by both UTP (**3.1**, Figure III.4) and ATP (**1.4**). The human $P2Y_4$ receptor is selectively activated by UTP, and ATP is a potent competitive antagonist at this receptor. However, the $P2Y_4$ receptor of several other species is activated by both UTP and ATP.[141,142,143] The high dependence of the human $P2Y_4$ receptor on uridine nucleotides for activation makes it difficult to find UTP analogues that are $P2Y_2$ receptor selective. However, in controlled clinical studies, UTP is used in preference to ATP as $P2Y_2$ receptor agonist because of the expected higher selectivity of pyrimidine nucleotides versus the other P2 receptors and because active ATP metabolites such as adenosine may interact with the P1 receptors leading to undesirable side effects.[144]

When tested under conditions excluding enzymatic conversion of nucleotides, UDP and ADP did not activate the $P2Y_2$ receptor, indicating that the receptor is selective for nucleoside triphosphates.[145] The phosphate groups of nucleotides are deprotonated at physiological pH ($pK_{a1} \approx 1$, $pK_{a2} \approx 6$),[146] thus, the nucleoside triphosphates are tetra-anions, while the diphosphates exhibit a tri-anionic form. Under physiological conditions, the anions may form complexes with divalent cations, such as Ca^{2+} or Mg^{2+}.

There is some evidence that the tetra-anionic forms of ATP and UTP and not the complexed forms bind to $P2Y_2$ receptors, and this may be true for all nucleotide receptors.[147]

A lot of efforts have been made to synthesize highly potent and selective agonists for the $P2Y_2$ receptor. The most important results towards this goal are summarized below.

1.3.1.1 Phosphate Chain Modifications

UTPγS (**3.2**, Figure III.4), a phosphate chain modified nucleotide, is a relatively potent $P2Y_2$ receptor agonist and is more stable against hydrolyzing enzymes compared to UTP.[148] The same modification in ATP resulted in a 75-fold decrease in activity.[149]

The phosphate chain in UTP has also been modified by replacement of the β,γ-oxygen bridge by NH (**3.3**), CH_2 (**3.4**) or CF_2 (**3.5**) (Figure III.4). All these modifications resulted in a decrease in activity at $P2Y_2$ receptors (rank order of potency: O > NH > CF_2 > CH_2). Exchange of the β,γ-oxygen in ATP had similar effects.

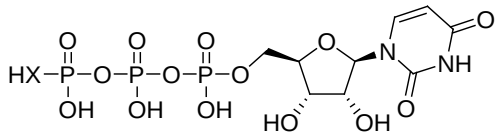

3.1: X = O
3.2: X = S

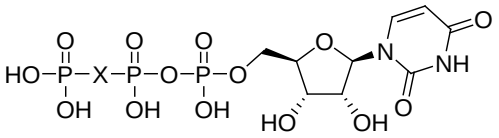

3.3: X = NH
3.4: X = CH_2
3.5: X = CF_2

Figure III.4

In order to obtain metabolic stable agonists, Cosyn *et al*.[150] decided to replace the α-phosphate group of UTP by an isosteric phosphonate group (**3.6**). Unfortunately **3.6** exhibited nearly quantitative hydrolysis to the corresponding 5'-phosphonate **3.7** during the receptor binding experiments (Figure III.5). Surprisingly, when tested in its pure form, **3.7** showed partial $P2Y_2$ agonist activity while being inactive at the $P2Y_4$ receptor.

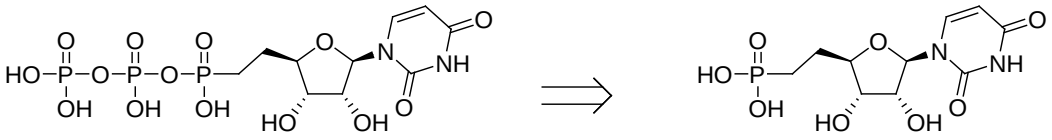

3.6 **3.7**

Figure III.5

1.3.1.2 Dinucleotides

Diadenosine polyphosphates are relatively potent agonists at $P2Y_2$ receptors but are physiologically unstable and are quickly degraded to ATP, ADP, AMP and mainly to adenosine.[151] The most potent dinucleotide, Ap_4A (**3.8**, Figure III.6), contains four phosphate groups which connect two adenosine residues. Ap_4A is only 3-fold less potent than ATP but also interacts with $P2Y_4$ and P2X receptor subtypes.

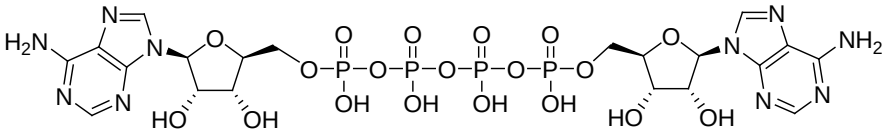

3.8

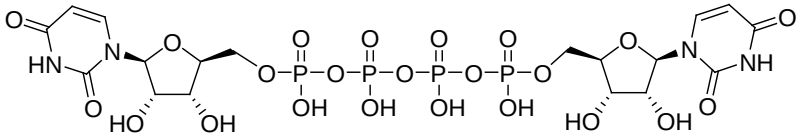

3.9

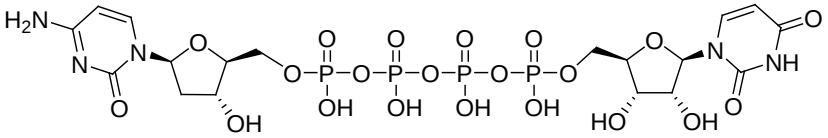

3.10

Figure III.6

Diuridine polyphosphates have the advantage of being more $P2Y_2$ selective than adenine dinucleotides since they do not or only weakly interact with other purine nucleotide sensitive P2 receptor subtypes. In addition, they are not degraded to adenosine, which may activate P1 purinergic receptors. Up_4U (diquafosol, INS-365, **3.9**, Figure III.6) is the most potent $P2Y_2$ agonist in this group, exhibiting similarly high activity as UTP.[152,153]

A synthetic mixed dinucleotide consisting of 2'-deoxycytidine and uridine connected via their 5'-positions by a tetraphosphate chain (denufosol, Up_4dC, INS-37217, **3.10**, Figure III.6), is a potent, selective, and highly stable $P2Y_2$ agonist that has been tested as an inhalable drug in a number of clinical trials for the treatment of cystic fibrosis.[154,155]

1.3.1.3 Uracil Modifications

From a series of UTP derivatives in which the oxygen in position 4 of the uracil moiety was replaced by various substituents the sulfur-containing 4-thioUTP (**3.11**) showed the most promising $P2Y_2$ activity, while all other variations (methoxy, hexyloxy, methylthio, amino, morpholino, hexylamino and cyclopentylamino) caused significant loss in $P2Y_2$ activity in comparison with UTP.[135] In addition, 2-thioUTP (**3.12**) behaved as a very potent $P2Y_2$ receptor agonist with increased selectivity versus $P2Y_4$ receptors (Figure III.7).

A bromine atom has been introduced in the 5-position (**3.13**, Figure III.7) of UTP. This modification led to a 15-fold decrease in activity. 5-Alkyl-substituted UTP derivatives were found to be full agonists at $P2Y_2$ receptors of NG108-15 cells, but less potent than UTP. The activity decreased with increasing size of the 5-substituent: H > methyl > ethyl > isopropyl > propyl > butyl.[156]

The N3-hydrogen does not appear to be essential since compound **3.14**, which is lacking the 3-NH, is still quite active. Replacement (**3.15**) or reorientation (**3.16**) of the uracil ring resulted in less potent analogues (Figure III.7).[157]

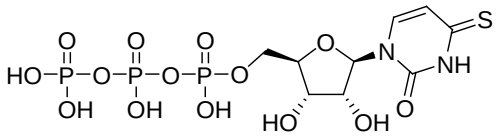

3.11

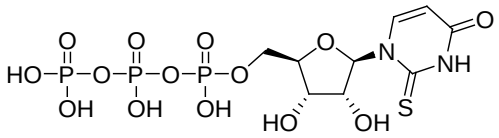

3.12

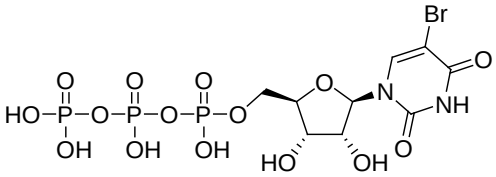

3.13

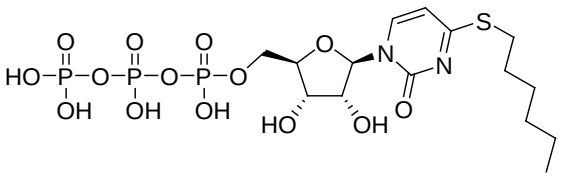

3.14

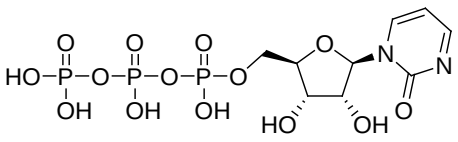

3.15

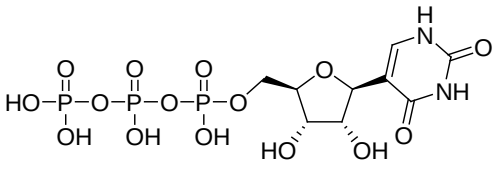

3.16

Figure III.7

1.3.1.4 Ribose Modifications

Removal of the 2'- or 3'-hydroxyl group of UTP caused a significant loss in $P2Y_2$ receptor activity. The 2',3'-dideoxy derivative of UTP was inactive. 2'-Amino-2'-deoxy UTP (**3.17**) and the *arabino* isomer of UTP (**3.18**) were equipotent to ATP at the $P2Y_2$ receptor and showed a moderate selectivity over the $P2Y_4$ receptor, while other 2'-modifications decreased the $P2Y_2$ receptor potency (Figure III.8).

Replacement of the sugar by a bicyclo[3.1.0]hexane system, which mimics a ribofuranose rigidified in the northern conformation, was well tolerated by the $P2Y_2$ receptor. (*N*)-methanocarba-UTP (**3.19**, Figure III.8) was almost equipotent to UTP.[158]

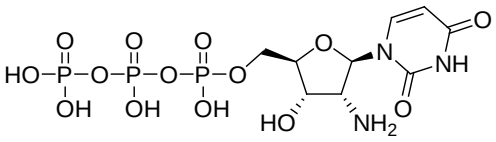

3.17

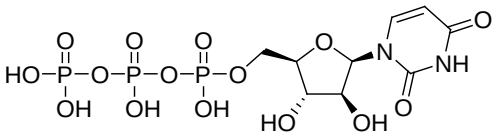

3.18

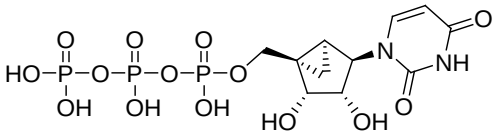

3.19

Figure III.8

1.3.1.5 Combined Modifications

Combination of a 2-thiouracil modification with a β-D-arabinofuranose (**3.20**) demonstrated moderately potent and highly selective agonist activity at the $P2Y_2$ receptor, while the 2'-amino-2'-deoxy ribose analogue (**3.21**) was 6 times more potent than the natural ligand UTP and 300-fold selective in activation of the $P2Y_2$ receptor in comparison with the $P2Y_4$ receptor. The potency of **3.21** is greatly reduced upon acetylation (**3.22**) and reduced to a lesser degree upon trifluoroacetylation (**3.23**) (Figure III.9).

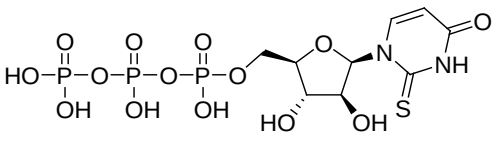

3.20

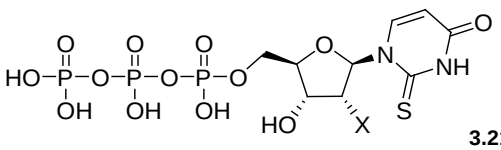

3.21: X = NH_2
3.22: X = $NHCOCH_3$
3.23: X = $NHCOCF_3$

Figure III.9

In vitro pharmacological data for the most potent $P2Y_2$ receptor agonists currently known are presented in Table III.1. EC_{50} values represent the half maximal effective concentration in an assay of $P2Y_2$ and $P2Y_4$ receptor-stimulated phospholipase C activity. The structure-activity relationship of the different phosphate chain, uracil and ribose UTP modifications is summarized in Figure III.10.

Table III.1. *In vitro* pharmacological data for the most potent $P2Y_2$ receptor agonists currently known.

Compound	Name	EC_{50} ($P2Y_2$) nM	EC_{50} ($P2Y_4$) nM
1.4	ATP	85	Antagonist
3.1	UTP	49	73
3.2	UTPγS	240	1600
3.8	Ap_4A	180	Inactive
3.9	Up_4U (diquafosol)	60	200
3.10	Up_4dC (denufosol)	220	800
3.11	4-thioUTP	26	23
3.12	2-thioUTP	35	350
3.17	2'-amino-2'-deoxyUTP	62	1200
3.18	*arabino*-UTP	87	710
3.19	(*N*)-methanocarba-UTP	85	91
3.21	2'-amino-2'-deoxy-2-thioUTP	8	2400

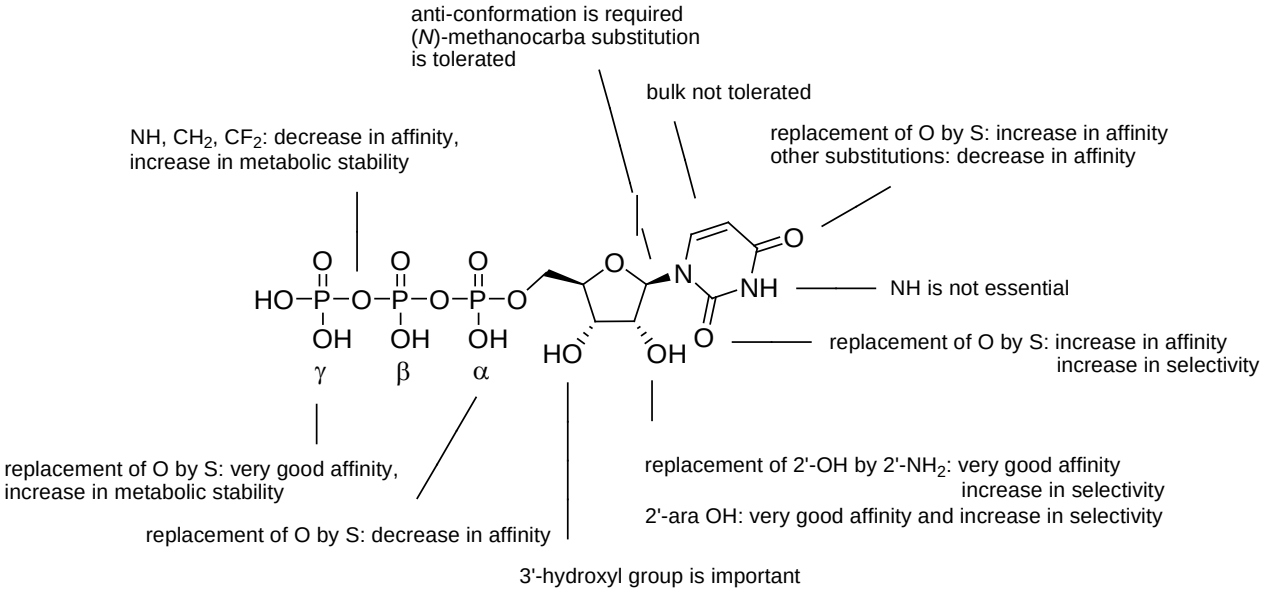

Figure III.10. Structure-activity relationship of UTP derivatives as $P2Y_2$ agonists.

1.3.2 Therapeutic Potential of $P2Y_2$ Receptor Agonists

1.3.2.1 Cystic Fibrosis

Cystic fibrosis (CF) is a recessive genetic disease caused by mutations in the cystic fibrosis transmembrane regulator gene (CFTR). A deletion of phenylalanine at position 508 (ΔF508) accounts for more than 70% of all cases of CF. The disease generally has multiple manifestations like pancreatic dysfunction, diabetes mellitus, ileus and male infertility. Depending on the mutation there are more or less severe symptoms. The most prominent manifestation accounting for 90% of mortality is pulmonary disease, characterized by desiccated mucus, impaired mucociliary clearance and secondary bacterial infections. Mutated CFTR in lung epithelium causes decreased chloride secretion and excessive sodium absorption, leading to a reduction in airway surface liquid (ASL). Depletion of a specific part of the ASL, the periciliary liquid, leads to defective ciliary function and cough clearance. Subsequently, thickened mucus plaques adhere to the airway surface, generating hypoxic regions and promoting bacterial infections. CF has affected approximately 80 000 individuals worldwide and their main life expectancy is currently about 37 years.[159]

In healthy people, airway hydration is regulated by CFTR proteins, the so called cystic fibrosis transmembrane conductance regulator Cl^- channels (Figure III.11). Activation of these Cl^- channels, via $P2Y_2$ or A_{2B}, results in an increased Cl^- secretion and a decreased Na^+ absorption due to the downregulation of the epithelial Na^+ channels (ENaC). However, in cystic fibrosis, mutations in de CFTR gene result in a decreased function or expression of the CFTR proteins. Consequently, the ENaC activity is up-regulated (Na^+ influx ↑) and the cell depends only on the Ca^{2+} activated Cl^- channels (CaCC) for Cl^- secretion. As a result, Cl^- secretion is limited and airway epithelia will be dehydrated with reduced mucociliary clearance and a propensity for chronic infection of the respiratory tract with resulting inflammation, progressive airway damage and bronchiectasis.[160,161]

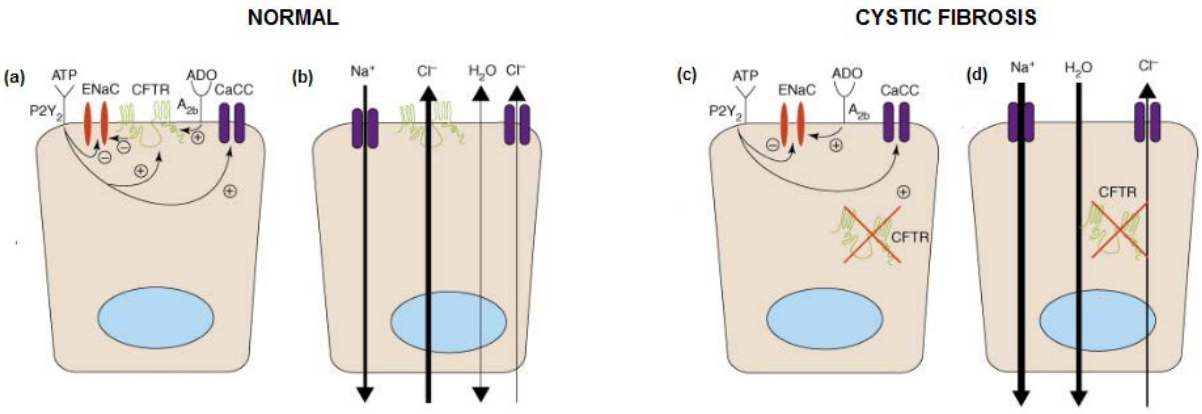

Figure III.11. Regulation of the ASL volume homeostasis by ATP release. (a) Normal airway epithelia exhibit ATP-mediated $P2Y_2$ receptor regulation and ADO-mediated A_{2B} receptor regulation of CFTR; (b) Normal airway epithelia balance: Na^+ absorption against Cl^- secretion to maintain ASL homeostasis; (c) CF airway epithelia do not (or less) express functional CFTR proteins resulting in an A_{2B} mediated activation of ENaC; (d) CF airway epithelia balance: increased salt and water absorption leading to a reduction in ASL.[162]

Studies using *in vitro* models of airway epithelia have shown the important role of the $P2Y_2$ receptor in regulating ion transport in epithelial cells. Activation of ion transport by $P2Y_2$ receptors in both normal and CF airway epithelia leads to liquid secretion (Figure III.11).[163] Taken this into account, the impaired ion transport in the bronchi of CF patients can be bypassed by stimulation of $P2Y_2$ receptors. Subsequently, it was found that UTP stimulated mucin secretion from goblet cells[164] and increased the beat frequency of cilia in isolated normal and CF epithelial cells.[165] A knockout study confirmed previous pharmacological data and identified $P2Y_2$ receptors as the crucial luminal P2 receptor in respiratory epithelium.[166]

The natural ligand UTP, has high potency, but limited metabolic stability and thus has a relatively short duration of action when administered via inhalation. Therefore, Inspire Pharmaceuticals, Inc. has developed a series of new, highly selective and potent $P2Y_2$ receptor agonists with enhanced metabolic stability. Some of the most promising compounds were used in clinical studies evaluating the effects of inhaled $P2Y_2$ agonists on sputum expectoration and mucociliary clearance in smokers and patients with a variety of airway disorders, including CF.[163] Denufosol (**3.10**, Up_4dC, INS37217) received fast-track and orphan drug status in US and orphan drug status in Europe as a treatment for CF. A first phase III trial of denufosol in CF (TIGER-I) demonstrated an improved lung function versus placebo in patient having minimally impaired to normal baseline lung function characteristic of early CF lung disease. However, results from a second phase III trial (TIGER-II) were disappointing and did not confirm the promising result from TIGER-I.[167]

1.3.2.2 Dry Eye Syndrome

$P2Y_2$ receptors can be found on the ocular surface (e.g., cornea, conjunctiva, …) where they play an important role in the regulation of conjunctival mucin and Cl^- secretion. Activation of the $P2Y_2$ receptor stimulates chlorine and water secretion from conjunctival epithelial cells, leading to a better lubrification of the ocular surface.[168,169] In 1999, Inspire Pharmaceuticals, Inc. started to test diquafosol (**3.9**, Up_4U) for the treatment of dry eye syndrome. Unfortunately, diquafosol failed in late phase III trial.

1.3.2.3 Cancer

$P2Y_1$ and $P2Y_2$ receptors are, perhaps, the most widely studied purinoceptor subtypes in cancer.[170] Whereas the role of $P2Y_1$ receptors in cancer is to decrease cellular proliferation, the $P2Y_2$ receptor usually increases cell numbers. Indeed, in most physiological conditions, activation of human $P2Y_2$ receptors causes an increase in cell proliferation. This is reflected in some cancer types such as melanoma and lung cancer.[171,172] However, in other cancer types such as esophageal cancer and some colorectal cancers, activation of $P2Y_2$ receptors causes a decrease in cellular proliferation. For these types of cancer, $P2Y_2$ receptor agonists have been suggested as novel therapeutics.[173,174]

1.3.2.4 Antihypertensiva

Studies performed in various species have showed that systemic activation of $P2Y_2$ receptors lowers blood pressure and inhibits renal Na^+ reabsorption. Based on these effects, it is suggested that $P2Y_2$ receptor agonists may have potential in the treatment of hypertension.[175]

1.3.2.5 Vaginal Humidifier

Due to the fact that $P2Y_2$ receptors are expressed in cervical and vaginal tissues, it is thought that $P2Y_2$ receptor agonists may be an alternative and effective therapy to alleviate postmenopausal symptoms of vaginal dryness by increasing mucin production as well as by enhancing pelvic blood flow.[176]

1.3.3 $P2Y_2$ Receptor Antagonists

Studies with antagonists are important to elucidate the physiological roles of receptors. Unfortunately, subtype-selective P2-receptor antagonists are not available. All known P2-receptor antagonists block several subtypes of P2-receptors. Nevertheless, the combined use of subtype preferential agonists and antagonists may allow the pharmacological characterization of different P2Y-subtypes.[134]

1.3.3.1 Standard P2 Antagonists

The standard P2 receptor antagonists Reactive Blue 2 (RB-2, **3.24**) and suramin (**3.25**) block the human $P2Y_2$ receptor with moderate potency (Figure III.12). Both appear to be competitive antagonists. RB-2 is one of the most potent $P2Y_2$ receptor antagonists known to date (IC_{50} ~ 1 µM). It is an anthraquinone derivative that bears three negatively charged sulfonate groups and may be *meta*- or *para*-sulfonated or a mixture of both isomer.[130] Suramin, a polysulfonated naphthalene derivative of relatively high molecular weight, exhibits an IC_{50} value of ca. 50 µM. When given at high micromolar concentrations, suramin affects all nucleotide-sensitive P2Y receptors with the exception of the $P2Y_4$ receptor.

In addition to $P2Y_2$-antagonistic activity, RB-2 and suramin interact with a number of other receptors and proteins, including other P2Y receptor subtypes, P2X receptors,[177] ectonucleotidases,[178] kinases (RB-2),[179] and G proteins (suramin).[180] The promiscuity of these molecules limits their usefulness as pharmacological tools.

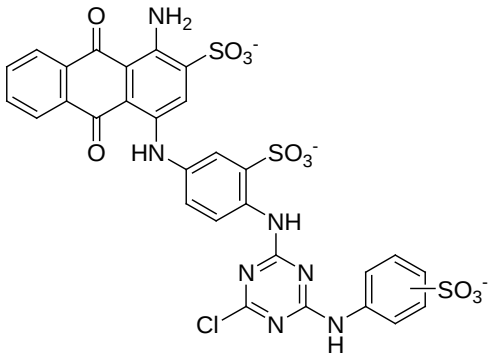

3.24

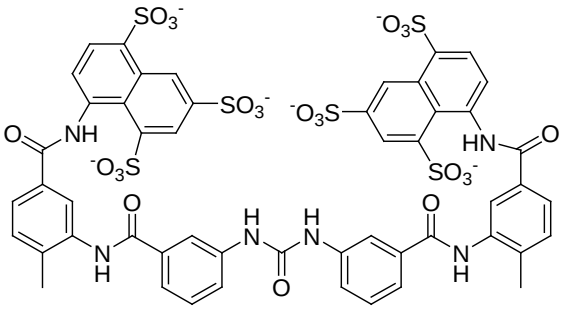

3.25

Figure III.12

1.3.3.2 Anthraquinones

In 2007, Müller and coworkers synthesized a series of simplified RB-2 analogues. Compound **3.26** (PSB-716, Figure III.13) appeared to be a relatively potent $P2Y_2$ antagonist with an IC_{50} value of 9 µM. In contrast to RB-2, **3.26** seems to be selective versus other P2Y subtypes as well as nucleotide-metabolizing enzymes.[181]

1.3.3.3 Thiouracil Derivative AR-C118925

The natural ligand UTP served as a lead compound for the development of new $P2Y_2$ receptor antagonists. Structural modifications to eliminate efficacy and to improve the pharmacokinetic properties led to the development of thiouracil derivative AR-C118925 (**3.27**, Figure III.13). This analogue contains a heterocyclic substituent in the 5 position and a substituent at N-1 that mimics the ribose triphosphate group. AR-C118925 appears to be a selective and competitive $P2Y_2$ receptor antagonist and showed an IC_{50} value of ca. 1 µM.[130]

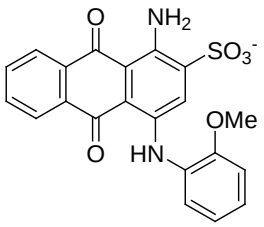

3.26

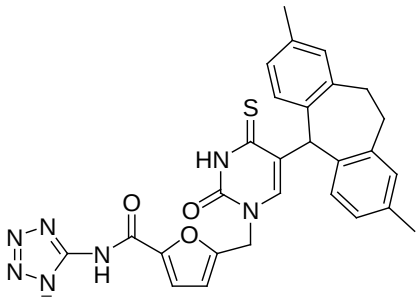

3.27

Figure III.13

1.3.3.4 Flavonoids

Flavonoids are secondary plant metabolites found in fruits, vegetables, bark and flowers of many higher plants. A series of 40 flavonoids was investigated at $P2Y_2$ receptors and several flavones were found to block $P2Y_2$ receptors in the low micromolar range. The post potent compounds were kaempferol (**3.28**), tangeretin (**3.29**) and heptamethoxyflavone (**3.30**) (Figure III.14).[182]

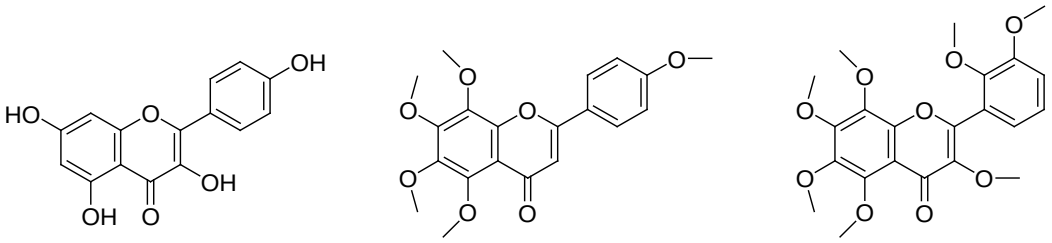

3.28 **3.29** **3.30**

Figure III.14

1.3.4 Therapeutic Potential of $P2Y_2$ Receptor Antagonists

1.3.4.1 Inflammation

$P2Y_2$ receptors are expressed by endothelial cells and cells of the immune system (e.g., T-cells, neutrophils, eosinophils and macrophages), and thus appear to play a role in defense mechanisms and inflammatory processes. Antagonists are considered to have potential anti-inflammatory properties.[147]

1.3.4.2 Coronary Vasospastic Disorders

$P2Y_2$ receptor antagonists are though as potential therapeutics of coronary vasospastic disorders since stimulation of $P2Y_2$, besides P2X receptors, mediates contraction of human coronary arteries.[183]

1.3.4.3 Neuroprotective Agents

P2 receptor antagonists, including RB-2, have been reported to exhibit neuroprotective properties. They may be useful for the treatment of epileptic seizures, strokes and neurodegenerative diseases, such as Alzheimer's and Parkinson's disease.[147]

1.3.5 Molecular Modeling of the $P2Y_2$ Receptor

The first site-directed mutagenesis and molecular modeling of transmembrane helical domains 6 and 7 (TMs 6 and 7) of the $P2Y_2$ receptor were reported by Erb *et al*.[184] In 2006, a molecular model was provided by a molecular dynamics simulation in a phospholipidic and aqueous environment. In contrast with the earlier one, this model contained not only seven TMs but also all extracellular and intracellular hydrophilic loops.[185] Recently, Hillman *et al*. published a more detailed and refined model generated in homology to the crystal structure of bovine rhodopsin.[186]

A binding pocket could be determined in the upper third part of the receptor molecule (Figure III.15). So far, the structure of this pocket is rather unclear but amino acids from the sixth (TM6) and seventh transmembrane (TM7) helices and from the second extracellular loop (EL2) have shown to be involved. An entry channel between TM5 and TM6 was found to lead to this binding site. In addition, this channel provides a binding pocket for larger ligands like dinucleotides.

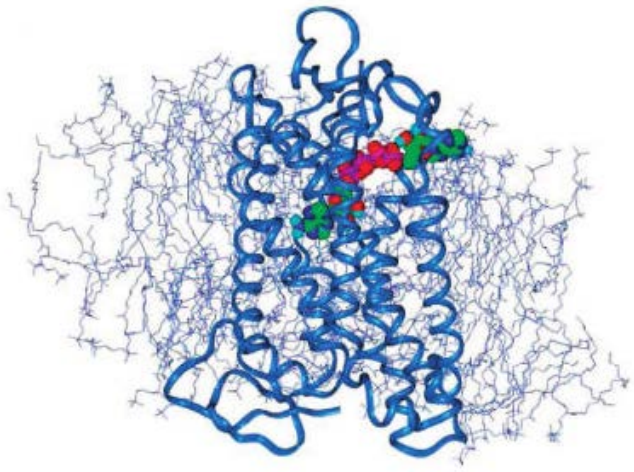

Figure III.15. Computer generated model of the $P2Y_2$ receptors embedded in a lipid bilayer with Ap_4A into the binding site.[186]

Binding of ATP and UTP led to an induced fit of the receptor protein. UTP induced a larger protein rearrangement than ATP because the protein has to adapt itself more strongly to the smaller UTP molecule, resulting in the formation of more stable hydrogen bonds in the UTP-$P2Y_2$ complex compared to that of the ATP-$P2Y_2$ complex. As a consequence, UTP is a slightly more potent and efficacious agonist than ATP.

On the other hand, for the large dinucleotide Ap_4A (**3.8**), a lower degree of induced fit by the protein is observed, and the ligand has to adapt its conformation in order to fit into the binding site. Although the dinucleotides (being large molecules) can have more interactions with the receptor protein than the mononucleotides, their potency is lower. This may be explained by their suboptimal fit into the receptor binding site. As seen in Figure III.15, part of the dinucleotide Ap_4A sticks out of the receptor protein.

Dinucleotide binding would result in reduced flexibility of the receptor protein, including EL2, which is part of the binding pocket for mononucleotides.[186]

The homology model of the $P2Y_2$ receptor has allowed to identify the amino acid residues with important roles as gate keepers in ligand binding and in activating and stabilizing the receptor. Since our work does not rely on the available structural information of the $P2Y_2$ receptor, we prefer not go in too much detail about available models and refer the interested reader to the original papers.[184,185,186]

2 URIDINE 5'-PHOSPHONATE ANALOGUES

2.1 OBJECTIVES

The major limitations associated with known agonists for the $P2Y_2$ receptor are (i) the lack of selectivity vs. closely related P2Y receptor subtypes and (ii) their fast degradation by nucleotide-hydrolyzing ecto-enzymes, which results in a relative short duration of action.[130] In that context, it was recently explored to what extent replacement of the α-phosphate group of UTP (**3.1**) by an isosteric phosphonate affected $P2Y_2$ receptor activity.[150] Since the carbon-phosphorus bond cannot be hydrolyzed, this analogue was expected to exhibit prolonged metabolic stability. While Cosyn *et al*. initially focused on a diphosphophosphonate mimic of UTP (**3.6**), it was fortuitously discovered that its synthetic precursor **3.7** was also capable of activating the $P2Y_2$ receptor, while being inactive at the $P2Y_4$ receptor (Figure III.16).[150]

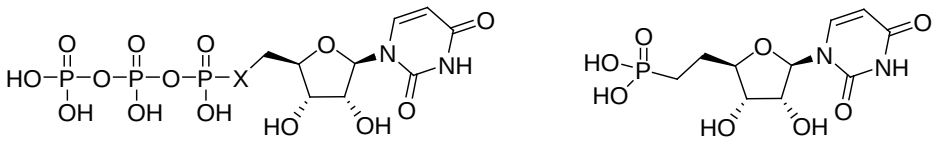

3.1: X = O
3.6: X = CH_2

3.7

Figure III.16.

In this chapter, we explore the influence of further modifications of the 5'-methylene phosphonate **3.7** on activity at the $P2Y_2$ receptor. A preliminary report from Astra-Zeneca indicated that incorporation of large semiplanar, hydrophobic aromatic rings at position 5 of thiouridine triphosphate may be accommodated by the $P2Y_2$ receptor but tend to preclude the conformational change required for receptor activation.[187] Therefore, we introduced several (hetero)aromatic substituents at the 5-position of the 5'-methylene phosphonate analogue **3.7**. In addition, we also envisaged replacement of the 2'-OH group of **3.7** with a 2'-chloro and a 2'-amino group. In the case of UTP, the latter modification was associated with increased $P2Y_2$ selectivity while maintaining excellent potency.

Finally, another phosphonate bio-isostere of uridine 5'-monophosphate (UMP), obtained by the inversion of the 4'-CH_2-O group of UMP, was also explored.

2.2 CHEMISTRY

2.2.1 Synthesis of 5-Modified 5'-Methylene Phosphonate Uridine Analogues

Different methods for the preparation of isosteric phosphonate analogues of nucleoside phosphates have been reported. Most often these involve a Wittig-type[188] or an Arbuzov[189] reaction. In addition, Barton *et al*.[190] published a radical approach for the introduction of the carbon-phosphorous bond. We decided to follow the method described by Xu *et al*.[191] in which the isosteric analogue was prepared by treatment of a suitable protected uridine 5'-aldehyde with a stabilized [Ph_3P=CHPO$(OEt)_2$] ylide (Scheme III.1). Starting from uridine (**3.31**), 5',6'-vinyl phosphonate **3.33** was synthesized by oxidation of 2',3'-*O*-isopropylidene-uridine **3.32** to an 5'-aldehyde intermediate, which was immediately reacted with freshly prepared [(diethoxyphosphinyl)methylidene] triphenylphosphorane **3.72**.[191] Catalytic hydrogenation of the obtained olefin in the presence of palladium on carbon gave access to the corresponding saturated phosphonate ester **3.34**.

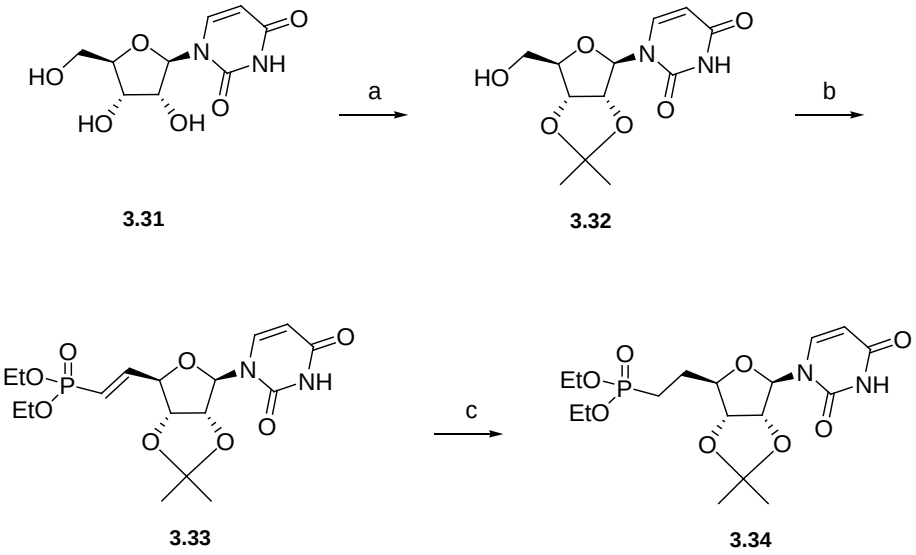

Scheme III.1. Reagents and conditions. (a) 2,2-dimethoxypropane, *p*-toluenesulfonic acid, acetone, 5 h, 80%; (b) (i) IBX, CH_3CN, 80 °C, 6 h; (ii) [(Diethoxyphosphinyl)methylidene] triphenylphosphorane (**3.72**), DMSO, rt, overnight, 59% over 2 steps; (c) H_2, Pd/C, MeOH, rt, overnight, 76%.

C-5 selective NBS-mediated bromination[116] of phosphonate **3.34** followed by a Suzuki-Miyaura coupling with a number of commercial aryl and heteroaryl boronic acids gave access to a series of C-5 substituted analogues. The latter transformation took place in a DMF-H_2O solution and was catalyzed by Pd$(PPh_3)_4$. Sodium carbonate was used for the activation of the boronic acids.[192] One-pot deprotection of the phosphonate diester and the 2',3'-*O*-isopropylidene group by consecutive treatment with TMSBr and TFA afforded the desired phosphonates **3.44-3.51** in variable yields (Scheme III.2).[193]

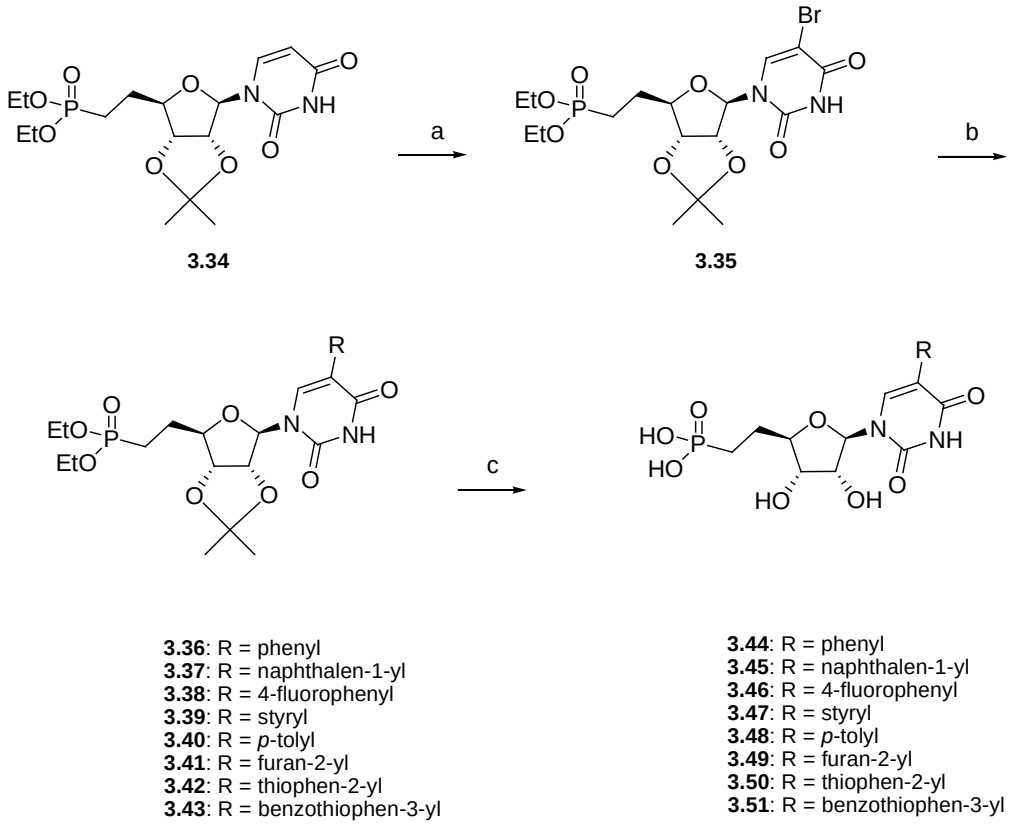

3.34 **3.35**

3.36: R = phenyl
3.37: R = naphthalen-1-yl
3.38: R = 4-fluorophenyl
3.39: R = styryl
3.40: R = *p*-tolyl
3.41: R = furan-2-yl
3.42: R = thiophen-2-yl
3.43: R = benzothiophen-3-yl

3.44: R = phenyl
3.45: R = naphthalen-1-yl
3.46: R = 4-fluorophenyl
3.47: R = styryl
3.48: R = *p*-tolyl
3.49: R = furan-2-yl
3.50: R = thiophen-2-yl
3.51: R = benzothiophen-3-yl

Scheme III.2. Reagents and conditions. (a) NBS, DMF, rt, overnight, 79%; (b) R-B(OH)$_2$, Na_2CO_3, $Pd(PPh_3)_4$, DMF, H_2O, reflux, 4 h, 39-76%; (c) (i) TMSBr, CH_2Cl_2, rt, overnight; (ii) 50% aq. TFA, H_2O, rt, 4 h, 11-78%.

2.2.2 Synthesis of 2'-Amino and 2'-Chloro 5'-Methylene Phosphonate Uridine Analogues

The synthesis of 2'-amino 5'-methylene phosphonate **3.56** started from intermediate **3.34** and is depicted in Scheme III.3. After deprotection of the 2' and 3' hydroxyl groups of **3.34**, 2',2-*O*-anhydro analogue **3.53** was formed using diphenyl carbonate, $NaHCO_3$ in DMF or thionyl chloride in CH_3CN followed by the addition of NaOAc.[194] Introduction of the azide group at the 2' position was accomplished via opening of **3.53** with NaN_3 in DMF.[195] Interestingly, these conditions caused concomitant incomplete hydrolysis of the phosphonate ester to afford **3.54**. Azide-mediated conversion of a phosphonate diester to its mono-ester was previously reported by Holy.[196] Staudinger reduction[197] of the azide followed by deprotection of mono ethylphosphonate **3.55** resulted in the desired 2'-amino uridine 5'-phosphonate analogue **3.56**.[198]

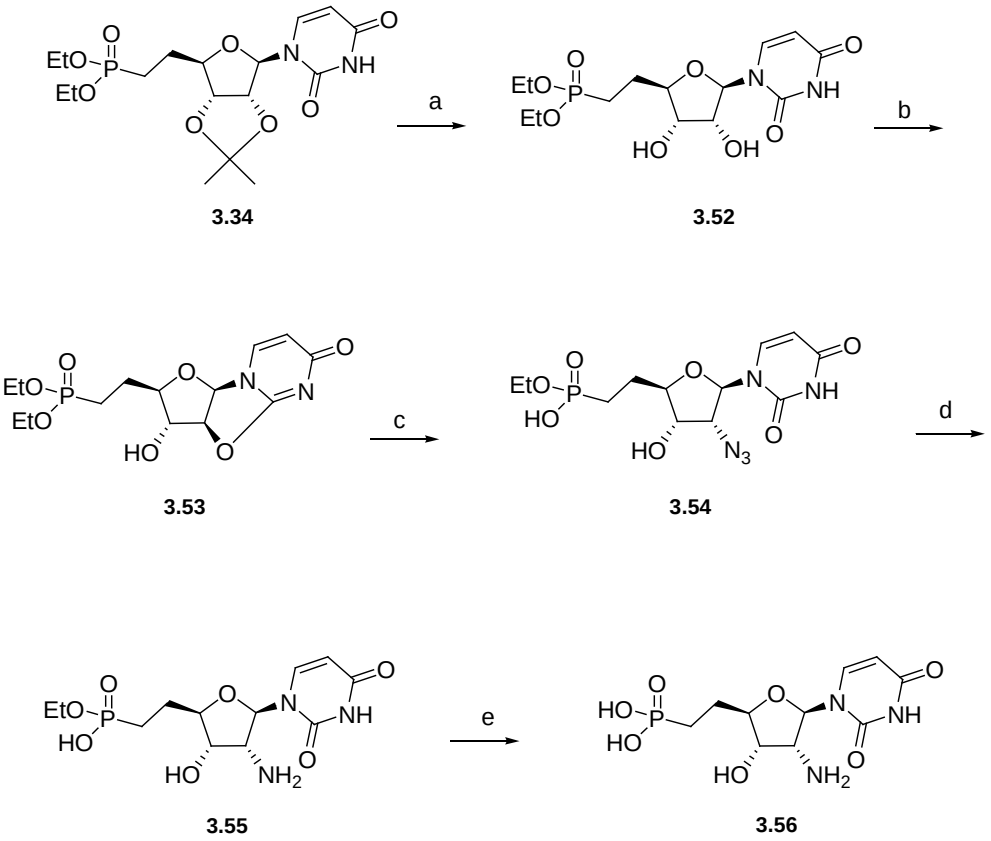

Scheme III.3. Reagents and conditions. (a) 50% aq. HCOOH, rt, 4.5 h, 57% or 50% aq. TFA, 0 °C → rt, 2 h, 64%; (b) (i) $SOCl_2$, CH_3CN, rt, 2 h; (ii) NaOAc, DMF, 85 °C, 3 h, 92% over 2 steps or $(PhO)_2CO$, $NaHCO_3$, DMF, reflux, 1.5 h, 65 %; (c) NaN_3, DMF, 130 °C, overnight, quant. yield; (d) PPh_3, THF, H_2O, rt, overnight, quant. yield; (e) TMSBr, CH_2Cl_2, rt, overnight, 78%.

Similarly, treatment of **3.53** with a 2N HCl in diethylether solution followed by the hydrolysis of the phosphonate diester resulted in the 2'-chloro analogue **3.58** (Scheme III.4).[113]

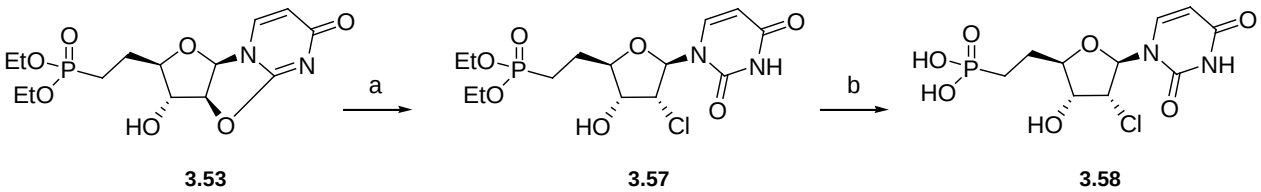

Scheme III.4. Reagents and conditions. (a) 2N HCl in Et_2O, dioxane, rt, overnight, 54%; (b) TMSBr, CH_2Cl_2, rt, overnight, 58%.

2.2.3 Synthesis of 4'-O-CH_2 Phosphonate Analogue **3.68**

The formation of 4'-O-CH_2 phosphonate **3.68** started with the synthesis of glycal **3.64** (Scheme III.5). Since the direct oxidation of 2'-deoxyuridine into 2'-deoxyuridine-5'-carboxylic acid using TEMPO/BAIB[199] and PDC failed, 2'-deoxyuridine was first tritylated followed by the silyl protection of 3'-OH. After removal of the trityl group, the 5'-OH group was oxidized with TEMPO/BAIB to furnish carboxylic acid **3.62**. Treatment of compound **3.62** with NH_4F in MeOH[200] followed by a decarboxylative elimination[201] afforded glycal **3.64** in moderate yield.

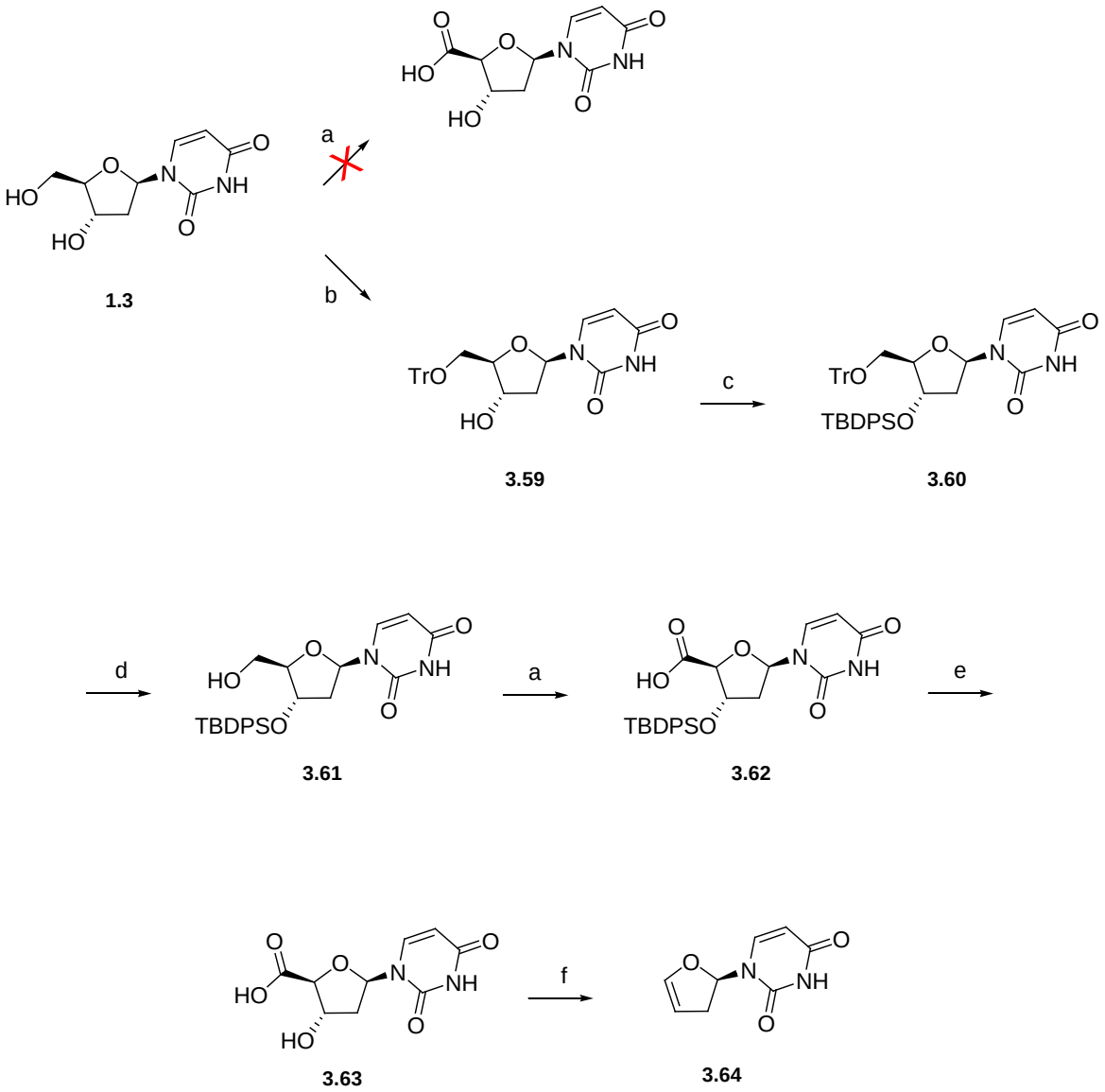

1.3 **3.59** **3.60** **3.61** **3.62** **3.63** **3.64**

Scheme III.5. Reagents and conditions. (a) TEMPO, BAIB, CH_3CN, H_2O, rt, 16 h, 78% for **3.61** → **3.62**; (b) trityl chloride, pyridine, 65 °C, overnight, 61%; (c) TBDPSCl, imidazole, DMF, rt, overnight, 100%; (d) $ZnBr_2$, CH_2Cl_2/*i*PrOH (85:15), rt, overnight, 60%; (e) NH_4F, MeOH, rt, overnight, 100%; (f) dimethylformamide dineopentyl acetal, DMF, 130 °C, 20 min, 46%.

Treatment of glycal **3.64** with phenylselenyl chloride at -70 °C followed by the addition of silver perchlorate in the presence of diethyl(hydroxymethyl)phosphonate afforded phosphonate **3.65** in 35% overall yield.[202] Compound **3.65** was further transformed into olefin **3.66** via sodium periodate oxidation of selenium and subsequent elimination.[202] OsO_4-promoted dihydroxylation in the presence of *N*-methylmorpholine-*N*-oxide[203] followed by TMSBr hydrolysis of the phosphonate ester groups provided compound **3.68** in moderate yield. A positive NOE was observed between the H-1' and H-4' of compound **3.66**, confirming the *cis* stereo-arrangement of the uracil base and the phosphonomethoxy side chain (Scheme III.6).

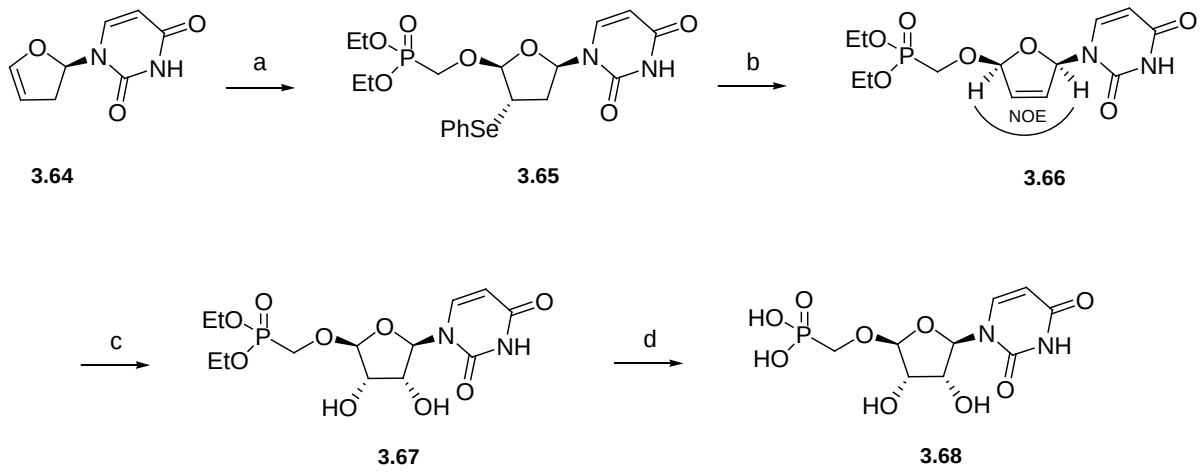

3.64 **3.65** **3.66**

3.67 **3.68**

Scheme III.6. Reagents and conditions. (a) (i) PhSeCl, CH_2Cl_2, -70 °C, 1 h; (ii) $HOCH_2PO(OEt)_2$, $AgClO_4$, CH_2Cl_2, CH_3CN, -70 °C → 0 °C, 15 min, 35% over 2 steps; (b) $NaIO_4$, $NaHCO_3$, MeOH, rt , 1 h then 80 °C, 75 min, 68%; (c) OsO_4, NMO, acetone-water (5:1), rt, 48 h, 60%; (d) TMSBr, 2,6-lutidine, DMF, 0 °C → rt, overnight, 50%.

Assignment of the stereochemical arrangement in **3.65** was based on mechanistic considerations as depicted in Figure III.17.[202] The sterically favored α side approach of the electrophile generated the energetically more stable selenium and/or oxonium transition intermediate **I** in preference to the less favorable **II**.

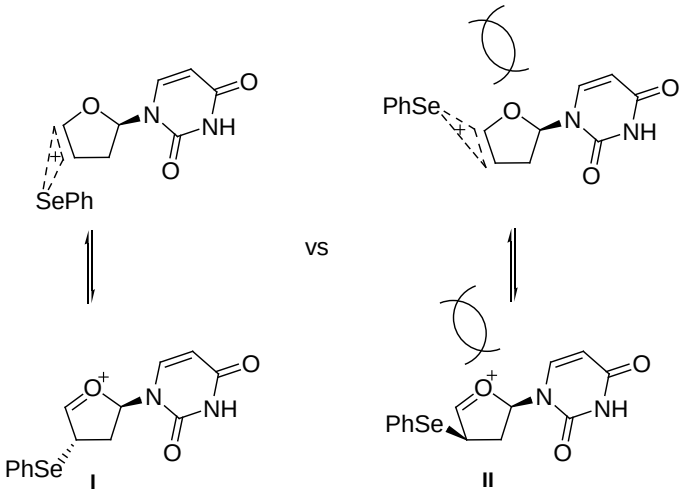

Figure III.17

2.3 PHARMACOLOGICAL EVALUATION

Activities of analogues at the $P2Y_2$ receptor were determined measuring PLC-dependent phosphoinositide hydrolysis in 1321N1 human astrocytoma cells stably expressing the human $P2Y_2$ receptor (performed under the guidance of Prof. Dr. Kendall Harden at the Department of Pharmacology, University of North Carolina School of Medicine, Chapel Hill, NC 27599, USA).[204,205] Neither UTP nor any of the phosphonate analogues promoted inositol phosphate accumulation in wild-type 1321N1 cells (Fig. III.18A). In contrast, quantification of inositol phosphate accumulation in $P2Y_2$ receptor-expressing 1321N1 cells revealed that the newly synthesized 5'-methylene-phosphonate analogues are P2Y2 receptor agonists (Fig III.18B).

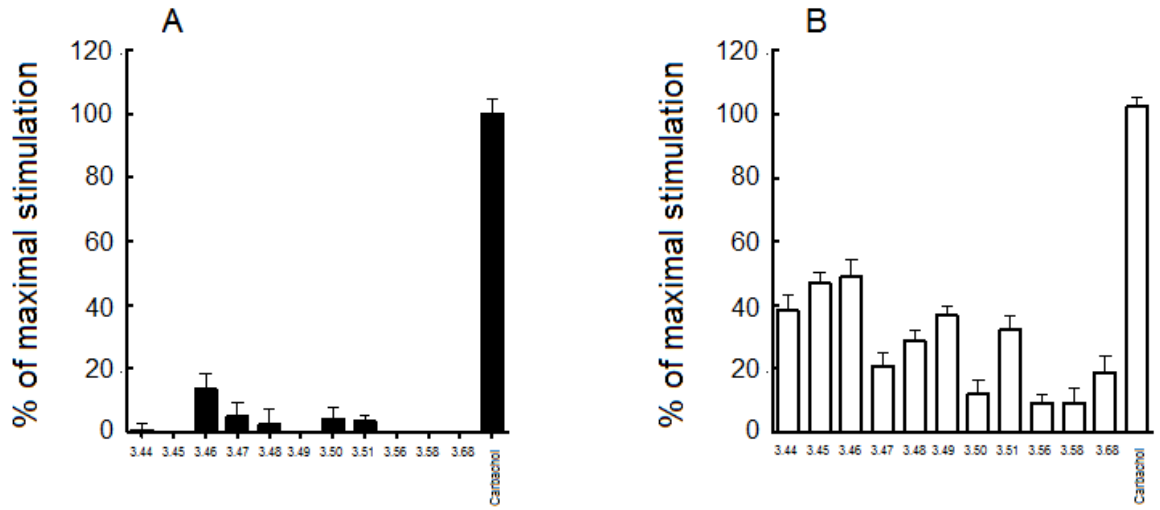

Figure III.18. Inositol phosphate production in (A) wild type 1321N1 human astrocytoma cells and (B) 1321N1 cells stably expressing the human $P2Y_2$ receptor.

None of the analogues produced maximal effects as great as UTP when tested at 100 μM concentration. Therefore, full concentration effect curves were carried out with each of the analogues to more clearly assess their maximal effects relative to UTP and to establish their relative potencies as $P2Y_2$ receptor agonists. To enhance clarity of comparison of the relative activities of these analogues, the data are arbitrarily presented in four separate panels (Fig. III.19).

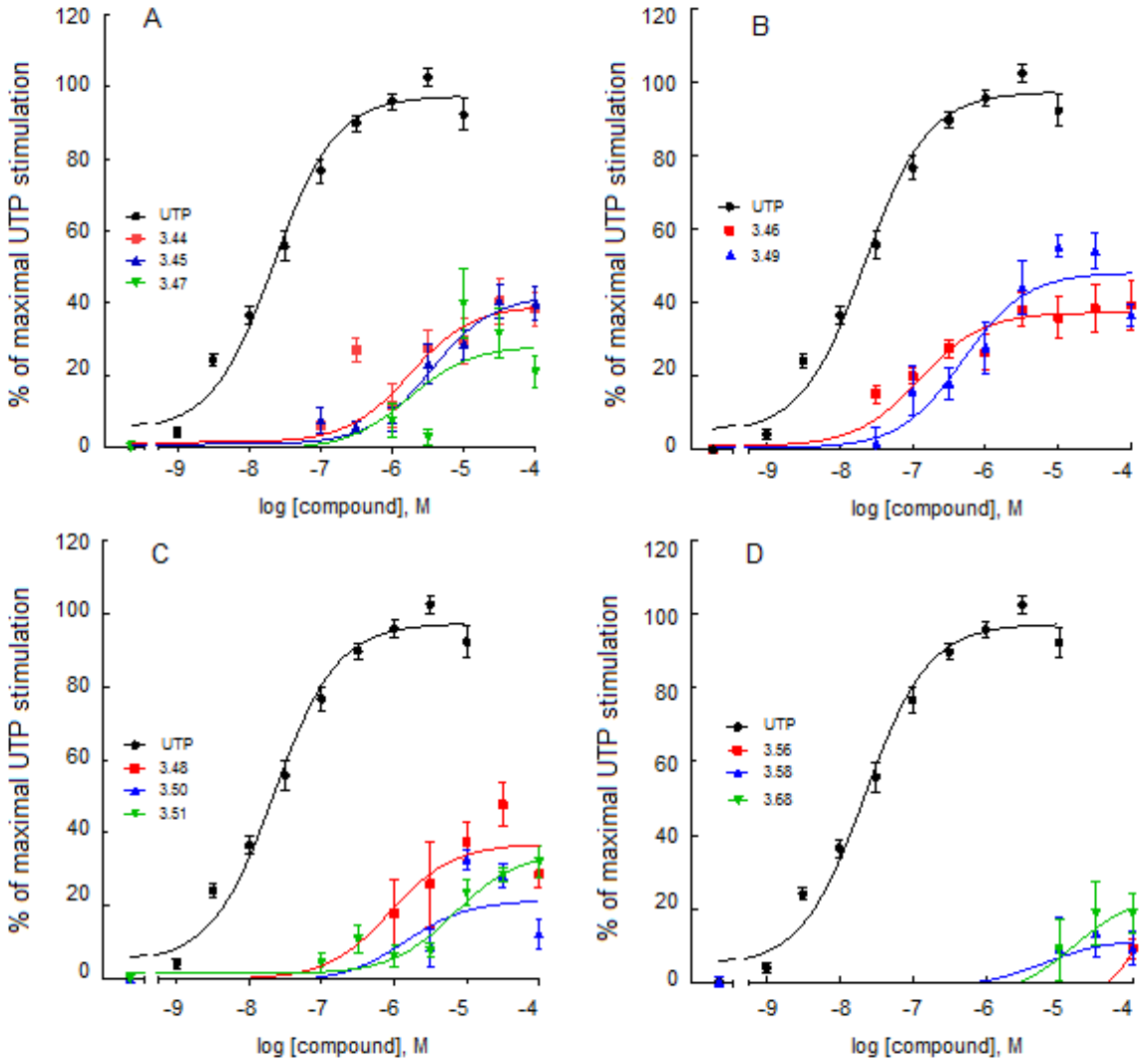

Figure III.19. Concentration dependent activation of the $P2Y_2$ receptor by phosphonate nucleotide derivatives.

The 5-modified uridine 5'-phosphonate analogues activated the $P2Y_2$ receptor with a range of apparent potencies, and the maximal effect observed with each of these molecules was only 30-40% of that observed with UTP. Preferred modifications at position 5 of the uracil moiety of compound **3.7** included phenyl (**3.44**), 1-naphthyl (**3.45**), 4-fluorophenyl (**3.46**), 2-furanyl (**3.49**) and *p*-tolyl (**3.48**) (Fig. III.19). The most potent agonist was the 5-(4-fluorophenyl) analogue (**3.46**), which activated the receptor with a slightly higher potency (EC_{50} = 170 ± 100 nM) than analogue **3.49** (EC_{50} = 560 ± 240 nM).

Both 2'-modified analogues (**3.56** and **3.58**) were essentially inactive at the $P2Y_2$ receptor. The negative impact of the replacement of a 2'-OH by a 2'-NH_2 group, may indicate that these phosphonates have a different mode of binding to the $P2Y_2$ receptor, since a similar modification on UTP was well tolerated.

Compound **3.68** was significantly less potent than the lead phosphonate indicating that replacement of the 5'-CH_2 group by an oxygen tends to reduce agonist activity.

The activities of the two most potent new compounds **3.46** and **3.49** were directly compared to the 5-unsubstituted parent compound **3.7** (Fig. III.20). Both analogues produced maximal effects at the $P2Y_2$ receptor that were similar to that of **3.7**, but were approximately 10-fold more potent than **3.7**.

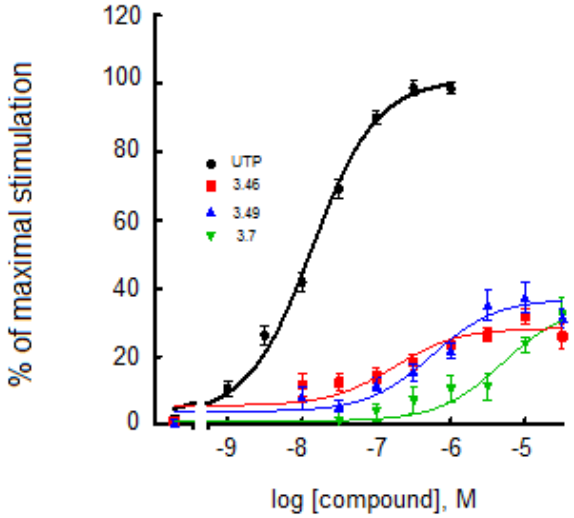

Figure III.20. Comparison of the concentration dependence of the most potent phosphonates for activation of the $P2Y_2$ receptor.

The idea that these modified uridine 5'-phosphonate analogues are orthosteric ligands that exhibit less intrinsic efficacy than UTP was examined by assessing their capacity at high concentrations to inhibit the effect of a near-maximal concentration of UTP (Fig. III.21A). No inhibitory effect on the action of UTP was observed with any of these phosphonate analogues. Concentration effect curves for UTP also were carried out in the absence and presence of a high (100 µM) concentration of **3.46** or **3.49** to determine whether the activity of these molecules was consistent with that of agonists acting at the orthosteric or an allosteric site of the $P2Y_2$ receptor. The data presented in Figure III.21 are consistent with the idea that these uridine 5'-phosphonate analogues act at an allosteric site rather than the orthosteric binding pocket to produce their effect on $P2Y_2$ receptor activity.

A possible binding site for the agonists might be a site that is close to the terminal end of the dinucleotides, i.e. the far site U of Up_4U (**3.8**). If this should be true then the behavior in combination with UTP should be very different from the combination with Up_4U. To test this hypothesis, an experiment in which the capacity of different C-5 modified uridine 5'-phosphonates to lower the IP_3 concentration produced by Up_4U stimulation will be done in the near future.

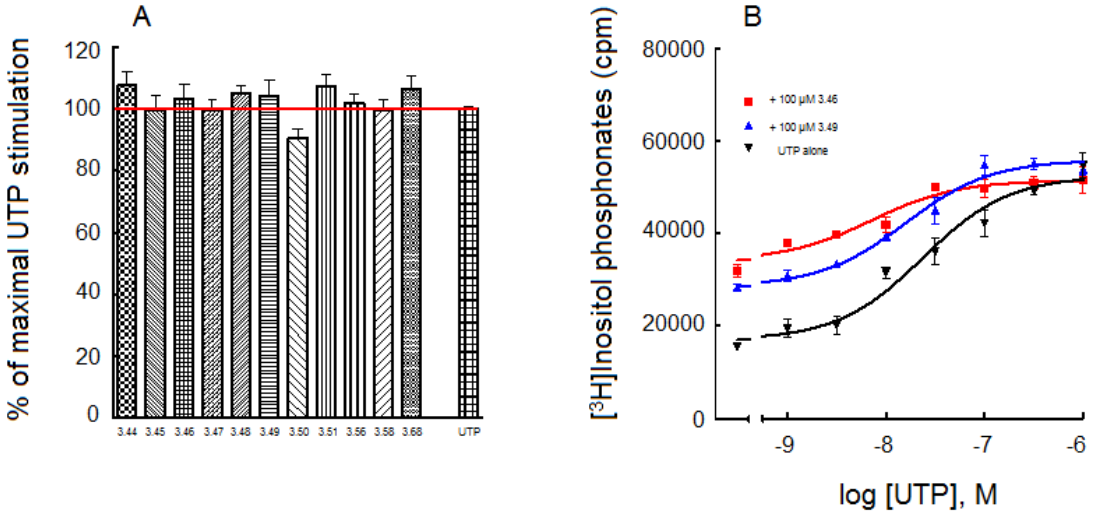

Figure III.21. Effect of high concentrations of phosphonate analogues on the $P2Y_2$ receptor-mediated activity of UTP. (A) Lack of effect of the broad range of phosphonate analogues on response to UTP. The effects of 100 µM concentrations of the indicated phosphonates were tested in the presence of 100 nM UTP in 1321N1-$P2Y_2$ cells as described in Methods. (B) Concentration dependent effects of UTP in the presence of the most potent phosphonate analogues. 1321N1-$P2Y_2$ cells were incubated with various concentrations UTP in the absence or presence of 100 µM **3.46** or **3.49**.

Interestingly, compound **3.69**, a regioisomer of **3.44**, with a 6-phenyl substituent,[193] exhibited clearly lower apparent efficacy and potency in activating the $P2Y_2$ receptor (Figure III.22).

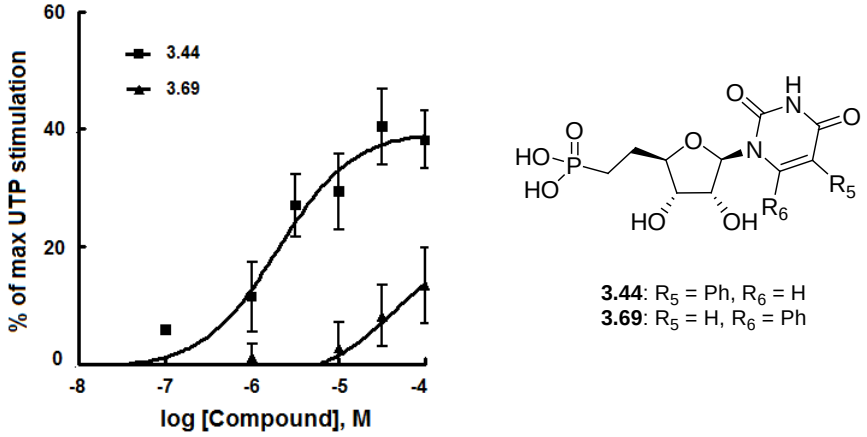

Figure III.22. Comparison of the concentration dependent activation of the $P2Y_2$ receptor by the 5-, and 6-phenyl substituted 5'-methylene phosphonate analogues **3.44** and **3.69**.

2.4 CONFORMATIONAL ANALYSIS

The conformational behavior of nucleosides is considered to be of great importance for their interactions with target proteins and thus for their biological activity. The complete definition of the conformation of a nucleoside involves the determination of three principal structural parameters:1) the glycosyl torsion angle χ, which determines the relative position of the base to the sugar moiety (*syn* or *anti*); 2) the torsion angle γ, which determines the orientation of the 5'-OH group with respect to C3'; and 3) the puckering of the furanose ring and its deviation from planarity.[206]

The sugar puckering of natural *ribo*- and deoxyribonucleosides in solution appears as a dynamic equilibrium between two major conformers, the North (*N*) and the South (*S*), with a very low energy barrier between the two states (Figure III.23).[206,207]

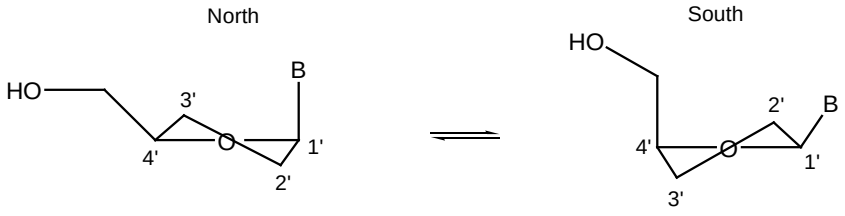

Figure III.23. Rapidly equilibrium North and South conformation of nucleosides.

Davies *et al.*[208] derived the following equations that relate the fraction of the North conformer X_N with the values of the vicinal three scalar couplings that can be measured between the protons of the ring:

$$J_{H1',H2'} = 9.3\ (1-X_N)$$
$$J_{H2',H3'} = 4.6X_N + 5.3\ (1-X_N)$$
$$J_{H3',H4'} = 9.3X_N$$

To assess the impact of the presence of a substituent at the C-5 position of the uracil base on the relative proportions of Northern and Southern conformers, these scalar couplings were measured at five different temperatures for the 5-phenyl substituted uridine phosphonate **3.44**, while the same was done for the non C-5 substituted uridine phosphonate **3.7**. The fraction of the *N*-type conformer was obtained by minimizing the sum of square difference between the experimental couplings and those calculated from the above equations. The results are shown in Table III.2.

Table III.2. ^{1}H-NMR derived mole fraction of the *N*-type conformer of **3.7** and **3.44** at different temperatures (Measurements are performed under the supervision of Prof. Dr. José Martens at the NMR and Structure Analysis Unit, Department of Organic Chemistry, UGent).

	X_N	
T [°C]	**3.7**	**3.44**
20	55.5	52.9
27	54.8	53.1
35	54.4	54.1
42	54.1	53.8
50	54.0	53.0

For analogue **3.7**, the Northern and Southern conformers are nearly equally present, with a small preference for the Northern. From Table III.2, it appears that **3.44** has similar North/South populations as **3.7**. It can therefore be concluded that the implantation of a phenyl group at the C-5 position appears to have no effect on the conformational state of the ribofuranose ring. Interestingly, this is in contrast to the effect of implanting a phenyl ring at C-6 of the base (**3.69**) as was published recently by Nencka *et al*.,[193] that clearly shows an enhanced preference for the Northern conformation.

As mentioned above, another aspect of the conformation is the orientation of the base relative to the ring structure, which is assumed to be either *syn* (with the oxygen at position C-2 lying immediately above the furanose ring) or *anti* (with the oxygen at position C-2 pointing away from the furanose ring). The NOESY spectrum of compound **3.7** showed clear cross-peaks from the H-6 proton to the H-3' and both H-5' protons, confirming that the *anti* rotamer could be adopted. When a bulky group is implanted at the C-5 position, it is positioned further away from the ribose ring and the conformational implications for the five ring appeared to be negligible.

2.5 PHOTOPHYSICAL EVALUATION

The application of fluorescent nucleoside analogues as molecular probes provides a new tool for studying the uptake and metabolism of the corresponding analogues as described in PART I - Chapter 2. In the phosphonate series **3.44-3.51**, several phosphonate analogues showed fluorescence properties. A photophysical evaluation (performed in the Laboratory of General Biochemistry and Physical Pharmacy, UGent) of compound **3.46** is depicted in Figure III.24. The 5-(4-fluorophenyl)uridine 5'-phosphonate analogue showed an excitation maximum of 328 nm and an emission maximum of 360 nm.

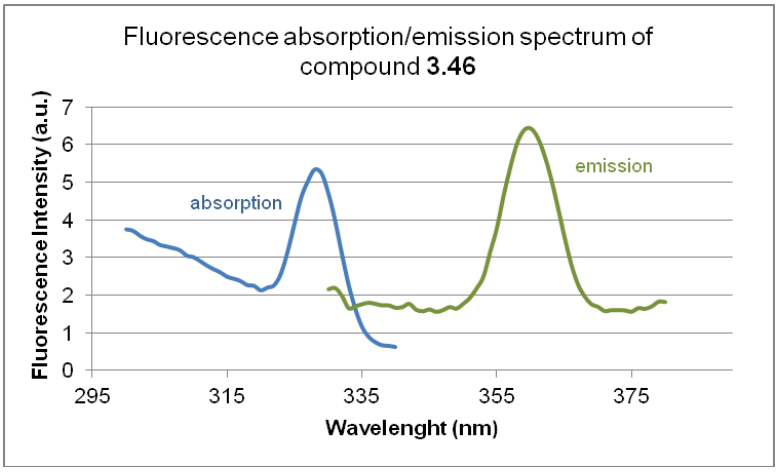

Figure III.24. Excitation and emission spectrum of compound **3.46**.

2.6 CONCLUSIONS

In this study we explored the influence of modifications of uridine 5'-methylene phosphonate (**3.7**) on the activity at the human $P2Y_2$ receptor. A Suzuki–Miyaura coupling of a suitable 5-bromo precursor with aryl and heteroaryl boronic acids allowed to generate a small series of C-5 substituted analogues of **3.7**. All 5-modified analogues caused $P2Y_2$-dependent IP_3 accumulation. Interestingly, none of the phosphonate analogues had the same maximal activity as UTP. Within this series, a 5-(2-furanyl) modification (**3.49**) gave the highest efficacy, while 5-(4-fluorophenyl) substitution (**3.46**) afforded the highest potency. Remarkably, these analogues failed to inhibit activity of UTP down to the level of activity seen with the 5-modified analogues alone as would be expected for classical partial agonists. A possible explanation for this phenomenon is that these phosphonates are producing their effects by interacting with a receptor site distinct from the orthosteric site. Phosphonate **3.49** may become a useful, metabolically stable tool compound for further pharmacological characterization of the $P2Y_2$ receptor.

2.7 EXPERIMENTAL PART

2.7.1 Synthesis

2',3'-*O*-Isopropylidene-β-D-uridine (3.32)

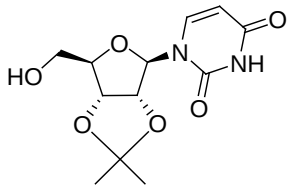

p-Toluenesulfonic acid (300 mg, 1.52 mmol) was added to a suspension of uridine (3.71 g, 15.19 mmol) in dry action (150 mL) and 2,2-dimethoxypropane (10 mL). The reaction was stirred at room temperature for 5 h. The mixture was concentrated *in vacuo* and the residue dissolved in EtOAc. The organic phase was washed with sat. aq. $NaHCO_3$, dried with $MgSO_4$, filtered and evaporated to dryness. Purification on a silica gel column (CH_2Cl_2/MeOH 95:5) afforded compound **3.32** as a white solid (3.45 g, 80%).

^{1}H NMR (300 MHz, DMSO-d_6): δ 1.29 (3H, s, CH_3), 1.49 (3H, s, CH_3), 3.57 (1H, dd, *J*= 4.5 Hz, *J*= 8.7 Hz, H-5'a), 4.06 (1H, dd, *J*= 4.2 Hz, *J*= 8.1 Hz, H-5'b), 4.73-4.76 (1H, m, H-4'), 4.89 (1H, dd, *J*= 2.7 Hz, *J*= 6.6 Hz, H-3'), 5.08 (1H, app t, *J*= 4.8 Hz, H-2'), 5.63 (1H, d, *J*= 8.1 Hz, CH=CH), 5.83 (1H, d, *J*= 2.7 Hz, H-1'), 7.79 (1H, d, *J*= 8.1 Hz, CH=CH). The spectrum is accordance with the literature report.[209]

^{13}C NMR (75 MHz, DMSO-d_6): δ 25.19 (CH_3), 27.06 (CH_3), 61.27 (C-5'), 80.48 (C-3'), 83.68 (C-4'), 86.52 (C-2'), 91.12 (C-1'), 101.74 (C-5), 112.96 (isopropylidene), 141.92 (C-6), 150.34 (C-2), 163.18 (C-4).

Exact mass (ESI-MS) for $C_{12}H_{17}N_2O_6$ $[M+H]^+$ found, 285.1086; calcd, 285.1081.

1-[5,6-Dideoxy-6-(diethoxyphosphinyl)-2,3-*O*-isopropylidene-β-D-*ribo*-hex-5-enofuranosyl]uracil (3.33)

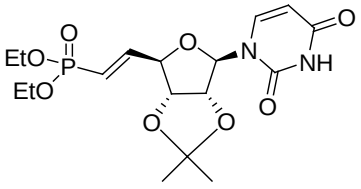

IBX (3.23 g, 11.49 mmol) was added to a solution of **3.32** (2.18 g, 7.66 mmol) in CH_3CN (60 mL) and the resulted suspension was stirred at 80 °C for 6 h. After cooling in an ice bath (15 min), the solid was

removed by filtration and washed with cold CH_3CN. The solvent was evaporated and the residue was co-distilled with toluene. The residue was dissolved in anhydrous DMSO (20 mL) and freshly prepared **3.72** in DMSO (20 mL) was added. After 20 h, the mixture was poured into water and extracted with CH_2Cl_2. The combined organic layers were dried over $MgSO_4$, filtered and concentrated *in vacuo*. The residue was lyophilized to remove the remaining DMSO and purified on a silica gel column (CH_2Cl_2/MeOH 95:5 and acetone/pentane 50:50) yielding 1.88 g mg (59%) of **3.33** as a foam.

^{1}H NMR (300 MHz, DMSO-d_6): δ 1.22 (6H, t, *J*= 6.9 Hz, 2 x *O*CH_2CH_3), 1.30 (3H, s, CH_3), 1.50 (3H, s, CH_3), 3.88-4.01 (4H, m, 2 x *O*CH_2CH_3), 4.58-4.61 (1H, m, H-4'), 4.84 (1H, dd, *J*= 4.5 Hz, *J*= 6.6 Hz, H-3'), 5.13 (1H, dd, *J*= 1.5 Hz, *J*= 6.3 Hz, H-2'), 5.63 (1H, d, *J*= 8.1 Hz, CH=CH), 5.82 (1H, d, *J*= 1.5 Hz, H-1'), 5.93-6.05 (1H, m, H-6'), 6.62-6.77 (1H, m, H-5'), 7.73 (1H, d, *J*= 8.1 Hz, CH=CH), 11.43 (1H, s, 3-NH). The spectrum is accordance with the literature report.[150]

Exact mass (ESI-MS) for $C_{17}H_{26}N_2O_8P$ $[M+H]^+$ found, 417.1442; calcd, 417.1421.

1-[5,6-Dideoxy-6-(diethoxyphosphinyl)-2,3-*O*-isopropylidene-β-D-*ribo*-hexofuranosyl]uracil (3.34)

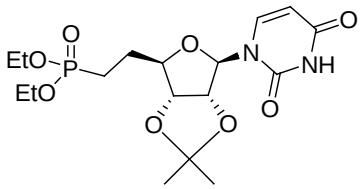

To a solution of compound **3.33** (921 mg, 2.21 mmol) in MeOH (15 mL) was added 10% Pd/C. The reaction mixture was stirred under hydrogen atmosphere overnight. The catalyst was removed by filtration through Celite and the filtrate was evaporated to yield pure compound **3.34** (707 mg, 76%) as a colourless solid.

^{1}H NMR (300 MHz, DMSO-d_6): δ 1.22 (6H, t, *J*= 7.1 Hz, 2 x *O*CH_2CH_3), 1.29 (3H, s, CH_3), 1.48 (3H, s, CH_3), 1.72 (4H, m, H-5'a,b and H-6'a,b), 3.92-4.02 (5H, m, 2 x *O*CH_2CH_3 and H-4'), 4.64 (1H, dd, *J*= 4.7 Hz, *J*= 6.5 Hz, H-3'), 5.00 (1H, dd, *J*= 2.3 Hz, *J*= 6.5 Hz, H-2'), 5.64 (1H, dd, *J*= 2.0 Hz, *J*= 7.9 Hz, CH=CH), 5.75 (1H, d, *J*= 2.9 Hz, H-1'), 7.70 (1H, d, *J*= 7.9 Hz, CH=CH), 11.40 (1H, s, 3-NH). The spectrum is accordance with the literature report.[150]

Exact mass (ESI-MS) for $C_{17}H_{28}N_2O_8P$ $[M+H]^+$ found, 419.1605; calcd, 419.1578.

1-[5,6-Dideoxy-6-(diethoxyphosphinyl)-2,3-*O*-isopropylidene-β-D-*ribo*-hexofuranosyl]-5-bromouracil (3.35)

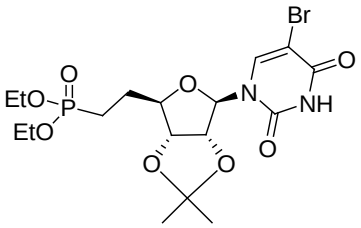

To a solution of compound **3.34** (399 mg, 0.95 mmol) in DMF (8 mL) was added *N*-bromosuccinimide (NBS, 187 mg, 1.05 mmol) under N_2. The reaction mixture was stirred at room temperature for 16 hours. DMF was removed *in vacuo* and the residue was purified by column chromatography (CH_2Cl_2/MeOH 95:5) to afford compound **3.35** (376 mg, 79%) as a colourless oil.

^{1}H NMR (300 MHz, DMSO-d_6): δ 1.20-1.28 (9H, m, 2 x OCH_2CH_3 and CH_3), 1.47 (3H, s, CH_3), 1.69-1.92 (4H, m, H-5'a,b and H-6'a,b), 3.90-4.04 (5H, m, 2 x OCH_2CH_3 and H-4'), 4.64-4.67 (1H, m, H-3'), 5.04 (1H, dd, *J*= 2.1 Hz, *J*= 6.6 Hz, H-2'), 5.73 (1H, d, *J*= 2.1 Hz, H-1'), 8.23 (1H, s, H-6), 11.91 (1H, s, 3-NH).

^{31}P NMR (DMSO-d_6): δ 31.53.

^{13}C NMR (75 MHz, DMSO-d_6): δ 16.25 (OCH_2CH_3), 16.32 (OCH_2CH_3), 19.89 (C-6'), 21.76 (C-5'), 25.24 (CH_3), 27.00 (CH_3), 60.91 (OCH_2CH_3), 61.00 (OCH_2CH_3), 82.61 (C-3'), 83.38 (C-2'), 85.65 (C-4', d, *J*= 17.9 Hz), 91.77 (C-1'), 96.12 (C-5), 113.49 (isopropylidene), 142.53 (C-6), 149.56 (C-2), 159.23 (C-4).

Exact mass (ESI-MS) for $C_{17}H_{27}BrN_2O_8P$ $[M+H]^+$ found, 497.0697; calcd, 497.0683.

General procedure for the synthesis of 5-modified nucleoside phosphonates via Suzuki-Miyaura coupling

A mixture of compound **3.35** (1 equiv.), aryl boronic acid (2 equiv.), $Pd(PPh_3)_4$ (0.1 equiv.) and Na_2CO_3 (3.3 equiv.) in DMF and degassed H_2O was heated (± 130 °C, oil bath) under argon for 6 h or until TLC indicated consumption of all starting material. The mixture was then concentrated and co-distilled with toluene. The residue was purified by column chromatography affording 5-modified analogues in moderate yield.

1-[5,6-Dideoxy-6-(diethoxyphosphinyl)-2,3-*O*-isopropylidene-β-D-*ribo*-hexofuranosyl]-5-phenyluracil (3.36)

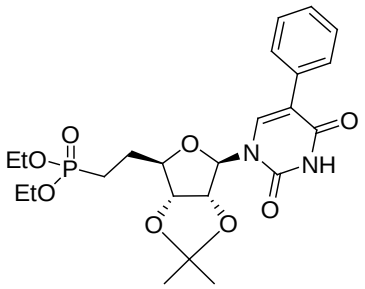

Reaction of compound **3.35** (78 mg, 0.16 mmol) with phenylboronic acid (39 mg, 0.32 mmol), $Pd(PPh_3)_4$ (18 mg, 0.016 mmol) and Na_2CO_3 (55 mg, 0.52 mmol) in DMF (4 mL) and degassed H_2O (0.5 mL) was performed as described in the general procedure for the synthesis of 5-modified phosphonates. Purification of the crude on a silica gel column (CH_2Cl_2/MeOH 95:5) afforded compound **3.36** as a colourless oil (33 mg, 43%).

^{1}H NMR (300 MHz, DMSO-d_6): δ 1.18-1.23 (6H, m, 2 x OCH_2CH_3), 1.30 (3H, s, CH_3), 1.49 (3H, s, CH_3), 1.74-1.89 (4H, m, H-5'a,b and H-6'a,b), 3.91-4.02 (5H, m, 2 x OCH_2CH_3 and H-4'), 4.67-4.71 (1H, m, H-3'), 5.14 (1H, dd, *J*= 2.4 Hz, *J*= 6.6 Hz, H-2'), 5.85 (1H, d, *J*= 2.1 Hz, H-1'), 7.29-7.41 (3H, m, Ph), 7.52-7.55 (2H, m, Ph), 7.91 (1H, s, H-6), 11.62 (1H, s, 3-NH).

^{31}P NMR (DMSO-d_6): δ 31.55.

^{13}C NMR (75 MHz, DMSO-d_6): δ 16.22 (OCH_2CH_3), 16.30 (OCH_2CH_3), 19.88 (C-6'), 21.74 (C-5'), 25.26 (CH_3), 27.03 (CH_3), 60.89 (OCH_2CH_3), 61.02 (OCH_2CH_3), 82.76 (C-3'), 83.42 (C-2'), 85.55 (C-4', d, *J*= 17.9 Hz), 91.96 (C-1'), 113.44 and 113.85 (isopropylidene and C-5), 127.39, 128.05, 128.27, 132.69 and 140.40 (Ph and C-6), 149.70 (C-2), 162.21 (C-4).

Exact mass (ESI-MS) for $C_{23}H_{32}N_2O_8P$ $[M+H]^+$ found, 495.1891; calcd, 495.1891.

1-[5,6-Dideoxy-6-(diethoxyphosphinyl)-2,3-*O*-isopropylidene-β-D-*ribo*-hexofuranosyl]-5-(naphthalen-1-yl)uracil (3.37)

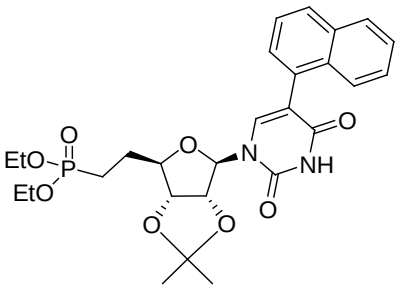

Reaction of compound **3.35** (63 mg, 0.13 mmol) with naphthalene-1-boronic acid (45 mg, 0.25 mmol), $Pd(PPh_3)_4$ (15 mg, 0.013 mmol) and Na_2CO_3 (44 mg, 0.42 mmol) in DMF (3 mL) and degassed H_2O (0.4 mL) was performed as described in the general procedure for the synthesis of 5-modified phosphonates. Purification of the crude on a silica gel column (CH_2Cl_2/MeOH 96:4) afforded compound **3.37** as a colourless solid (42 mg, 61%).

^{1}H NMR (300 MHz, DMSO-d_6): δ 1.19 (6H, dt, *J*= 1.5 Hz, *J*= 7.2 Hz, 2 x *O*CH_2CH_3), 1.31 (3H, s, CH_3), 1.50 (3H, s, CH_3), 1.74-1.91 (4H, m, H-5'a,b and H-6'a,b), 3.90-4.04 (5H, m, 2 x *O*CH_2CH_3 and H-4'), 4.71 (1H, dd, *J*= 4.5 Hz, *J*= 6.3 Hz, H-3'), 5.18 (1H, dd, *J*= 2.4 Hz, *J*= 6.6 Hz, H-2'), 5.87 (1H, d, *J*= 2.1 Hz, H-1'), 7.49-7.55 (2H, m, naphthalene), 7.69 (1H, dd, *J*= 1.8 Hz, *J*= 8.4 Hz, naphthalene), 7.90-7.95 (3H, m, naphthalene), 8.06 (1H, s, H-6), 8.12 (1H, *d*, *J*= 1.2 Hz, naphthalene), 11.69 (1H, s, 3-NH).

^{31}P NMR (DMSO-d_6): δ 31.58.

^{13}C NMR (75 MHz, DMSO-d_6): δ 16.21 (*O*CH_2CH_3), 16.28 (*O*CH_2CH_3), 19.87 (C-6'), 21.74 (C-5'), 25.30 (CH_3), 27.05 (CH_3), 61.01 (2 x *O*CH_2CH_3), 82.80 (C-3'), 83.47 (C-2'), 85.56 (C-4'), 92.28 (C-1'), 113.40 and 113.66 (isopropylidene and C-5), 126.09, 126.19, 126.49, 126.82, 127.28, 127.42, 127.94, 130.42, 132.12, 132.78 and 140.89 (naphthalene and C-6), 149.80 (C-2), 162.51 (C-4).

Exact mass (ESI-MS) for $C_{27}H_{34}N_2O_8P$ $[M+H]^+$ found, 545.2076; calcd, 545.2047.

1-[5,6-Dideoxy-6'-(diethoxyphosphinyl)-2,3-*O*-isopropylidene-β-D-*ribo*-hexofuranosyl]-5-(4-fluorophenyl)uracil (3.38)

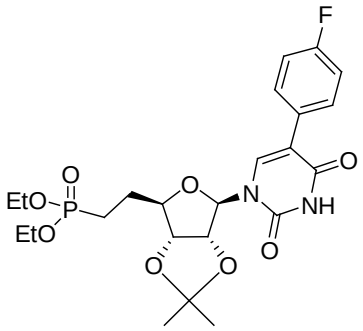

Reaction of compound **3.35** (78 mg, 0.16 mmol) with 4-fluorophenylboronic acid (44 mg, 0.31 mmol), $Pd(PPh_3)_4$ (18 mg, 0.016 mmol) and Na_2CO_3 (54 mg, 0.51 mmol) in DMF (4 mL) and degassed H_2O (0.5 mL) was performed as described in the general procedure for the synthesis of 5-modified phosphonates. Purification of the crude on a silica gel column (CH_2Cl_2/MeOH 95:5) afforded compound **3.38** as a colourless solid (56 mg, 70%).

^{1}H NMR (300 MHz, DMSO-d_6): δ 1.18 (6H, dt, *J*= 0.9 Hz, *J*= 7.2 Hz, 2 x *O*CH_2CH_3), 1.27 (3H, s, CH_3), 1.47 (3H, s, CH_3), 1.72-1.89 (4H, m, H-5'a,b and H-6'a,b), 3.92-4.02 (5H, m, 2 x *O*CH_2CH_3 and H-4'), 4.69 (1H, dd, *J*= 4.8 Hz, *J*= 6.6 Hz, H-3'), 5.14 (1H, dd, *J*= 2.4 Hz, *J*= 6.9 Hz, H-2'), 5.83 (1H, d, *J*= 2.4 Hz, H-1'), 7.19-7.25 (2H, m, subs Ph), 7.57-7.63 (2H, m, subs Ph), 7.92 (1H, s, H-6), 11.64 (1H, s, 3-NH).

^{31}P NMR (DMSO-d_6): δ 31.56.

^{13}C NMR (75 MHz, DMSO-d_6): δ 16.22 (*O*CH_2CH_3), 16.29 (*O*CH_2CH_3), 19.89 (C-6'), 21.75 (C-5'), 25.27 (CH_3), 27.03 (CH_3), 61.03 (2 x *O*CH_2CH_3), 82.77 (C-3'), 83.40 (C-2'), 85.56 (C-4', d, *J*= 17.9 Hz), 92.01 (C-1'), 112.89, 113.46, 114.74 and 115.02 (subs Ph, isopropylidene and C-5), 129.08, 130.24 and 130.35 (subs Ph), 140.45 (C-6), 149.71 (C-2), 159.94 (subs Ph), 162.26 (C-4).

Exact mass (ESI-MS) for $C_{23}H_{31}FN_2O_8P$ $[M+H]^+$ found, 513.1815; calcd, 513.1797.

1-[5,6-Dideoxy-6-(diethoxyphosphinyl)-2,3-*O*-isopropylidene-β-D-*ribo*-hexofuranosyl]-5-styryluracil (3.39)

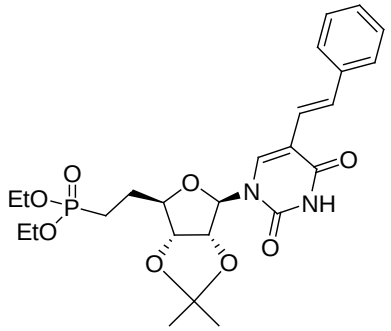

Reaction of compound **3.35** (91 mg, 0.18 mmol) with *trans*-2-phenylvinylboronic acid (56 mg, 0.37 mmol), $Pd(PPh_3)_4$ (21 mg, 0.018 mmol) and Na_2CO_3 (64 mg, 0.60 mmol) in DMF (4 mL) and degassed H_2O (0.5 mL) was performed as described in the general procedure for the synthesis of 5-modified phosphonates. Purification of the crude on a silica gel column (CH_2Cl_2/MeOH 95:5) afforded compound **3.39** as a colourless solid (72 mg, 76%).

^{1}H NMR (300 MHz, DMSO-d_6): δ 1.18 (6H, app dt, *J*= 1.2 Hz, *J*= 6.9 Hz, 2 x *O*CH_2CH_3), 1.28 (3H, s, CH_3), 1.48 (3H, s, CH_3), 1.71-1.88 (4H, m, H-5'a,b and H-6'a,b), 3.90-4.01 (5H, m, 2 x *O*CH_2CH_3 and H-4'), 4.68 (1H, dd, *J*= 4.8 Hz, *J*= 6.6 Hz, H-3'), 5.06 (1H, dd, *J*= 2.4 Hz, *J*= 6.6 Hz, H-2'), 5.80 (1H, d, *J*= 2.4 Hz, H-1'), 6.88 (1H, d, *J*= 16.2 Hz, styrene), 7.20-7.25 (1H, m, styrene), 7.33 (2H, d, *J*= 7.8 Hz, styrene), 7.43-7.48 (3H, m, styrene), 7.94 (1H, H-6).

^{31}P NMR (DMSO-d_6): δ 31.51.

^{13}C NMR (75 MHz, DMSO-d_6): δ 16.22 (OCH$_2$CH$_3$), 16.30 (OCH$_2$CH$_3$), 19.90 (C-6'), 21.76 (C-5'), 25.29 (CH$_3$), 27.02 (CH$_3$), 60.99 (2 x OCH$_2$CH$_3$), 82.64 (C-3'), 83.49 (C-2'), 85.41 (C-4', d, J= 17.6 Hz), 91.34 (C-1'), 111.22 (C-5), 113.54 (isopropylidene), 120.83, 125.99, 127.42, 128.32, 128.74 and 137.43 (styrene), 140.09 (C-6), 149.26 (C-2), 162.21 (C-4).

Exact mass (ESI-MS) for $C_{25}H_{34}N_2O_8P$ $[M+H]^+$ found, 521.2049; calcd, 521.2047.

1-[5,6-Dideoxy-6-(diethoxyphosphinyl)-2,3-*O*-isopropylidene-β-D-*ribo*-hexofuranosyl]-5-(*p*-tolyl)uracil (3.40)

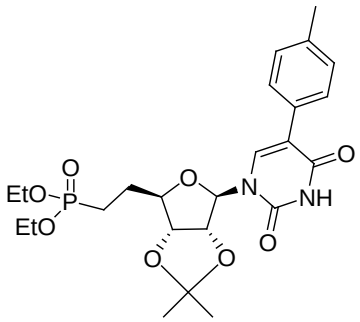

Reaction of compound **3.35** (63 mg, 0.13 mmol) with 4-methylphenylboronic acid (36 mg, 0.25 mmol), Pd(PPh$_3$)$_4$ (15 mg, 0.013 mmol) and Na$_2$CO$_3$ (45 mg, 0.42 mmol) in DMF (3 mL) and degassed H$_2$O (0.4 mL) was performed as described in the general procedure for the synthesis of 5-modified phosphonates. Purification of the crude on a silica gel column (CH$_2$Cl$_2$/MeOH 97:3) afforded compound **3.40** as a colourless solid (29 mg, 46%).

^{1}H NMR (300 MHz, CDCl$_3$): δ 1.24-1.33 (9H, m, 2 x OCH$_2$CH$_3$ and CH$_3$) 1.54 (3H, s, CH$_3$), 1.72-2.07 (4H, m, H-5'a,b and H-6'a,b), 2.71 (3H, s, *p*-tolyl), 4.01-4.13 (5H, m, 2 x OCH$_2$CH$_3$ and H-4'), 4.64 (1H, dd, J= 4.5 Hz, J= 6.3 Hz, H-3'), 5.04 (1H, dd, J= 2.1 Hz, J= 6.3 Hz, H-2'), 5.67 (1H, d, J= 2.4 Hz, H-1'), 7.16-7.79 (4H, m, *p*-tolyl), 8.00 (1H, H-6).

^{31}P NMR (CDCl$_3$): δ 31.27.

^{13}C NMR (75 MHz, CDCl$_3$): δ 16.62 (OCH$_2$CH$_3$), 16.70 (OCH$_2$CH$_3$), 25.46 (C-6'), 27.27 (C-5'), 29.82 (CH$_3$), 31.48 (CH$_3$), 38.38 (*p*-tolyl), 59.75 (OCH$_2$CH$_3$), 62.14 (OCH$_2$CH$_3$), 83.60 (C-3'), 84.56 (C-2'), 86.95 (C-4'), 94.17 (C-1'), 115.12 and 115.97 (isopropylidene and C-5), 128.36, 129.12, 129.50, 138.40 and 139.41 (*p*-tolyl and C-6), 149.83 (C-2), 162.71 (C-4).

Exact mass (ESI-MS) for $C_{24}H_{34}N_2O_8P$ $[M+H]^+$ found, 509.2076; calcd, 509.2047.

1-[5,6-Dideoxy-6-(diethoxyphosphinyl)-2,3-*O*-isopropylidene-β-D-*ribo*-hexofuranosyl]-5-(furan-2-yl)uracil (3.41)

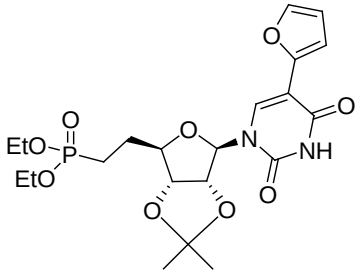

Reaction of compound **3.35** (93 mg, 0.19 mmol) with furan-2-boronic acid (42 mg, 0.37 mmol), $Pd(PPh_3)_4$ (22 mg, 0.019 mmol) and Na_2CO_3 (65 mg, 0.62 mmol) in DMF (4.5 mL) and degassed H_2O (0.6 mL) was performed as described in the general procedure for the synthesis of 5-modified phosphonates. Purification of the crude on a silica gel column (CH_2Cl_2/MeOH 95:5) afforded compound **3.41** as a brown solid (36 mg, 40%).

^{1}H NMR (300 MHz, DMSO-d_6): δ 1.16-1.28 (6H, m, 2 x OCH_2CH_3) 1.28 (3H, s, CH_3), 1.48 (3H, s, CH_3), 1.76-1.81 (4H, m, H-5'a,b and H-6'a,b), 3.82-4.07 (5H, m, 2 x OCH_2CH_3 and H-4'), 4.58-4.68 (1H, m, H-3'), 5.03-5.13 (1H, m, H-2'), 5.84-5.86 (1H, m, H-1'), 6.50-6.54 (1H, m, furan), 6.83-6.88 (1H, m, furan), 7.61-7.66 (1H, m, furan), 8.02 (1H, app d, *J*= 4.8 Hz, H-6).

^{31}P NMR (DMSO-d_6): δ 31.63.

^{13}C NMR (75 MHz, DMSO-d_6): δ 16.29 (OCH_2CH_3), 16.37 (OCH_2CH_3), 20.00 (C-6'), 21.98 (C-5'), 25.31 (CH_3), 27.07 (CH_3), 60.99 and 61.11 (2 x OCH_2CH_3), 82.83 (C-3'), 83.74 (C-2'), 85.89 (C-4', d, *J*= 17.6 Hz), 92.37 (C-1'), 105.72 and 108.40 (furan), 111.73 (C-5), 113.46 (isopropylidene), 128.83 and 131.55 (furan), 141.79 (C-6), 149.24 (C-2), 160.37 (C-4).

Exact mass (ESI-MS) for $C_{21}H_{30}N_2O_9P$ $[M+H]^+$ found, 485.1708; calcd, 485.1683.

1-[5,6-Dideoxy-6-(diethoxyphosphinyl)-2,3-*O*-isopropylidene-β-D-*ribo*-hexofuranosyl]-5-(thiophen-2-yl)uracil (3.42)

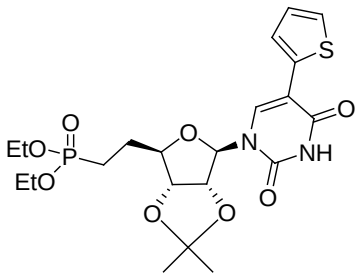

Reaction of compound **3.35** (81 mg, 0.16 mmol) with thiophene-2-boronic acid (42 mg, 0.33 mmol), $Pd(PPh_3)_4$ (19 mg, 0.016 mmol) and Na_2CO_3 (57 mg, 0.54 mmol) in DMF (4 mL) and degassed H_2O

(0.5 mL) was performed as described in the general procedure for the synthesis of 5-modified phosphonates. Purification of the crude on a silica gel column (CH_2Cl_2/MeOH 95:5) afforded compound **3.42** as a colourless solid (32 mg, 39%).

^{1}H NMR (300 MHz, DMSO-d_6): δ 1.1-1.22 (6H, m, 2 x OCH_2CH_3) 1.28 (3H, s, CH_3), 1.48 (3H, s, CH_3), 1.68-1.91 (4H, m, H-5'a,b and H-6'a,b), 3.90-3.97 (5H, m, 2 x OCH_2CH_3 and H-4'), 4.67-4.69 (1H, m, H-3'), 5.13-5.15 (1H, m, H-2'), 5.82 (1H, m, H-1'), 7.05-7.07 (1H, m, thiophene), 7.46-7.47 (2H, m, thiophene), 8.20 (1H, s, H-6).

^{31}P NMR (DMSO-d_6): δ 31.64.

^{13}C NMR (75 MHz, DMSO-d_6): δ 16.25 (OCH_2CH_3), 16.33 (OCH_2CH_3), (C-6 and C-5' not visible), 25.31 (CH_3), 27.07 (CH_3), 60.99 (2 x OCH_2CH_3), 82.87 (C-3'), 83.57 (C-2'), 85.86 (C-4'), 93.79 (C-1'), 108.56 (C-5), 113.40 (isopropylidene), 128.73-138.33 (thiophene), (C-6, C-2 and C-4 not visible).

Exact mass (ESI-MS) for $C_{21}H_{30}N_2O_8PS$ $[M+H]^+$ found, 501.1453; calcd, 501.1455.

1-[5,6-Dideoxy-6-(diethoxyphosphinyl)-2,3-*O*-isopropylidene-β-D-*ribo*-hexofuranosyl]-5-(benzothiophen-3-yl)uracil (3.43)

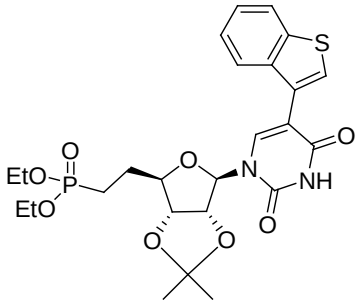

Reaction of compound **3.35** (105 mg, 0.21 mmol) with 1-benzothiophen-3-yl-boronic acid (77 mg, 0.42 mmol), $Pd(PPh_3)_4$ (24 mg, 0.021 mmol) and Na_2CO_3 (74 mg, 0.70 mmol) in DMF (5 mL) and degassed H_2O (0.7 mL) was performed as described in the general procedure for the synthesis of 5-modified phosphonates. Purification of the crude on a silica gel column (CH_2Cl_2/MeOH 95:5) afforded compound **3.43** as a brown solid (49 mg, 42%).

^{1}H NMR (300 MHz, $CDCl_3$): δ 1.25-1.32 (9H, m, 2 x OCH_2CH_3 and CH_3), 1.55 (3H, s, CH_3), 1.77-1.93 (2H, m, H-6'a and H-6'b), 1.98-2.08 (2H, m, H-5'a and H-5'b), 4.02-4.12 (5H, m, 2 x OCH_2CH_3 and H-4'), 4.61 (1H, t, *J*= 5.7 Hz, H-3'), 5.00 (1H, app d, *J*= 6.6 Hz, H-2'), 5.70 (1H, app s, H-1'), 7.32-7.41 (2H, m, benzothiophene), 7.46-7.48 (1H, m, benzothiophene), 7.54 (1H, s, H-6), 7.67 (1H, d, *J*= 7.8 Hz, benzothiophenyl), 7.86 (1H, d, *J*= 7.8 Hz, benzothiophene), 9.53 (1H, br s, 3-NH).

^{31}P NMR (DMSO-d_6): δ 31.01.

^{13}C NMR (75 MHz, $CDCl_3$): δ 16.52 (OCH_2CH_3), 16.60 (OCH_2CH_3), 21.04 (C-6'), 22.94 (C-5'), 25.48 (CH_3), 27.31 (CH_3), 61.81 (OCH_2CH_3), 83.43 (C-3'), 84.41 (C-2'), 86.64 (C-4', d, *J*= 17.9 Hz), 93.79 (C-1'), 110.69 and 115.11 (C-5 and isopropylidene), 122.48, 123.08, 124.65, 124.71, 126.86, 126.94 and 137.70 (benzothiophene), 140.15 and 140.39 (C-6 and benzothiophene), 149.54 (C-2), 162.12 (C-4).

Exact mass (ESI-MS) for $C_{25}H_{32}N_2O_8PS$ $[M+H]^+$ found, 551.1620; calcd, 551.1612.

General procedure for the deprotection of 5-modified nucleoside phosphonates

The phosphonic ester (1 equiv.) was dissolved in dry CH_2Cl_2 under argon. TMSBr (2 equiv.) was added and the resulting solution was stirred overnight. The solvents were evaporated and the residue was co-distilled with toluene. Then, water was added followed by TFA (50%) and the mixture was stirred for 4 h. The solvent was evaporated and subsequently portioned between EtOAc/Et_2O (1:1) and water. The organic phase was washed with water and the water layers were combined and lyophilized. Purification of the crude using RP-HPLC (Phenomenex Luna C-18, H_2O/0.1% HCOOH in CH_3CN, 90:10 → 0:100 in 23 min, flow 17.5 mL/min) afforded compounds **3.44-3.51** in moderate yield.

1-[5,6-Dideoxy-6-(dihydroxyphosphinyl)-β-D-*ribo*-hexofuranosyl]-5-phenyluracil (3.44)

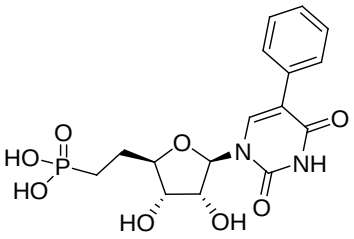

Reaction of compound **3.36** (32 mg, 0.068 mmol) with TMSBr (18 µL, 1.35 mmol) in dry CH_2Cl_2 (1.4 mL) followed by reaction with 1.4 mL 50% aq. TFA in water (0.7 mL) as described in the general procedure for the deprotection of 5-modified nucleoside phosphonates, afforded compound **3.44** as a white powder (14.1 mg, 55%).

^{1}H NMR (300 MHz, DMSO-d_6): δ 1.40-1.43 (2H, m, H-6'a and H-6'b), 1.80-1.84 (2H, m, H-5'a and H-5'b), 3.82-3.83 (2H, m, H-3' and H-4'), 4.19 (1H, t, *J*= 5.1 Hz, H-2'), 5.72 (1H, d, *J*= 4.5 Hz, H-1'), 7.26-7.40 (3H, m, Ph), 7.51-7.54 (2H, m, Ph), 7.64 (1H, s, H-6).

^{31}P NMR (DMSO-d_6): δ 25.89.

^{13}C NMR (75 MHz, DMSO-d_6): δ (C-6' not visible), 26.89 (C-5'), 72.46 (C-3'), 72.52 (C-2'), 83.48 (C-4', d, *J*= 15.9 Hz), 89.54 (C-1'), 113.97 (C-5), 127.36, 128.16, 128.22 and 132.80 (Ph), 138.34 (C-6), 150.11 (C-2), 162.07 (C-4).

Exact mass (ESI-MS) for $C_{16}H_{18}N_2O_8P$ $[M-H]^-$ found, 397.0815; calcd, 397.0806.

1-[5,6-Dideoxy-6-(dihydroxyphosphinyl)-β-D-*ribo*-hexofuranosyl]-5-(naphthalen-1-yl)uracil (3.45)

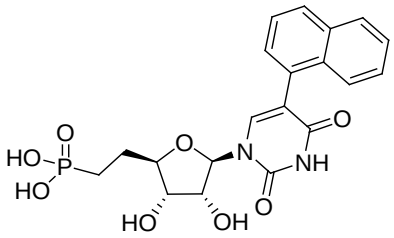

Reaction of compound **3.37** (70 mg, 0.073 mmol) with TMSBr (19 µL, 1.46 mmol) in dry CH_2Cl_2 (1.5 mL) followed by reaction with 1.5 mL 50% aq. TFA in water (0.7 mL) as described in the general procedure for the deprotection of 5-modified nucleoside phosphonates, afforded compound **3.45** as a white powder (22.6 mg, 39%).

^{1}H NMR (300 MHz, DMSO-d_6): δ 1.60 (2H, app br s, H-6'a and H-6'b), 1.78-1.84 (2H, m, H-5'a and H-5'b), 3.77-3.85 (2H, m, H-3' and H-4'), 4.25 (1H, t, *J*= 5.4 Hz, H-2'), 5.73 (1H, d, *J*= 4.8 Hz, H-1'), 7.29-7.41 (3H, m, naphthalene), 7.52-7.69 (2H, m, naphthalene), 7.69 (1H, s, H-6), 11.57 (1H, s, 3-NH).

^{31}P NMR (DMSO-d_6): δ 25.71.

^{13}C NMR (75 MHz, DMSO-d_6): δ 23.80 (C-6'), 27.04 (C-5'), 72.56 (C-3'), 72.62 (C-2'), 83.52 (C-4'), 89.83 (C-1'), 113.94 (C-5), 126.19, 126.27, 126.58, 126.78, 127.50, 128.22, 130.51, 132.23 and 132.91 (naphthalene), 138.95 (C-6), 150.21 (C-2), 162.32 (C-4).

Exact mass (ESI-MS) for $C_{20}H_{20}N_2O_8P$ $[M-H]^-$ found, 447.0969; calcd, 447.0963.

1-[5,6-Dideoxy-6-(dihydroxyphosphinyl)-β-D-*ribo*-hexofuranosyl]-5-(4-fluorophenyl)uracil (3.46)

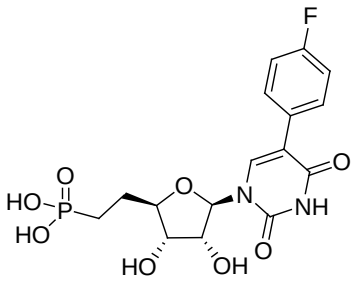

Reaction of compound **3.38** (56 mg, 0.11 mmol) with TMSBr (29 µL, 2.20 mmol) in dry CH_2Cl_2 (2.2 mL) followed by reaction with 2.2 mL 50% aq. TFA in water (1.1 mL) as described in the general procedure for the deprotection of 5-modified nucleoside phosphonates, afforded compound **3.46** as a white powder (26.1 mg, 57%).

^{1}H NMR (300 MHz, DMSO-d_6): δ 1.62 (2H, app br s, H-6'a and H-6'b), 1.79 (2H, app br s, H-5'a and H-5'b), 3.77-3.84 (2H, m, H-3' and H-4'), 4.26 (1H, t, *J*= 5.1 Hz, H-2'), 5.73 (1H, d, *J*= 4.8 Hz, H-1'), 7.21 (2H, t, *J*= 8.7 Hz, subs Ph), 7.56-7.60 (2H, m, subs Ph), 7.70 (1H, s, H-6), 11.59 (1H, s, 3-NH).

^{31}P NMR (DMSO-d_6): δ 26.17.

^{13}C NMR (75 MHz, DMSO-d_6): δ (C-6' not visible), 27.05 (C-5'), 72.57 (C-3'), 72.60 (C-2'), 83.65 (C-4'), 89.67 (C-1'), 113.11 (C-5), 114.92, 115.20, 129.21, 129.25, 130.29 and 130.40 (subs Ph), 138.44 (C-6), 150.18 (C-2), 160.01 (subs Ph), 162.17 (C-4).

Exact mass (ESI-MS) for $C_{16}H_{17}FN_2O_8P$ $[M-H]^-$ found, 415.0722; calcd, 415.0712.

1-[5,6-Dideoxy-6-(dihydroxyphosphinyl)-β-D-*ribo*-hexofuranosyl]-5-styryluracil (3.47)

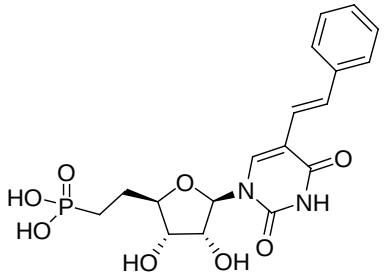

Reaction of compound **3.39** (72 mg, 0.14 mmol) with TMSBr (36 µL, 2.75 mmol) in dry CH_2Cl_2 (2.8 mL) followed by reaction with 2.8 mL 50% aq. TFA in water (1.4 mL) as described in the general procedure for the deprotection of 5-modified nucleoside phosphonates, afforded compound **3.47** as a white powder (6.5 mg, 11%).

^{1}H NMR (300 MHz, DMSO-d_6): δ 1.60 (2H, br s, H-6'a and H-6'b), 1.87 (2H, br s, H-5'a and H-5'b), 3.78-3.86 (2H, m, H-3' and H-4'), 4.15 (1H, app s, H-2'), 5.75-5.76 (1H, m, H-1'), 6.98 (1H, d, *J*= 16.2 Hz, styrene), 7.15-7.57 (6H, m, styrene), 7.78 (1H, s, H-6).
^{31}P NMR (DMSO-d_6): δ 24.42.

^{13}C NMR (175 MHz, DMSO-d_6): δ 24.35 (C-6'), 27.07 (C-5'), 72.35 (C-3'), 72.72 (C-2'), 83.48 (C-4'), 88.68 (C-1'), 111.27 (C-5), 121.28, 125.97, 127.27, 128.20, 128.57 and 137.57 (styrene), 138.78 (C-6), 149.62 (C-2), 162.04 (C-4).

Exact mass (ESI-MS) for $C_{18}H_{20}N_2O_8P$ $[M-H]^-$ found, 423.0954; calcd, 423.0963.

1-[5,6-Dideoxy-6-(dihydroxyphosphinyl)-β-D-*ribo*-hexofuranosyl]-5-(*p*-tolyl)uracil (3.48)

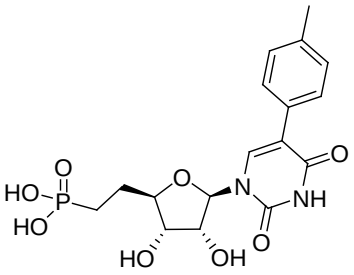

Reaction of compound **3.40** (29 mg, 0.058 mmol) with TMSBr (15 µL, 1.15 mmol) in dry CH_2Cl_2 (1.2 mL) followed by reaction with 1.2 mL 50% aq. TFA in water (0.6 mL) as described in the general procedure for the deprotection of 5-modified nucleoside phosphonates, afforded compound **3.48** as a white powder (4.3 mg, 18%).

^{1}H NMR (300 MHz, DMSO-d_6): δ 1.40-1.99 (4H, m, H-6'a,b and H-5'a,b), 2.34 (3H, s, *p*-tolyl), 3.77-3.82 (2H, m, H-3' and H-4'), 4.22 (1H, m, H-2'), 5.73 (1H, d, *J*= 4.5 Hz, H-1'), 7.19 (2H, d, *J*= 7.5 Hz, *p*-tolyl), 7.42 (2H, d, *J*= 7.8 Hz, *p*-tolyl), 7.62 (1H, s, H-6).

^{31}P NMR (DMSO-d_6): δ 25.55.

^{13}C NMR (75 MHz, DMSO-d_6): δ 20.61 (*p*-tolyl), (C-6' not visible), 27.00 (C-5'), 72.33 (C-3'), 72.42 (C-2'), 83.64 (C-4'), 89.28 (C-1'), 113.74 (C-5), 127.85, 128.58, 129.71 and 136.47 (*p*-tolyl), 137.58 (C-6), 149.92 (C-2), 161.95 (C-4).

Exact mass (ESI-MS) for $C_{17}H_{20}N_2O_8P$ $[M-H]^-$ found, 411.0970; calcd, 411.0963.

1-[5,6-Dideoxy-6-(dihydroxyphosphinyl)-β-D-*ribo*-hexofuranosyl]-5-(furan-2-yl)uracil (3.49)

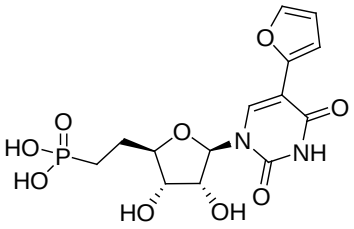

Reaction of compound **3.41** (32 mg, 0.067 mmol) with TMSBr (18 µL, 1.34 mmol) in dry CH_2Cl_2 (1.4 mL) followed by reaction with 1.4 mL 50% aq. TFA in water (0.7 mL) as described in the general procedure for the deprotection of 5-modified nucleoside phosphonates, afforded compound **3.49** as a white powder (5.8 mg, 22%).

^{1}H NMR (300 MHz, DMSO-d_6): δ 1.61 (2H, br s, H-6'a and H-6'b), 1.83-1.91 (2H, m, H-5'a and H-5'b), 3.80-3.82 (2H, m, H-3' and H-4'), 4.12 (1H, s, H-2'), 5.73 (1H, d, *J*= 3.9 Hz, H-1'), 6.51 (1H, d, *J*= 1.8 Hz, furan), 6.87 (1H, d, *J*= 3.3 Hz, furan), 7.66 (1H, s, furan), 7.82 (1H, s, H-6).

^{31}P NMR (DMSO-d_6): δ 25.08.

^{13}C NMR (75 MHz, DMSO-d_6): δ (C-6' not visible), 27.12 (C-5'), 72.58 and 73.34 (C-2' and C-3'), 83.56 (C-4'), 89.56 (C-1'), 105.69, 108.10 and 111.56 (C-5 and furan), 134.25 (C-6), 141.81 and 146.08 (furan), 149.42 (C-2), 160.07 (C-4).

Exact mass (ESI-MS) for $C_{14}H_{16}N_2O_9P$ $[M-H]^-$ found, 387.0604; calcd, 387.0599.

1-[5,6-Dideoxy-6-(dihydroxyphosphinyl)-β-D-*ribo*-hexofuranosyl]-5-(thiophen-2-yl)uracil (3.50)

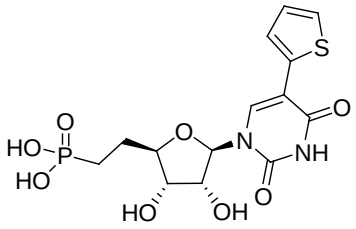

Reaction of compound **3.42** (32 mg, 0.063 mmol) with TMSBr (17 µL, 1.26 mmol) in dry CH_2Cl_2 (1.3 mL) followed by reaction with 1.2 mL 50% aq. TFA in water (0.6 mL) as described in the general procedure for the deprotection of 5-modified nucleoside phosphonates, afforded compound **3.50** as a white powder (9.3 mg, 37%).

^{1}H NMR (300 MHz, DMSO-d_6): δ 1.61 (2H, br s, H-6'a and H-6'b), 1.75-1.91 (2H, m, H-5'a and H-5'b), 3.80-3.85 (2H, m, H-3' and H-4'), 4.22-4.28 (1H, m, H-2'), 5.71 (1H, d, *J*= 4.5 Hz, H-1'), 7.02-7.10 (1H, m, thiophene), 7.46 (1H, d, *J*= 5.1 Hz, thiophene), 7.50 (1H, s, thiophene), 7.96 (1H, s, H-6).

^{31}P NMR (DMSO-d_6): δ 25.42.

^{13}C NMR (175 MHz, DMSO-d_6): δ 24.21 (C-6'), 26.99 (C-5'), 72.36 (C-3'), 72.73 (C-2'), 83.68 (C-4'), 89.80 (C-1'), 108.63 (C-5), 123.20, 125.80, 126.54 and 133.39 (thiophene), 135.82 (C-6), 149.48 (C-2), 161.30 (C-4).

Exact mass (ESI-MS) for $C_{14}H_{16}N_2O_8PS$ $[M-H]^-$ found, 403.0343; calcd, 403.0371.

1-[5,6-Dideoxy-6-(dihydroxyphosphinyl)-β-D-*ribo*-hexofuranosyl]-5-(benzothiophen-3-yl)uracil (3.51)

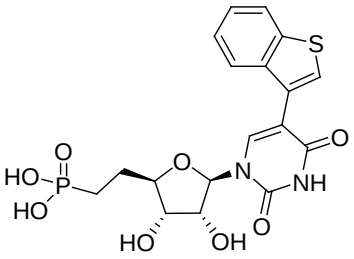

Reaction of compound **3.43** (49 mg, 0.088 mmol) with TMSBr (23 µL, 1.76 mmol) in dry CH_2Cl_2 (1.8 mL) followed by reaction with 1.8 mL 50% aq. TFA in water (0.9 mL) as described in the general procedure for the deprotection of 5-modified nucleoside phosphonates, afforded compound **3.51** as a white powder (31.5 mg, 78%).

^{1}H NMR (300 MHz, DMSO-d_6): δ 1.59 (2H, br s, H-6'a and H-6'b), 1.76-1.80 (2H, m, H-5'a and H-5'b), 3.76-3.83 (2H, m, H-3' and H-4'), 4.21-4.4.24 (1H, m, H-2'), 5.77 (1H, d, *J*= 4.8 Hz, H-1'), 7.36-7.44 (2H, m, benzothiophene), 7.63-7.66 (1H, m, benzothiophene), 7.78 (2H, app d, *J*= 7.2 Hz, benzothiophene and H-6), 7.98-8.02 (1H, m, benzothiophene), 11.66 (1H, s, 3-NH).

^{31}P NMR (DMSO-d_6): δ 26.13.

^{13}C NMR (75 MHz, DMSO-d_6): δ (C-6' not visible), 26.65 (C-5'), 72.49 (C-3'), 72.44 (C-2'), 83.47 (C-4'), 89.37 (C-1'), 109.30 (C-5), 123.05, 124.28, 124.39, 126.65, 128.23, 138.02, 139.14 and 139.68 (benzothiophenyl and C-6), 150.29 (C-2), 162.00 (C-4).

Exact mass (ESI-MS) for $C_{18}H_{18}N_2O_8PS$ $[M-H]^-$ found, 453.0531; calcd, 453.0527.

1-[5,6-Dideoxy-6-(diethoxyphosphinyl)-β-D-*ribo*-hexofuranosyl]uracil (3.52)

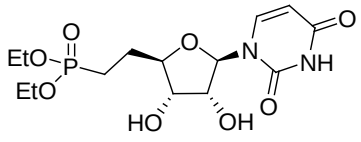

1st Method: A solution of **3.34** (428 mg, 1.02 mmol) and 50% aqueous HCOOH (10 mL) was stirred for 4,5 h at room temperature. The mixture was evaporated *in vacuo* and purified on a silica column using CH_2Cl_2/MeOH (90:10) as a solvent. Compound **3.52** was obtained as a colourless solid (220 mg, 57%).

2nd Method: Compound **3.34** (340 mg, 0.81 mmol) was dissolved in 50% aqueous TFA at 0 °C. After stirring for 2 hours at room temperature, the mixture was evaporated to dryness. The crude was

purified using column chromatography (CH_2Cl_2/MeOH 95:5 → 90:10) yielding compound **3.52** as a colourless solid (198 mg, 64%).

^{1}H NMR (300 MHz, DMSO-d_6): δ 1.23 (6H, t, *J*= 6.9 Hz, 2 x *O*CH_2CH_3), 1.72-1.86 (4H, m, H-5'a,b and H-6'a,b), 3.32-3.83 (2H, m, H-3' and H-4'), 3.93-4.11 (5H, m, 2 x *O*CH_2CH_3 and H-2'), 5.12 (1H, d, *J*= 5.7 Hz, 3'-OH), 5.35 (1H, d, *J*= 5.7 Hz, 2'-OH), 5.63 '1H, d, *J*= 8.1 Hz, CH=CH), 5.68 (1H, d, *J*= 5.1 Hz, H-1'), 7.59 (1H, d, *J*= 8.1 Hz, CH=CH), 11.34 (1H, s, 3-NH).

^{31}P NMR (DMSO-d_6): δ 31.86.

^{13}C NMR (75 MHz, DMSO-d_6): δ 16.26 and 16.33 (2 x *O*CH_2CH_3), 19.99 (C-6'), 21.85 (C-5'), 61.95 (2 x *O*CH_2CH_3), 72.40 and 72.57 (C-2' and C-3'), 82.65 (C-4, d, *J*= 17.3 Hz), 88.93 (C-1'), 102.06 (C-5), 141.42 (C-6), 150.61 (C-2), 163.03 (C-4).

Exact mass (ESI-MS) for $C_{14}H_{24}N_2O_8P$ $[M+H]^+$ found, 379.1262; calcd, 379.1265.

1-[2,2-Anhydro-5,6-dideoxy-6-(diethoxyphosphinyl)-β-D-*arabino*-hexofuranosyl]uracil (3.53)

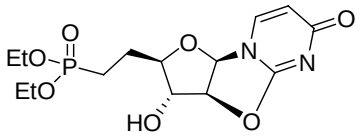

1st Method: Compound **3.52** (205 mg, 0.54 mmol) was dissolved into a mixed solution of thionyl chloride (0.17 mL) and CH_3CN (1.4 mL) with vigorously stirring at room temperature. After 2 h, the mixture was poured into water and extracted with CH_2Cl_2. The combined organic layers were dried over $MgSO_4$, filtered and concentrated *in vacuo*. Without further purification, the 2,3-sulfonyl derivative of **3.52** and sodium acetate (223 mg, 2.72 mmol) were heated in DMF at about 85 °C. After stirring for 3 h, solvents were removed *in vacuo* and the crude purified on a silica gel column (CH_2Cl_2/MeOH (95:5 → 80:20)) yielding 180 mg (92%) of **3.53** as a white foam.

2nd Method: Diphenyl carbonate (33 mg, 0.15 mmol) and sodium bicarbonate (1 mg, 0.012 mmol) were added to the DMF (0.7 mL) solution of **3.52** (53 mg, 0.14 mmol). The mixture was heated to reflux, and carbon dioxide was generated. After 1.5 hour, the darkened solution was concentrated *in vacuo* and the crude purified on a silica gel column (CH_2Cl_2/MeOH 90:10) affording **3.53** in a 65% yield.

^{1}H NMR (300 MHz, DMSO-d_6): δ 1.14-1.23 (7H, m, 2 x *O*CH_2CH_3 and H-5'a), 1.59-1.68 (3H, m, H-5'b and H-6'a,b), 3.84-3.94 (4H, m, 2 x *O*CH_2CH_3), 4.00-4.10 (1H, m, H-4'), 4.32 (1H, app s, H-3'), 5.19 (1H, d, *J*= 5.7 Hz, H-2'), 5.87 (1H, d, *J*= 7.5 Hz, CH=CH), 6.30 (1H, d, *J*= 5.7 Hz, H-1'), 7.91 (1H, d, *J*= 7.5 Hz, CH=CH).

^{31}P NMR (DMSO-d_6): δ 31.02.

^{13}C NMR (75 MHz, $CDCl_3$): δ 16.45 and 16.53 (2 x OCH_2CH_3), 21.08 (C-6'), 22.99 (C-5'), 62.14 and 62.23 (2 x OCH_2CH_3), (C3' under $CDCl_3$ peak), 87.72 (C-4', d, *J*= 16.7 Hz), 89.49 (C-2'), 90.31 (C-1'), 109.94 (C-5), 136.16 (C-6), 160.19 (C-2), 172.90 (C-4).

Exact mass (ESI-MS) for $C_{14}H_{22}N_2O_7P$ $[M+H]^+$ found, 361.1157; calcd, 361.1159.

1-[2-Azido-2,5,6-trideoxy-6-(ethoxyhydroxyphosphinyl)-β-D-*ribo*-hexofuranosyl]uracil (3.54)

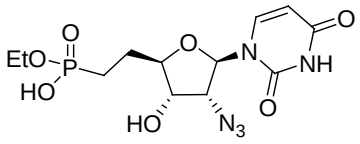

A suspension of compound **3.53** (33 mg, 0.092 mmol) and NaN_3 (37 mg, 0.56 mmol) in 0.7 mL DMF was heated overnight at 150 °C. The mixture was cooled to room temperature and evaporated *in vacuo*. The crude was dissolved in CH_2Cl_2/MeOH (8:2) and filtrated. Solvents were removed to afford compound **3.54** in quantitative yield (yellow oil).

^{1}H NMR (300 MHz, DMSO-d_6): δ 1.08-1.20 (3H, m, OCH_2CH_3), 1.48-1.70 (2H, m, H-6'a,b), 1.76-1.91 (2H, m, H-5'a,b), 3.75-3.89 (3H, m, OCH_2CH_3 and H-2'), 4.13-4.17 (1H, m, H-4'), 4.24-4.26 (1H, m, H-3'), 5.66-5.74 (2H, m, H-1' and CH=CH), 7.94-8.02 (1H, m, CH=CH).

^{31}P NMR (DMSO-d_6): δ 25.36.

Exact mass (ESI-MS) for $C_{12}H_{19}N_5O_7P$ $[M+H]^+$ found, 376.0997; calcd, 376.1017.

1-[2-Amino-2,5,6-trideoxy-6-(ethoxyhydroxyphosphinyl)-β-D-*ribo*-hexofuranosyl]uracil (3.55)

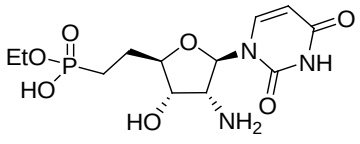

Compound **3.54** (24 mg, 0.065 mmol) and PPh_3 (34 mg, 0.13 mmol) were dissolved in THF (1 mL). After stirring for 10 minutes, H_2O was added (17 µL). After stirring overnight, the volatiles were removed *in vacuo*. The residue dissolved in water, washed with EtOAc/Et_2O (1:1) and lyophilized. Compound **3.55** was obtained in quantitative yield (light yellow solid).

^{1}H NMR (300 MHz, DMSO-d_6): δ 1.02-1.15 (3H, m, OCH_2CH_3), 1.21-1.52 (2H, m, H-6'a,b), 1.76 (2H, br s, H-5'a,b), 3.56-3.77 (3H, m, OCH_2CH_3 and H-2'), 4.04-4.10 (1H, m, H-4'), 4.22 (1H, app s, H-3'), 5.83-5.88 (1H, m, CH=CH), 6.27 (1H, app d, *J*= 5.4 Hz, H-1'), 7.91-7.93 (1H, d, *J*= 7.5 Hz, CH=CH).

^{31}P NMR (D_2O-d_6): δ 26.76.

Exact mass (ESI-MS) for $C_{12}H_{19}N_3O_7P$ $[M-H]^-$ found, 348.0954; calcd, 348.0966.

1-[2-Amino-2,5,6-trideoxy-6-(dihydroxyphosphinyl)-β-D-*ribo*-hexofuranosyl]uracil (3.56)

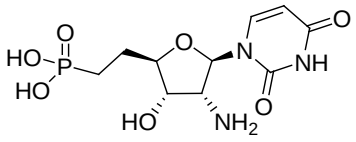

To a solution of compound **3.55** (24 mg, 0.067 mmol) in CH_2Cl_2 (1.9 mL) was added TMSBr (89 µL, 0.67 mmol). After stirring overnight, the volatiles were removed *in vacuo*. The residue was dissolved in water, washed with EtOAc/Et_2O (1:1) and lyophilized. The crude was purified using flash chromatography (*i*PrOH/NH_4OH/H_2O 6:3:1) yielding compound **3.56** (18.6 mg, 78%) as a light yellow powder. Compound **3.56** was isolated in the bis ammonium salt form.

^{1}H NMR (300 MHz, D_2O): δ 1.61-1.78 (2H, m, H-6'a,b), 1.89-1.95 (2H, m, H-5'a,b), 4.00-4.01 (1H, m, H-2'), 4.12-4.18 (1H, m, H-4'), 4.34-4.37 (1H, m, H-3'), 5.93 (1H, d, *J*= 7.8 Hz, CH=CH), 6.06 (1H, app d, *J*= 6.6 Hz, H-1'), 7.73 (1H, d, *J*= 8.4 Hz, CH=CH).

^{31}P NMR (D_2O-d_6): δ 24.03.

^{13}C NMR (75 MHz, D_2O): δ 24.10 (C-6', d, *J*= 133.9 Hz), 27.29 (C-5', d, *J*= 3.5 Hz), 55.79 (C-2'), 71.65 (C-3'), 86.20 (C-4', d, *J*= 17.3 Hz), 87.27 (C-1'), 102.90 (C-5), 141.67 (C-6), 151.88 (C-2), 166.21 (C-4).

Exact mass (ESI-MS) for $C_{10}H_{15}N_3O_7P$ $[M-H]^-$ found, 320.0646; calcd, 320.0653.

1-[2-Chloro-2,5,6-trideoxy-6-(diethoxyphosphinyl)-β-D-*ribo*-hexofuranosyl]uracil (3.57)

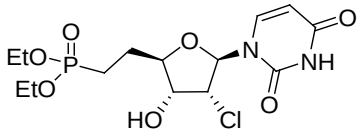

To a solution of compound **3.53** (76 mg, 0.21 mmol) in dry DMF (0.5 mL) was added 2N HCl in diethylether (1.4 mL). After stirring overnight, the mixture was concentrated *in vacuo* and the residue purified on a silica gel column (CH_2Cl_2/MeOH 90:10) affording **3.57** as a colourless solid (45 mg, 54%).

^{1}H NMR (300 MHz, DMSO-d_6): δ 1.23 (6H, t, *J*= 7.2 Hz, 2 x *O*CH_2CH_3), 1.65-1.98 (4H, m, H-5'a,b and H-6'a,b), 3.87-3.89 (1H, m, H-4'), 3.94-4.02 (5H, m, 2 x *O*CH_2CH_3 and H-3'), 4.73 (1H, app t, *J*= 6.0 Hz, H-2'), 5.69 (1H, d, *J*= 8.1 Hz, CH=CH), 5.89 (1H, d, *J*= 5.1 Hz, 3'-OH), 5.96 (1H, d, *J*= 6 Hz, H-1'), 7.63 (1H, d, *J*= 8.4 Hz, CH=CH), 11.45 (1H, s, 3-NH).

^{31}P NMR (DMSO-d_6): δ 32.03.

^{13}C NMR (75 MHz, DMSO-d_6): δ 16.43 and 16.50 (2 x *O*CH_2CH_3), 20.06 (C-6'), 21.92 (C-5'), 61.12, 61.16 and 61.23 (C-2' and 2 x *O*CH_2CH_3), 71.93 (C-3'), 83.57 (C-4', d, *J*= 16.8 Hz), 88.83 (C-1'), 102.62 (C-5), 140.71 (C-6), 150.69 (C-2), 163.07 (C-4).

Exact mass (ESI-MS) for $C_{14}H_{23}ClN_2O_7P$ $[M+H]^+$ found, 397.0942; calcd, 397.0926.

1-[2-Chloro-2,5,6-trideoxy-6-(dihydroxyphosphinyl)-β-D-*ribo*-hexofuranosyl]uracil (3.58)

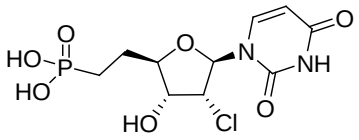

To a solution of **3.57** (41 mg, 0.10 mmol) in CH_2Cl_2 (1.5 mL) was added TMSBr (27 µL, 0.20 mmol). After stirring overnight, the volatiles were removed *in vacuo*. The residue was dissolved in water, washed with EtOAc/Et_2O (1:1) and lyophilized. The crude was purified using flash chromatography (*i*PrOH/NH_4OH/H_2O 6:3:1) yielding 58% of compound **3.58** (21.8 mg, white powder). Compound **3.58** was isolated in the bis ammonium salt form.

^{1}H NMR (300 MHz, D_2O): δ 1.60-1.82 (2H, m, H-6'a and H-6'b), 1.94-2.05 (2H, m, H-5'a and H-5'b), 4.13-4.19 (1H, m, H-4'), 4.27 (1H, app t, *J*= 5.4 Hz, H-3'), 4.66 (1H, app t, *J*= 5.1 Hz, H-2'), 5.92 (1H, d, *J*= 8.4 Hz, CH=CH), 6.08 (1H, d, *J*= 4.8 Hz, H-1'), 7.71 (1H, d, *J*= 8.1 Hz, CH=CH).

^{31}P NMR (D_2O): δ 24.24.

^{13}C NMR (75 MHz, D_2O): δ 24.17 (C-6', d, *J*= 133.6 Hz), 27.08 (C-5', d, *J*= 3.8 Hz), 61.39 (C-2'), 72.56 (C-3'), 84.25 (C-4', d, *J*= 17.9 Hz), 90.27 (C-1'), 102.73 (C-5), 141.52 (C-6), 151.69 (C-2), 166.25 (C-4).

Exact mass (ESI-MS) for $C_{10}H_{13}ClN_2O_7P$ $[M-H]^-$ found, 339.0154; calcd, 339.0154.

2'-Deoxy-5'-*O*-triphenylmethyl-β-D-uridine (3.59)

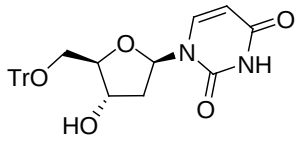

To a solution of 2'-deoxyuridine (5.30 g, 23.22 mmol) in anhydrous pyridine (50 mL) was added triphenylmethyl chloride (7.28 g, 26.11 mmol). The mixture was heated to 65 °C and stirred overnight. Then it was diluted with CH_2Cl_2 (50 mL), washed with saturated aqueous $NaHCO_3$ (3 x 100 mL), and dried over anhydrous $MgSO_4$. The solvent was removed under reduced pressure and the resulting residue was purified by column chromatography (CH_2Cl_2/MeOH 96:4), affording compound **3.59** (6.65 g, 61%) as a white foam.

^{1}H NMR (300 MHz, DMSO-d_6): δ 2.18 (1H, app t, *J*= 6.6 Hz, H-2'a and H-2'b), 3.15-3.20 (1H, m, H-5'a), 3.24-3.33 (1H, m, H-5'b), 3.86-3.90 (1H, m, H-4'), 4.25-4.30 (1H, m, H-3'), 5.34-5.40 (2H, m, 3'-OH and CH=CH), 6.15 (1H, app t, *J*= 6.3 Hz, H-1'), 7.25-7.41 (15H, m, Tr), 7.63 (1H, d, *J*= 8.4 Hz, CH=CH), 11.33 (1H, s, 3-NH).

^{13}C NMR (75 MHz, DMSO-d_6): δ 63.82 (C-5'), 70.04 (C-3'), 84.26 and 85.40 (C-1' and C-4'), 86.47 (Tr), 101.72 (C-5), 127.29, 128.11 and 128.43 (Tr), 140.56 (C-6), 143.60 (Tr), 150.48 (C-2), 163.18 (C-4).

Exact mass (ESI-MS) for $C_{28}H_{27}N_2O_5$ $[M+H]^+$ found, 471.1919; calcd, 471.1915.

3'-*O*-*tert*-Butyldiphenylsilyl-2'-deoxy-5'-*O*-triphenylmethyl-β-D-uridine (3.60)

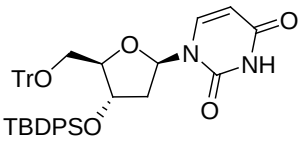

To a solution of compound **3.59** (6.65 g, 14.13 mmol) in DMF (50 mL) were added imidazole (4.62 g, 67.82 mmol) and *tert*-butyldiphenylchlorosilane (5.8 mL, 22.61 mmol) at rt. The mixture was stirred at the same temperature overnight. After being quenched with water, the mixture was extracted with Et_2O three times and dried over $MgSO_4$. The solvents were evaporated and the residue was purified on a silica gel column (CH_2Cl_2/MeOH 99:1) to give compound **3.60** (10.02 g, 100%) as a white foam.

^{1}H NMR (300 MHz, DMSO-d_6): δ 0.97 (9H, s, TBDPS), 2.02-2.09 (1H, m, H-2'a), 2.19-2.27 (1H, m, H-2'b), 3.03-3.08 (2H, m, H-5'a and H-5'b), 4.01-4.05 (1H, m, H-4'), 4.39-4.43 (1H, m, H-3'), 5.30 (1H, dd, *J*= 1.8 Hz, *J*= 8.1 Hz, CH=CH), 6.18 (1H, app t, *J*= 6.3 Hz, H-1'), 7.20-7.57 (25H, m, Tr and TBDPS), 7.67-7.70 (1H, m, CH=CH), 11.30 (1H, s, 3-NH).

Exact mass (ESI-MS) for $C_{44}H_{45}N_2O_5Si$ $[M+H]^+$ found, 709.3094; calcd, 709.3092.

3'-*O*-*tert*-Butyldiphenylsilyl-2'-deoxy-β-D-uridine (3.61)

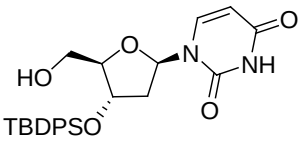

Compound **3.60** (10.02 g, 14.14 mmol) was dissolved in a mixture of $ZnBr_2$ (51.83 g, 230.16 mmol) in CH_2Cl_2/*i*PrOH (230 mL, 195:35) and stirred overnight at room temperature. The reaction was quenched with water and extracted with CH_2Cl_2 (3 x 100 mL). The combined organic layers were dried over $MgSO_4$ and evaporated to dryness. The resulting residue was purified by column chromatography (CH_2Cl_2/MeOH 96:4), affording compound **3.61** (3.97 g, 60%) as a white solid.

^{1}H NMR (300 MHz, DMSO-d_6): δ 1.05 (9H, s, TBDPS), 1.92-2.02 (1H, m, H-2'a), 2.10-2.17 (1H, m, H-2'b), 3.15-3.22 (1H, m, H-5'a), 3.30-3.41 (1H, m, H-5'b), 3.92-3.93 (1H, m, H-4'), 4.41-4.43 (1H, m, H-3'), 4.95 (1H, app t, *J*= 5.1 Hz, 5'-OH), 5.61 (1H, app dd, *J*= 2.1 Hz, *J*= 8.1 Hz, CH=CH), 6.26-6.31 (1H, m, H-1'), 7.42-7.53 (6H, m, TBDPS), 7.59-7.63 (4H, m, TBDPS), 7.78 (1H, d, *J*= 8.1 Hz, CH=CH), 11.30 (1H, s, 3-NH).

^{13}C NMR (75 MHz, DMSO-d_6): δ 18.99 (TBDPS), 27.04 (TBDPS), 61.42 (C-5'), 74.32 (C-3'), 84.71 (C-4'), 88.11 (C-1'), 102.30 (C-5'), 128.41, 128.43, 130.55, 133.24, 135.62 and 136.64 (TBDPS), 140.83 (C-6), 150.84 (C-2), 163.74 (C-4).

Exact mass (ESI-MS) for $C_{25}H_{31}N_2O_5Si$ $[M+H]^+$ found, 467.1992; calcd, 467.1997.

3'-*O*-*tert*-Butyldiphenylsilyl-2'-deoxy-β-D-uridine-5'-carboxylic acid (3.62)

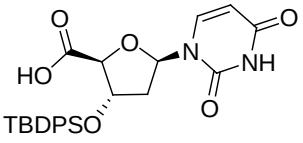

Alcohol **3.61** (1.12 g, 2.39 mmol) was dissolved in CH_3CN (20 mL). BAIB (1.69 g, 5.25 mmol) was added followed by water (20 mL). The mixture was then treated with TEMPO (78 mg, 0.48 mmol) and stirred for 16 h. The reaction mixture was concentrated under reduced pressure and the crude purified

on a silica gel column (CH_2Cl_2/MeOH 95:5 → 80:20) yielding compound **3.62** as a white foam (0.90 g, 78%).

^{1}H NMR (300 MHz, DMSO-d_6): δ 1.06 (9H, s, TBDPS), 1.87-1.96 (1H, m, H-2'a), 2.12-2.19 (1H, m, H-2'b), 4.50 (1H, app s, H-4'), 4.65 (1H, d, *J*= 3.9 Hz, H-3'), 5.69 (1H, app dd, *J*= 2.1 Hz, *J*= 8.1 Hz, CH=CH), 6.45 (1H, dd, *J*= 5.4 Hz, *J*= 9.3, H-1'), 7.42-7.53 (6H, m, TBDPS), 7.62-7.65 (4H, m, TBDPS), 8.10 (1H, d, *J*= 7.8 Hz, CH=CH), 11.36 (1H, app d, *J*= 1.8 Hz, 3-NH).

^{13}C NMR (75 MHz, DMSO-d_6): δ 18.69 (TBDPS), 26.63 (TBDPS), 76.48 (C-3'), 84.37 (C-4'), 85.68 (C-1'), 102.09 (C-5'), 128.00, 128.05, 130.17, 130.21, 132.33, 132.46, 135.26 and 135.28 (TBDPS), 140.40 (C-6), 150.49 (C-2), 163.04 (C-4), 171.71 (C-5').

Exact mass (ESI-MS) for $C_{25}H_{29}N_2O_6Si$ $[M+H]^+$ found, 481.1795; calcd, 481.1789.

2'-Deoxy-β-D-uridine-5'-carboxylic acid (3.63)

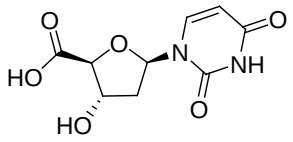

A solution of compound **3.62** (273 mg, 0.57 mmol) and NH_4F (42 mg, 1.14 mmol) in MeOH (2 mL) was stirred overnight at room temperature. The reaction mixture was evaporated and the residue dissolved in water, washed with EtOAc and lyophilized to obtain pure compound **3.63** as a white solid (140 mg, 100%).

^{1}H NMR (300 MHz, D_2O): δ 1.99-2.08 (1H, m, H-2'a), 2.23-2.30 (1H, m, H-2'b), 4.26 (1H, d, *J*= 1.5 Hz, H-4'), 4.49-4.54 (1H, m, H-3'), 5.80 (1H, d, *J*= 8.1 Hz, CH=CH), 6.30 (1H, dd, *J*= 5.7 Hz, *J*= 8.7 Hz, H-1'), 8.36 (1H, d, *J*= 8.1 Hz, CH=CH). (The ^{1}H NMR spectrum is accordance with the literature report.[201])

Exact mass (ESI-MS) for $C_9H_9N_2O_6$ $[M-H]^-$ found, 241.0470; calcd, 241.0466.

(2*R*)-1-[(2,3-Dihydrofuran-2-yl]uracil (3.64)

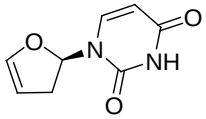

2'-Deoxyuridine-5'-carboxylic acid **3.63** (120 mg, 0.50 mmol) and dimethylformamide dineopentyl acetal (0.44 mL, 1.59 mmol) in DMF (5 mL) were heated at 130 °C. After 20 min the reaction mixture

was cooled and evaporated *in vacuo*. The crude was dissolved in CH_2Cl_2 and extracted with brine. The organic layer was dried over $MgSO_4$, filtered and concentrated. Purification using silica column chromatography (CH_2Cl_2/MeOH 96:4) afforded compound **3.64** (41 mg, 46%) as a colourless solid.

^{1}H NMR (300 MHz, DMSO-d_6): δ 2.55-2.64 (1H, m, H-2'a), 3.02-3.13 (1H, m, H-2'b), 5.14 (1H, app q, *J*= 2.4 Hz, H-3'), 5.64 (1H, d, *J*= 8.1 Hz, CH=CH), 6.54 (1H, app q, *J*= 4.2 Hz, H-1'), 6.60 (1H, app q, *J*= 3.0 Hz, H-4'), 7.33 (1H, d, *J*= 7.8 Hz, CH=CH), 11.35 (1H, s, 3-NH). (The ^{1}H NMR spectrum is accordance with the literature report.[201])

^{13}C NMR (75 MHz, DMSO-d_6): δ 34.39 (C-2'), 84.13 (C-1'), 100.06 (C-3'), 102.90 (C-5), 140.01 (C-6), 144.83 (C-4'), 150.24 (C-2), 163.10 (C-4).

Exact mass (ESI-MS) for $C_8H_9N_2O_3$ $[M+H]^+$ found, 181.0164; calcd, 181.0608.

(2*R*,4*S*,5*R*)-1-[5-((Diethoxyphosphinyl)methoxy)-4-(phenylselenyl)tetrahydrofuran-2-yl]uracil (3.65)

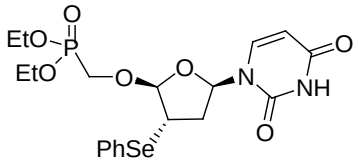

A solution of phenylselenyl chloride (44 mg, 0.23 mmol) in CH_2Cl_2 (0.1 mL) was added dropwise to a solution of glycal **3.64** (41 mg, 0.23 mmol) in CH_2Cl_2 (0.7 mL). After the mixture was stirred at -70 °C for 1 h, the solvent was removed under reduced pressure and the crude dissolved in CH_2Cl_2 (0.5 mL). Diethyl(hydroxymethyl)phosphonate (74 µL, 0.50 mmol) was added and the solution was cooled to -70 °C. Over 3 minutes a solution of silver perchlorate (52 mg, 0.25 mmol) in CH_3CN (0.1 mL) was added and the mixture was allowed to warm to 0 °C and poured into an aq. $NaHCO_3$ solution. The organic phase was separated, dried over $MgSO_4$ and evaporated *in vacuo*. The residual oil was purified on silica (CH_2Cl_2/MeOH 96:4) yielding compound **3.65** (40 mg, 35%) as a colourless solid.

^{1}H NMR (300 MHz, $CDCl_3$): δ 1.26 (6H, app dt, *J*= 1.5 Hz, *J*= 7.2 Hz, 2 x *O*CH_2CH_3), 2.41-2.45 (2H, m, H-2'a and H-2'b), 3.59-3.67 (1H, m, H-5'a), 3.79-3.90 (2H, m, H-5'b and H-3'), 4.03-4.13 (4H, m, 2 x *O*CH_2CH_3), 5.09 (1H, app s, H-4'), 5.74 (1H, app dd, *J*= 2.4 Hz, *J*= 8.4 Hz, CH=CH), 6.48 (1H, app t, *J*= 7.2 Hz, H-1'), 7.23-7.33 (3H, m, Ph), 7.49-7.55 (2H, m, Ph), 7.61 (1H, d, *J*= 8.4 Hz, CH=CH), 8.51 (1H, s, 3-NH).

^{31}P NMR ($CDCl_3$): δ 20.12.

^{13}C NMR (75 MHz, $CDCl_3$): δ 16.65 and 16.72 (2 x *O*CH_2CH_3), 36.27 (C-2'), 43.79 (C-3'), 60.47 (C-5'), 62.82 and 62.91 (2 x *O*CH_2CH_3), 86.53 (C-1'), 103.84 (C-4'), 110.04 (C-5), 127.36, 128.89, 129.73 and 135.12 (Ph), 140.41 (C-6), 150.51 (C-2), 162.78 (C-4).
Exact mass (ESI-MS) for $C_{19}H_{26}N_2O_7PSe$ $[M+H]^+$ found, 505.0630; calcd, 505.0637.

(2*R*,5*R*)-1-[2,5-Dihydro-5-((diethoxyphosphinyl)methoxy)-furan-2-yl]uracil (3.66)

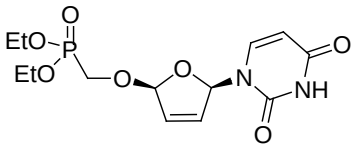

To a solution of compound **3.65** (41 mg, 0.082 mmol) in MeOH (0.7 mL) was added dropwise a suspended solution of sodium bicarbonate (12 mg, 0.14 mmol) and sodium periodate (22 mg, 0.10 mmol) in water (0.7 mL). After being stirred at rt for 1 h, the mixture was heated at 80 °C for 75 min. Volatiles were removed *in vacuo* and the residue was suspended in CH_2Cl_2, filtered through Celite and dried over $MgSO_4$. After evaporation under reduced pressure, the crude was purified on a silica gel column (CH_2Cl_2/MeOH 96:4) to give compound **3.66** (19 mg, 68%) as a yellow oil.

^{1}H NMR (300 MHz, $CDCl_3$): δ 1.31-1.36 (6H, m, 2 x *O*CH_2CH_3), 3.87-3.94 (1H, m, H-5'a), 4.03-4.22 (5H, m, H-5'b and 2 x *O*CH_2CH_3), 5.71 (1H, d, *J*= 7.8 Hz, CH=CH), 5.80 (1H, app s, H-4'), 6.10 (1H, app d, *J*= 6.0 Hz, H-2'), 6.28-6.31 (1H, m, H-3'), 6.97 (1H, app s, H-1'), 7.39 (1H, d, *J*= 8.1 Hz, CH=CH), 9.21 (1H, s, 3-NH).

^{31}P NMR ($CDCl_3$): δ 20.21.

^{13}C NMR (75 MHz, $CDCl_3$): δ 16.18 and 16.25 (2 x *O*CH_2CH_3), 61.17, 62.36 and 63.41 (2 x *O*CH_2CH_3 and C-5'), 87.77 (C-1'), 102.92 (C-5), 108.38 (C-4'), 130.11 (C-2'), 131.73 (C-3'), 139.77 (C-6), 150.21 (C-2), 162.78 (C-4).

Exact mass (ESI-MS) for $C_{13}H_{20}N_2O_7P$ $[M+H]^+$ found, 347.0999; calcd, 347.1003.

(2*R*,3*R*,4*S*,5*R*)-1-[5-((Diethoxyphosphinyl)methoxy)-3,4-dihydroxy-tetrahydrofuran-2-yl]uracil (3.67)

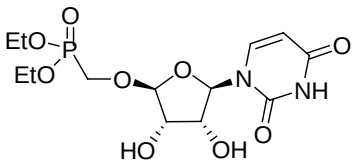

Compound **3.66** (37 mg, 0.11 mmol) was dissolved in a 5:1 acetone-water mixture (4 mL) and treated with osmium tetraoxide (0.19 mL [4 wt% solution], 0.032 mmol) and *N*-methylmorpholine-*N*-oxide (32

mg, 0.26 mmol). After stirring for 48 h, the mixture was quenched with a saturated solution of $Na_2S_2O_3$ (4 mL) and stirred for 30 min. The black mixture was extracted with EtOAc three times and the combined organic layers were dried over $MgSO_4$ and evaporated. Chromatography of the residue on silica gel (CH_2Cl_2/MeOH 90:10) yielded diol **3.67** as a colourless solid (24 mg, 60%).

^{1}H NMR (300 MHz, DMSO-d_6): δ 1.23 (6H, t, *J*= 6.9 Hz, 2 x OCH_2CH_3), 3.88-3.91 (3H, m, H-3', H-5'a and H-5'b), 4.02-4.10 (4H, m, 2 x OCH_2CH_3), 4.93 (1H, app s, H-4'), 5.52 (1H, d, *J*= 6.0 Hz, 2'-OH), 5.60 (1H, d, *J*= 4.2 Hz, 3'-OH), 5.65 (1H, d, *J*= 8.1 Hz, CH=CH), 6.06 (1H, d, *J*= 6.9 Hz, H-1'), 7.49 (1H, d, *J*= 8.1 Hz, CH=CH).

^{31}P NMR (DMSO-d_6): δ 20.55.

^{13}C NMR (75 MHz, DMSO-d_6): δ 16.44 and 16.51 (2 x OCH_2CH_3), 59.50 (C-5'), 62.35 and 62.43 (2 x OCH_2CH_3), 73.07 (C-2'), 73.53 (C-3'), 87.78 (C-1'), 103.17 (C-5), 107.95 (C-4'), 140.47 (C-6), 151.13 (C-2), 163.12 (C-4).

Exact mass (ESI-MS) for $C_{13}H_{22}N_2O_9P$ $[M+H]^+$ found, 381.1035; calcd, 381.1057.

(2*R*,3*R*,4*S*,5*R*)-1-[3,4-Dihydroxy-5-(phosphonomethoxy)-tetrahydrofuran-2-yl]uracil (3.68)

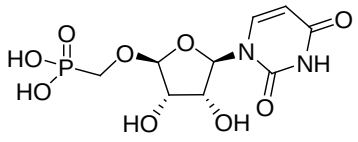

Compound **3.67** (23 mg, 0.061 mmol) was dissolved in dry DMF (3.8 mL) and cooled to 0 °C. The solution was then treated with 2,6-lutidine (71 µL, 0.61 mmol) followed by the dropwise addition of TMSBr (41 µL, 0.30 mmol). The mixture was allowed to warm to rt and stirred for 16 h. The solvent was evaporated and subsequently portioned between EtOAc/Et_2O (1:1) and water. The organic phase was washed with water and the water layers were combined and lyophilized. The crude was purified using flash chromatography (*i*PrOH/NH_4OH/H_2O 6:3:1) yielding compound **3.68** (9.0 mg, 50%) as a white powder. Compound **3.68** was isolated in the bis ammonium salt form.

^{1}H NMR (300 MHz, CD_3OD): δ 3.47-3.55 (1H, m, H-5'a), 3.80-3.87 (1H, m, H-5'b), 4.09 (1H, app d, *J*= 4.2 Hz, H-3'), 4.40-4.44 (1H, m, H-2'), 4.96 (1H, app s, H-4'), 5.84 (1H, d, *J*= 8.1 Hz, CH=CH), 6.25 (1H, d, *J*= 6.6 Hz, H-1'), 7.91 (1H, d, *J*= 7.8 Hz, CH=CH).

^{31}P NMR (CD_3OD): δ 14.09.

^{13}C NMR (75 MHz, CD_3OD): δ 64.88 (C-5'), 66.99 (C-2'), 73.62 (C-3'), 89.86 (C-1'), 104.15 (C-5), 110.40 (C-4'), 143.28 (C-6), 152.96 (C-2), 166.08 (C-4).

Exact mass (ESI-MS) for $C_9H_{12}N_2O_9P$ $[M-H]^-$ found, 323.0296; calcd, 323.0286.

(Diethoxyphosphinyl)methyl triflate (3.70)

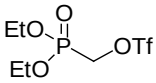

To a stirred solution of diethyl(hydroxymethyl)phosphonate (4.17 g, 24.80 mmol) and 2,6-lutidine (3.59 mL, 29.52 mmol) in anhydrous CH_2Cl_2 (40 mL), trifluoromethanesulfonic anhydride (5.0 mL, 28.52 mmol) was added dropwise at -50 °C. The resulting mixture was allowed to warm to 0 °C over 3 h and was then diluted with diethylether. The ethereal solution was successively washed with water and 1N HCl and dried over $MgSO_4$. After concentration *in vacuo*, compound **3.70** was obtained as a yellowish oil (6.07 g, 82%), which was used in the next step without purification.

^{1}H NMR (300 MHz, $CDCl_3$): δ 1.38 (6H, t, *J*= 7.1 Hz, 2 x *O*CH_2CH_3), 4.19-4.29 (4H, m, 2 x *O*CH_2CH_3), 4.63 (2H, d, *J*= 8.8 Hz, CH_2). (The ^{1}H NMR spectrum is accordance with the literature report.[191])

[(Diethoxyphosphinyl)methyl]triphenylphosphonium triflate (3.71)

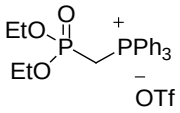

Compound **3.70** (6.07 g, 20.24 mmol) was added dropwise to a stirred solution of triphenylphosphine (6.11 g, 23.28 mmol) in 12 mL anhydrous CH_2Cl_2 at 0 °C. The mixture was allowed to warm to room temperature and then stirred overnight. The solvent was removed under reduced pressure and the crude purified on a silica gel column affording compound **3.71** (7.49 g, 66%) as a white solid.

^{1}H NMR (300 MHz, $CDCl_3$): δ 1.12 (6H, t, *J*= 7.1 Hz, 2 x *O*CH_2CH_3), 3.91-4.06 (4H, m, 2 x *O*CH_2 CH_3), 4.09-4.22 (2H, dd, *J*= 16.1 Hz and *J*= 20.2 Hz, CH_2), 7.65-7.90 (15H, m, PPh_3). (The ^{1}H NMR spectrum is accordance with the literature report.[191])

[(Diethoxyphosphinyl)methyl]triphenylphosphorane (3.72)

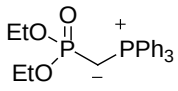

To a stirred suspension of a NaH (60% dispersion in mineral oil, 257 mg, 6.42 mmol) in anhydrous THF (10 mL) was added triphenylphosphonium triflate salt **3.71** (1.53 g, 2.72 mmol) in anhydrous THF (10 mL) at 0 °C. The resulting mixture was stirred at 0 °C for 30 min. The solvent was removed under

reduced pressure and the residue washed with anhydrous CH_2Cl_2 and filtered. After concentration of the extracts, a slightly yellow oil (compound **3.72**) was obtained, that was used immediately as reagent for the synthesis of α,β-unsaturated phosphonate esters.

^{1}H NMR (300 MHz, $CDCl_3$): δ 1.12 (6H, t, *J*= 7.1 Hz, 2 x *O*CH_2CH_3), 1.27 (1H, d, *J*= 7.5 Hz, CH), 3.81-3.93 (4H, m, 2 x *O*CH_2CH_3), 7.40-7.74 (15H, m, PPh_3). (The ^{1}H NMR spectrum is accordance with the literature report.[191])

2.7.2 Experimental Assays

Assay of PLC Activity Stimulated by the $P2Y_2$ Receptor

A stable cell line for study of the human $P2Y_2$ receptor was generated by retroviral expression of the receptor in 1321N1 human astrocytoma cells, which do not natively express P2Y receptors. Agonist-induced [^{3}H]inositol phosphate production was measured in 1321N1 cells plated to 20,000 cells/well on 96-well plates two days prior to assay. Sixteen hours before the assay, the inositol lipid pool of the cells was radiolabeled by incubation in 100 µL of serum-free inositol-free Dulbecco's modified Eagle's medium, containing 1.0 µCi of myo-[^{3}H]inositol. No changes of medium were made subsequent to the addition of [^{3}H]inositol. On the day of the assay, cells were challenged with 25 µL of the five-fold concentrated solution of receptor agonists in 200 mM Hepes, pH 7.3 in HBSS, containing 50 mM LiCl for 30 min at 37 °C. Incubations were terminated by aspiration of the drug-containing medium and addition of 450 µL of ice-cold 50 mM formic acid. [^{3}H]Inositol phosphate accumulation was quantified using scintillation proximity assay methodology as previously described in detail.[205]

Data Analysis

Agonist potencies (EC_{50} values) were determined from concentration-response curves by non-linear regression analysis using the GraphPad software package Prism (GraphPad, San Diego, CA). All experiments examining the activity of newly synthesized molecules also included full concentration effect curves for UTP at the $P2Y_2$ receptor. Each concentration of drug was tested in triplicate assays, and concentration effect curves for each test drug were repeated in at least three separate experiments with freshly diluted molecule. The results are presented as mean ± SEM from multiple experiments or in the case of concentration effect curves from a single experiment carried out with triplicate assays that were representative of results from multiple experiments.

PART IV

SYNTHESIS OF 5-SUBSTITUTED 2’-DEOXYURIDINE-5’-PHOSPHONATE ANALOGUES AND EVALUATION OF THEIR ANTIVIRAL ACTIVITY

1 INTRODUCTION

During the past two decades, antiviral drugs have become crucial in the management of several viral infections, including human HSV, HIV, HBV, HCV and cytomegalovirus (HCMV) infections. Prominent among these drugs are nucleoside analogues, which can act as potent antiviral agents owing to their ability to inhibit viral polymerases, which have key roles in the various viral life cycles.[210]

1.1 2'-DEOXYPYRIMIDINES AS ANTIVIRAL AGENTS

Many 2'-deoxypyrimidine derivatives have been synthesized and evaluated for their antiviral activities. Several analogues showed activity against DNA viruses (e.g., HSV, varicella zoster virus, Epstein-Barr virus (EBV) and HBV), however, some nucleosides of this class are cytotoxic to the host cells due to the poor selectivity of their triphosphate metabolites toward the viral DNA polymerases vs. the cellular host polymerases.

1.1.1 5-Modified 2'-Deoxyuridine Analogues

5-Iodo-2'-deoxyuridine (**4.1**, IdU), originally designed as a potential antitumor drug, was the first 2'-deoxynucleoside which showed selective and potent anti-herpes activity. Subsequently, 5-trifluoromethyl-2'-deoxyuridine (**4.2**, trifluridine) and 5-ethyl-2'-deoxyuridine (**4.3**, EdU) proved active against herpes simplex viruses and are currently used for the treatment of herpetic keratitis (Figure IV.1). IdU, trifluridine and EdU are phosphorylated to their monophosphates by virus-encoded thymidine kinases, followed by two phosphorylation steps by host kinases. Once converted into their active triphosphates, the latter act as selective inhibitors of HSV DNA polymerases.[211]

Introduction of a (*E*)-5-(2-bromovinyl) moiety at position 5 of 2'-deoxyuridine resulted in analogue **1.10** (Figure IV.1), which proved highly potent and active against herpes simplex virus 1 and VZV. BVDU has been used for many years, albeit at a limited scale, for the topical treatment of herpetic keratitis and for the oral treatment of VZV infections.[212]

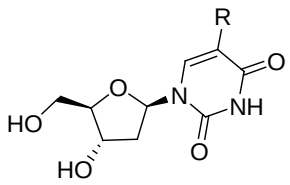

4.1: R = I
4.2: R = CF_3
4.3: R = Et

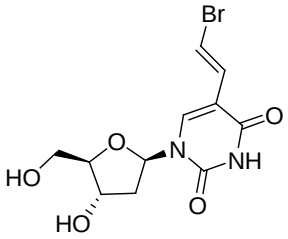

1.10

Figure IV.1

During the last decade, many publications have appeared on the synthesis and antiviral activity of 5-modified 2'-deoxyuridine analogues. Several substituents have been introduced at C-5, including alkoxymethyl groups,[213] azoles[214] and alkyloximes.[214] Several analogues proved moderately to highly active against HSV. These results showed that modification at position 5 of 2'-deoxyuridine represents an interesting approach in the search for new anti-herpes agents.

1.1.2 Bicyclic Nucleoside Analogues (BCNs)

Bicyclic nucleoside analogues with a furanopyrimidine base moiety (Figure IV.2) were discovered serendipitously as unwanted by-products from the Pd-catalyzed coupling of 5-iodo pyrimidine nucleosides with terminal alkynes. Bicyclic nucleoside analogue **4.4**, which shows structural resemblance to compound **1.68**, is inactive against HSV-1/2, CMV and VZV *in vitro*. However, several analogues containing a longer aliphatic chain (R = *n*-C_8H_{17} to *n*-$C_{10}H_{21}$) substituted at position 6 of the furanopyrimidine base showed highly potent and specific activity against VZV. With an EC_{50} of 0.008-0.01 µM, derivative **4.5** was the most potent compound in this series. Introduction of a substituted phenyl group at position 6 increased antiviral activity: compound **4.6** (FV 100) showed an EC_{50} value of 0.1-0.5 nM against VZV, being at least 1000 times more active than acyclovir.[215,216]

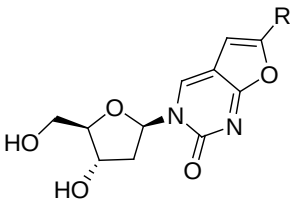

4.4: X = H
4.5: X = *n*-C_8H_{17}
4.6: X = 4-pentylphenyl

Figure IV.2

1.1.3 Carba 2'-Deoxyuridine Analogues

The carba analogs of some 2'-deoxypyrimidine nucleosides were tested for their antiviral potency and showed activity against HSV-1/2. Among them, carba-IdU (**4.7**) and carba-BVDU (**4.8**) showed comparable potency and selectivity against HSV-1/2 as their parent nucleosides (IdU and BVDU). Interestingly, also their (+)-enantiomers **4.9** and **4.10** were active against HSV-1 (Figure IV.3).[217,218]

1.1.4 1,5-Anhydro-2,3-dideoxy-D-*arabino*-hexitol Analogues

1,5-Anhydro-2,3-dideoxy-D-*arabino*-hexitol nucleosides (Figure IV.3) can be considered as 'ring-expanded' 2'-deoxynucleoside analogs where a methyl group is inserted between the ring oxygen and the anomeric carbon atom. Among them, 1,5-anhydro-2,3-dideoxy-2-(5-iodouracil-1-yl)-D-*arabino*-hexitol (**4.11**) and 1,5-anhydro-2,3-dideoxy-2-(5-trifluoromethyluracil-1-yl)-D-*arabino*-hexitol (**4.12**) showed potent activity against HSV-1 (EC_{50}: 0.025 µg/mL for both) and HSV-2 (EC_{50}: 0.5 µg/mL and 0.38 µg/mL, respectively), comparable to acyclovir.[219,220,221]

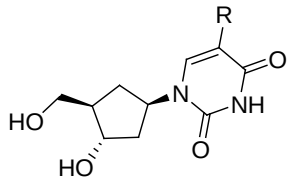

4.7: R = I
4.8: R = (*E*)-2-bromovinyl

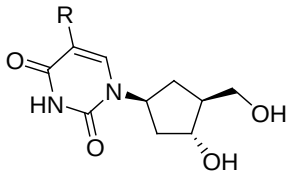

4.9: R = I
4.10: R = (*E*)-2-bromovinyl

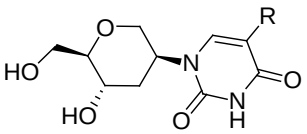

4.11: R = I
4.12: R = CF_3

Figure IV.3

1.1.5 Conformational Preference of 2'-Deoxypyrimidines as Antiviral Agents

For antiviral 2'-deoxyribonucleosides, where the desired biological response is principally derived from the incorporation of the drug into DNA, the ability of the molecule to interact effectively with three activating kinases and the target cellular or viral DNA polymerase is of vital importance. Although the sugar ring of nucleosides is flexible and can adopt several conformations, two identifiable dynamically interconverting conformations have been observed in solution: North and South. When nucleosides bind to the active site of enzymes, one conformer interacts selectively with the enzyme. For this reason, locked nucleosides ((North)-methanocarbathymidine (*N*-MCT) and (South)-methanocarbathymidine (*S*-MCT) (Figure IV.4)) have been used to probe the conformational preference of individual enzymatic steps. The herpes kinases showed a distinct bias for *S*-MCT, while DNA polymerases almost exclusively incorporate the *N*-MCT-5'-TP. As a result, only *N*-MCT demonstrated potent antiviral activity against herpes simplex viruses 1 and 2 and Kaposi's sarcoma-associated herpesvirus.[222]

This differential conformational preference of the activating kinases and the target polymerases make the development of new antiviral nucleosides very challenging: for the activation into their active form the nucleoside analogues should adopt the Southern conformation, while for their antiviral activity against DNA polymerases the Northern conformation is preferred.[222]

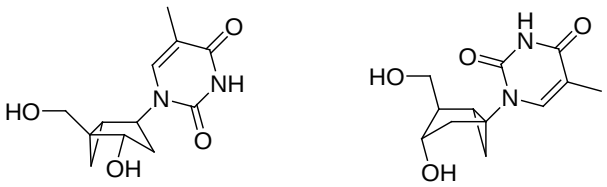

N-MCT *S*-MCT

Figure IV.4. Bicyclo[3.1.0]hexane nucleosides locked in two non-equilibrating North (*N*-MCT) and South (*S*-MCT) conformations.[222]

1.2 NUCLEOSIDE PHOSPHONATES AS ANTIVIRAL AGENTS

Structural modifications, either on the base or the sugar moiety of a natural nucleoside is a commonly used method in the search for new antiviral agents. One should keep in mind that the viral nucleic acid biosynthesis can only be disturbed when the nucleoside analogue is converted into its corresponding triphosphate form.[223] The first step in this process, the phosphorylation of the nucleoside analogue into its 5'-monophosphate counterpart by nucleoside kinases, is often rate limiting in the conversion to the active metabolite. One way to overcome this bottleneck is to devise prodrugs that are capable of delivering the nucleoside monophosphate intracellularly.[224,225] Another approach to bypass the first phosphorylation step is to use phosphonate analogs, that, after intracellular conversion into their corresponding diphosphophosphonate forms, can exhibit antiviral activities.

Currently, three acyclic nucleoside phosphonate prodrugs have been licensed for the treatment of viral infections: adefovir dipivoxil (**4.13**) for the treatment of chronic hepatitis B, tenofovir disoproxil fumarate (**4.14**) for the treatment of HIV & HBV infections and cidofovir (**4.15**) for the treatment of CMV retinitis in AIDS patients. Likewise, a few nucleoside phosphonates with a cyclic sugar moiety (e.g., **4.16, 4.17** and **4.18**) were identified as potent antiviral agents without possessing cytotoxic activity (Figure IV.5).[226]

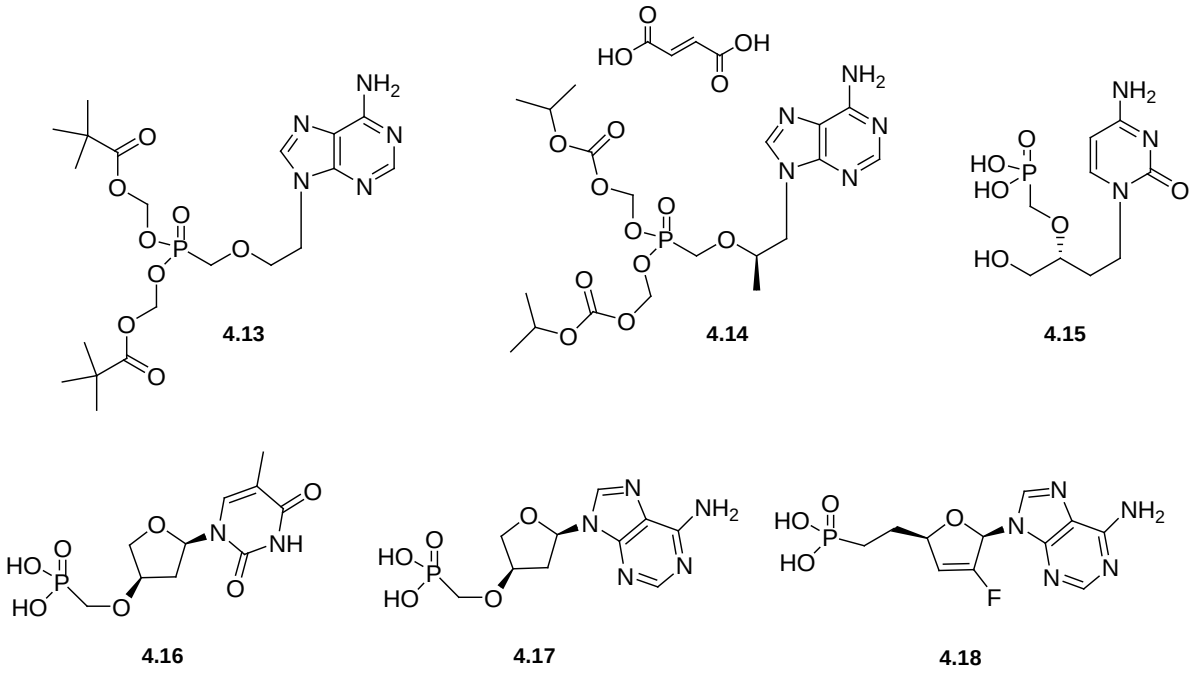

Figure VI.5

2 5-MODIFIED 2'-DEOXYURIDINE 5'-PHOSPHONATE ANALOGUES

2.1 OBJECTIVES

Modification of naturally occurring nucleosides is an important area in the development of new antiviral agents. A number of C-5 modified 2'-deoxypyrimidine analogues are known to possess potent and selective antiviral activity (cf. infra). However, relatively few examples of 5-(hetero)aryl-modified nucleosides with promising antiviral activity have been reported.[227] This may be due to the fact that these nucleosides are not efficiently converted into their triphosphate form. This led us to investigate a small series of 2'-deoxyuridine analogues that combine different aromatic substituents at position 5 of the base with a 5'-methylene phosphonate group to bypass a possibly difficult first intracellular phosphorylation step. All compounds will be evaluated against a panel of different viruses.

2.2 CHEMISTRY

2.2.1 Attempted Synthesis of 2'-Deoxyuridine 5'-Methylene Phosphonate **4.24**

The synthesis of the target phosphonate is depicted in Scheme IV.1 and started from 2'-deoxyuridine. After protection of the 3'- and 5'-OH as TBDMS ethers, the primary hydroxyl group was selectively deprotected using HF·pyridine.[228] Conversion of nucleoside **4.20** to the vinylic phosphonate **4.21** was accomplished following the same two-step procedure as described for **3.33**. Catalytic hydrogenation of **4.21** in the presence of Pd/C followed by the treatment of **4.22** with a 1M TBAF solution afforded phosphonate **4.23**. Treatment of **4.23** with TMSBr in CH_2Cl_2 to deprotect the phosphonate ester caused concomitant anomerisation as revealed by ^{1}H NMR analysis of the anomeric mixture. Attempts to separate **4.24** and **4.25** using flash chromatography and RP-HPLC were unsuccessful.

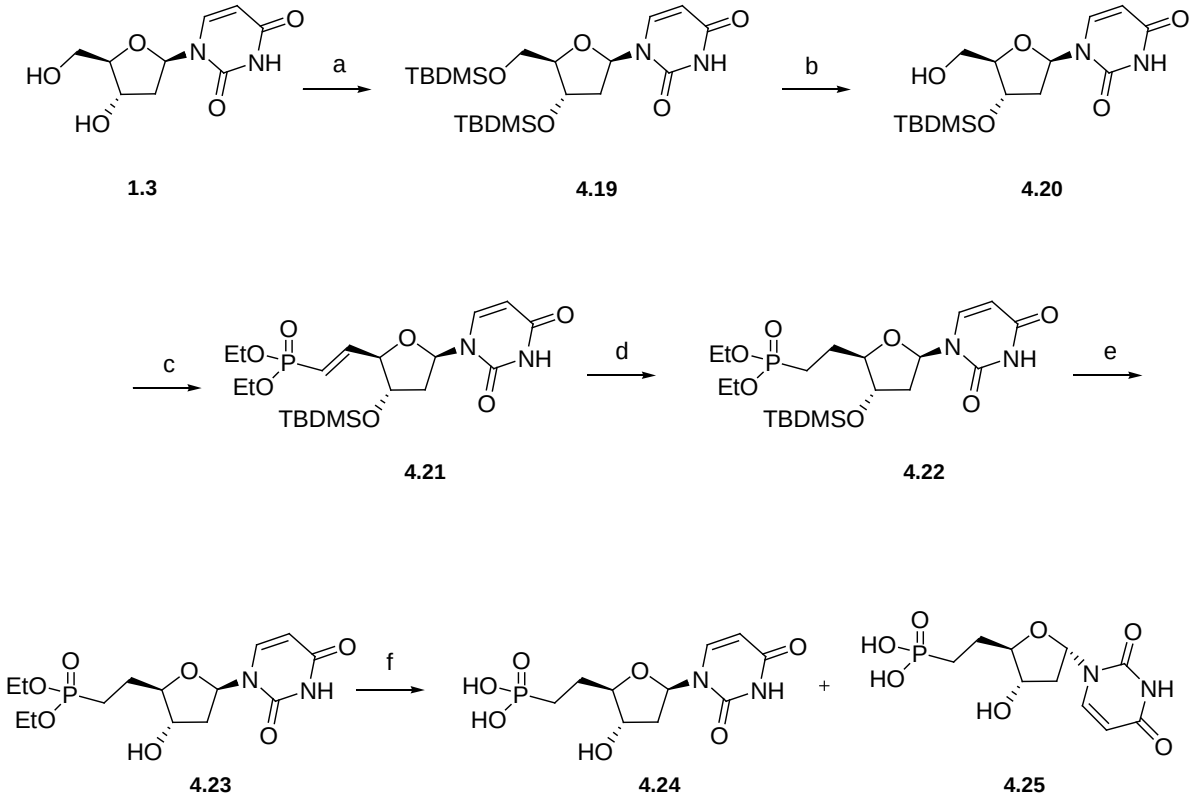

Scheme IV.1. Reagents and conditions. (a) TBDMSCl, imidazole, DMF, rt, 20 h, 100%; (b) HF·pyridine, THF, 0 °C → rt, 2 h, 43%; (c) (i) IBX, CH_3CN, 80 °C, 6 h; (ii) **3.72**, DMSO, rt, 20 h, 41% over 2 steps; (d) H_2, Pd/C, MeOH, rt, overnight, 97%; (e) 1M TBAF in THF, rt, 3 h, 69%; (f) TMSBr, CH_2Cl_2, rt, overnight, 65%.

To avoid the anomerisation issue, we attempted to deprotect **4.23** in the presence of TMSBr under different reaction conditions. Following the reaction via ^{31}P NMR, we observed anomerisation immediately after addition of TMSBr. Attempts at different temperatures learned that no reaction occurred under -20 °C, and that anomerisation started simultaneously with the phosphonate hydrolysis, even at low temperature. Also the addition of an acid scavenger (e.g., bis(trimethylsilyl)acetamide or 2,6-lutidine) could not prevent anomerisation.[229]

Finally, we tried to obtain phosphonate **4.24** by removing the phosphonate protecting groups prior to desilylation of 3'-OH. Unfortunately, treatment of **4.22** with TMSBr in CH_2Cl_2 resulted again in a mixture of **4.24** and **4.25**. Under these reaction conditions, the 3'-OH protecting group was removed as well. (Scheme IV.2).

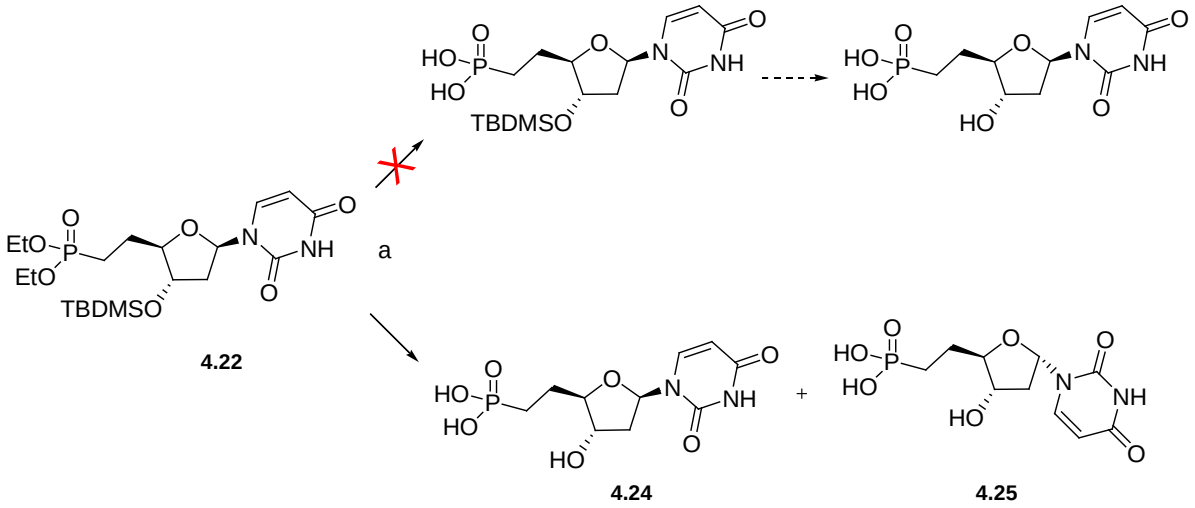

Scheme IV.2. Reagents and conditions. (a) TMSBr, CH_2Cl_2, rt, overnight, 22%.

2.2.2 Synthesis of 5-Modified 2'-Deoxyuridine 5'-Methylene Phosphonate Analogues

A series of 5-modified 2'-deoxyuridine 5'-methylene phosphonate analogs could be obtained using the same strategy described for the synthesis of compounds **3.44-3.51**. Starting from **4.22**, selective bromination[116] followed by a palladium-catalyzed cross-coupling[192] with four commercial aryl and heteroaryl boronic acids gave access to a compounds **4.27-4.31** (Scheme IV.3). After removing the silyl protecting group with TBAF, deprotection of the phosphonate esters was performed using TMSBr in CH_2Cl_2. Except for the furan derivative, which degraded during the last step, final deprotection resulted in a 2:1 mixture of the α- and β-isomer, which could be separated using RP-HPLC.

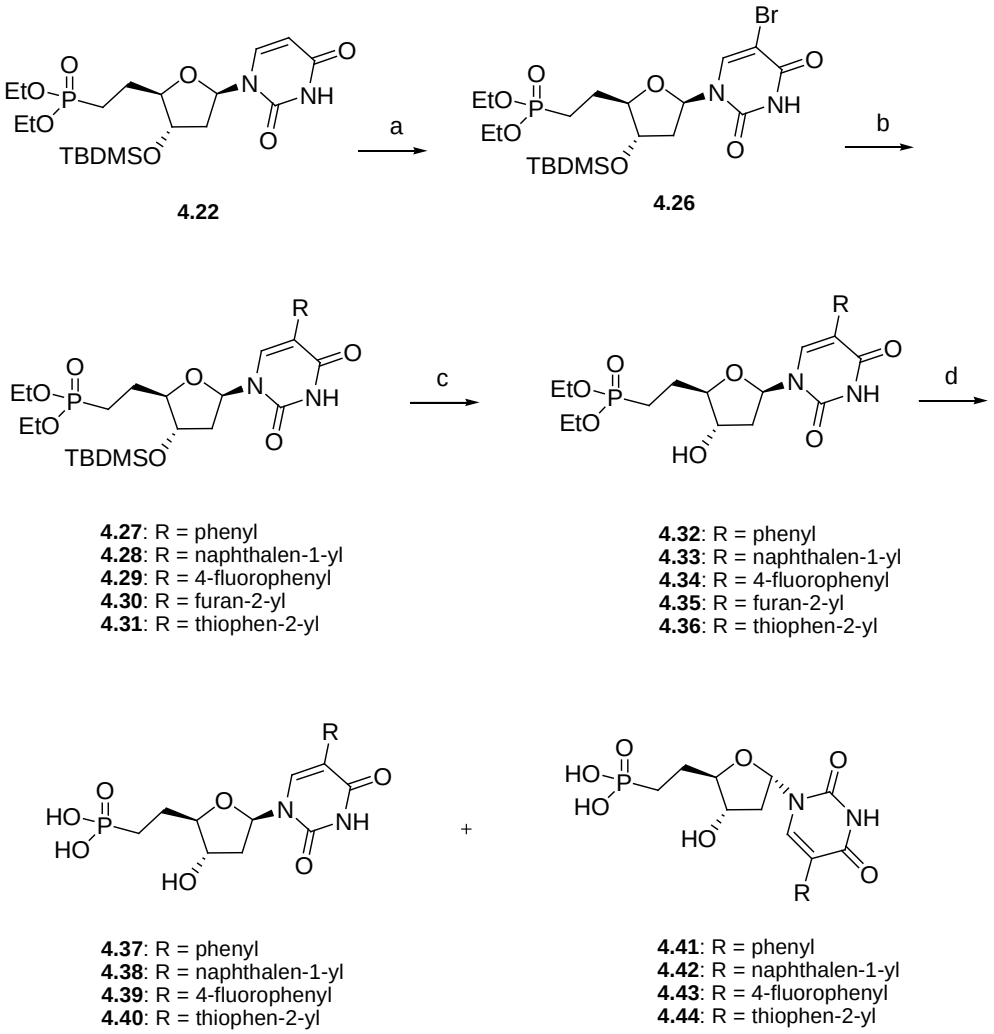

Scheme IV.3. Reagents and conditions. (a) NBS, DMF, rt, overnight, 49%; (b) R-B(OH)$_2$, Na_2CO_3, $Pd(PPh_3)_4$, DMF, H_2O, reflux, 4 h, 75-91%; (c) 1M TBAF in THF, rt, 1 h, 32-71%; (d) TMSBr, CH_2Cl_2, rt, overnight, 4-19%.

From a chemical point of view, it would have been interesting to investigate the influence of a 6 modification on the anomerisation during phosphonate deprotection. We anticipate that introduction of a 6-substituent could have a bigger impact on this phenomenon than a 5 modification. Introduction of an electron withdrawing group is believed to reduce or prevent isomerisation whereas an electron donating group could facilitate isomerisation. Unfortunately, a shortage of time prevented us to explore this hypothesis.

2.3 STRUCTURE ANALYSIS

To identify the α- and β-isomers of the 5-modified 2'-deoxyuridine 5'-methylene phosphonate analogues, a stereochemical assignment of compound **4.37** was performed in the NMR and Structure Analysis Unit of the Department of Organic Chemistry (UGent). The 2D ROESY spectrum of compound **4.37** is depicted in Figure IV.6. A clear rOe contact between H-4' and H-2'b (proton down) and a much weaker interaction between H-6 and H-2'b proved that H-4' and H-6 were not positioned at the same side of the furanose ring. The β-configuration of the nucleobase was further established by the presence of a strong interaction between H-6 and H-5'a,b (Figure IV.6).

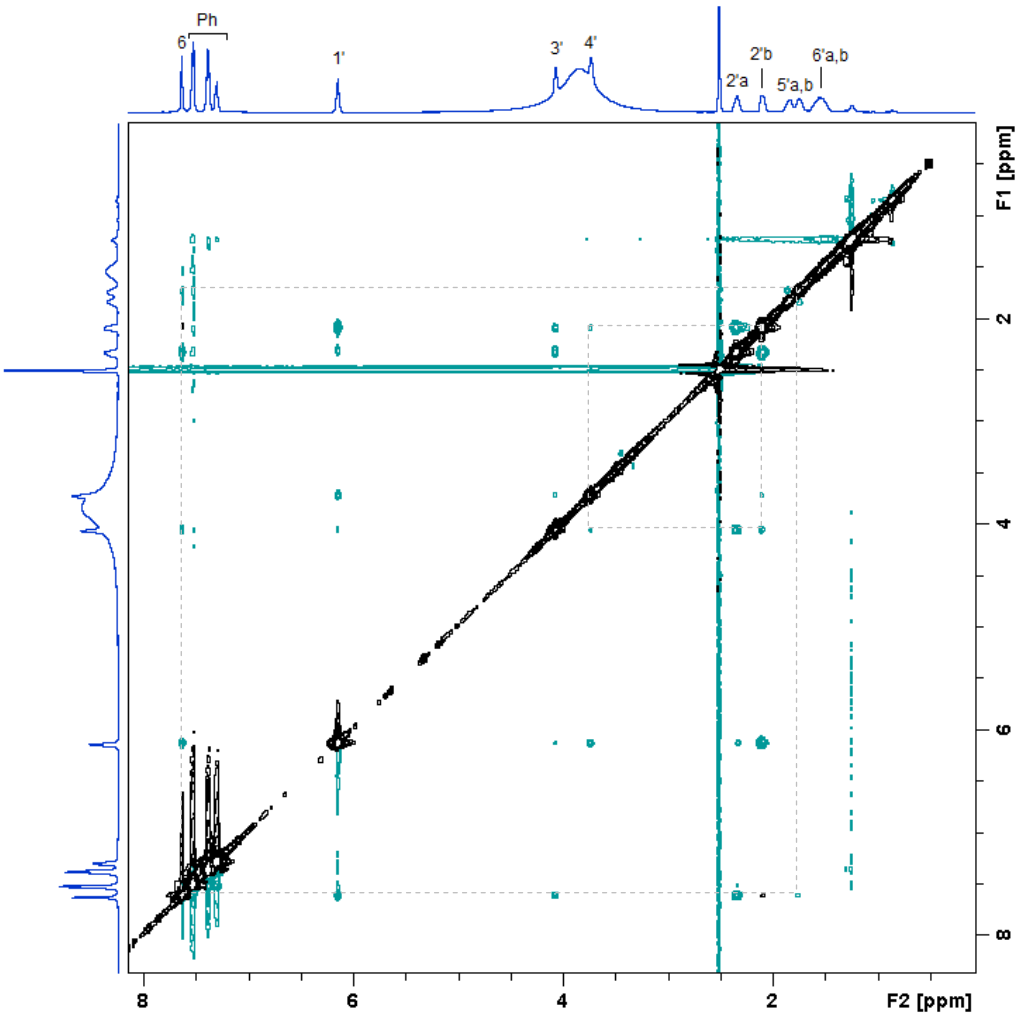

Figure IV.6. 2D ROESY (500.13 MHz, 298.0 K) spectrum of compound **4.37**.

2.4 BIOLOGICAL EVALUATION

All compounds were evaluated for their antiviral activity against a broad panel of viruses including HSV-1 (KOS), HSV-2 (G), vaccinia virus (VV), vesicular stomatitis virus (VSV), thymidine kinase deficient HSV-1 TK$^-$ (KOS ACV^r), HCMV and VZV in HEL (human embryonic lung) cell cultures; and HIV-1 (III_B) and HIV-2 (ROD) in human T-lymphocyte (CEM) cell cultures (performed in the Laboratory of Virology and Chemotherapy (Rega Institute, K.U.Leuven)) (Tables IV.1-IV.3). The activities of the compounds were compared with reference antiviral drugs: brivudin, cidofovir, acyclovir and ganciclovir.

Table IV.1. Antiviral activity and cytotoxicity of 5-modified 2'-deoxyuridine phosphonate analogues against HSV-1, HSV-2, VV, VSV and HSV-1 TK$^-$ in HEL cell cultures.

Compound	EC_{50}[a] (μM)					MCC[b] (μM)
	HSV-1 (KOS)	HSV-2 (G)	VV	VSV	HSV-1 TK$^-$ (KOS ACV^r)	
4.37	> 100	> 100	> 100	> 100	> 100	> 100
4.38	> 100	> 100	> 100	> 100	> 100	> 100
4.39	> 100	> 100	> 100	> 100	> 100	> 100
4.40	> 100	> 100	> 100	> 100	> 100	> 100
4.41	> 100	> 100	> 100	> 100	> 100	> 100
4.42	> 100	> 100	> 100	> 100	> 100	> 100
4.43	> 100	> 100	> 100	> 100	> 100	> 100
4.44	> 100	> 100	> 100	> 100	> 100	> 100
Brivudin	0.4	250	10	> 250	250	> 250
Cidofovir	2	1	10	> 250	2	> 250
Acyclovir	0.2	0.2	> 250	> 250	112	> 250
Ganciclovir	0.01	0.01	> 100	> 100	20	> 100

[a]50%-Effective concentration or compound concentration required to reduce virus-induced cytopathogenicity by 50%.

[b]Minimum cytotoxic concentration or compound concentration required to cause a microscopically detectable alteration of normal cell morphology.

Table IV.2. Antiviral activity and cytotoxicity of 5-modified 2'-deoxyuridine phosphonate analogues against different HCMV and VZV strains in HEL cell cultures.

Compound	EC_{50}[a] (µM)				Cytotoxicity (µM)	
	HCMV AD-169	HCMV Davis	VZV OKA	VZV TK^- 07/1	Cell morphology[b] (MCC)	Cell growth[c] (CC_{50})
4.37	> 100	> 100	> 100	> 100	> 100	
4.38	45	45	100	100	> 100	> 100
4.39	> 20	41	> 20	> 20	≥ 100	> 100
4.40	55	63	> 100	> 100	> 100	100
4.41	> 100	> 100	> 100	> 100	> 100	
4.42	45	> 20	100	100	≥ 100	> 100
4.43	> 100	> 100	> 100	> 100	> 100	
4.44	> 100	> 100	> 100	> 100	> 100	
Acyclovir			1.3	37	> 440	
Brivudin			0.026	12	> 300	
Ganciclovir	7.9	7.0			≥ 394	141
Cidofovir	0.67	0.95			≥ 317	63

[a]Effective concentration required to reduce virus-induced cytopathicity by 50%. Virus input was 100 plaque forming units (PFU).

[b]Minimum cytotoxic concentration or compound concentration that caused a microscopically detectable alteration of cell morphology.

[c]50%-Cytotoxic concentration or compound concentration required to reduce cell growth by 50%.

Table IV.3. Antiviral activity of 5-modified 2'-deoxyuridine phosphonate analogues in human T-lymphocyte (CEM) cell cultures.

Compound	EC_{50}[a](μM)		CC_{50}[b] (μM)
	HIV-1	HIV-2	
4.37	> 250	> 250	> 250
4.38	> 50	> 50	> 250
4.39	> 50	> 50	> 250
4.40	> 50	> 50	> 250
4.41	> 50	> 50	> 250
4.42	> 50	> 50	> 250
4.43	> 50	≥ 50	> 250
4.44	>50	> 50	> 250

[a]EC_{50} = effective concentration or compound concentration required to protect CEM cells against the cytopathogenicity of HIV by 50%

[b]CC_{50} = 50%-cytostatic concentration for the proliferation on T-lymphocyte CEM cells

None of the tested compounds showed toxicity to any of the tested cell lines. However, the final compounds **4.37-4.40** and **4.41-4.44** failed to show antiviral activity against HSV-1, HSV-2, VV, VSV, HSV-1 TK^- and different VZV strains (Tables IV.1 and IV.2). Also in the human T-lymphocyte (CEM) cell cultures (Table IV.3), none of these compounds showed activity against HIV-1 or HIV-2. Very weak antiviral activity was observed for the β-analogue **4.39** and the α-analogue **4.42** against HCMV Davies and HCMV AD-169, respectively, while compounds **4.38** and **4.40**, showed weak antiviral activity against both HCMV strains. The most active compound of this series, analogue **4.38**, was at least 6 or 50 times less active than ganciclovir and cidofovir, respectively.

2.5 CONCLUSIONS

This chapter described the synthesis, stereochemical assignment and antiviral activity of a small series of 2'-deoxyuridine analogues that combined different aromatic substituents at position 5 of the base with a 5'-methylene phosphonate modification at the sugar moiety. All compounds were synthesized via an 8-step procedure, featuring a Wittig reaction and Suzuki-Miyaura coupling. An unexpected anomerisation during the last step of the synthesis allowed us to investigate the β- as well as the α-anomers of the corresponding phosphonates. None of these analogues exhibited significant antiviral activity.

2.6 EXPERIMENTAL PART

2.6.1 Synthesis

3',5'-Di-*O*-*tert*-butyldimethylsilyl-2'-deoxy-β-D-uridine (4.19)

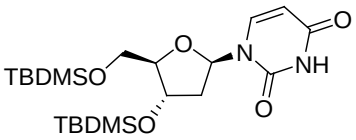

2'-Deoxyuridine (5.64 g, 24.72 mmol) was dissolved in dry DMF (50 mL). Imidazole (7.41 g, 108.77 mmol) and *tert*-butyldimethylsilyl chloride (9.32 g, 61.8 mmol) were added with stirring. After 20 h at rt, TLC in CH_2C_2/MeOH (95:5) showed a single spot. DMF was removed *in vacuo* and the residue was dissolved in CH_2Cl_2. The mixture was washed with a sat. aq. $NaHCO_3$ solution, followed by brine. The organic layer was dried over $MgSO_4$ and filtered. After evaporation, no further purification was needed to obtain pure compound **4.19** as a white foam (11.72 g, 100%).

^{1}H NMR (300 MHz, DMSO-d_6): δ 0.071-0.092 (12H, m, 2 x TBDMS), 0.86-0.89 (18H, m, 2 x TBDMS), 2.08-2.28 (2H, m, H-2'a and H-2'b), 3.67-3.81 (3H, m, H-4', H-5'a and H-5'b), 4.35-4.39 (1H, m, H-3'), 5.58 (1H, d, *J*= 8.1 Hz, CH=CH), 6.13 (1H, t, *J*= 6.6 Hz, H-1'), 7.28 (1H, d, *J*= 8.1 Hz, CH=CH), 11.33 (1H, s, 3-NH).

^{13}C NMR (75 MHz, DMSO-d_6): δ -5.58, -4.98 and -4.77 (TBDMS), 17.98 (TBDMS), 25.66 and 25.75 (TBDMS), 62.36 (C-5'), 71.43 (C-3'), 84.05 (C-1'), 86.67 (C-4'), 101.70 (C-5), 140.20 (C-6), 150.36 (C-2), 163.04 (C-4).

Exact mass (ESI-MS) for $C_{21}H_{41}N_2O_5Si_2$ $[M+H]^+$ found, 457.2747 ; calcd, 457.2549.

3'-*O*-*tert*-Butyldimethylsilyl-2'-deoxy-β-D-uridine (4.20)

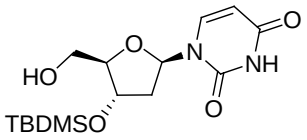

In a 250 mL polyethylene vial, compound **4.19** (1.41 g, 3.09 mmol) was dissolved in THF (32 mL). The vial was cooled to 0 °C and hydrogen fluoride-pyridine complex buffered with pyridine (19 mL of a stock solution made from 5 mL of pyridine, 12.5 mL of THF and 4.5 mL of hydrogen fluoride-pyridine) was added. The reaction mixture was stirred at 0 °C for 1 h and another hour at rt. Then it was carefully poured into a sat. $NaHCO_3$ solution. The organic layer was separated and the aqueous layer

was extracted with EtOAc. The combined organic extracts were dried over $MgSO_4$, filtered and concentrated. The crude residue was purified by flash chromatography over silica gel (CH_2Cl_2/MeOH 97:3) to give 455 mg of compound **4.20** (white solid, 43%).

^{1}H NMR (300 MHz, DMSO-d_6): δ 0.081 (6H, s, TBDMS), 0.87 (9H, s, TBDMS), 2.04-2.21 (2H, m, H-2'a and H-2'b), 3.54 (2H, dd, *J*= 4.2 Hz, *J*= 9.0 Hz, H-5'a and H-5'b), 3.76 (1H, dd, *J*= 3.6 Hz, *J*= 6.6 Hz, H-4'), 4.39-4.43 (1H, m, H-3'), 5.06 (1H, t, *J*= 5.4 Hz, 5'-OH), 5.63 (1H, d, *J*= 7.8 Hz, CH=CH), 6.14 (1H, t, *J*= 7.5 Hz, H-1'), 7.81 (1H, d, *J*= 7.8 Hz, CH=CH), 11.29 (1H, s, 3-NH).

^{13}C NMR (75 MHz, DMSO-d_6): δ -4.98 and -4.82 (TBDMS), 17.70 (TBDMS), 25.68 (TBDMS), 60.87 (C-5'), 72.03 (C-3'), 83.98 (C-1'), 87.42 (C-4'), 101.86 (C-5), 147 (C-6), 150.48 (C-2), 163.35 (C-4).

Exact mass (ESI-MS) for $C_{15}H_{27}N_2O_5Si$ $[M+H]^+$ found, 343.1707; calcd, 343.1684.

1-[3-*O*-*tert*-Butyldimethylsilyl-2,5,6-trideoxy-6-(diethoxyphosphinyl)-β-D-*ribo*-hex-5-enofuranosyl]uracil (4.21)

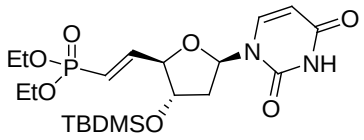

IBX (550 mg, 1.97 mmol) was added to a solution of **4.20** (449 mg, 1.31 mmol) in CH_3CN (12 mL) and the resulted suspension was stirred at 80 °C for 6 h. After cooling in an ice bath (15 min), the solid was removed by filtration and washed with cold CH_3CN. The solvent was evaporated and the residue was co-distilled with toluene. The residue was dissolved in anhydrous DMSO (3.4 mL) and freshly prepared **3.72** in DMSO (3.4 mL) was added. After 20 h, the mixture was poured into water and extracted with CH_2Cl_2. The combined organic layers were dried over $MgSO_4$, filtered and concentrated *in vacuo*. The residue was lyophilized to remove the remaining DMSO and purified on a silica gel column (CH_2Cl_2/MeOH 98:2) yielding 257 mg (41%) of **4.21** as a colourless solid.

^{1}H NMR (300 MHz, DMSO-d_6): δ 0.070 (6H, s, TBDMS), 0.87 (9H, s, TBDMS), 1.23 (6H, app dt, *J*= 1.5 Hz, *J*= 6.9 Hz, 2 x OCH_2CH_3), 2.13-2.22 (1H, m, H-2'a), 2.34-2.43 (1H, m, H-2'b), 3.92-4.03 (4H, m, 2 x OCH_2CH_3), 4.20-4.25 (1H, m, H-4'), 4.38-4.45 (1H, m, H-3'), 5.64 (1H, d, *J*= 7.8 Hz, CH=CH), 5.96-6.09 (1H, m, H-6'), 6.16 (1H, dd, *J*= 6.0 Hz, *J*= 7.5 Hz, H-1'), 6.60-6.75 (1H, m, H-5'), 7.68 (1H, d, *J*= 8.4 Hz, CH=CH), 11.34 (1H, s, 3-NH).

^{31}P NMR (DMSO-d_6): δ 17.21.

^{13}C NMR (75 MHz, DMSO-d_6): δ -5.02 and -4.87 (TBDMS), 16.10 and 16.18 (2 x OCH_2CH_3), 17.60 (TBDMS), 25.57 (TBDMS), 61.21 and 61.31 (2 x OCH_2CH_3), 74.36 (C-3'), 84.27 and 85.27 (C-1' and C-4'), 102.07 (C-5), 118.48 (C-6'), 141.38 (C-6), 147.81 (C-5'), 150.29 (C-2), 162.98 (C-4).

Exact mass (ESI-MS) for $C_{20}H_{36}N_2O_7PSi$ $[M+H]^+$ found, 475.2035; calcd, 475.2024.

1-[3-*O*-*tert*-Butyldimethylsilyl-2,5,6-trideoxy-6-(diethoxyphosphinyl)-β-D-*ribo*-hexofuranosyl]-uracil (4.22)

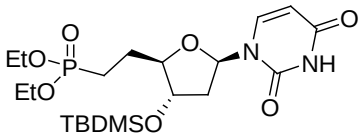

To a solution of compound **4.21** (257 mg, 0.54 mmol) in MeOH (8 mL) was added 10% Pd/C. The reaction mixture was stirred under hydrogen atmosphere overnight. The catalyst was removed by filtration through Celite and the filtrate was evaporated to yield pure compound **4.22** (250 mg, 97%) as a colourless solid.

^{1}H NMR (300 MHz, DMSO-d_6): δ 0.084 (6H, app d, *J*= 2.4 Hz, TBDMS), 0.87 (9H, s, TBDMS), 1.22 (6H, t, *J*= 6.9 Hz, 2 x OCH_2CH_3), 1.65-1.86 (4H, m, H-5'a, H-5'b, H-6'a and H-6'b), 2.00-2.15 (1H, m, H-2'a), 2.22-2.31 (1H, m, H-2'b), 3.68-3.72 (1H, m, H-3'), 3.92-4.04 (4H, m, 2 x OCH_2CH_3), 4.23-4.29 (1H, m, H-4'), 5.62 (1H, d, *J*= 8.1 Hz, CH=CH), 6.10 (1H, t, *J*= 6.6 Hz, H-1'), 7.59 (1H, d, *J*= 8.4 Hz, CH=CH), 11.32 (1H, s, 3-NH).

^{31}P NMR (DMSO-d_6): δ 31.72.

^{13}C NMR (75 MHz, DMSO-d_6): δ -5.04, -4.99 and -4.73 (TBDMS), 16.21 and 16.28 (2 x OCH_2CH_3), 17.58 (TBDMS), 20.04 (C-6'), 21.90 (C-5'), 25.61 and 25.77 (TBDMS), 60.90 and 60.97 (2 x OCH_2CH_3), 73.84 (C-3'), 83.61 and 84.95 (C-1' and C-4'), 102.10 (C-5), 141.03 (C-6), 150.40 (C-2), 163.11 (C-4).

Exact mass (ESI-MS) for $C_{20}H_{38}N_2O_7PSi$ $[M+H]^+$ found, 477.2119; calcd, 477.2180.

1-[2,5,6-Trideoxy-6-(diethoxyphosphinyl)-β-D-*ribo*-hexofuranosyl]uracil (4.23)

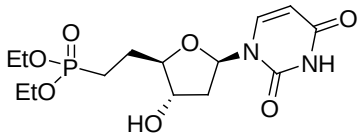

Compound **4.22** (309 mg, 0.65 mmol) was dissolved in 4.1 mL THF and a TBAF solution in THF (1M, 1.44 mL, 1.44 mmol) was added at rt. After stirring for 3 h the reaction mixture was evaporated *in vacuo* and poured on a silica column (CH_2Cl_2/MeOH 92:8) to give compound **4.23** (162 mg, 69%) as a colourless solid.

^{1}H NMR (300 MHz, DMSO-d_6): δ 1.23 (6H, t, *J*= 6.9 Hz, 2 x OCH_2CH_3), 1.68-1.82 (4H, m, H-5'a, H-5'b, H-6'a and H-6'b), 2.04-2.24 (2H, m, H-2'a and H-2"), 3.66-3.68 (1H, m, H-4'), 3.92-4.08 (5H, m, 2 x OCH_2CH_3 and H-3'), 5.30 (1H, d, *J*= 4.5 Hz, 3'-OH), 5.63 (1H, d, *J*= 8.7 Hz, CH=CH), 6.10 (1H, t, *J*= 6.6 Hz, H-1'), 7.58 (1H, d, *J*= 7.8 Hz, CH=CH), 11.31 (1H, s, 3-NH).

^{31}P NMR (DMSO-d_6): δ 31.89.

^{13}C NMR (75 MHz, DMSO-d_6): δ 16.26 and 16.33 (2 x OCH_2CH_3), 20.14 (C-6'), 22.00 (C-5'), 60.89 and 61.00 (2 x OCH_2CH_3), 72.52 (C-3'), 83.65 and 85.43 (C-1' and C-4'), 102.08 (C-5), 140.79 (C-6), 150.45 (C-2), 163.10 (C-4).

Exact mass (ESI-MS) for $C_{14}H_{24}N_2O_7P$ $[M+H]^+$ found, 363.1308; calcd, 363.1316.

1-[2,5,6-Trideoxy-6-(dihydroxyphosphinyl)-β-D-*ribo*-hexofuranosyl]uracil (4.24) and 1-[2,5,6-trideoxy-6-(dihydroxyphosphinyl)-α-D-*ribo*-hexofuranosyl]uracil (4.25)

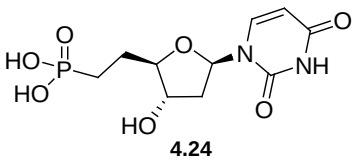

4.24

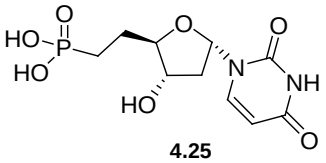

4.25

1st Method: To a solution of **4.23** (40 mg, 0.11 mmol) in CH_2Cl_2 (1.6 mL) was added TMSBr (29 µL, 0.22 mmol). After stirring overnight, the volatiles were removed *in vacuo*. The residue was dissolved in water, washed with EtOAc/Et_2O (1:1) and lyophilized. A 2:3 mixture of compounds **4.24** and **4.25** (25 mg, 65%) was obtained as a yellow powder.

2nd Method: To a solution of **4.22** (27 mg, 0.062 mmol) in CH_2Cl_2 (0.9 mL) was added TMSBr (16 µL, 0.12 mmol). After stirring overnight, the volatiles were removed *in vacuo*. The residue was dissolved in water, washed with EtOAc/Et_2O (1:1) and lyophilized. A 2:3 mixture of compounds **4.24** and **4.25** (4.1 mg, 22%) was obtained as a yellow powder.

^{1}H NMR (300 MHz, D_2O): δ 1.48-1.91 (4.4H, m, H-5'a, H-5'b, H-6'a, H-6'b and minor isomer H-2'a), 2.12-2.17 (0.6H, major isomer, m, H-2'b), 2.34-2.38 (0.6H, major isomer, m, H-2'a), 2.72-2.80 (0.4 H, minor isomer, m, H-2'b), 3.94-4.00 (0.4H, minor isomer, m, H-3'), 4.31-4.37 (1.6H, m, major isomer H-3' and H-4'), 5.85 (0.6H, major isomer, d, *J*= 7.8 Hz, CH=CH), 5.89 (0.4H, minor isomer, d, *J*= 8.1 Hz, CH=CH), 6.15 (0.6H, major isomer, dd, *J*= 2.7 Hz, *J*= 7.5 Hz, H-1'), 6.25 (0.4H, minor isomer, app t, *J*= 6.9 Hz, H-1'), 7.73 (0.4H, minor isomer, d, *J*= 8.4 Hz, CH=CH), 7.93 (0.6H, major isomer, d, *J*= 8.1 Hz, CH=CH).

^{31}P NMR (DMSO-d_6): δ 23.63.

^{13}C NMR (75 MHz, DMSO-d_6): δ 24.65 (major isomer, C-6'), 26.40 (minor isomer, C-6'), 28.06 (major isomer, C-5') 28.25 (minor isomer, C-5'), 72.72 (major isomer, C-3'), 72.86 (minor isomer, C-3'), 83.86, 85.25, 89.00 and 89.14 (C-1' and C-4'), 101.13 (major isomer, C-5), 102.33 (minor isomer, C-5), 140.64 (minor isomer, C-6), 141.67 (major isomer, C-6), 150.62 (minor isomer, C-2), 150.74 (major isomer, C-2), 163.29 (minor isomer, C-4), 163.56 (major isomer, C-4).

Exact mass (ESI-MS) for $C_{10}H_{14}N_2O_7P$ $[M-H]^-$ found, 305.0539; calcd, 305.0544.

1-[3-*O*-*tert*-Butyldimethylsilyl-2,5,6-trideoxy-6-(diethoxyphosphinyl)-β-D-*ribo*-hexofuranosyl]-5-bromouracil (4.26)

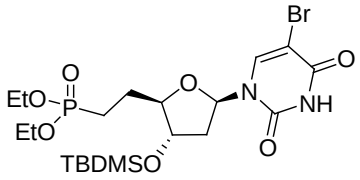

To a solution of compound **4.22** (950 mg, 1.99 mmol) in DMF (15 mL) was added *N*-bromosuccinimide (NBS, 390 mg, 2.19 mmol) under N_2. The reaction mixture was stirred at room temperature for 16 hours. DMF was removed *in vacuo* and the residue was purified by column chromatography (CH_2Cl_2/MeOH 97:3) to afford **4.26** (538 mg, 49%) as a white foam.

^{1}H NMR (300 MHz, $CDCl_3$): δ 0.082 (6H, app d, *J*= 1.8 Hz, TBDMS), 0.89 (9H, s, TBDMS), 1.34 (6H, t, *J*= 6.9 Hz, 2 x *O*CH_2CH_3), 1.82-2.02 (4H, m, H-5'a, H-5'b, H-6'a and H-6'b), 2.09-2.16 (1H, m, H-2'a), 2.29-2.32 (1H, m, H-2'b), 3.81-3.84 (1H, m, H-4'), 4.07-4.19 (5H, m, 2 x *O*CH_2CH_3, H-3'), 6.13 (1H, t, *J*= 6.3 Hz, H-1'), 7.65 (1H, s, H-6), 9.83 (1H, s, 3-NH).

^{31}P NMR ($CDCl_3$): δ 30.90.

^{13}C NMR (75 MHz, $CDCl_3$): δ -4.83 and -4.56 (TBDMS), 16.46 and 16.54 (2 x *O*CH_2CH_3), 17.89 (TBDMS), 21.38 (C-6'), 23.28 (C-5'), 25.68 (TBDMS), 40.85 (C-2'), 61.80 and 61.83 (2 x *O*CH_2CH_3), 74.50 (C-3'), 85.57 C-1'), 86.53 (C-4', d, *J*= 17.0 Hz), 97.10 (C-5), 139.01 (C-6), 149.47 (C-2), 159.03 (C-4).

Exact mass (ESI-MS) for $C_{20}H_{37}BrN_2O_7PSi$ $[M+H]^+$ found, 555.1323; calcd, 555.1286.

General procedure for the synthesis of 5-modified nucleoside phosphonates via Suzuki-Miyaura coupling

A mixture of compound **4.26** (1 equiv.), aryl boronic acid (2 equiv.), $Pd(PPh_3)_4$ (0.1 equiv.) and Na_2CO_3 (3.3 equiv.) in DMF and degassed H_2O was heated (± 130 °C, oil bath) under argon for 6 h or until TLC indicated consumption of all starting material. The mixture was then concentrated and co-distilled

with toluene. The residue was purified by column chromatography (CH_2Cl_2/MeOH 94:6-98:2) affording the 5-modified analogues in moderate yield.

1-[3-*O*-*tert*-Butyldimethylsilyl-2,5,6-trideoxy-6-(diethoxyphosphinyl)-β-D-*ribo*-hexofuranosyl]-5-phenyluracil (4.27)

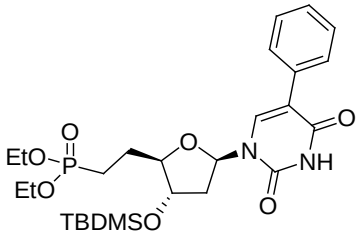

Reaction of compound **4.26** (153 mg, 0.27 mmol) with phenylboronic acid (68 mg, 0.55 mmol), $Pd(PPh_3)_4$ (32 mg, 0.027 mmol) and Na_2CO_3 (96 mg, 0.91 mmol) in DMF (6.5 mL) and degassed H_2O (0.8 mL) was performed as described in the general procedure to yield compound **4.27** as a colourless solid (120 mg, 79%).

^{1}H NMR (300 MHz, $CDCl_3$): δ 0.084 (6H, s, TBDMS), 0.90 (9H, s, TBDMS), 1.25-1.32 (6H, m, 2 x OCH_2CH_3), 1.73-2.04 (4H, m, H-5'a, H-5'b, H-6'a and H-6'b), 2.11-2.20 (1H, m, H-2'a), 2.31-2.39 (1H, m, H-2'b), 3.83-3.86 (1H, m, H-4'), 4.00-4.11 (5H, m, 2 x OCH_2CH_3 and H-3'), 6.23 (1H, app t, *J*= 6.6 Hz, H-1'), 7.33-7.71 (6H, m, Ph and H-6).

^{31}P NMR ($CDCl_3$): δ 30.69.

^{13}C NMR (75 MHz, $CDCl_3$): δ -4.73 and -4.46 (TBDMS), 16.48 and 16.56 (2 x OCH_2CH_3), 18.00 (TBDMS), 21.44 (C-6'), 23.34 (C-5'), 25.80 (TBDMS), 40.67 (C-2'), 61.86 and 61.94 (2 x OCH_2CH_3), 74.75 (C-3'), 85.30 (C-1'), 86.42 (C-4', d, *J*= 17.0 Hz), 115.67 (C-5), 128.07-133.10 (Ph), 136.95 (C-6), 150.02 (C-2), 162.39 (C-4).

Exact mass (ESI-MS) for $C_{26}H_{42}N_2O_7PSi$ $[M+H]^+$ found, 553.2485; calcd, 553.2493.

1-[3-*O*-*tert*-Butyldimethylsilyl-2,5,6-trideoxy-6-(diethoxyphosphinyl)-β-D-*ribo*-hexofuranosyl]-5-(naphthalen-1-yl)uracil (4.28)

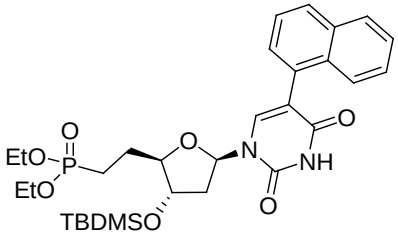

Reaction of compound **4.26** (122 mg, 0.22 mmol) with naphthalene-1-boronic acid (75 mg, 0.44 mmol), $Pd(PPh_3)_4$ (25 mg, 0.022 mmol) and Na_2CO_3 (77 mg, 0.72 mmol) in DMF (5 mL) and degassed H_2O (0.7 mL) was performed as described in the general procedure to afford compound **4.28** as a colourless solid (120 mg, 91%).

^{1}H NMR (300 MHz, $CDCl_3$): δ 0.056 (6H, s, TBDMS), 0.87 (9H, s, TBDMS), 1.15-1.24 (6H, m, 2 x OCH_2CH_3), 1.77-2.03 (4H, m, H-5'a, H-5'b, H-6'a and H-6'b), 2.12-2.18 (1H, m, H-2'a), 2.26-2.31 (1H, m, H-2'b), 3.82 (1H, app s, H-4'), 3.95-4.13 (5H, m, 2 x OCH_2CH_3 and H-3'), 6.24 (1H, app t, *J*= 6.6 Hz, H-1'), 7.42-7.82 (7H, m, naphthalene), 7.98 (1H, s, H-6), 8.43 (1H, s, 3-NH).

^{31}P NMR ($CDCl_3$): δ 30.95.

^{13}C NMR (75 MHz, $CDCl_3$): δ -4.87 and -4.62 (TBDMS), 16.28 and 16.36 (2 x OCH_2CH_3), 17.85 (TBDMS), 21.31 (C-6'), 23.21 (C-5'), 25.65 (TBDMS), 40.50 (C-2'), 61.63 and 61.71 (2 x OCH_2CH_3), 74.63 (C-3'), 85.26 (C-1'), 86.29 (C-4', d, *J*= 17.0 Hz), 115.45 (C-5), 125.89-133.22 (naphthalene), 136.91 (C-6), 149.88 (C-2), 162.26 (C-4).

Exact mass (ESI-MS) for $C_{30}H_{44}FN_2O_7PSi$ $[M+H]^+$ found, 571.2430; calcd, 603.2650.

1-[3-*O*-*tert*-Butyldimethylsilyl-2,5,6-trideoxy-6-(diethoxyphosphinyl)-β-D-*ribo*-hexofuranosyl]-5-(4-fluorophenyl)uracil (4.29)

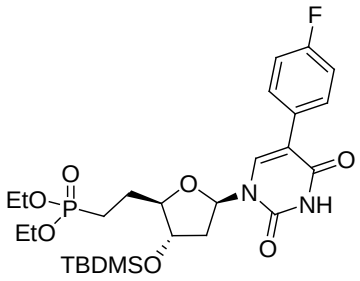

Reaction of compound **4.26** (163 mg, 0.29 mmol) with 4-fluorophenylboronic acid (82 mg, 0.59 mmol), $Pd(PPh_3)_4$ (34 mg, 0.029 mmol) and Na_2CO_3 (102 mg, 0.97 mmol) in DMF (7 mL) and degassed H_2O (0.9 mL) was performed as described in the general procedure to yield compound **4.29** as a colourless solid (141 mg, 84%).

^{1}H NMR (300 MHz, $CDCl_3$): δ 0.010 (6H, s, TBDMS), 0.80-0.84 (9H, m, TBDMS), 1.21 (6H, app q, *J*= 7.2 Hz, 2 x OCH_2CH_3), 1.68-1.94 (4H, m, H-5'a, H-5'b, H-6'a and H-6'b), 2.02-2.11 (1H, m, H-2'a), 2.23-2.31 (1H, m, H-2'b), 3.74-3.78 (1H, m, H-4'), 3.93-4.02 (5H, m, 2 x OCH_2CH_3 and H-3'), 6.14 (1H, app t, *J*= 6.9 Hz, H-1'), 6.99-7.04 (2H, m, subs Ph), 7.34-7.42 (3H, m, subs Ph and H-6), 8.25 (1H, s, 3-NH).

^{31}P NMR ($CDCl_3$): δ 30.74.

^{13}C NMR (75 MHz, $CDCl_3$): δ -4.41 and -4.14 (TBDMS), 16.83 and 16.91 (2 x OCH_2CH_3), 18.33 (TBDMS), 21.79 (C-6'), 23.69 (C-5'), 26.09 (TBDMS), 41.14 (C-2'), 62.07 and 62.19 (2 x OCH_2CH_3), 75.07 (C-3'), 85.78 (C-1'), 86.73 (C-4', d, *J*= 17.0 Hz), 115.19 (C-5), 128.61-132.59 (subs Ph), 136.93 (C-6), 149.74 (C-2), 161.91 (C-4).

Exact mass (ESI-MS) for $C_{26}H_{41}FN_2O_7PSi$ $[M+H]^+$ found, 571.2430; calcd, 571.2399.

1-[3-*O*-*tert*-Butyldimethylsilyl-2,5,6-trideoxy-6-(diethoxyphosphinyl)-β-D-*ribo*-hexofuranosyl]-5-(furan-2-yl)uracil (4.30)

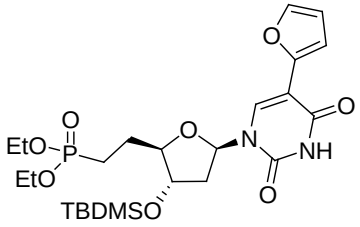

Reaction of compound **4.26** (47 mg, 0.085 mmol) with furan-2-boronic acid (20 mg, 0.18 mmol), $Pd(PPh_3)_4$ (10 mg, 0.0085 mmol) and Na_2CO_3 (30 mg, 0.28 mmol) in DMF (2 mL) and degassed H_2O (0.3 mL) was performed as described in the general procedure to afford compound **4.30** as a colourless solid (36 mg, 77%).

^{1}H NMR (300 MHz, $CDCl_3$): δ 0.0080 (6H, s, TBDMS), 0.80-0.84 (9H, m, TBDMS), 1.23 (6H, app dt, *J*= 2.1 Hz, *J*= 6.9 Hz, 2 x OCH_2CH_3), 1.73-1.99 (4H, m, H-5'a, H-5'b, H-6'a and H-6'b), 2.04-2.13 (1H, m, H-2'a), 2.23-2.31 (1H, m, H-2'b), 3.76-3.78 (1H, m, H-4'), 3.97-4.09 (5H, m, 2 x OCH_2CH_3 and H-3'), 6.16 (1H, app t, *J*= 6.6 Hz, H-1'), 6.36 (1H, dd, *J*= 2.1 Hz, *J*= 3.6 Hz, furan), 6.97 (1H, d, *J*= 3.6 Hz, furan), 7.28 (1H, d, *J*= 1.2 Hz, furan), 7.71 (1H, s, H-6).

^{31}P NMR ($CDCl_3$): δ 30.92.

^{13}C NMR (75 MHz, $CDCl_3$): δ -4.71 and -4.44 (TBDMS), 16.53 and 16.61 (2 x OCH_2CH_3), 18.02 (TBDMS), 21.49 (C-6'), 23.38 (C-5'), 25.81 (TBDMS), 40.97 (C-2'), 61.75 and 61.88 (2 x OCH_2CH_3), 74.66 (C-3'), 85.43 (C-1'), 86.55 (C-4', *J*= 16.8 Hz), 107.39, 109.50 and 111.97 (C-5 and furan), 133.13 (C-6), 141.34 (furan), 145.86 (furan), 149.35 (C-2), 160.11 (C-6).

Exact mass (ESI-MS) for $C_{24}H_{40}N_2O_8PSi$ $[M+H]^+$ found, 571.2275; calcd, 543.2286.

1-[3-*O*-*tert*-Butyldimethylsilyl-2,5,6-trideoxy-6-(diethoxyphosphinyl)-β-D-*ribo*-hexofuranosyl]-5-(thiophen-2-yl)uracil (4.31)

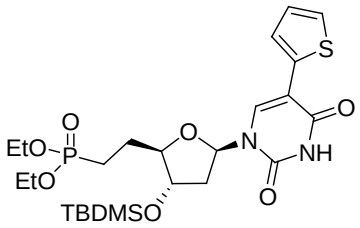

Reaction of compound **4.26** (155 mg, 0.28 mmol) with thiophene-2-boronic acid (71 mg, 0.56 mmol), $Pd(PPh_3)_4$ (32 mg, 0.028 mmol) and Na_2CO_3 (98 mg, 0.92 mmol) in DMF (6.7 mL) and degassed H_2O (0.8 mL) was performed as described in the general procedure to yield compound **4.31** as a colourless solid (117 mg, 75%).

^{1}H NMR (300 MHz, $CDCl_3$): δ 0.090 (6H, s, TBDMS), 0.90 (9H, s, TBDMS), 1.26-1.37 (6H, m, 2 x OCH_2CH_3), 1.83-2.08 (4H, m, H-5'a, H-5'b, H-6'a and H-6'b), 2.14-2.23 (1H, m, H-2'a), 2.32-2.40 (1H, m, H-2'b), 3.85-3.90 (1H, m, H-4'), 4.06-4.18 (5H, m, 2 x OCH_2CH_3 and H-3'), 6.23 (1H, app t, *J*= 6.3 Hz, H-1'), 7.01-7.04 (1H, m, thiophene), 7.25-7.29 (1H, m, thiophene), 7.39-7.44 (1H, m, thiophene), 7.69 (1H, s, H-6), 9.97 (1H, s, 3-NH).

^{31}P NMR ($CDCl_3$): δ 30.80.

^{13}C NMR (75 MHz, $CDCl_3$): δ -4.77 and -4.50 (TBDMS), 16.48 and 16.56 (2 x OCH_2CH_3), 17.95 (TBDMS), 21.46 (C-6'), 23.36 (C-5'), 25.74 (TBDMS), 40.91 (C-2'), 61.79 and 61.86 (2 x OCH_2CH_3), 74.64 (C-3'), 85.62 (C-1'), 86.55 (C-4', d, *J*= 16.8 Hz), 110.20 (C-5), 124.42, 125.37, 127.10 and 133.63 (thiophene), 134.32 (C-6), 149.39 (C-2), 161.27 (C-4).

Exact mass (ESI-MS) for $C_{24}H_{40}N_2O_7PSSi$ $[M+H]^+$ found, 559.2058; calcd, 559.2058.

1-[2,5,6-Trideoxy-6-(diethoxyphosphinyl)-β-D-*ribo*-hexofuranosyl]-5-phenyluracil (4.32)

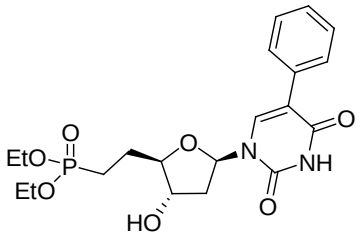

Compound **4.27** (115 mg, 0.21 mmol) was dissolved in THF (1.3 mL). A solution of 1 M TBAF in THF (0.46 mmol, 0.46 mL) was added. After stirring for 1 h at room temperature, the reaction was completed. The solvent was evaporated and the dry residue was purified by column chromatography (CH_2Cl_2/MeOH 96:4) to give pure compound **4.32** (65 mg, colourless solid) in 71% yield.

^{1}H NMR (300 MHz, DMSO-d_6): δ 1.18 (6H, dt, *J*= 1.8 Hz, *J*= 6.9 Hz, 2 x OCH_2CH_3), 1.75-1.83 (4H, m, H-5'a, H-5'b, H-6'a and H-6'b), 2.06-2.14 (1H, m, H-2'a), 2.36-2.51 (1H, m, H-2'b), 3.71-3.72 (1H, m, H-4'), 3.89-3.99 (4H, m, 2 x OCH_2CH_3), 4.06-4.12 (1H, m, H-3'), 5.29 (1H, d, *J*= 4.5 Hz, 3'-OH), 6.17 (1H, t, *J*= 6.9 Hz, H-1'), 7.29-7.40 (3H, m, Ph), 7.51-7.54 (2H, m, Ph), 7.63 (1H, s, H-6).

^{31}P NMR (DMSO-d_6): δ 31.80.

^{13}C NMR (75 MHz, DMSO-d_6): δ 16.13 and 16.20 (2 x OCH_2CH_3), 20.17 (C-6'), 22.03 (C-5'), 60.93 and 61.01 (2 x OCH_2CH_3), 72.80 (C-3'), 84.46 (C-1'), 85.74 (C-4', d, *J*= 17.0 Hz), 113.07 (C-5), 114.76, 115.04, 129.29, 129.34, 130.23 and 130.34 (Ph), 137.87 (C-6), 149.89 (C-6), 162.05 (C-4).

Exact mass (ESI-MS) for $C_{20}H_{28}N_2O_7P$ $[M+H]^+$ found: 439.1639, calcd: 439.1686.

1-[2,5,6-Trideoxy-6-(diethoxyphosphinyl)-β-D-*ribo*-hexofuranosyl]-5-(naphthalen-1-yl)uracil (4.33)

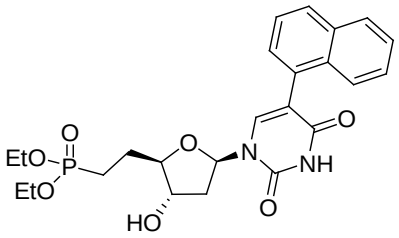

Compound **4.28** (120 mg, 0.20 mmol) was deprotected using the same procedure as described for the synthesis of compound **4.32**. Compound **4.33** was obtained as a colourless solid in a 65% yield (63 mg).

^{1}H NMR (300 MHz, $CDCl_3$): δ 1.17-1.25 (6H, m, 2 x OCH_2CH_3), 1.77-2.02 (4H, m, H-5'a, H-5'b, H-6'a and H-6'b), 2.12-2.21 (1H, m, H-2'a), 2.40-2.53 (1H, m, H-2'b), 3.91-4.07 (5H, m, 2 x OCH_2CH_3 and H-4'), 4.16-4.20 (1H, m, H-3'), 5.28 (1H, s, 3'-OH), 6.26 (1H, t, *J*= 6.6 Hz, H-1'), 7.40-7.46 (2H, m, naphthalene), 7.53-7.58 (2H, m, naphthalene), 7.75-7.84 (3H, m, naphthalene), 7.96 (1H, s, H-6).

^{31}P NMR ($CDCl_3$): δ 31.46.

^{13}C NMR (75 MHz, $CDCl_3$): δ 16.37 and 16.49 (2 x OCH_2CH_3), 21.07 (C-6'), 22.96 (C-5'), 40.06 (C-2'), 61.99 and 62.06 (2 x OCH_2CH_3), 73.85 (C-3'), 85.43 (C-1'), 86.25 (C-4', d, *J*= 16.2 Hz), 115.60 (C-5), 126.03, 126.31, 126.36, 127.25, 127.62, 128.09, 128.30, 130.00, 132.88 and 133.34 (naphthalene), 137.17 (C-6), 150.29 (C-6), 162.61 (C-4).

Exact mass (ESI-MS) for $C_{24}H_{30}N_2O_7P$ $[M+H]^+$ found: 489.1814, calcd: 489.1785.

1-[2,5,6-Trideoxy-6-(diethoxyphosphinyl)-β-D-*ribo*-hexofuranosyl]-5-(4-fluorophenyl)uracil (4.34)

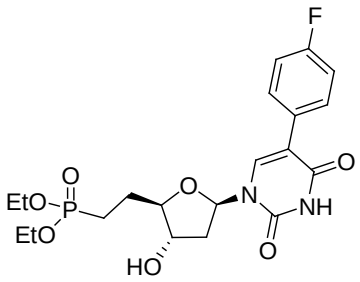

Compound **4.29** (135 mg, 0.24 mmol) was deprotected using the same procedure as described for the synthesis of compound **4.32**. Compound **4.34** was obtained as a colourless solid in a 32% yield (35 mg).

^{1}H NMR (300 MHz, DMSO-d_6): δ 1.18 (6H, dt, *J*= 2.4 Hz, *J*= 6.9 Hz, 2 x *O*CH_2CH_3), 1.70-1.82 (4H, m, H-5'a, H-5'b, H-6'a and H-6'b), 2.05-2.13 (1H, m, H-2'a), 2.37-2.44 (1H, m, H-2'b), 3.70-3.71 (1H, m, H-4'), 3.89-3.99 (4H, m, 2 x *O*CH_2CH_3), 4.06-4.09 (1H, m, H-3'), 5.28 (1H, d, *J*= 4.5 Hz, 3'-OH), 6.16 (1H, t, *J*= 7.2 Hz, H-1'), 7.17-7.23 (2H, m, subs Ph), 7.55-7.60 (2H, m, subs Ph), 7.64 (1H, s, H-6), 11.53 (1H, s, 3-NH).

^{31}P NMR (DMSO-d_6): δ 31.80.

^{13}C NMR (75 MHz, DMSO-d_6): δ 16.22 and 16.30 (2 x *O*CH_2CH_3), 20.29 (C-6'), 22.15 (C-5'), 60.91 and 61.03 (2 x *O*CH_2CH_3), 72.80 (C-3'), 84.61 (C-1'), 85.86 (C-4', d, *J*= 16.7 Hz), 113.07 (C-5), 114.76, 115.04, 129.29, 129.34, 130.23 and 130.34 (subs Ph), 137.87 (C-6), 149.89 (C-6), 162.05 (C-4).

Exact mass (ESI-MS) for $C_{20}H_{27}FN_2O_7P$ $[M+H]^+$ found, 457.1547; calcd, 457.1534.

1-[2,5,6-Trideoxy-6-(diethoxyphosphinyl)-β-D-*ribo*-hexofuranosyl]-5-(furan-2-yl)uracil (4.35)

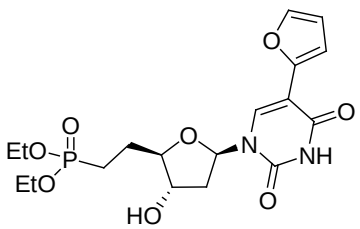

Compound **4.30** (113 mg, 0.21 mmol) was deprotected using the same procedure as described for the synthesis of compound **4.32**. Compound **4.35** was obtained as a colourless solid in a 42% yield (38 mg).

^{1}H NMR (300 MHz, $CDCl_3$): δ 1.32 (6H, dt, *J*= 1.5 Hz, *J*= 6.9 Hz, 2 x OCH_2CH_3), 1.87-2.13 (4H, m, H-5'a, H-5'b, H-6'a and H-6'b), 2.20-2.29 (1H, m, H-2'a), 2.46-2.54 (1H, m, H-2'b), 3.96-3.99 (1H, m, H-4'), 4.05-4.18 (4H, m, 2 x OCH_2CH_3), 4.23-4.29 (1H, m, H-3'), 6.28 (1H, t, *J*= 6.3 Hz, H-1'), 6.43 (1H, dd, *J*= 1.8 Hz, *J*= 3.3 Hz, furan), 7.02 (1H, d, *J*= 3.6 Hz, furan), 7.34 (1H, d, *J*= 1.2 Hz, furan), 7.80 (1H, s, H-6).

^{31}P NMR ($CDCl_3$): δ 31.57.

^{13}C NMR (75 MHz, $CDCl_3$): δ 16.72 and 16.80 (2 x OCH_2CH_3), 21.26 (C-6'), 23.15 (C-5'), 40.49 (C-2'), 62.27 and 62.36 (2 x OCH_2CH_3), 74.02 (C-3'), 85.65 (C-1'), 86.55 (C-4', d, *J*= 14.3 Hz), 107.60, 109.65, 112.19 (furan and C-5), 133.51 (C-6), 141.49 (furan), 146.12 (furan), 149.88 (C-6), 160.54 (C-4).

Exact mass (ESI-MS) for $C_{18}H_{26}N_2O_8P$ $[M+H]^+$ found: 429.1421, calcd: 429.1421.

1-[2,5,6-Trideoxy-6-(diethoxyphosphinyl)-β-D-*ribo*-hexofuranosyl]-5-(thiophen-2-yl)uracil (4.36)

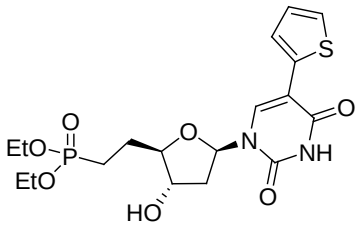

Compound **4.31** (117 mg, 0.21 mmol) was deprotected using the same procedure as described for the synthesis of compound **4.32**. Compound **4.36** was obtained as a colourless solid in a 63% yield (59 mg).

^{1}H NMR (300 MHz, $CDCl_3$): δ 1.31 (6H, app dt, *J*= 2.1 Hz, *J*= 6.9 Hz, 2 x OCH_2CH_3), 1.86-2.08 (4H, m, H-5'a, H-5'b, H-6'a and H-6'b), 2.18-2.27 (1H, m, H-2'a), 2.46-2.54 (1H, m, H-2'b), 3.97-3.98 (1H, m, H-4'), 4.04-4.15 (4H, m, 2 x OCH_2CH_3), 4.19-4.26 (1H, m, H-3'), 5.30 (1H, s, 3'-OH), 6.25 (1H, app t, *J*= 6.6 Hz, H-1'), 6.97-7.00 (1H, m, thiophene), 7.24 (1H, d, *J*= 4.8 Hz, thiophene), 7.36 (1H, d, *J*= 3.0 Hz, thiophene), 7.69 (1H, s, H-6).

^{31}P NMR ($CDCl_3$): δ 31.48.

^{13}C NMR (75 MHz, $CDCl_3$): δ 16.50 and 16.58 (2 x OCH_2CH_3), 21.10 (C-6'), 23.00 (C-5'), 40.27 (C-2'), 62.07 and 62.17 (2 x OCH_2CH_3), 73.80 (C-3'), 85.72 (C-1'), 86.40 (C-4', d, *J*= 15.9 Hz), 110.19 (C-5), 124.35, 125.45, 127.08 and 133.64 (thiophene), 134.55 (C-6), 149.77 (C-2), 161.52 (C-4).

Exact mass (ESI-MS) for $C_{18}H_{26}N_2O_7PS$ $[M+H]^+$ found, 445.1210; calcd, 445.1193.

General procedure for the deprotection of 5-modified nucleoside phosphonates

The phosphonic ester (1 equiv.) was dissolved in CH_2Cl_2 under argon. TMSBr (2 equiv.) was added and the resulting solution was stirred overnight. The solvent was evaporated and the residue dissolved in a mixture of EtOAc/Et_2O (1:1) and water. The organic phase was washed with water and the water layers were combined and lyophilized. Purification of the crude using RP-HPLC (Phenomenex Luna C-18, H_2O/0.1% HCOOH in CH_3CN, 90:10 → 0:100 in 23 min, flow 17.5 mL/min) afforded 2 series of compounds: the α- (retention time ≥ 12 min) and β-isomer (retention time ≈ 10-11 min) of each phosphonate.

1-[2,5,6-Trideoxy-6-(dihydroxyphosphinyl)-β-D-*ribo*-hexofuranosyl]-5-phenyluracil (4.37) and 1-[2,5,6-trideoxy-6-(dihydroxyphosphinyl)-α-D-*ribo*-hexofuranosyl]-5-phenyluracil (4.41)

Reaction of compound **4.32** (27 mg, 0.061 mmol) with TMSBr (16 µL, 0.12 mmol) in CH_2Cl_2 (0.9 mL) as described in the general procedure affording the β- (**4.37**, 0.9 mg, 4%) and α-isomer (**4.41**, 3.2 mg, 14%) as white powders.

Compound **4.37**:

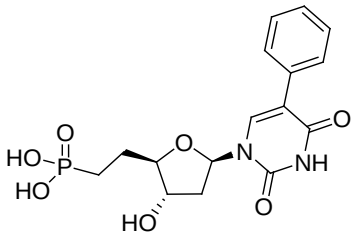

^{1}H NMR (300 MHz, DMSO-d_6): δ 1.52-1.55 (2H, m, H-6'a and H-6'b), 1.79-1.91 (2H, m, H-5'a and H-5'b), 2.07-2.11 (1H, m, H-2'a), 2.29-2.38 (1H, m, H-2'b), 3.73 (1H, app s, H-4'), 4.06 (1H, app s, H-3'), 6.14 (1H, t, *J*= 6.6 Hz, H-1'), 7.27-7.40 (3H, m, Ph), 7.51-7.54 (2H, m, Ph), 7.63 (1H, s, H-6).

^{31}P NMR (DMSO-d_6): δ 24.44.

^{13}C NMR (175 MHz, DMSO-d_6): δ C-6', C-5' and C-2' not visible, 72.78 (C-3'), 84.31 (C-1'), 86.69 (C-4', d, *J*= 19.3 Hz), 113.89 (C-5), 127.32, 128.11, 128.23 and 132.93 (Ph), 137.59 (C-6), 149.86 (C-6), 162.08 (C-4).

Exact mass (ESI-MS) for $C_{16}H_{18}N_2O_7P$ $[M-H]^-$ found, 381.0836; calcd, 381.0857.

Compound **4.41**:

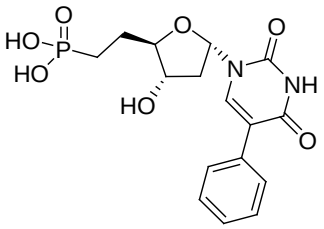

^{1}H NMR (300 MHz, DMSO-d_6): δ 1.49-1.57 (4H, m, H-5'a, H-5'b, H-6'a and H-6'b), 1.98 (1H, app d, *J*= 14.1 Hz, H-2'a), 2.57-2.65 (1H, m, H-2'b), 4.11 (1H, app s, H-4'), 4.23 (H, app s, H-3'), 6.14 (1H, app d, *J*= 6.6 Hz, H-1'), 7.27-7.38 (3H, m, Ph), 7.51-7.54 (2H, m, Ph), 8.16 (1H, s, H-6).

^{31}P NMR (DMSO-d_6): δ 23.62.

^{13}C NMR (75 MHz, DMSO-d_6): δ C-6', C-5' and C-2' not visible, 73.25 (C-3'), 86.00 (C-1' and C-4'), 113.32 (C-5), 128.50-134.13 (Ph), 139.88 (C-6), 150.71 (C-2), 162.88 (C-4).

Exact mass (ESI-MS) for $C_{16}H_{18}N_2O_7P$ $[M-H]^-$ found, 381.0851; calcd, 381.0857.

1-[2,5,6-Trideoxy-6-(dihydroxyphosphinyl)-β-D-*ribo*-hexofuranosyl]-5-(naphtalen-1-yl)uracil (4.38) and 1-[2,5,6-trideoxy-6-(dihydroxyphosphinyl)-α-D-*ribo*-hexofuranosyl]-5-(naphthalen-1-yl)uracil (4.42)

Reaction of compound **4.33** (63 mg, 0.13 mmol) with TMSBr (34 µL, 0.26 mmol) in CH_2Cl_2 (1.9 mL) as described in the general procedure affording the β- (**4.38**, 7.05 mg, 13%) and α-isomer (**4.42**, 8.77 mg, 16%) as white powders.

Compound **4.38**:

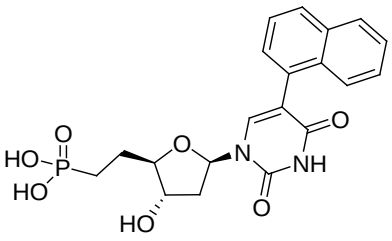

^{1}H NMR (300 MHz, DMSO-d_6): δ 1.47 (2H, app br s, H-6'a and H-6'b), 1.80 (2H, app br s, H-5'a and H-5'b), 2.13 (1H, app br s, H-2'a), 2.27 (1H, app br s, H-2'b), 3.79 (1H, app s, H-4'), 4.09-4.14 (1H, m, H-3'), 6.14 (1H, app s, H-1'), 7.49-8.27 (8H, m, naphthalene and H-6).

^{31}P NMR (DMSO-d_6): δ 20.97.

^{13}C NMR (175 MHz, $CDCl_3$): δ 22.59 (C-6'), 28.10 (C-5'), 39.40 (C-2'), 73.22 (C-3'), 84.41 (C-1'), 87.44 (C-4'), C-5 not visible, 126.52, 127.63, 129.20, 126.84, 138.12 and 141.10 (naphthalene and C-6), (C-2 and C-4 not visible).

Exact mass (ESI-MS) for $C_{20}H_{20}N_2O_7P$ $[M-H]^-$ found: 431.1041, calcd: 431.1014.

Compound **4.42**:

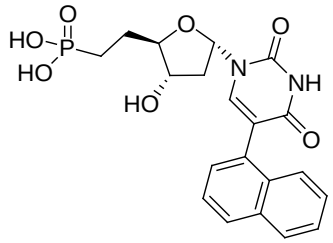

^{1}H NMR (300 MHz, DMSO-d_6): δ 1.59 (4H, app br s, H-5'a, H-5'b, H-6'a and H-6'b), 1.99-2.06 (1H, m, H-2'a), 2.52-2.70 (1H, m, H-2'b), 4.13 (1H, app s, H-4'), 4.27 (1H, app s, H-3'), 6.18 (1H, app d, *J*= 5.7 Hz, H-1'), 7.46-7.52 (2H, m, naphthalene), 7.66 (2H, d, *J*= 8.4 Hz, naphthalene), 7.88-7.91 (3H, m, naphthalene), 8.12 (1H, s, naphthalene), 8.31 (1H, s, H-6).

^{31}P NMR (DMSO-d_6): δ 24.28.

^{13}C NMR (75 MHz, DMSO-d_6): δ C-6', C-5' and C-2' not visible, 72.61 (C-3'), 85.41 (C-1' and C-4'), 112.48 (C-5), 125.95-132.84 (naphthalene), 139.65 (C-6), 150.02 (C-2), 162.35 (C-4).

Exact mass (ESI-MS) for $C_{20}H_{20}N_2O_7P$ $[M-H]^-$ found: 431.1009, calcd: 431.1014.

1-[2,5,6-Trideoxy-6-(dihydroxyphosphinyl)-β-D-*ribo*-hexofuranosyl]-5-(4-fluorophenyl)uracil (4.39) and 1-[2,5,6-trideoxy-6-(dihydroxyphosphinyl)-α-D-*ribo*-hexofuranosyl]-5-(4-fluorophenyl)uracil (4.43)

Reaction of compound **4.34** (36 mg, 0.078 mmol) with TMSBr (21 µL, 0.16 mmol) in CH_2Cl_2 (1.0 mL) as described in the general affording the β- (**4.39**, 1.69 mg, 6%) and α-isomer (**4.43**, 3.19 mg, 12%) as white powders.

Compound **4.39**:

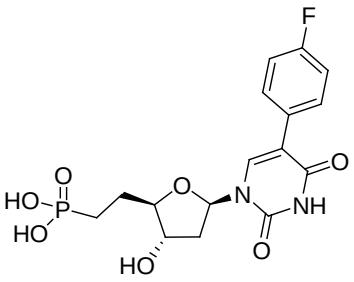

^{1}H NMR (300 MHz, DMSO-d_6): δ 1.43 (2H, app br s, H-6'a and H-6'b), 1.76 (2H, app br s, H-5'a and H-5'b), 2.09 (1H, app br s, H-2'a), 2.28 (1H, app br s, H-2'b), H-4' under H_2O peak, 4.08 (1H, app s, H-3'), 6.09 (1H, app s, H-1'), 7.21-7.62 (5H, m, subs Ph and H-6).
^{31}P NMR (DMSO-d_6): δ 20.60.

^{13}C NMR (175 MHz, DMSO-d_6): δ (C-6', C-5' and C-2' not visible), 72.41 (C-3'), 84.25 (C-1'), 87.76 (C-4'), 115.31 (C-5), 130.56 (subs Ph), (C-6, C-2 and C-4 not visible).

Exact mass (ESI-MS) for $C_{16}H_{17}FN_2O_7P$ $[M-H]^-$ found: 399.0762, calcd: 399.0763.

Compound **4.43**:

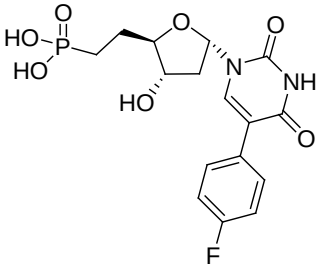

^{1}H NMR (300 MHz, DMSO-d_6): δ 1.44-1.58 (4H, m, H-5'a, H-5'b, H-6'a and H-6'b), 1.99 (1H, d, *J*= 13.5 Hz, H-2'a), 2.52-2.65 (1H, m, H-2'b), 4.11 (1H, app s, H-4'), 4.20-4.25 (1H, m, H-3'), 6.12 (1H, app d, *J*= 6.9 Hz, H-1'), 7.19 (2H, app t, *J*= 8.7 Hz, subs Ph), 7.54-7.59 (2H, m, subs Ph), 8.15 (1H, s, H-6), 8.33 (1H, s, subs Ph).

^{31}P NMR (DMSO-d_6): δ 22.19.

^{13}C NMR (75 MHz, DMSO-d_6): δ (C-6', C-5' and C-2' not visible), 72.22 (C-3'), 85.16 (C-1'), 111.49 (C-5), 114.67, 114.96, 129,57 and 129.67 (subs Ph), 139.00 (C-6), 149.84 (C-2), 162.04 (C-4).

Exact mass (ESI-MS) for $C_{16}H_{17}FN_2O_7P$ $[M-H]^-$ found: 399.0743, calcd: 399.0763.

1-[2,5,6-Trideoxy-6-(dihydroxyphosphinyl)-β-D-*ribo*-hexofuranosyl]-5-(thiophen-2-yl)uracil (4.40) and 1-[2,5,6-trideoxy-6-(dihydroxyphosphinyl)-α-D-*ribo*-hexofuranosyl]-5-(thiophen-2-yl)uracil (4.44)

Reaction of compound **4.36** (59 mg, 0.13 mmol) with TMSBr (35 µL, 0.27 mmol) in CH_2Cl_2 (2.0 mL) as described in the general procedure affording the β- (**4.40**, 5.2 mg, 10%) and α-isomer (**4.44**, 9.6 mg, 19%) as white powders.

Compound **4.40**:

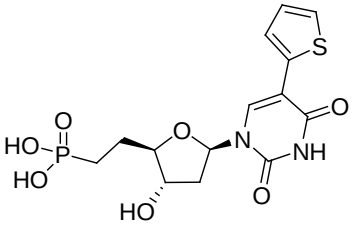

^{1}H NMR (300 MHz, DMSO-d_6): δ 1.50 (2H, app br s, H-6'a and H-6'b), 1.80 (2H, app br s, H-5'a and H-5'b), 2.04-2.12 (1H, m, H-2'a), 2.27-2.31 (1H, m, H-2'b), 3.80 (1H, app br s, H-4'), 4.09 (1H, app br s, H-3'), 6.10 (1H, d, *J*= 6.6 Hz, H-1'), 7.06 (1H, t, *J*= 4.8 Hz, thiophene), 7.45 (2H, app dd, *J*= 4.8 Hz, *J*= 14.4 Hz, thiophene), 7.89 (1H, s, H-6).

^{31}P NMR (DMSO-d_6): δ 23.13.

^{13}C NMR (75 MHz, $CDCl_3$): δ (C-6', C-5' and C-2' not visible), 73.42 (C-3'), 85.35 (C-1'), 109.21 (C-5), 123.93-134.26 (thiophene), 135.74 (C-6), 149.97 (C-2), 161.94 (C-4).

Exact mass (ESI-MS) for $C_{14}H_{16}N_2O_7PS$ $[M-H]^-$ found:387.0377, calcd: 387.0421.

Compound **4.44**:

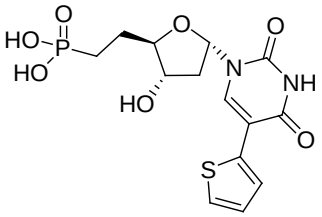

^{1}H NMR (300 MHz, DMSO-d_6): δ 1.40-1.72 (4H, m, H-5'a, H-5'b, H-6'a and H-6'b), 2.02 (1H, app d, *J*= 14.4 Hz, H-2'a), 2.59-2.68 (1H, m, H-2'b), 4.13 (1H, app d, *J*= 4.8 Hz, H-3'), 4.27 (4H, app s, H-4'), 6.16 (1H, app d, *J*= 5.7 Hz, H-1'), 7.04-7.07 (1H, dd, *J*= 3.6 Hz, *J*= 4.8 Hz, thiophene), 7.37-7.38 (1H, m, thiophene), 7.44-7.45 (1H, m, thiophene), 8.46 (1H, s, H-6).

^{31}P NMR (DMSO-d_6): δ 25.63.

^{13}C NMR (75 MHz, DMSO-d_6): δ 23.39 (C-6'), 25.19 (C-5'), (C-2' under DMSO peak), 72.59 (C-3'), 85.51 (C-1'), 88.91 (C-4'), 107.71 (C-5), 122.58-134.28 (thiophene), 136.98 (C-6), 149.53 (C-2), 161.87 (C-4).

Exact mass (ESI-MS) for $C_{14}H_{16}N_2O_7PS$ $[M-H]^-$ found: 387.0416, calcd: 387.0421.

2.6.2 Experimental Assays

Antiviral and Cytotoxicity Assays for Compounds 4.37-4.44

The antiviral activity of the new compounds was determined using a cytopathogenicity assay against herpes simplex virus type 1 (HSV-1) (KOS strain), herpes simplex virus type 2 (HSV-2) (G strain), vaccinia virus, vesicular stomatitis virus, HSV-1 TK^- KOS ACV^r in HEL cell cultures. Stock solutions of the test compounds were prepared in DMSO at a concentration of 10 mg/mL. Cells, grown to confluency in 96-well plates, were infected with 100 $CCID_{50}$ of virus, one $CCID_{50}$ being the 50% cell culture infective dose in the presence of varying concentrations of the test compounds. Cultures were further incubated until complete cytopathogenicity was observed in the infected and untreated virus control. The cytotoxicity of the compounds was evaluated in parallel with their antiviral activity in uninfected cells and is expressed as the minimum cytotoxic concentration (MCC) that causes a microscopically detectable alteration of normal cell morphology. The symbol ''>'' is used to indicate the highest concentration at which the compounds were tested and found not to be antivirally active.

For the anti-HCMV and anti-VZV assays, HEL fibroblasts were infected with 100 PFU per well. Compounds were added after a 1 h-incubation period, and the cells were further incubated at 37 °C. After 5 (VZV) and 7 days (HCMV) of incubation, plaques (VZV) or virus-induced cytopathogenicity (HCMV) was monitored microscopically after ethanol fixation and staining with Giemsa solution. The cytotoxicity of the compounds was evaluated in parallel with their antiviral activity in uninfected cells and is expressed as the minimum cytotoxic concentration that causes a microscopically detectable alteration of cell morphology (MCC) and the concentration required to reduce cell growth by 50% (CC_{50}).

Determination of the anti-HIV activity of the compounds was based on virus-induced cytopathogenicity of HIV-infected CEM cells, measured at day 4 to 5 post virus infection by the microscopically estimating virus-induced syncytia. Results are expressed as the 50% effective concentration (EC_{50}) as reported in Table IV.3. The cytostatic activity of the compounds was evaluated in parallel with their antiviral activity in uninfected cell cultures and is expressed as the 50%-inhibitory concentration for the proliferation of the T-lymphocyte CEM cells (CC_{50}).

GENERAL CONCLUSIONS

Modification of naturally occurring nucleosides is an important strategy in the search for new agents with therapeutic potential. Structural modifications of either the base or sugar moiety of nucleosides may afford promising tool compounds interfering with many therapeutically interesting targets. Based on this principle, 3'-deoxy-3'-arylthiourea derivatives of thymidine were earlier discovered as highly active to and selective inhibitors of human mitochondrial thymidine kinase 2. We aimed at synthesizing 3'-modified thymidine analogues in which the thiourea, known as a perpetrator of toxicity, was replaced with an alternative linker. Selected compounds, featuring a 1,2,3-triazole or an amino-tetrazole moiety, proved very potent inhibitors of TK-2 with IC_{50} values in the nanomolar range (Figure IV). A main drawback of these compounds is their difficult uptake into the mitochondria. Therefore, further research should be focused on a better mitochondrial uptake rather than an increased inhibitory activity. Concerning this issue, it would be of interest to investigate the use of mitochondrial targeting peptides or the introduction of lipophilic positively charged conjugates which improved the mitochondrial uptake of other compounds in the past.[230,231]

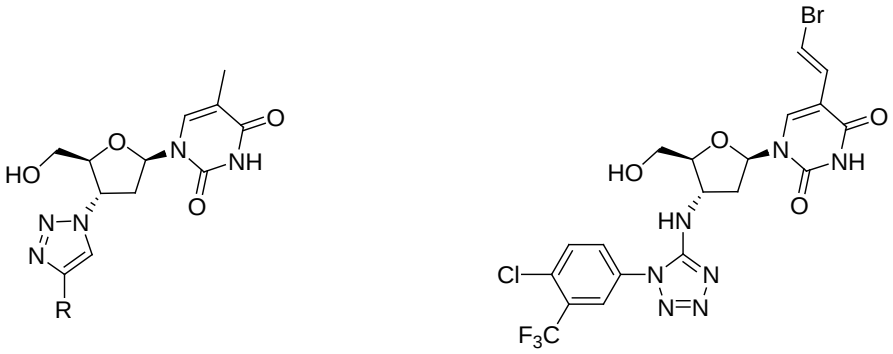

1.53: R = 4-chlorophenyl; IC_{50} = 46 nM
1.54: R = 3,4-dichlorophenyl; IC_{50} = 42 nM

1.90: R = CH_3; IC_{50} = 35 nM
1.100: R = bromovinyl; IC_{50} = 14 nM

Figure IV

Based on the reported close structural similarities between TK-2 and TMPKmt and the reasonable correlation of the IC_{50} values of known inhibitors of both targets, some analogues originally designed as TK-2 inhibitors, were also evaluated for their inhibitory activity against thymidylate kinase of *M. tuberculosis*. Several 3'-modified thymidine analogues showed inhibitory activity in the low micromolar range and represent valuable tools to gain further insight into the S.A.R. of TMPKmt inhibitors, further demonstrating that cross screening may be very useful and lead to the discovery of promising compounds against alternative targets with minimal efforts. With a K_i value of 0.17 µM, 5'-arylthiourea 4-thio-α-thymidine analogue **2.23** is one of the most potent TMPKmt inhibitors reported today (Figure V). This compound is capable of inhibiting mycobacterial growth at a concentration of 25 µg/mL, further promoting TMPKmt as an attractive target for further inhibitor design.

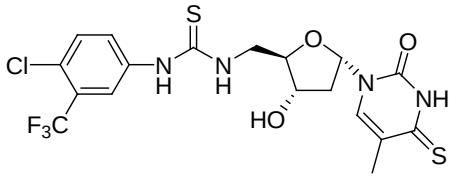

2.23

Figure V

In the third part of this thesis, new ligands for the $P2Y_2$ receptor were synthesized that combine an aromatic substituent at position 5 of the uracil base and a methylene phosphonate at C-5' of the ribofuranose ring. These compounds were synthesized via a 7-step procedure including a Wittig reaction and a Suzuki-Miyaura coupling. Within this series, all compounds activated the $P2Y_2$ receptor with a range of apparent potencies, and the maximal effect observed with each of these molecules was around 30-40% of that observed with UTP. Preferred modifications at position 5 of the uracil moiety of compound **3.7** are depicted in Figure VI. Remarkably, these analogues failed to inhibit activity of UTP down to the level of activity seen with the 5-modified analogues alone as would be expected for classical partial agonists. A possible explanation for this phenomenon is that these phosphonates are producing their effects by interacting with a receptor site distinct from the orthosteric site. Phosphonate **3.49** may become a useful tool compound for further pharmacological characterization of the $P2Y_2$ receptor.

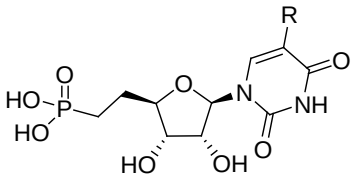

3.44: R = phenyl
3.45: R = naphthalen-1-yl
3.46: R = 4-fluorophenyl
3.48: R = *p*-tolyl
3.49: R = furan-2-yl

Figure VI

Exploration of a similar chemical strategy on different starting materials may allow to discover interesting probe compounds that are rather similar from a chemical point of view, but may show promising totally different biological activities. Therefore, several 5-modified 5'-methylene phosphonate 2'-deoxyuridine analogues were synthesized as possible antiviral agents. Hence, the only difference with those derivatives (PART IV) and those modulating the $P2Y_2$ receptor is that the latter feature a ribofuranose moiety (as present in the endogenous UTP agonist), while for the possible antiviral agents 2'-deoxyuridine was selected as a preferred scaffold for drugs acting against DNA viruses. A similar reaction sequence as for the $P2Y_2$ receptor ligands was used but resulted in a mixture of α- and β-analogues due to an unexpected anomerisation during the phosphonate deprotection step. This proves that, although the starting material is quite similar, a same reaction can give rise to different and something unexpected products. After separation of the α- and β-analogues, all compounds were tested against a broad panel of different viruses. Unfortunately, none of the 2'-deoxyuridine analogues exhibited significant antiviral activity.

REFERENCES

[1] Mathews, C. K. (**2000**), *Biochemistry,* (van Holde, K. E.; Ahern, K. G.) San Franciso: Addison Wesley Longman, Inc. 3th edition.

[2] Reichard, P. Interactions between deoxyribonucleotide and DNA synthesis. *Annu. Rev. Biochem*. **1988**, *57*, 349-374.

[3] Wright, J. A.; Chan, A. K.; Choy, B. K.; Hurta, R. A.; McClarty, G. A. and Tagger, A. Y. Regulation and drug resistance mechanisms of mammalian ribonucleotide reductase, and the significance to DNA synthesis. *Biochem. Cell Biol*. **1990**, *68*, 1364-1371.

[4] Arner, E. S. and Eriksson, S. Mammalian deoxyribonucleoside kinases. *Pharmacol. Therap*. **1995**, *67*, 155-186.

[5] Van Rompay, A. R.; Johansson, M. and Karlsson, A. Substrate specificity and phosphorylation of antiviral and anticancer nucleoside analogues by human deoxyribonucleoside kinases and ribonucleoside kinases. *Pharmacol. Ther*. **2003**, *100*, 119-139.

[6] Eriksson, S.; Munch-Petersen, B.; Johansson, K., Eklund, H. Structure and function of cellular deoxyribonucleoside kinases. *Cell. Mol. Life Sci*. **2002**, *59*, 1327-1346.

[7] Munch-Petersen, B.; Piskur, J.; Sθndergaard, L. Four deoxynucleoside kinase activities from *Drosophila melanogaster* are contained within a single monomeric enzyme, a new multifunctional deoxynucleoside kinase. *J. Biol. Chem.* **1998**, *273*, 3926-3931.

[8] Pérez-Pérez, M. J.; Priego, E-M.; Hernández, A-I.; Familiar, O.; Camarasa, M-J.; Negri, A.; Gago, F. and Balzarini, J. Structure, physiological role, and Specific inhibitors of human thymidine kinase 2 (TK2): present and future. *Med. Res. Rev.* **2008**, *28*, 797-820.

[9] Johansson, M.; Van Rompay, A. R.; Degreve, B.; Balzarini, J. and Karlsson, A. Cloning and characterization of the multisubstrate deoxyribonucleoside kinase of *Drosophila melanogaster*. *J. Biol. Chem.* **1999**, *274*, 23814-23819.

[10] Zheng, X.; Johansson, M. and Karlsson, A. Retroviral transduction of cancer cell lines with the gene encoding *Drosophila melanogaster* multisubstrate deoxyribonucleoside kinase. *J. Biol. Chem*. **2000**, *275*, 39125-39129.

[11] Bradshaw, H. D. Molecular-cloning and cell cycle specific regulation of a functional human thymidine gene. *Proc. Natl. Acad. Sci. USA,* **1983**, *80*, 5588-5591.

[12] Wang, L.; Munch-Petersen, B.; Sjöberg, A. H.; Hellman, U.; Bergman, T.; Jörnvall, H. and Eriksson, S. Human thymidine kinase 2: molecular cloning and characterization of the enzyme activity with antiviral and cytostatic nucleoside substrates. *FEBS Lett.* **1999**, *443*, 170-174.

[13] Arner, E. S.; Spasokoukotskaja, T. and Eriksson, S. Selective assays for thymidine kinase 1 and 2 and deoxycytidine kinase and their activities in extracts from human cells and tissues. *Biochem. Biophys. Res. Commun.* **1992**, *188*, 712-718.

[14] Johansson M. and Karlsson, A. Cloning of the cDNA and chromosome localization of the gene for human thymidine kinase 2*. J. Biol. Chem*. **1997**, *272*, 8454-8458.

[15] Bogenhagen, D. and Clayton, D. A. Thymidylate nucleotide supply for mitochondrial-DNA synthesis in mouse L-cells - Effect of 5-fluorodeoxyuridine and methotrexate in thymidine kinase plus and thymidine kinase minus cells. *J. Biol. Chem*. **1976**, *251*, 2938-2944.

[16] Munch-Petersen, B.; Cloos, L.; Tyrsted, G. and Eriksson S. Diverging substrate specificity of pure human thymidine kinases 1 and 2 against antiviral dideoxynucleosides. *J. Biol. Chem.* **1991**, *266*, 9032-9038.

[17] Eriksson, S.; Kierdaszuk, B.; Munch-Petersen, B.; Öberg, B. and Johansson N. G. Comparison of the substrate specificities of human thymidine kinase 1 and 2 and deoxycytidine kinase toward antiviral and cytostatic nucleoside analogs. *Biochem. Biophys. Res. Commun*. **1991**, *176*, 586-592.

[18] Wang, L.; Hellman, U. and Eriksson, S. Cloning and expression of human mitochondrial deoxyguanosine kinase cDNA. *FEBS Lett.* **1996**, *390*, 39-43.

[19] Eriksson, S.; Munch-Petersen, B.; Kierdaszuk, B. and Arnér, E. Expression and substrate specificities of human thymidine kinase 1, thymidine kinase 2 and deoxycytidine kinase. *Adv. Exp. Med. Biol.* **1991**, *309*, 239-243.

[20] Johansson, N. G. and Eriksson, S. Structure-activity relationships for phosphorylation of nucleoside analogs to monophosphates by nucleoside kinases. *Acta Biochim. Pol.* **1996**, *43*, 143-160.

[21] Lunato, A. J.; Wang, J.; Woollard, J. E.; Anisuzzaman, A. K.; Ji, W.; Rong, F. G.; Ikeda, S.; Soloway, A. H.; Eriksson, S.; Ives, D. H.; Blue, T. E. and Tjarks, W. Synthesis of 5-(carboranylalkylmercapto)-2′-deoxyuridines and 3-(carboranylalkyl) thymidines and their evaluation as substrates for human thymidine kinases 1 and 2. *J. Med. Chem.* **1999**, *42*, 3378-3389.

[22] Furman, P. A.; Fyfe, J. A.; St Clair, M. H.; Weinhold, K.; Rideout, J. L.; Freeman, G. A.; Lehrman, S. N.; Bolognesi, D. P.; Broder, S.; Mitsuya, H. and Barry, D. W. Phosphorylation of 3′-azido-3′-deoxythymidine and selective interaction of the 5′-triphosphate with human immunodeficiency virus reverse transcriptase. *Proc. Natl. Acad. Sci. USA,* **1986**, *83*, 8333-8337.

[23] Wang, J.; Su, C.; Neuhard, J. and Eriksson S. Expression of human mitochondrial thymidine kinase in *Escherichia coli*: correlation between the enzymatic activity of pyrimidine nucleoside analogues and their inhibitory effect on bacterial growth. *Biochem. Pharmacol.* **2000**, *59*, 1583-1588.

[24] Hernández, A. I.; Familiar, O.; Negri, A.; Rodríguez-Barrios, F.; Gago, F.; Karlsson, A.; Camarasa, M. J.; Balzarini, J. and Pérez-Pérez, M. J. *N*-1-substituted thymine derivatives as mitochondrial thymidine kinase (TK-2) inhibitors. *J. Med. Chem.* **2006**, *49*, 7766-7773.

[25] Barroso, J. F.; Elholm, M. and Flatmark, T. Tight binding of deoxyribonucleotide triphosphates to human thymidine kinase 2 expressed in *Escherichia coli*. Purification and partial characterization of its dimeric and tetrameric forms. *Biochemistry,* **2003**, *42*, 15158-15169.

[26] Gerth, M. L. and Lutz, S. Mutagenesis of non-conserved active site residues improves the activity and narrows the specificity of human thymidine kinase 2. *Biochem. Biophys. Res. Commun.* **2007**, *354*, 802-807.

[27] Kuo, W. L.; Hirschhorn, R.; Huie, M. L. and Hirschhorn, K. Localization and ordering of acid alpha-glucosidase (GAA) and thymidine kinase (TK1) by fluorescence in situ hybridization. *Hum. Genet*. **1996**, *97*, 404-406.

[28] Petty, E. M.; Miller, D. E.; Grant, A. L.; Collins, E. E.; Glover, T. W. and Law, D. J. FISH localization of the soluble thymidine kinase gene (TK1) to human 17q25, a region of chromosomal loss in sporadic breast tumors. *Cytogenet. Cell Genet*. **1996**, *72*, 319-321.

[29] Welin, M.; Kosinska, U.; Mikkelsen, N. E.; Carnrot, C.; Zhu, C. Y.; Wang, L.Y.; Eriksson, S.; Munch-Petersen, B. and Eklund, H. Structures of thymidine kinase 1 of human and mycoplasmic origin. *Proc. Natl. Acad. Sci. USA,* **2004**, *101*, 17970-17975.

[30] Johansson, K.; Ramaswamy, S.; Ljungcrantz, C.; Knecht, W.; Piskur, J.; Munch-Petersen, B.; Eriksson, S. and Eklund, H. Structural basis for substrate specificities of cellular deoxyribonucleoside kinases. *Nat. Struct. Biol.* **2001**, *8*, 616-20.

[31] Suzuki, N. N.; Koizumi, K.; Fukushima, M.; Matsuda, A. and Inagaki, F. Structural basis for the specificity, catalysis, and regulation of human uridine-cytidine kinase. *Structure*, **2004**, *12*, 751-64.

[32] Wild, K.; Bohner, T.; Folkers, G. and Schulz, G. E. The structures of thymidine kinase from herpes simplex virus type 1 in complex with substrates and a substrate analogue. *Protein Sci.* **1997**, *6*, 2097-106.

[33] Tang, Y.; Schon, E. A.; Wilichowski, E.; Vazquez-Memije, M. E.; Davidson, E. and King, M. P. Rearrangements of human mitochondrial DNA (mtDNA): New insights into the regulation of mtDNA copy number and gene expression. *Mol. Biol. Cell,* **2000***, 11*, 1471-1485.

[34] Gross, N. J.; Getz, G. S. and Rabinowitz, M. Apparent turnover of mitochondrial deoxyribonucleic acid and mitochondrial phospholipids in the tissues of the rat. *J. Biol. Chem.* **1969**, 244, 1552-1562.

[35] Dolce, V.; Fiermonte, G.; Runswick, M. J.; Palmieri, F. and Walker J. E. The human mitochondrial deoxynucleotide carrier and its role in the toxicity of nucleoside antivirals. *Proc. Natl. Acad. Sci. USA*, **2001**, 2284-2288.

[36] Bradshaw, P. C. and Samuels, D. C. A computational model of mitochondrial deoxynucleotide metabolism and DNA replication. *Am. J. Physiol. Cell Physiol.* **2005**, *288*, 989-1002.

[37] Samuels, D. C. Mitochondrial AZT Metabolism. *Life*, **2006**, *58*, 403-408.

[38] Pontarin, G.; Gallinaro, L.; Ferraro, P.; Reichard, P. and Bianchi, V. Origins of mitochondrial thymidine triphosphate: Dynamic relations to cytosolic pools. *Proc. Natl. Acad. Sci. USA*, **2003**, *100*, 12159-12164.

[39] Rampazzo, C.; Ferraro, P.; Pontatin, G.; Fabris, S.; Reichard, P. and Bianchi, V. Mitochondrial deoxyribonucleotides, pool sizes, synthesis, and regulation. *J. Biol. Chem*. **2004**, *279*, 17019-17026.

[40] Moraes, C. T.; Shanske, S.; Tritschler, H. J.; Aprille, J. R.; Andreetta, F.; Bonilla, E.; Schon, E. A. and Dimauro, S. mtDNA depletion with variable tissues expression: a novel genetic abnormality in mitochondrial diseases. *Am. J. Hum. Genet.* **1991**, *48*, 492-501.

[41] Vu, T. H.; Sciacco, M.; Tanji, K.; Nichter, C.; Bonilla, E.; Chatkupt, S.; Maertens, P.; Shanske, S.; Mendell, J.; Koenigsberger, M. R.; Sharer, L.; Schon, E. A.; DiMauro, S. and DeVivo, D. C. Clinical manifestations of mitochondrial DNA depletion. *Neurology*, **1998**, *50*, 1783-1790.

[42] Mandel, H.; Szargel, R.; Labay, V.; Elpeleg, O.; Saada, A.; Shalata, A.; Anbinder, Y.; Berkowitz, D.; Hartman, C.; Barak, M.; Eriksson, S. and Cohen; N. The deoxyguanosine kinase gene is mutated in individuals with depleted hepatocerebral mitochondrial DNA. *Nat. Genet.* **2001**, *29*, 337-341.

[43] Saada, A.; Shaag, A.; Mandel, H.; Nevo, Y.; Eriksson, S. and Elpeleg, O. Mutant mitochondrial thymidine kinase in mitochondrial DNA depletion myopathy. *Nat. Genet.* **2001**, *29*, 342-344.

[44] Mancuso, M.; Salviati, L.; Sacconi, S.; Otaegui, D.; Camano, P.; Marina, A.; Bacman, S.; Moraes, C. T.; Carlo, J. R.; Garcia, M.; Garcia-Alvarez, M.; Monzon, L.; Naini, A. B.; Hirano, M.; Bonilla, E.; Taratuto, A. L.; DiMauro, S. and Vu, T. H.; Mitochondrial DNA depletion - Mutations in thymidine kinase gene with myopathy and SMA. *Neurology*, **2000**, *59*, 1197-1202.

[45] Suomalainen, A. and Isohanni, P. Mitochondrial DNA depletion syndromes - Many genes, common mechanisms. *Neuromuscul. Disord.* **2010**, *20*, 429-437.

[46] Lewis, W.; Day, B. J. and Copeland, W. C. Mitochondrial toxicity of NRTI antiviral drugs: An integrated cellular perspective. *Nat. Rev. Drug Discov*. **2003**, *10*, 812-822.

[47] Bradshaw, P. C.; Li, J. and Samuels, D. C. A computational model of mitochondrial AZT metabolism. *Biochem. J*. **2005**, *392*, 363-373.

[48] Kohler, J. J. and Lewis, W. A brief overview of mechanisms of mitochondrial toxicity from NRTIs. *Environ. Mol. Mutagen*. **2007**, *48*, 166-172.

[49] Susan-Resiga, D.; Bentley, A. T.; Lynx, M. D.; LaClair, D. D. and McKee, E. E. Zidovudine inhibits thymidine phosphorylation in the isolated perfused rat heart. *Antimicrob. Agents Chemother*. **2007**, *51*, 1142-1149.

[50] Lynx, M. D. and McKee, E. E. 3'-Azido-3'-deoxythymide (AZT) is a competitive inhibitor of thymidine phosphorylation in isolated rat heart and liver mitochondria. *Biochem. Pharmacol*. **2006**, *72*, 239-243.

[51] Perez-Perez, M. J.; Hernandez, A. I.; Priego, E. M.; Rodriguez-Barrios, F.; Gago, F.; Camarasa, M. J. and Balzarini, J. Mitochondrial Thymidine Kinase Inhibitors. *Curr. Top. Med. Chem*. **2005**, *5*, 1205-1219.

[52] Balzarini, J.; Zhu, C. Y.; De Clercq, E.; Pérez-Pérez, M. J.; Chamorro, C.; Camarasa, M. J. and Karlsson, A. Novel ribofuranosylnucleoside lead compounds for potent and selective inhibitors of mitochondrial thymidine kinase-2. *Biochem. J.* **2000***, 351*, 167-171.

[53] Kierdaszuk, B.; Krawiec, K.; Kazimierczuk, Z.; Jacobsson, U.; Johansson, N. G.; Munch-Petersen, B.; Eriksson, S. and Shugar, D. Substrate/inhibitor properties of human deoxycytidine kinase (dCK) and thymidine kinases (TK1 and TK2) towards the sugar moiety of nucleosides, including O'-alkyl analogues. *Nucleosides Nucleotides,* **1999***, 18*, 1883-1903.

[54] Manfredini, S.; Baraldi, P. G.; Durini, E.; Porcu, L.; Angusti, A.; Vertuani, S.; Solaroli, N.; De Clercq, E.; Karlsson, A. and Balzarini, J. Design, synthesis and enzymatic activity of highly selective human mitochondrial thymidine kinase inhibitors. *Bioorg. Med. Chem. Lett.* **2001**, *11*, 1329-1332.

[55] Ciliberti, N.; Manfredini, S.; Angusti, A.; Durini, E.; Solaroli, N.; Vertuani, S.; Buzzoni, L.; Bonache, M. C.; Ben-Shalom, E.; Karlsson, A.; Saada, A. and Balzarini, J. Novel selective human mitochondrial kinase inhibitors: Design, synthesis and enzymatic activity. *Bioorg. Med. Chem.* **2007**, *15*, 3065-3081.

[56] Hernandez, A. I.; Balzarini, J.; Karlsson, A.; Camarasa, M. J. and Pérez-Pérez, M. J. Acyclic nucleoside analogues as novel inhibitors of human mitochondrial thymidine kinase. *J. Med. Chem.* **2002**, *45*, 4254-4263.

[57] Balzarini, J.; Hernández, A. I.; Roche, P.; Esnouf, R.; Karlsson, A.; Camarasa, M. J. and Pérez-Pérez, M. J. Non-nucleoside inhibitors of mitochondrial thymidine kinase (TK-2) differentially inhibit the closely related herpes simplex virus type 1 TK and *Drosophila melanogaster* multifunctional deoxynucleoside kinase. *Mol. Pharmacol.* **2003**, *63*, 263-270.

[58] Priego, E. M.; Balzarini, J.; Karlsson, A.; Camarasa, M. J. and Pérez-Pérez, M. J. Synthesis and evaluation of thymine-derived carboxamides against mitochondrial thymidine kinase (TK-2) and related enzymes. *Bioorg. Med. Chem.* **2004**, *12*, 5079-5090.

[59] Balzarini, J.; Van Daele, I.; Negri, A.; Solaroli, N.; Karlsson, A.; Liekens, S.; Gago, F. and Van Calenbergh, S. Human mitochondrial thymidine kinase is selectively inhibited by 3'-thiourea derivatives of beta-thymidine: identification of residues crucial for both inhibition and catalytic activity. *Mol. Pharmacol.* **2009**, *75*, 1127-1136.

[60] Onderwater, R. C. A.; Commandeur, J. N. M. and Vermeulen, N. P. E. Comparative cytotoxicity of *N*-substituted *N*'-(4-imidazole-ethyl)-thiourea in precision-cut rat liver slices. *Toxicology,* **2004**, *197*, 80-90.

[61] Wigerinck, P.; Van Aerschot, A.; Claes, P.; Balzarini, J.; De Clercq, E. and Herdewijn, P. 3'-(1,2,3-Triazol-1-yl)-2',3'-dideoxythymidine and 3'-(1,2,3-triazol-1-yl)-2',3'-dideoxyuridine. *J. Heterocycl. Chem.* **1989**, *26*, 1635-1642.

[62] Huisgen, R. (**1984**) *1,3-Dipolar Cycloaddition Chemistry*. Wiley: New York.

[63] Huisgen, R.; Szeimies, G. und Möbius, L. Kinetik der additionen organischer azide an CC-Mehrfachbindungen. *Chem. Ber.* **1967**, *100*, 2494-2507.

[64] Rostovtsev, V. V.; Green, L. G.; Fokin, V. V. and Sharpless, K. B. A stepwise Huisgen cycloaddition process: copper(I)-catalyzed regioselective "Ligation" of azides and terminal Alkynes. *Agew. Chemie*. **2002**, *114*, 2708-2711.

[65] Glinski, R. P.; Khan, M. S. and Kalamas, R. L. Nucleotide synthesis. IV. Phosphorylated 3'-amino-3'-deoxythymidine and 5'-amino-5'-deoxythymidine and derivatives. *J. Org. Chem.* **1973**, *38*, 4299-4305.

[66] Bessodes, M.; Koiotis, D. and Antonakis, K. Rapid and selective detritylation of primary alcohols using formic acid. *Tetrahedron Lett.* **1986**, *27*, 579-580.

[67] Cosyn, L.; Palaniappan, K. K.; Kim, S. K.; Duong, H. T.; Gao, Z. G.; Jacobson, K. A. and Van Calenbergh, S. 2-Triazole-substituted adenosines: A new class of selective A3 adenosine receptor agonists, partial agonists, and antagonists. *J. Med. Chem.* **2006**, *49*, 7373-7383.

[68] Zhang, L.; Chen, X.; Xue, P.; Sun, H. H. Y.; Williams, I. D.; Sharpless, K. B.; Fokin, V. V. and Jia, G. Ruthenium-catalyzed cycloaddition of alkynes and organic azides. *J. Am. Chem. Soc*. **2005**, *127*, 15998-15999.

[69] Van Daele, I.; Munier-Lehmann, H.; Froeyen, M.; Balzarini, J. and Van Calenbergh, S. Rational design of 5'-thiourea-substituted α-thymidine analogues as thymidine monophosphate kinase inhibitors capable of inhibiting mycobacterial growth. *J. Med. Chem.* **2007**, *50*, 5281-5292.

[70] Lavandera, I.; Fernández, S.; Ferrero, M.; De Clercq, E. and Gotor, V. Synthesis, protonation behavior, conformational analysis, and regioselective enzymatic acylation of the novel diamino

analogue of (*E*)-5-(2-bromovinyl)-2'-deoxyuridine (BVDU). *Nucleosides Nucleotides Nucleic Acids*, **2003**, *22*, 1939-1952.

[71] Bleackley, R. C.; Jones, A. S. and Walker, R. T. Incorporation of 5-substituted uracil derivatives into nucleic acids. III. Synthesis of 5-substituted uracils derived from 5-acetyluracil. *Tetrahedron,* **1976**, *32*, 2795-2797.

[72] Egeblad-Welin, L.; Sonntag, Y.; Eklund, H. and Munch-Petersen, B. Functional studies of active-site mutants from *Drosophila melanogaster* deoxyribonucleoside kinase. Investigations of the putative catalytic glutamate-arginine pair and of residues responsible for substrate specificity. *FEBS J*. **2007**, *274*, 1542-51.

[73] Van Poecke, S.; Negri, A.; Gago, F.; Van Daele, I.; Solaroli, N.; Karlsson, A.; Balzarini, J. and Van Calenbergh, S. 3'-[4-Aryl-(1,2,3-triazol-1-yl)]-3'-deoxythymidine analogues as potent and selective inhibitors of human mitochondrial thymidine kinase. *J. Med. Chem*. **2010**, *53*, 2902-2912.

[74] Berry, D. A.; Jung, K. Y.; Wise, D. S.; Sercel, A. D.; Pearson, W. H.; Mackie, H.; Randolph, J. B. and Somers, R. L. Pyrrolo-dC and pyrrolo-C: fluorescent analogs of cytidine and 2 '-deoxycytidine for the study of oligonucleotides*. Tetrahedron Lett.* **2004**, *45*, 2457-2461.

[75] Li, Y.; Soni, P. B.; Liu, L.; Zhang, X.; Liotta, D. C. and Lutz, S. Synthesis of fluorescent nucleoside analogs as probes for 2'-deoxyribonucleoside kinases. *Bioorg. Med. Chem. Lett.* **2010**, *20*, 841-843.

[76] Chu, C. K. and Chen, Y. Process for the deoxygenation of nucleosides. *WO Patent 9215598*, **1992**.

[77] Case, D. A.; Darden, T. A.; Cheatham, T. E.; Simmerling, C. L.; Wang, J.; Duke, R. E.; Luo, R.; Crowley, M.; Walker, R. C.; Zhang, W.; Merz, K. M.; Wang, B.; Hayik, S.; Roitberg, A.; Seabra, G.; Kolossvary, I.; Wong, K. F.; Paesani, F.; Vanicek, J.; Wu, X.; Brozell, S. R.; Steinbrecher, T.; Gohlke, H.; Yang, L.; Tan, C.; Mongan, J.; Hornak, V.; Cui, G.; Mathews, D. H.; Seetin, M. G.; Sagui, C. and Babin, V. Kollman, P. A. *AMBER 10*; University of California: San Francisco. **2008**.

[78] Celewicz, L.; Urjasz, W. and Golankiewicz, K. Synthesis of 3'-*N*-substituted 3'-amino-3'-deoxythymidine derivatives. *Nucleosides Nucleotides,* **1993**, *12*, 951-956.

[79] Cunha, S.; Costa, M. B.; Napolitano, H. B.; Lariucci, C. and Vencato, I. Study of *N*-benzoyl-activation in the $HgCl_2$-promoted guanylation reaction of thioureas. Synthesis and structural analysis of *N*-benzoyl-guanidines. *Tetrahedron*, **2001**, *57*, 1671-1675.

[80] Batey, R. A.; Powell, D. A. A general synthetic method for the formation of substituted 5-aminotetrazoles from thioureas: A strategy for diversity amplification. *Org. Lett.* **2000**, *2*, 3237-3240.

[81] Svetlik, J.; Hrusovsky, I. and Martvon, A. Reactions of asymmetric carbodiimides with azoimide. *Coll. Czech. Chem. Commun.* **1979**, *44*, 2982-2986.

[82] Kohli, V.; Blöcker, H. and Köster, H. The triphenylmethyl (trityl) group and its use in nucleotide chemistry. *Tetrahedron lett.* **1983**, *21*, 2683-2686.

[83] Cegielski; J. P.; Chin, D. P.; Espinal, M. A.; Frieden, T. R.; Rodriquez, C. R.; Talbot, E. A.; Weil, D. E.; Zaleskis, R. and Raviglione, M. C. The global tuberculosis situation. Progress and problems in the 20th century, prospects for the 21st century. *Infect. Dis. Clin. North Am.* **2002**, *16*, 1-58.

[84] WHO Library Cataloguing-in-Publication Data (**2010**) *Global tuberculosis control: WHO report 2010*.

[85] Niederweis, M. Mycobacterial porins – new channel proteins in unique outer membranes. *Mol. Microbiol.* **2003**, *49*, 1167-1177.

[86] Brennan, P. J. and Crick, D. C. Structure of the cell wall of mycobacteria. *Curr. Top. Med. Chem.* **2007**, *7*, 475-488.

[87] Varki, A. (**2009**), *Essentials of Glycobiology*, (Cummings, R. D.; Esko, J. D.; Freeze, H. H.; Stanley, P. S.; Bertozzi, C. R.; Hart, G. W. and Etzler, M. E.) New York: Cold Spring Harbor, 2nd edition.

[88] Frieden, T. R.; Sterling, T. R.; Munsiff, S. S.; Watt, C. J. and Dye, C. Tuberculosis. *Lancet*, **2003**, *362*, 887-899.

[89] Knechel, N. A. Tuberculosis: pathophysiology, clinical features, and diagnosis. *Crit. Care Nurse*. **2009**, *29*, 34-43.

[90] WHO Library Cataloguing-in-Publication Data (**2006**) Diagnostics for tuberculosis. Global demand and market potential.

[91] Centers for Disease Control and Prevention. The role of BCG vaccine in the prevention and control of tuberculosis in the United States. *MMWR*. **1996**, 45, No. RR-4.

[92] World Health Organization. (**2011**) *Pursue high-quality DOTS expansion and enhancement.* Retrieved July 15, 2011 from http://www.who.int./tb/dots.

[93] Andersen, P. TB vaccines: progress and problems. *Trends Immunol*. **2001**, *22*, 160-168.

[94] Fine, P. E. M. Variation in protection by BCG: implications of and for heterologous immunity. *Lancet*, **1995**, *346*, 1339-1345.

[95] Rouse, D. A. and Morris, S. L. Molecular mechanisms of isoniazid resistance in *Mycobacterium tuberculosis* and *Mycobacterium bovis. Infect. Immun.* **1995**, *63*, 1427-1433.

[96] Musser, J. M. Antimicrobial agent resistance in mycobacteria: molecular genetic insights. *Clin. Microbiol. Rev.* **1995**, *8*, 496-514.

[97] Campbell, E. A.; Korzheva, N. Mustaev, A.; Murakami, K.; Nair, S.; Goldfarb, A. and Darst, S. A. Structural mechanism for rifampicin inhibition of bacterial RNA polymerase. *Cell*, **2001**, *104*, 901-912.

[98] Johnson, R.; Streicher, E. M.; Louw, G. E.; Warren, R. M.; van Helden, P. D. and Victor, T. C. Drug resistance in *Mycobacterium tuberculosis*. *Curr. Issues Mol. Biol.* **2006**, *8*, 97-111.

[99] Goude, R.; Amin, A. G.; Chatterjee, D. and Parish, T. The arabinosyltransferase EmbC is inhibited by ethambutol in *Mycobacterium tuberculosis*. *Antimicrob. Agents Chemother*. **2009**, *53*, 4138-4146.

[100] Wang, F.; Langley, R.; Gulten, G.; Dover, L. G.; Besra, G. S.; Jacobs Jr., W. R. and Sacchettini, J. C. Mechanism of thioamide drug action against tuberculosis and leprosy. *J. Exp. Med.* **2007**, *204*, 73-78.

[101] Stanley, R. E.; Blaha, G.; Grodzicki, R. L.; Strickler, M. D. and Steitz, T. A. The structures of the anti-tuberculosis antibiotics viomycin and capreomycin bound to the 70S ribosome. *Nat. Struct. Mol. Biol.* **2010**, *17*, 189-193.

[102] [No authors listed]. Para-aminosalicylic acid. *Tuberculosis*, **2008**, *88*, 137-138.

[103] WHO Library Cataloguing-in-Publication Data (**2010**) *Treatment of tuberculosis: guidelines.* 4th edition.

[104] Gandhi, N. R.; Nunn, P.; Dheda, K.; Schaaf, H. S.; Zignol, M.; van Soolingen, D.; Jensen, P. and Bayona, J. Multidrug-resistant and extensively drug-resistant tuberculosis: a threat to global control of tuberculosis. *Lancet*, **2010**, *375*, 1830-1843.

[105] Lawn, S. D. and Wilkinson, R. Extensively drug resistant tuberculosis. *B. M. J*. **2006**, *333*, 559-560.

[106] Yan, H. and Tsai, M. D. Nucleoside monophosphate kinases: Structure, mechanism, and substrate specificity. *Adv. Enzymol. Related Areas Molec. Biol.* **1999**, *73*, 103-133.

[107] Li de la Sierra, I.; Munier-Lehmann, H.; Gilles, A. M.; Bârzu, O. and Delarue, M. X-ray Structure of TMP Kinase from *Mycobacterium tuberculosis* complexed with TMP at 1.95 Å Resolution. *J. Mol. Biol.* **2001**, *311*, 87-100.

[108] Ostermann, N.; Schlichting, I.; Brundiers, R.; Konrad, M.; Reinstein, J.; Veit, T.; Goody, R. S. and Lavie, A. Insights into the phosphoryltransfer mechanism of human thymidylate kinase gained from crystal structures of enzyme complexes along the reaction coordinate. *Structure*, **2000**, *8*, 629-642.

[109] Fioravanti, E.; Adam, V.; Munier-Lehmann, H. and Bourgeois, D. The crystal structure of *Mycobacterium tuberculosis* thymidylate kinase in complex with 3'-azidodeoxythymidine monophosphate suggests a mechanism for competitive inhibition. *Biochemistry*, **2005**, *44*, 130-137.

[110] Vanheusden, V.; Munier-Lehmann, H.; Froeyen, M.; Dugue, L.; Heyerick, A.; De Keukeleir, D.; Pochet, S.; Busson, R.; Herdewijn, P. and Van Calenbergh, S. 3'-*C*-Branched-chain-substituted nucleosides and nucleotides as potent inhibitors of *Mycobacterium tuberculosis* thymidine monophosphate kinase. *J. Med. Chem.* **2003**, *46*, 3811-3821.

[111] Munier-Lehman H.; Chaffotte A.; Pochet S.; Labesse G. Thymidylate kinase of *Mycobacterium tuberculosis*: A chimera sharing properties common to eukaryotic and bacterial enzymes. *Protein Science*, **2001**, *10*, 1195-1205.

[112] Haouz, A.; Vanheusden, V.; Munier-Lehmann, H.; Froeyen, M.; Herdewijn, P.; Van Calenbergh, S. and Delarue, M. Enzymatic and structural analysis of inhibitors designed against *M. tuberculosis* thymidylate kinase: new insights into the phosphoryl transfer mechanism, *J. Biol. Chem.* **2003**, *278*, 4963-4971.

[113] Vanheusden, V.; Munier-Lehmann, H.; Pochet, S.; Herdewijn, P. and Van Calenbergh, S. Synthesis and evaluation of thymidine-5'-*O*-monophosphate analogues as inhibitors of *Mycobacterium tuberculosis* thymidylate kinase. *Bioorg. Med. Chem. Lett*. **2002**, *12*, 2695-2698.

[114] Vanheusden, V.; Munier-Lehmann, H.; Froeyen, M.; Busson, R.; Rozenski, J.; Herdewijn, P. and Van Calenbergh, S. Discovery of bicyclic thymidine analogues as selective and high-affinity inhibitors of *Mycobacterium tuberculosis* thymidine monophosphate kinase. *J. Med. Chem.* **2004**, *47*, 6187-6194.

[115] Van Poecke, S.; Negri, A.; Janssens, J.; Solaroli, N.; Karlsson, A.; Gago, F.; Balzarini, J. and Van Calenbergh, S. Synthesis, modeling and evaluation of 3'-(1-aryl-1*H*-tetrazol-5-ylamino)-substituted 3'-deoxythymidine derivatives as potent and selective human mitochondrial thymidine kinase inhibitors *Org. Biomol. Chem*. **2011**, *9*, 892-901.

[116] Rai, D.; Johar, M.; Srivastav, N. C.; Manning, T.; Agrawal, B.; Kunimoto, D. Y. and Kumar, R. Inhibition of *Mycobacterium tuberculosis*, *Mycobacterium bovis*, and *Mycobacterium avium* by novel dideoxy nucleosides. *J. Med. Chem*. **2007**, *50*, 4766-4774.

[117] Imazawa, M. and Eckstein, F. Synthesis of 3'-azido-2',3'-dideoxyribofuranosylpurines. *J. Org. Chem.* **1978**, *43*, 3044-3048.

[118] Reviews about the use Lawesson's reagent: (a) Cava, M. M. and Levinson, M. I. Thionation reactions of Lawesson's reagents. *Tetrahedron*, **1985**, *41*, 5061-5087; (b) Jesberger, M.; Davis, T. P. and Barner, L. Applications of Lawesson's reagent in organic and organometallic syntheses. *Synthesis*, **2003**, *13*, 1929-1958; (c) Ozturk, T.; Ertas, E. and Mert. O. Use of Lawesson's reagent in organic synthesis. *Chem. Rev.* **2007**, *107*, 5210-5278.

[119] Neilson, T. and Werstiuk, E. S. Oligoribonucleotide Synthesis II. Preparation of 2'-*O*-tetrahydropyranyl derivatives of adenosine and cytidine necessary for insertion in stepwise synthesis. *Can. J. Chem.* **1971**, *49*, 493-499.

[120] Corey, E. J. and Venkateswarlu, A. Protection of hydroxyl groups as *tert*-butyldimethylsilyl derivatives. *J. Am. Chem. Soc*. **1972**, *94*, 6190-6191.

[121] Ward, D. I.; Jeffs, S. M.; Coe, P. L.; Walker, R. T. A mild procedure for the anomerization of 2'-deoxynucleosides. *Tetrahedron Lett.* **1993**, *34*, 6779-6782.

[122] Familiar, O.; Munier-Lehmann, H.; Ainsa, J. A.; Camarasa, M. J. & Perez-Perez, M. J. Design, synthesis and inhibitory activity against *Mycobacterium tuberculosis* thymidine monophosphate kinase of acyclic nucleoside analogues with a distal imidazoquinolinone. *Eur. J. Med. Chem*. **2010**, *45*, 5910-5918.

[123] Palomino, E.; Meltsner, B. R.; Kessel, D. and Horwitz, J. P. Synthesis and *in vitro* evaluation of some 4-thiopyrimidine nucleosides for prevention or reversal of AIDS-associated neurological disorders. *J. Med. Chem*. **1990**, *33*, 258-263.

[124] Blondin, C.; Serina, L.; Wiesmüller, L.; Gilles, A. M. and Bârzu, O. Improved spectrophotometric assay of nucleoside monophosphate kinase-activity using the pyruvate-kinase lactate-dehydrogenase coupling system. *Anal. Biochem*. **1994**, *220*, 219-221.

[125] Palomino, J. C.; Martin, A.; Camacho, M.; Guerrra, H. and Swings, J. F. Resazurin microtiter assay plate: Simple and inexpensive method for detection of drug resistance in *Mycobacterium tuberculosis. Antimicrob. Agents Chemother*. **2002**, *46*, 2720-2722.

[126] Ralevic, V. and Burnstock, G. Receptors for purines and pyrimidines. *Pharmacol. Rev*. **1998**, *50*, 413-492.

[127] Burnstock, G. **1978**. *A basis for distinguishing two types of purinergic receptor, in Cell Membrane Receptors for Drugs and Hormones: A Multidisciplinary Approach* (Straub, R. W. and Bolis, L.), New York: Raven Press.

[128] Fredholm, B. B.; Abbracchio, M. P.; Burnstock, G.; Daly, J. W.; Harden, K. T.; Jacobson, K. A.; Leff, P. and Williams, M. Nomenclature and classification of purinoceptors. *Pharmacol. Rev.* **1994**, *46*, 143-156.

[129] Burnstock, G. Purine and pyrimidine receptors. *Cell. Mol. Life Sci.* **2007**, *64*, 1471-1483.

[130] Brunschweiger, A. and Müller, C. E. P2 receptors activated by uracil nucleotides - an update. *Curr. Med. Chem.* **2006**, *13*, 289-312.

[131] Webb, T. E.; Simon, J.; Krishek, B. J.; Bateson, A. N.; Smart, T. G.; King, B. F.; Burnstock, G. and Barnard, E. A. Cloning and functional expression of a brain G-protein-coupled ATP receptor. *FEBS Lett*. **1993**, *324*, 219-225.

[132] Lustig, K. D.; Shiau, A. K.; Brake, A. J. and Julius, D. Expression cloning of an ATP receptor from mouse neuroblastoma-cells. *Proc. Natl. Acad. Sci. USA*, **1993**, *90*, 5113-5117.

[133] Zhong, X.; Kriz, R.; Seehra, J. and Kumar, R. *N*-linked glycosylation of platelet $P2Y_{12}$ ADP receptor is essential for signal transduction but not for ligand binding or cell surface expression. *FEBS Lett.* **2004**, *562*, 111-117.

[134] Von Kügelgen, I. Pharmacological profiles of cloned mammalian P2Y-receptor subtypes. *Pharmacol. Ther.* **2006**, *110*, 415-432.

[135] Shaver, S. R. P2Y receptors: biological advances and therapeutic opportunities. *Curr. Opin. Drug Discov. Devel.* **2001**, *4*, 665-670.

[136] Hoffmann, C.; Moro, S. Nicholas, R. A.; Harden, T. K. and Jacobson, K. A. The Role of amino acids in extracellular loops of the human $P2Y_1$ receptor in surface expression and activation processes. *J. Biol. Chem.* **1999**, *274*, 14639-14647.

[137] Ding, Z.; Kim, S.; Dorsam, R. T. Jin, J. and Kunapuli, S. P. Inactivation of the human $P2Y_{12}$ receptor by thiol reagents requires interaction with both extracellular cysteine residues, Cys17 and Cys270. *Blood*, **2003**, *101*, 3908-3914.

[138] Siu, F. K. Y.; Lam, I. P. Y.; Chu, J. Y. S. and Chow, B. K. C. Signaling mechanisms of secretin receptor. *Regul. Peptides*, **2006**, *137*, 95-104.

[139] Cressman, V. L.; Lazarowski, E.; Homolya, L.; Boucher, R. C.; Koller, B. H. and Grubb, B. R. Effect of loss of $P2Y_2$ receptor gene expression on nucleotide regulation of murine epithelial Cl^- transport. *J. Biol. Chem.* **1999**, *274*, 26461-26468.

[140] Parr, C. E.; Sullivan, D. M.; Paradiso, A. M.; Lazarowski, E. R.; Burch, L. H.; Olsen, J. C., Erb, L.; Weisman, G. A.; Boucher, R. C. and Turner, J. T. Cloning and expression of a human P2U nucleotide receptor, a target for cystic fibrosis pharmacotherapy. *Proc. Natl. Acad. Sci. USA,* **1994**, *91*, 3275-3279.

[141] Kennedy, C.; Qi, A. D.; Herold, C. L.; Harden, T. K. and Nicholas, R. A. ATP, an agonist at the rat $P2Y_4$ receptor, is an antagonist at the human $P2Y_4$ receptor. *Mol. Pharmacol.* **2000**, *57*, 926-931.

[142] Bogdanov, Y. D.; Wildman, S. S.; Clements, M. P.; King, B. F. and Burnstock, G. Molecular cloning and characterization of rat $P2Y_4$ nucleotide receptor. *Br. J. Pharmacol.* **1998**, *124*, 428-430.

[143] Webb, T. E.; Henderson, D. J.; Roberts, J. A. and Barnard, E. A. Molecular cloning and characterization of the rat $P2Y_4$ receptor. *J. Neurochem*. **1998**, *71*, 1348-1357.

[144] Jacobson, K. A.; Jarvis, M. F. and Williams, M. Purine and Pyrimidine (P2) Receptors as drug targets. *J. Med. Chem.* **2002**, *45*, 4057-4093.

[145] Nicholas, R. A.; Watt, W. C.; Lazarowski, E. R.; Li, Q. and Harden, T. K. Uridine nucleotide selectivity of three phospholipase C-activating P2 receptors: identification of a UDP-selective, a UTP-selective, and an ATP- and UTP-specific receptor. *Mol. Pharmacol.* **1996**, *50*, 224-229.

[146] Saenger, W. **1995**, *Principles of nucleic acid structure*. New York: Springer, 4th edition.

[147] Müller, C. E. P2-pyrimidinergic receptors and their ligands. *Curr. Pharm. Design*. **2002**, *8*, 2353-2370.

[148] Lazarowski, E. R.; Watt, W. C.; Stutts, M. J.; Brown, H. A.; Boucher, R. C.; Harden, T. K. Enzymatic synthesis of UTP gamma S, a potent hydrolysis resistant agonist of P-2U-purinoceptors. *Br. J. Pharmacol.* **1996**, *117*, 203-209.

[149] Lazarowski, E. R.; Watt, W. C.; Stutts, M. J.; Boucher, R. C. and Harden, T. K. Pharmacological selectivity of the cloned human P-2U-purinoreceptor – Potent activation by diadenosine tetraphosphate. *Br. J. Pharmacol.* **1995**, *116*, 1619-1627.

[150] Cosyn, L.; Van Calenbergh, S.; Joshi, B. V.; Ko, H.; Carter, R. L.; Harden, T. K. and Jacobson, K. A. Synthesis and P2Y receptor activity of nucleoside 5'-phosphonate derivatives. *Bioorg. Med. Chem. Lett*. **2009**, *19*, 3002-3005.

[151] Verspohl, E. J.; Blackburn, G. M.; Hohmeier, N.; Hagemann, J. and Lempka, M. Synthetic, nondegradable diadenosine polyphosphates and diinosine polyphosphates: Their effects on insulin-secreting cells and cultured vascular smooth muscle cells. *J. Med. Chem*. **2003**, *46*, 1554-1562.

[152] Pendergast, W.; Yerxa, B. R.; Douglass, J. G.; Shaver, S. R.; Dougherty, R. W.; Redick, C. C.; Sims, I. F. and Rideout, J. L. Synthesis and P2Y receptor activity of a series of uridine dinucleoside 5'-polyphosphates. *Bioorg. Med. Chem. Lett.* **2001**, *11*, 157-160.

[153] Nichols, K. K.; Yerxa, B. and Kellerman, D. J. Diquafosol tetrasodium: a novel dry eye therapy. *Exp. Opin. Investig. Drugs*, **2004**, *13*, 47-54.

[154] [No authors listed] Diquafosol: DE 089, diquafosol tetrasodium, INS 365, INS 365 Ophthalmic, INS 365 Respiratory, KPY 998. *Drugs R. D*. **2003**, *4*, 359-362.

[155] Deterding, R.; Retsch-Bogart, G.; Milgram, L.; Gibson, R.; Daines, C.; Zeitlin, P. L.; Milla, C.; Marshall, B.; Lavange, L.; Engels, J.; Mathews, D.; Gorden, J.; Schaberg, A.; Williams, J. and Ramsey, B. Safety and tolerability of denufosol tetrasodium inhalation solution, a novel P2Y(2) receptor agonist: Results of a phase 1/phase 2 multicenter study in mild to moderate cystic fibrosis. *Pediatr. Pulmonol*. **2005**, *39*, 339-348.

[156] Knoblauch, B.; Müller, C. E.; Jarlebark, L.; Lawoko, G.; Kottke, T.; Wikstrom, M. A. and Heilbronn, E. 5-substituted UTP derivatives as P2Y(2) receptor agonists. *Eur. J. Med. Chem.* **1999**, *34*, 809-824.

[157] Jacobson, K. A.; Constanzi, S.; Ivanov, A.; Tchilibon, S.; Besada, P.; Gao, Z.-G.; Maddileti, S.; Harden, T. K. Structure activity and molecular modeling analyses of ribose- and base-modified uridine 5'-triphosphate analogues at the human P2Y(2) and P2Y(4) receptors. *Biochem. Pharmacol.* **2006**, *71*, 540-549.

[158] Kim, H. S.; Ravi, R. G.; Marquez, V. E.; Maddileti, S.; Wihlborg, A. K.; Erlinge, D.; Malmsjo, M.; Boyer, J. L.; Harden, T. K. and Jacobson, K. A. Methanocarba modification of uracil and adenine

nucleotides: High potency of northern ring conformation at P2Y(1), P2Y(2), P2Y(4), and P2Y(11) but not P2Y(6) receptors. *J. Med. Chem.* **2002**, *45*, 208-218.

[159] Cymberknoh, M. C.; Shoseyov, D. and Kerem, E. Managing cystic fibrosis. Strategies that increase life expectancy and improve quality of life. *Am. J. Respir. Crit. Care Med.* **2011**, *183*, 1463-1471.

[160] Nichols, D.; Chmiel, J. and Berger, M. Chronic inflammation in the cystic fibrosis lung: alteration in inter- and intracellular signaling. *Clinic. Rev*. *Allerg. Immunol.* **2008**, *34*, 146-162.

[161] Kellerman, D.; Mospan, A. R.; Engels, J.; Schaberg, A.; Gorden, J. A. and Smiley, L. Denufosol: A review of studies with inhaled $P2Y_2$ agonists that led to Phase 3. *Pulm. Pharmacol. Ther*. **2008**, *21*, 600-607.

[162] Boucher, R. C. Cystic fibrosis: a disease of vulnerability to airway surface dehydration. *Trends Mol. Med.* **2007**, *13*, 231-240.

[163] Kellerman, D.; Evans, R.; Mathews, D. and Shaffer, C. Inhaled $P2Y_2$ receptor agonists as a treatment for patients with cystic fibrosis lung disease. *Adv. Drug Del. Rev.* **2002**, *54*, 1463-1474.

[164] Kim, K. C.; Park, H. R.; Shin, C. Y.; Akiyama, T. and Ko, K. H. Nucleotide-induced mucin release from primary hamster tracheal surface epithelial cells involved the P_{2u} purinoreceptor. *Eur. Respir. J*. **1996**, *9*, 542-548.

[165] Morse, D. M.; Smullen, J. L. and Davis, C. W. Differential effects of UTP, ATP, and adenosine on ciliary activity of human nasal epithelial cells. *Am. J. Physiol. Cell Physiol*. **2001**, *280*, C1485-C1497.

[166] Cressman, V. L.; Lazarowski, E. R.; Homolya, L.; Boucer, R. C.; Koller, B. H.; Grubb, B. R. Effect of loss of P2Y(2) receptor gene expression on nucleotide regulation of murine epithelial Cl^- transport. *J. Biol. Chem.* **1999**, *274*, 26461-26468.

[167] Accurso, F. J.; Moss, R. B.; Wilmott, R. W.; Anbar, R. D.; Schaberg, A. E.; Durham, T. A.; Ramsey, B. W. and the TIGER-1 Investigator Study Group. Denufosol tetrasodium in patients with cystic fibrosis and normal to mildly impaired lung function. *Am. J. Respir. Crit. Care Med.* **2011**, *183*, 627-634.

[168] Jumblatt, E. E. and Jumblatt, M. M. Regulation of ocular mucin secretion by P2Y(2) nucleotide receptors in rabbit and human conjunctiva. *Exp. Eye. Res*. **1998**, *67*, 341-346.

[169] Murakami, T.; Fujihara, T.; Horibe, Y. and Nakamura, M. Diquafosol elicits increases in net Cl^- transport through $P2Y_2$ receptor stimulation in rabbit conjunctiva. *Ophtalmic. Res*. **2004**, *36*, 89-93.

[170] White, N. and Burnstock, G. P2 receptors and cancer. *Trends Pharmacol. Sci.* **2006**, *27*, 211-217.

[171] White, N.; Ryten, M.; Clayton, E.; Butler, P. and Burnstock, G. P2Y purinergic receptors regulate the growth of human melanomas. *Cancer Lett*. **2005**, *224*, 81-91.

[172] Schafer, R.; Sedehizade, F.; Welte, T. and Reiser, G. ATP- and UTP-activated P2Y receptors differently regulate proliferation of human lung epithelial tumor cells. *Am. J. Physiol. Lung Cell. Mol. Physiol.* **2003**, *285*, L376-L385.

[173] Höpfner, M.; Maaser, K.; Barthel, B.; von Lampe, B.; Hanski, C.; Riecken, E. O.; Zeitz, M. and Scherübl, H. Growth inhibition and apoptosis induced by $P2Y_2$ receptors in human colorectal carcinoma cells: involvement of intracellular calcium and cyclic adenosine monophosphate. *Int. J. Colorectal Dis.* **2001**, *16*, 154-166.

[174] Maaser, K.; Höpfner, M.; Kap, H.; Sutter, A. P.; Barthel, B.; von Lampe, B.; Zeitz, M.Scherübl, H. Extracellular nucleotides inhibit growth of human oesophageal cancer cells via $P2Y_2$-receptors. *Br. J. Cancer*, **2002**, *86*, 636-644.

[175] Rieg, T.; Gerasimova, M.; Boyer, J. L.; Insel, P. A. and Vallon, V. $P2Y_2$ receptor activation decreases blood pressure and increases renal Na^+ excretion. *Am. J. Physiol. Regul. Integr. Comp. Physiol.* **2011**, in press.

[176] Min, K.; Munarriz, R.; Yerxa, B. R.; Goldstein, I.; Shaver, S. R.; Cowlen, M. S. and Traish, A. M. Selective $P2Y_2$ receptor agonists stimulate vaginal moisture in ovariectomized rabbits. *Fertil. Steril*. **2003**, *79*, 393-398.

[177] Jacobson, K. A.; King, B. F. and Burnstock, G. Pharmacological characterization of P2 (nucleotide) receptors. *Celltransmission*, **2000**, *16*, 3-16.

[178] Iqbal, J.; Vollmayer, P.; Braun, N.; Zimmermann, H. and Müller, C. E. A capillary electrophoresis method for the characterization of ecto-nucleoside triphosphate diphosphohydrolases (NTPDases) and the analysis of inhibitors by in-capillary enzymatic microreaction. *Purinergic Signal.* **2005**, *1*, 349-358.

[179] Claes, P.; Van Kolen, K.; Roymans, D.; Blero, D.; Vissenberg, K.; Erneux, C.; Verbelen, J. P.; Esmans, E. L. and Slegers, H. Reactive blue 2 inhibition of cyclic AMP-dependent differentiation of rat C6 glioma cells by purinergic receptor-independent inactivation of phosphatidylinositol 3-kinase. *Biochem. Pharmacol*. **2004**, *67*, 1489-1498.

[180] Chung, W. C. and Kermode, J. C. Suramin disrupts receptor-G protein coupling by blocking association of G protein alpha and beta gamma subunits. *J. Pharmacol. Exp. Ther.* **2005**, *313*, 191-198.

[181] Weyler, S.; Baqi, Y.; Hillmann, P.; Kaulich, M.; Hunder, A. M.; Müller, I. and Müller, C. E. Combinatorial synthesis of anilinoanthraquinone derivatives and evaluation as non-nucleotide-derived $P2Y_2$ receptor antagonists. *Bioorg. Med. Chem. Lett*. **2007**, *18*, 223-227.

[182] Kaulich, M.; Streicher, F.; Mayer, R.; Müller, I. and Müller, C. E. Flavonoids - Novel lead compounds for the development of $P2Y_2$ receptor antagonists. *Drug Dev. Res.* **2003**, *59*, 72-81.

[183] Malmsjö, M.; Hou, M.; Harden, T. K.; Pendergast, W.; Pantev, E.; Edvinsson, L. and Erlinge, D. J. Characterization of contractile P2 receptors in human coronary arteries by use of the stable pyrimidines uridine 5'-*O*-thiodiphosphate and uridine 5'-*O*-3-thiotriphosphate. *Pharmacol. Exp. Ther.* **2000**, *293*, 755-760.

[184] Erb, L.; Garrad, R.; Wang, Y.; Quinn, T.; Turner, J. T. and Weisman, G. A. Site-directed mutagenesis of P2U purinoceptors. *J. Biol. Chem.* **1995**, *270*, 4185-4188.

[185] Ivanov, A. A.; Costanzi, S. and Jacobson, K. A. Defining the nucleotide binding sites of P2Y receptors using rhodopsin-based homology modeling. *J. Comput. Aided Mol. Des.* **2006**, *20*, 417-426.

[186] Hillmann, P.; Ko, G. Y.; Spinrath, A.; Raulf, A.; von Kügelgen, I.; Wolff, S. C.; Nicholas, R. A.; Kostenis, E.; Höltje, H. D. and Müller, C. E. Key determinants of nucleotide-activated G protein-coupled $P2Y_2$ receptor function revealed by chemical and pharmacological experiments, mutagenesis and homology modeling. *J. Med. Chem*. **2009**, *52*, 2762-2775.

[187] Astra Pharm. Ltd*. et al*. Novel thiouridine triphosphate derivatives. *Exp. Opin. Ther. Patents.* **1999**, *9*, 205-207.

[188] Jones, G. H. and Moffatt, J. G. The synthesis of 6'-deoxyhomonucleoside-6'-phosphonic acids. *J. Am. Chem. Soc.* **1968**, *90*, 5337-5338.

[189] Padyukova, N. S.; Karpeisky, M. Y.; Kolobushkina, L. I. and Mikhailov, S. N. A new scheme for the synthesis of 5'-nucleotide phosphonate analogs. *Tetrahedron Lett.* **1987**, *28*, 3623-3626.

[190] Barton, D. H. R.; Stephane D. G.; Quiclet-Sire, B. and Samadi, M. New synthesis of sugar, nucleoside and α-amino acid phosphonates. *Tetrahedron*, **1992**, *48*, 1627-1636.

[191] Xu, Y.; Flavin, M. T. and Xu, Z. Preparation of new Wittig reagents and their application to the synthesis of α,β-unsaturated phosphonates. *J. Org. Chem*. **1996**, *61*, 7697-7701.

[192] Pomeisl, K.; Holý, A. and Pohl, R. Pd-catalyzed Suzuki-Miyaura coupling reactions in the synthesis of 5-aryl-1-[2-(phosphonomethoxy)ethyl]uracils as potential multisubstrate inhibitors of thymidine phosphorylase. *Tetrahedron Lett*. **2007**, *48*, 3065-3067.

[193] Nencka, R.; Sinnaeve, D.; Karalic, I.; Martins, J. C. and Van Calenbergh, S. Synthesis of C-6-substituted uridine phosphonates through aerobic ligand-free Suzuki-Miyaura cross-coupling. *Org. Biomol. Chem.* **2010**, *8*, 5234-5246.

[194] Verheyden, J. P. H.; Wagner, D. and Moffatt, J. G. Synthesis of some pyrimidine 2'-amino-2'-deoxynucleosides. *J. Org. Chem.* **1971**, *36*, 250-254.

[195] Hampton, A. and Nichol, A. W. Nucleotides. V. Purine ribonucleoside 2',3'-cyclic carbonates. Preparation and use for the synthesis of 5'-monosubstituted nucleosides. *Biochemistry*, **1966**, *5*, 2076-2082.

[196] Holy, A. Simple method for cleavage of phosphonic acid diesters to monoesters. *Synthesis-Stuttgart*. **1998**, 381-385.

[197] (a) Staudinger, H. and Meyer, J. Uber neue organische phosphorverbindungen III. Phosphinmethylenderivate und phosphinimine. *Helv. Chim. Acta*. **1919**, *2*, 635-646; (b) Scriven, E. F. V. Azides: Their preparation and synthetic uses. *Chem. Rev.* **1988**, *88*, 297-368.

[198] Kifli, N.; Htar, T. T.; De Clercq, E.; Balzarini, J. and Simons, C. Novel bicyclic sugar modified nucleosides: synthesis, conformational analysis and antiviral evaluation. *Bioorg. Med. Chem.* **2004**, *12*, 3247-3257.

[199] Epp, J. B. and Widlanski, T. S. Facile preparation of nucleoside-5'-carboxylic acids. *J. Org. Chem.* **1999**, *64*, 293-295.

[200] Zhang, W. and Robins, M. J. Removal of silyl protecting groups from hydroxyl functions with ammonium fluoride in methanol. *Tetrahedron Lett*. **1992**, *33*, 1177-1180.

[201] Zemlicka, J.; Gasser, R.; Freisler, J. V. and Horwitz, J. P. Nucleosides. XV. Decarboxylative elimination of 2'-deoxyuridine uronic acids. *J. Am. Chem. Soc.* **1972**, *94*, 3213-3218.

[202] Kim, C. U.; Luh, B. Y. and Martin, J. C. Regiospecific and highly stereoselective electrophilic addition to furanoid glycals: synthesis of phosphonate nucleotide analogues with potent activity against HIV. *J. Org. Chem.* **1991**, *56*, 2642-2647.

[203] Paquette, L. A.; Seekamp, C. K. and Kahane, A. L. Conformational restriction of nucleosides by spirocyclic annulation at C4' including synthesis of the complementary dideoxy and didehydrodideoxy analogues. *J. Org. Chem.* **2003**, *68*, 8614-8624.

[204] Nicholas, R. A.; Lazarowski, E. R.; Watt, W. C.; Li, Q. and Harden, T. K. Uridine nucleotide selectivity of three phospholipase C-activating P-2 receptors: Identification of a UDP-selective, a UTP-selective, and an ATP- and UTP-specific receptor. *Mol. Pharmacol.* **1996**, *50*, 224-229.

[205] Bourdon, D. M.; Wing, M. R.; Edwards, E. B.; Sondek, J. and Harden, T. K. Quantification of isoenzyme-specific activation of phospholipase C-beta 2 by Rac GTPases and phospholipase C-epsilon by Rho GTPases in an intact cell assay system. *Methods Enzymol.* **2006**, *406*, 489-499.

[206] Altona, C. and Sundaralingam, M. Conformational-analysis of sugar ring in nucleosides and nucleotides – improved method for interpretation of proton magnetic-resonance coupling constants. *J. Am. Chem. Soc.* **1973**, *95*, 2333-2344.

[207] Altona, C. and Sundaralingam, M. Conformational-analysis of sugar ring in nucleosides and nucleotides - new description using concept of pseudorotation*. J. Am. Chem. Soc.* **1972**, *94*, 8205-8212.

[208] Davies, D. B. and Danyluk, S. S. Nuclear magnetic-resonance studies of 5'-ribonucleotide and deoxyribonucleotide structures is solution. *Biochemistry*, **1974**, *13*, 4417-4434.

[209] Tiecco, M.; Profio, P. D.; Germani, R. and Savelli, G. Synthesis of novel 5'-uridine-head amphiphiles as model for DNA molecular recognition. *Nucleosides Nucleotides Nucleic acids*, **2009**, *28*, 911-923.

[210] De Clercq, E. and Holý, A. Acyclic nucleoside phosphonates: a key class of antiviral drugs. *Nat. Rev. Drug Discov.* **2005**, *4*, 928-940.

[211] Schinazi, R. F. **2004**. *Frontiers in nucleosides and nucleic acids*. (Liotta, D. C.) USA: IHL Press, 4th edition.

[212] De Clercq, E. Discovery and development of BVDU (brivudin) as a therapeutic for the treatment of herpes zoster. *Biochem. Pharmacol.* **2004**, *68*, 2301-2315.

[213] Brulikova, L. and Hlavac, J. Synthesis, reactivity and biological activity of 5-alkoxymethyluracil analogues. *Beilstein J. Org. Chem*. **2011**, *7*, 678-698.

[214] Ivanov, A. V.; Simonyan, A. R.; Belanov, E. F. and Aleksandrova, L. A. Synthesis and antiviral activity of new 5-substituted 2'-deoxyuridine derivatives. *Russ. J. Bioorg. Chem.* **2005**, *31*, 556-562.

[215] McGuigan, C.; Yarnold, C. J.; Jones, G.; Velázquez, S.; Barucki, H.; Brancale, A.; Andrei, G.; Snoeck, R.; De Clercq, E. and Balzarini, J. Potent and selective inhibition of varicella-zoster virus (VZV) by nucleoside analogues with an unusual bicyclic base. *J. Med. Chem.* **1999**, *42*, 4479-4484.

[216] McGuigan, C. and Balzarini, J. FV100 as a new approach for the possible treatment of varicella-zoster virus infection. *J. Antimicrob. Chem.* **2009**, *64*, 671-673.

[217] Herdewijn, P.; De Clercq, E.; Balzarini, J. and Vanderhaeghe, H. Synthesis and antiviral activity of the carbocyclic analogues of (*E*)-5-(2-halovinyl)-2'-deoxyuridines and (*E*)-5-(2-halovinyl)-2'-deoxy-cytidines. *J. Med. Chem.* **1985**, *28*, 550-555.

[218] Balzarini, J.; Baumgartner, H.; Bodenteich, M.; De Clercq, E. and Griengl, H. Synthesis and antiviral activity of the enantiomeric forms of carba-5-iodo-2'-deoxyuridine and carba-(*E*)-5-(2-bromovinyl)-2'-deoxyuridine. *J. Med. Chem.* **1989**, *32*, 1861-1865.

[219] Verheggen, I.; Van Aerschot, A.; Toppet, S.; Snoeck, R.; Janssen, G.; Balzarini, J.; De Clercq, E. and Herdewijn, P. Synthesis and antiherpes virus activity of 1,5-anhydrohexitol nucleosides. *J. Med. Chem.* **1993**, *36*, 2033-2040.

[220] Verheggen, I.; Van Aerschot, A.; Van Meervelt, L.; Rozenski, J.; Wiebe, L.; Snoeck, R.; Andrei, G.; Balzarini, J.; Claes, P.; De Clerq, E. and Herdewijn, P. Synthesis, biological evaluation, and structure analysis of a series of new 1,5-anhydrohexitol nucleosides. *J. Med. Chem.* **1995**, *38*, 826-835.

[221] Ostrowski, T.; Wroblowski, B.; Busson, R.; Rozenski, J.; De Clercq, E.; Bennett, M. S.; Champness, J. N.; Summers, W. C.; Sanderson, M. R. and Herdewijn, P. 5-Substituted pyrimidines with a 1,5-anhydro-2,3-dideoxy-D-*arabino*-hexitol moiety at N-1: Synthesis, antiviral activity, conformational analysis, and interaction with viral thymidine kinase. *J. Med. Chem*. **1998**, *41*, 4343-4353.

[222] Marquez, V. E.; Hughes, S. H.; Sei, S. and Agbaria, R. The history of *N*-methanocarbathymidine: The investigation of a conformational concept leads to the discovery of a potent and selective nucleoside antiviral agent. *Antiviral. Res.* **2006**, *71*, 268-275.

[223] Berdis, A. J. DNA Polymerases as therapeutic targets. *Biochemistry*, **2008**, *47*, 8253-8260.

[224] Sastry, J. K.; Nehete, P. N.; Khan, S.; Nowak, B. J.; Plunkett, W.; Arlinghaus, R. B. and Farquhar, D. Membrane-permeable dideoxyuridine 5'-monophosphate analog inhibits human-immunodeficiency-virus infection. *Mol. Pharmacol.* **1992**, *41*, 441-445.

[225] Puech, F.; Gosselin, G.; Lefebvre, I.; Pompon, A.; Aubertin, A. M.; Kirn, A. and Imbach, J. L. Intracellular delivery of nucleoside monophosphates through a reductase-mediated activation process. *Antiviral Res.* **1993**, *22*, 155-174.

[226] De Clercq, E. The clinical potential of the acyclic (and cyclic) nucleoside phosphonates. The magic of the phosphonate bond. *Biochem. Pharmacol.* **2011**, *82*, 99-109.

[227] Wigerinck, P.; Kerremans, L.; Claes, P.; Snoeck, R.; Maudgal, P.; De Clercq, E. and Herdewijn, P. Synthesis and antiviral activity of 5-thien-2-yl-2'-deoxyuridine analogues. *J. Med. Chem.* **1993**, *36*, 538-543.

[228] Evano, G.; Schaus, J. V. and Panek, J. S. A convergent synthesis of the macrocyclic core of cytotrienins: application of RCM for macrocyclization. *Org. Letters*, **2004**, *6*, 525-528.

[229] Van Aerschot, A.; Jie, L. and Herdewijn, P. Synthesis of 5'-*O*-phosphonomethyl-2',3'-didehydro-2',3'-dideoxyuridine by use of P-methoxybenzyl as a N^3-protecting group. *Tetrahedron Lett.* **1991**, *32*, 1905-1908.

[230] Murphy, M. P. and Smith, R. A. J. Targeting antioxidants to mitochondria by conjugation to lipophilic cations. *Annu. Rev. Pharmacol. Toxicol*. **2007**. *47,* 629-656.

[231] Szeto, H. H. Cell-permeable, mitochondrial-targeted, peptide antioxidants. *AAPS J*., **2006**, *8*, E277-E283.

SCIENTIFIC CV

PERSONALIA

Surname and name:	Van Poecke Sara
Date of birth:	October 23th 1983
Place of birth:	Lokeren
E-mail:	saravanpoecke@hotmail.com
Nationality:	Belgian

EDUCATION

2007 - present	PhD in Pharmaceutical Sciences, University of Ghent
2001 - 2007	Master in Pharmaceutical Sciences, *magna cum laude*, University of Ghent
1995 - 2001	Secondary education, Technique-Sciences, Sint-Carolus, Sint-Niklaas

ADDITIONAL TRAINING

2011	Three-day transferable skills training (Project management)

WORKING EXPERIENCE

2007 - 2011	PhD in Pharmaceutical Sciences, Laboratory of Medicinal Chemistry, University of Ghent
2008 - 2011	Teaching in work colleges Medicinal Chemistry

SUPERVISION OF MASTER STUDENTS IN PHARMACEUTICAL SCIENCES

2008	Aji Thomas; Synthesis of pyrimidine nucleosides and nucleotides with therapeutic potential
2009	Jolien Janssens; Synthesis of substrate-based inhibitors for thymidine kinase 2 (TK-2)
2010	Lynn Vander Stricht; Synthesis of nucleoside 5'-phosphonate analogues as potential $P2Y_2$-receptor ligands

SCIENTIFIC PUBLICATIONS IN PEER-REVIEWED JOURNALS

- Haemers, T.; Wiesner, J.; Van Poecke, S.; Goeman, J.; Henschker, D.; Beck, E.; Jomaab, H. and Van Calenbergh, S. Synthesis of α-substituted fosmidomycin analogues as highly potent *Plasmodium falciparum* growth inhibitors. *Bioorg. Med. Chem. Lett*. **2006**, *16*, 1888-1894.

- Van Poecke, S.; Negri, A.; Gago, F.; Van Daele, I.; Solaroli, N.; Karlsson, A.; Balzarini, J. and Van Calenbergh, S. 3'-[4-Aryl-(1,2,3-triazol-1-yl)]-3'-deoxythymidine analogues as potent and selective inhibitors of human mitochondrial thymidine kinase. *J. Med. Chem*. **2010**, *53*, 2902-2912.

- Van Poecke, S.; Negri, A.; Janssens, J.; Solaroli, N.; Karlsson, A.; Gago, F.; Balzarini, J. and Van Calenbergh, S. Synthesis, modeling and evaluation of 3'-(1-aryl-1*H*-tetrazol-5-yl-amino)-substituted 3'-deoxythymidine derivatives as potent and selective human mitochondrial thymidine kinase inhibitors. *Org. Biomol. Chem.* **2011**, *9*, 892-901.

- Van Poecke, S.; Munier-Lehmann, H.; Helynck, O.; Froeyen, M. and Van Calenbergh, S. Synthesis and inhibitory activity of thymidine analogues targeting *Mycobacterium tuberculosis* Thymidine Monophosphate Kinase. *Bioorg. Med. Chem*. Accepted.

- Van Poecke, S.; Sinnaeve, D.; Martins, J. C.; Balzarini, J. and Van Calenbergh, S. Synthesis of 5-substituted 2'-deoxyuridine-5'-phosphonate analogues and evaluation of their antiviral activity. Nucleosides Nucleotides Nucleic Acids. Submitted.

- Van Poecke, S.; Barrett, M. O.; Kumar, T. S.; Sinnaeve, D.; Martins, J. C. Harden, T. K. Jacobson, K. A. and Van Calenbergh, S. Synthesis and $P2Y_2$ receptor agonist activities of uridine 5'-phosphonate analogues. Submitted.

CONFERENCES

- New Drugs and Drug Candidates: Recent Achievements in Medicinal Chemistry
  Braine l'Alleud, Belgium, October 26, 2007

- Vlaams Jongerencongres van de Chemie
  Antwerp, Belgium, April 4, 2008

- XIVth Symposium on Chemistry of Nucleic Acid Components
  Cesky, Krumlov, Czech Republic, June 8-13, 2008

- Belgian Organic Synthesis Symposium (Boss)
  Ghent, Belgium, July 13-18, 2008

- Small Molecules, Antibodies and Natural Products: Multiple Faces of Medicinal Chemistry
  Leuven, Belgium, November 7, 2008

- 12th Sigma Aldrich Organic Synthesis Meeting
  Spa, Belgium, December 4-5, 2008
  Poster Presentation: Synthesis of highly active and selective inhibitors of thymidine kinase 2

- KVCV - Does size matter, a one day symposium
  Brussels, Belgium, November 2, 2009

- 13th Sigma Aldrich Organic Synthesis Meeting
  Spa, Belgium, December 3-4, 2009
  Poster Presentation: 3'-Deoxy-3'-substituted thymidines: a new class of thymidine kinase 2 inhibitors

- 10th Flemish Youth Conference of Chemistry
  Blankenberge, Belgium, March 1-2, 2010
  Oral Communication: Synthesis of highly active and selective inhibitors of thymidine kinase 2

- 21st International Symposium on Medicinal Chemistry (EFMC-ISMC 2010)
  Brussels, Belgium, September 5-9, 2010
  Poster Presentation: Synthesis of nucleoside 5'-phosphonate analogues as potential $P2Y_2$ receptor ligands

- XVth Symposium on Chemistry of Nucleic Acid Components

  Cesky, Krumlov, Czech Republic, June 5-10, 2011

  Poster Presentation: Synthesis of nucleoside 5'-phosphonate analogues as potential $P2Y_2$ receptor ligands